Characterisation of the centrosome protein Cep63

Nicola J. Brown

University College London

and

Cancer Research UK London Research Institute

PhD Supervisor: Dr Vincenzo Costanzo

A thesis submitted for the degree of

Doctor of Philosophy

University College London

September 2011

Declaration

I Nicola Brown confirm that the work presented in this thesis is my own. Where information has been derived from other sources, I confirm that this has been indicated in the thesis.

Abstract

In dividing cells, centrosomes act as the primary microtubule organising centre to orchestrate mitotic spindle assembly. Bipolar spindle assembly is responsible for accurate segregation of sister chromatids, such that each daughter cell receives an identical copy of the genome. Changes in centrosome number can lead to a lack of mitotic fidelity and genome instability. Chromosomes are replicated in a controlled and timely fashion and the same is true for centrosomes so that cells enter mitosis with two centrosomes. Further to their role in spindle assembly, centrosomes are also important in cell cycle regulation and DNA damage checkpoint signalling. Centrosomes are particularly important in the regulation of neuroepithelial cell division in the developing brain: all known incidences of primary microcephaly are caused by mutations in centrosome or spindle pole proteins.

Xenopus laevis Cep63 is a target of DNA damage kinase, ATM, and it's important for the formation of bipolar mitotic spindles (Smith et al., 2009). Therefore, Cep63 is an exciting candidate for maintenance of genome stability. Human Cep63 has been identified as a centrosome protein (Andersen et al., 2003), but its function was uncharacterised. In this thesis Cep63 was shown to be a constitutive centrosome protein, which plays a role in the regulation of centriole duplication. Cep152 was identified as a Cep63 interacting protein; and Cep63 and Cep152 are dependent on each other for their centrosomal localisation. Cep152 is required for centriole duplication via recruitment of essential duplication factors, Plk4 and CPAP, to the centrosome (Dzhindzhev et al., 2010b, Cizmecioglu et al., 2010, Hatch et al., 2010b). Furthermore, mouse embryonic fibroblasts in which the Cep63 gene is disrupted show decreased centriole numbers and signs of genome instability. Intriguingly, preliminary analysis of mouse embryos points to a potential link between Cep63 deficiency and microcephaly. We propose that Cep63 and Cep152 function together to ensure correct centrosomal levels of the essential centriole duplication factors Plk4 and CPAP.

Acknowledgements

First of all, thank you to Vincenzo for giving me the fantastic opportunity of working in the Costanzo lab and being a part of Clare Hall. My thanks also go to my thesis committee; Simon Boulton and Svend Petersen-Mahrt for guidance during my studies; and to Mark Petronczki, whose advice, criticism, and encouragement has been invaluable. Thanks to all of my colleagues, past and present: your help and your company have been much appreciated over the past four years and have made our lab a great place to work. Thank you especially to Liz Garner, Alessia Errico, and Simona Fiorani for help with writing and editing this thesis and for inspiration throughout.

Last, but not least, thank you to my partner James, who now understands more about centrosomes than any good software engineer really should.

Table of Contents

Table of figures

List of tables

Abbreviations

AP	Affinity Purified
APC/C	Anaphase Promoting Complex/Cyclosome
Aph	Aphidicolin
ATM	Ataxia Telangiectasia Mutated
ATR	ATM and Rad3 related
BER	Break Excision Repair
BSA	Bovine Serum Albumin
C152	Cep152, Centrosome protein of 152 kDa
C63	Cep63, Centrosome protein of 63 kDa
Cdk	Cyclin dependent kinase
cDNA	complementary DNA
CSF	Cytostatic Factor
DAPI	4,6-diamidino-2-phenylindole
ddH2O	double distilled water
DNA	Deoxyribonucleic acid
DSB	double strand break (in DNA)
EM	Electron Microscopy
ES	Embryonic Stem (cell)
FACS	Fluorescence Activated Cell Sorting
FCS	Foetal Calf Serum
G1	Gap phase 1
G2	Gap phase 1
GAPDH	Glyceraldehyde-3-phosphate dehydrogenase
GDP	Guanosine diphosphate
GEF	GTP Exchange Factor
GFP	Green Fluorescent Protein
GT	Gene-Trap
GTP	Guanosine triphosphate
HR	Homologous Recombination
HU	Hydroxyurea
IF	Immunofluorescence
IP	Immunoprecipitation
IR	Irradiation
M	Mitosis
MBP	Maltose Binding Protein
MCC	Mitotic Checkpoint Complex
MCPH	Primary Autosomal Recessive Microcephaly
MEF	Mouse Embryonic Fibroblast
MOPD II	Majewski Osteodysplastic Primordial Dwarfism type II
MPF	Maturation Promoting Factor
M/R/N	Mre11/Rad50/Nbs1
mRNA	messenger RNA
MT	Microtubule
MTOC	Microtubule Organising Centre
NE	Neuroepithelial
NER	Nucleotide Excision Repair

NHEJ	Non-Homologous End Joining
NPM	Nucleophosmin
NuMA	Nuclear Mitotic Apparatus Protein
Orc	Origin Recognition Complex
pADPr	poly adenosine diphosphate (ADP) ribose
PBS (-Tw)	phosphate buffered saline (plus 0.1% Tween 20)
PCM	Pericentriolar Material
PI	Propidium Iodide
Plk	Polo like kinase
RNA	Ribonucleic Acid
RNAi	RNA interference
RT-PCR	Reverse Transcription-PCR
S	S phase, Synthesis
SAC	Spindle Assembly Checkpoint
SDS	Sodium Dodecyl Sulfate
SDS-PAGE	SDS-Poly Acrylamide Gel Electrophoresis
Sgo1	Shugoshin 1
siRNA	short interfering RNA
TACC	Transforming Acid Coiled Coil protein
TBS (-Tw)	Tris Buffered Saline (plus 0.1% Tween 20)
TOG	Tumour Over-expressed Gene
TX	Triton X-100
UV	Ultra Violet radiation
WB	Western blot
WT	Wild Type
XCep152	*Xenopus laevis* Cep152
XCep63	*Xenopus laevis* Cep63
YFP	Yellow Fluorescent Protein
γ-IR	gamma-Irradiation
γ-TuRC	gamma-Tubulin Ring Complex

Chapter 1. Introduction

1.1 The eukaryotic cell cycle

Cell division is the process by which a mother cell duplicates its content and divides in two, forming two daughter cells. In single celled organisms, each cell division produces a whole new organism, whereas in large multicellular organisms such as mammals, cell division is required during development to produce the many different cell types that make up the body from one fertilised egg cell. Cell division is also required in fully developed mammals for the generation of new tissues: there is a high turnover of the body's cells throughout life for tissue maintenance and repair after injury.

The entire process of duplication of the genetic information through to division into two new cells is called "the cell cycle". Each cell contains the genetic information required for all cell types in the entire organism and in order for the genetic information to be maintained "word for word" throughout all of the trillions of cell divisions from fertilisation of a vertebrate egg to development of a fully formed organism, and through life the cell cycle has to be strictly controlled. Each cell can only divide when it has faithfully copied the genetic information so that an identical copy can be passed to each daughter cell. Genetic information is stored as deoxyribonucleic acid (DNA), which is packaged by cellular proteins into chromosomes. During cell division DNA is first duplicated in S phase (Synthesis) then segregated equally into two daughter cells in mitosis (M) by the action of the mitotic spindle (figure 1).

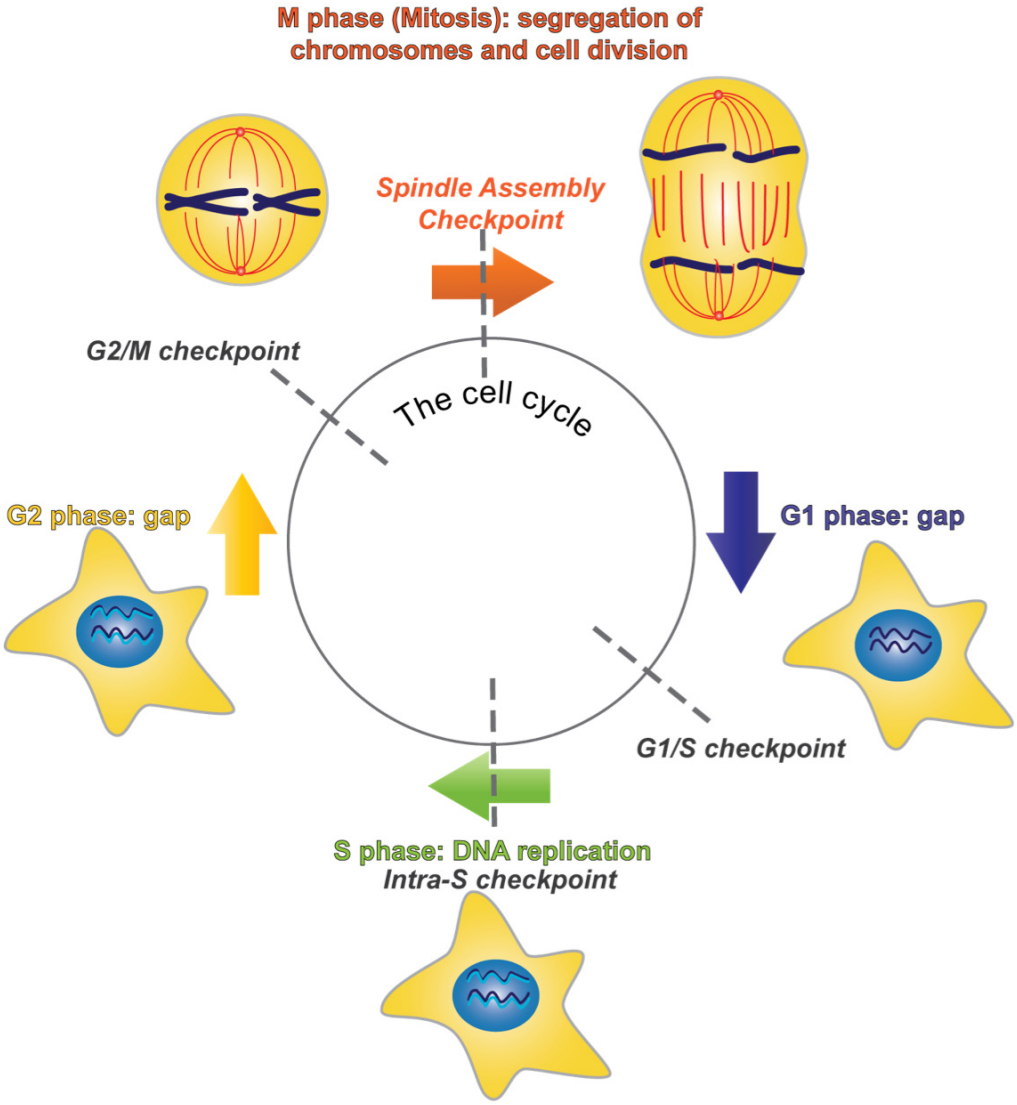

Figure 1 The cell cycle
DNA is replicated during S (synthesis) phase and duplicated chromosomes are then segregated equally into two daughter cells during mitosis. Chromosomes are aligned and attached to the mitotic spindle (red lines) such that sister chromatids are attached to spindle microtubules emanating from opposite spindle poles. When all chromatids are attached in a bipolar fashion the spindle assembly checkpoint is satisfied and anaphase occurs (mitosis, right). Cell cycle checkpoints regulate cell cycle progression at the stages indicated by dashed lines. The G1/S, intra-S and G2/M checkpoints are activated in response to DNA damage and halt cell cycle progression by inhibition of the appropriate Cdk-Cyclin pair. The spindle assembly checkpoint is activated by chromatids that are not properly attached to the mitotic spindle and halts mitosis by inhibiting the onset of anaphase. Gap phases separate S phase and mitosis in vertebrate somatic cell cycles to allow growth and the opportunity for cell cycle regulation by internal or external stimuli.

The equal segregation of chromosomes during cell division in human cells was first visualised by Walther Flemming in 1879 (figure 2, reproduced from (Paweletz, 2001)). Upon entry into mitosis, during prophase, replicated chromosomes (pairs of sister chromatids) condense, and duplicated centrosomes nucleate microtubules. Mitotic spindle formation begins between the two centrosomes. In prometaphase nuclear envelope breakdown occurs and spindle microtubules begin to attach to kinetochores on chromosomes, which is a highly dynamic process. In metaphase, chromosomes are aligned at the equator by the action of spindle microtubules and associated motor proteins, such that sister chromatids are attached to microtubules from opposite spindle poles (equatorial plate, figure 2). When all chromosomes are attached to the mitotic spindle in a bipolar fashion, the synchronous separation of sister chromosomes occurs (anaphase). In telophase, chromosomes at spindle poles start to de-condense; the nuclear envelope starts to reform; and the contractile ring assembles in the middle of the cell. The cytoplasm is divided in two by the contractile ring, made from actin and myosin filaments, in cytokinesis. Chromosomes continue to de-condense and nuclear envelope formation is completed (reconstruction phase, figure 2).

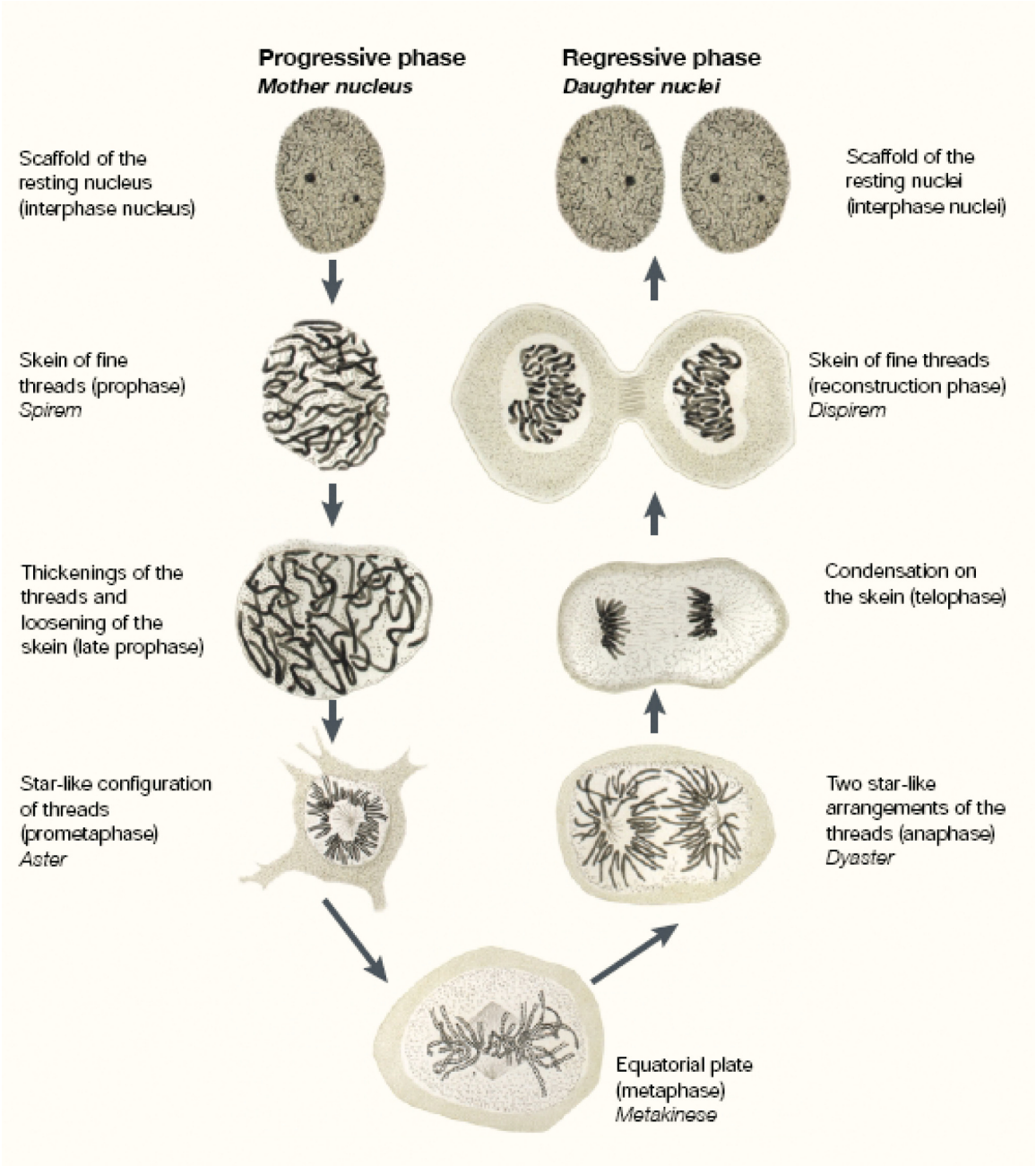

Figure 2 Walter Flemming's drawings of cell division stages
Diagram from Walther Flemming, Zellsubstanz, Kern und Zellteilung (1882) "Cell substance, nucleus and cell division". Taken from (Paweletz, 2001). These detailed drawing of the stages of cell division illustrate the condensation of duplicated chromosomes, their alignment at metaphase and their equal segregation into two daughter cells.

It is of extreme importance that DNA replication, the duplication of chromosomes, is carried out with precision to ensure that copies are identical. As follows, it is important that chromosomes are segregated equally during mitosis when the cell divides in two. Errors in DNA replication or unequal segregation of chromosomes lead to genetic instability and cancer (Negrini et al., 2010).

Theodor Boveri first documented these ideas in the 1880s: Boveri postulated that abnormal cell divisions led to tumour formation and that different chromosomes carried different genetic traits, so chromosomes had to be inherited equally by the two daughter cells during cell division. Boveri also put forward the idea that the cell cycle contains "checkpoints", which control the cell cycle and prevent amplification of cells with genetic errors, as documented by Bignold *et al.*(Bignold et al., 2006). These theories were based on earlier work carried out by Hansemann in the late 1800s, who documented the presence of abnormal asymmetric mitoses in carcinomas (Bignold et al., 2006).

The importance of accurate duplication and segregation of chromosomes during cell division has been documented and discussed for over a hundred years, and nowadays we know that the control of the cell cycle by regulatory proteins ensures fidelity. First of all, DNA replication is highly regulated to ensure that it takes place once and only once per cell cycle, and secondly, the duplicated chromosomes are equally segregated between the two daughter cells. Cells can only enter mitosis once the genome has been fully replicated and separation of the sister chromatids can only occur once all sister chromatids are attached to opposite spindle poles. In mammalian cells, S phase and M phase are separated by gap phases (G1 and G2), which allow for cell growth and the regulation of cell cycle progression by internal or external signals (figure 1). Accurate cell cycle control is crucial for the maintenance of genome stability.

1.1.1 Cell cycle control

Progression of the cell cycle is driven by protein kinases that phosphorylate a range of substrate proteins required for each stage of the cell cycle. These kinases that control cell cycle progression are thus called cyclin-dependent kinases (Cdks). Oscillations of the activity of Cdks are regulated, in part, by the periodic translation and proteolytic degradation of their cyclin partner, on which they rely for full activation. The first indication that the cell cycle could be regulated by protein degradation came from work carried out in the 1980s, which identified cyclin as a protein that was degraded periodically at a specific point in the cell cycle in fertilised sea urchin eggs (Evans et al., 1983). Further work showed that the addition of Cyclin B protein to *Xenopus laevis* egg extracts satisfied the requirement for protein synthesis for entry and progression through mitosis (Murray and Kirschner, 1989, Murray et al., 1989).

From biochemical studies of fertilised eggs and from genetic studies in yeast, it is now known that the cell cycle is controlled by different Cdk-cyclin pairs and that the periodic activation and inhibition of these kinases drives cell cycle progression (figure 3). Internal and external signalling pathways regulate cell cycle progression by controlling the activity of Cdk-cyclin complexes (Morgan, 2007). The cell cycle progresses in one direction only, due to Cdk-cyclins activating the Cdk-cyclin pair required for the next stage in the cycle. Timing of Cdk-cyclin activation depends on cyclin protein levels in the cell, removal of inhibitory phosphorylation on the kinase moiety and changes in levels of Cdk inhibitor proteins (figure 3).

S-phase and M-phase Cdks are held inactive during G1 by the specific degradation of their cyclin partners, suppression of cyclin gene expression, and the presence of specific Cdk inhibitors. G1 Cdks activate the S-phase Cdks and promote their own destruction ensuring directionality of the cell cycle. S-phase cyclins then activate proteins required for DNA replication. Cyclin B levels rise at the end of S-phase, which is required for activation of the M-phase Cdk, Cdk1. Full activation of Cdk1-cyclin B requires the removal of inhibitory phosphorylation on Cdk1 by Cdc25 phosphatase. Active Cdk1-

Cyclin B promotes its own activation, which provides a switch-like entry into mitosis (figure 4, bottom panel). Inhibitory phosphorylation is maintained by Wee1 kinase (Russell and Nurse, 1987), but when Cdk1-cyclin B is activated it inactivates its inhibitor, Wee1, and activates its activator, Cdc25 (Norbury et al., 1991). However, Cdk1-cylin B also activates the APC/C and therefore brings about its own degradation. APC/C activity is responsible for two key activities to allow mitotic exit: firstly, it degrades the protein that holds sister chromatids together so that they can be separated to opposite sides of the cell; secondly, it degrades cyclin B and consequently inactivates Cdk1.

Cdk1-cyclin B is the main regulator of mitotic events, but Cdk2-Cyclin A is also active during mitosis. Cdk2-cyclin A is required for mitosis up until mid-prophase (Furuno et al., 1999). Cdk2-cyclin A increases Cdk1-cylin B activity by activating Cdc25B and by stabilising cyclin B protein levels (Mitra and Enders, 2004, Lukas et al., 1999).

From **The Cell Cycle: Principles of Control** by David O Morgan

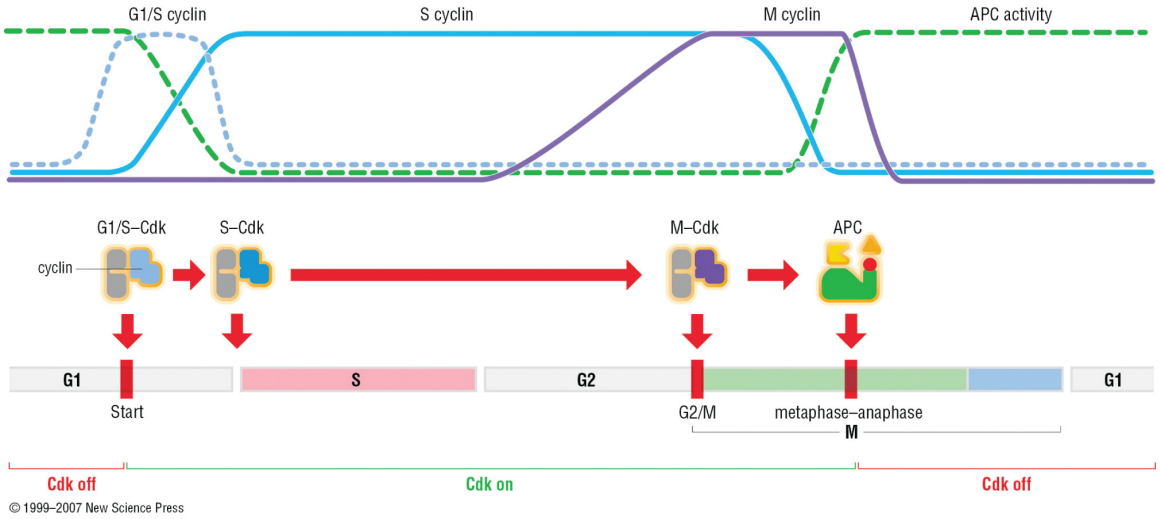

Figure 3 Cell cycle control by Cdk-cyclin complexes
Figure taken from The Cell Cycle: Principles of Control by David O Morgan (New Press Ltd. 2007). Cyclin dependent kinase (Cdk) activity is regulated by binding of cyclin partners, inhibitory phosphorylation and Cdk inhibitors. Cdks are only active as a Cdk-cyclin complex. Cyclin levels are regulated by selective degradation during the cell cycle. Active G1/S Cdk-cyclin complexes commits a cell to enter a new cell cycle at the start checkpoint in late G1. G1/S Cdk-cyclins then activate S phase cyclins, which are required for initiation of DNA replication, and promote their own degradation. The M-phase Cdk-cyclin complex is activated after completion of S phase, which causes entry into mitosis. M phase Cdk-cyclin activates the APC/C (Anaphase Promoting Complex/Cyclosome), which causes anaphase and leads to degradation of M phase cyclin. APC/C activity remains high until late G1 and thus keeps the Cdk activity low.

1.1.2 DNA damage checkpoints

When DNA damage occurs, the cell surveillance mechanisms, checkpoints, are activated. The purpose of checkpoints is to halt cell cycle progression, allowing time for DNA repair to occur, and to activate DNA repair mechanisms. DNA damage checkpoints are crucial in maintaining the integrity of the genome (Jackson and Bartek, 2009). Mutation of checkpoint genes causes DNA lesions to go undetected and therefore promotes the accumulation of mutations. Multiple mutations are required for a cell to become cancerous, thus oncogenesis is promoted if checkpoints are less efficient at recognising or repairing damaged DNA (Hanahan and Weinberg, 2011).

DNA damage checkpoints consist of DNA damage sensor and mediator proteins that recognise DNA lesions and activate the signal transducer proteins, and effector proteins that halt the cell cycle (figure 4). DNA damage checkpoints at different stages of the cell cycle have different effector proteins, but the same sensor, mediator and transducer proteins are used throughout the cell cycle. ATM (ataxia telangiectasia mutated) and ATR (ATM and Rad3 related) are two important DNA damage activated kinases. It is important to know that ATM and ATR do not carry out their function in isolation: there are many different mediator proteins that help to amplify the signal and aid recognition of damaged DNA, reviewed in (Sancar et al., 2004), (Zhou and Elledge, 2000) and (Stucki and Jackson, 2006).

ATM and ATR are both members of the phosphoinositide 3-kinase-like family and they phosphorylate a range of protein substrates. ATM is the main sensor of γ-irradiation induced DNA damage, which primarily causes double strand breaks whereupon ATM phosphorylates and activates the checkpoint kinase Chk2. ATR is the primary sensor of UV induced DNA damage in the cell, and signals via Chk1. However, the pathways do overlap: ATR can activate ATM in response to UV (Stiff et al., 2006) and ATM can activate ATR by mediating DNA double strand break resection to expose single strand DNA (Jazayeri et al., 2006).

At the G1/S phase transition, DNA damage causes inactivation of Cdk2-Cyclin E/A and thus prevents replication initiation. A long-term response is mediated via p53, which results in the prevention of S-phase gene transcription (Sancar et al., 2004). When DNA damage is encountered during S phase, the intra-S phase checkpoint is activated and the cell cycle is arrested in S phase by the inhibition Cdk-Cyclins required for replication origin firing. Thus late origin firing is prevented and replication cannot be completed until the damage has been repaired. During replication the ATR-Chk1-Cdc25 checkpoint pathway is active, which targets Cdc25 phosphatase for degradation. Cdc25 phosphatase is required for removal of the inhibitory phosphorylation from Cdk1 and therefore its degradation inhibits Cdk1 activation and the onset of mitosis.

The G2/M checkpoint prevents entry into mitosis in the presence of DNA damage (figure 4). DNA damage is recognised by ATM or ATR, which phosphorylate and activate Chk2 and Chk1 respectively. Chk1 and Chk2 inhibit Cdc25A phosphatase and activate Wee1 kinase. Upon phosphorylation by Chk1 or Chk2, Cdc25A binds to 14-3-3 proteins, which causes Cdc25A to be sequestered in the cytoplasm and degraded via ubiquitin-mediated proteasome degradation. Wee1 is phosphorylated by Chk1, which activates its kinase activity and results in the maintenance of inhibitory Cdk1 phosphorylation (O'Connell et al., 1997). Thus, in the presence of DNA damage Cdk1 is held inactive by inhibition of its activator, Cdc25, and activation of its inhibitor, Wee1, which prevents entry into mitosis.

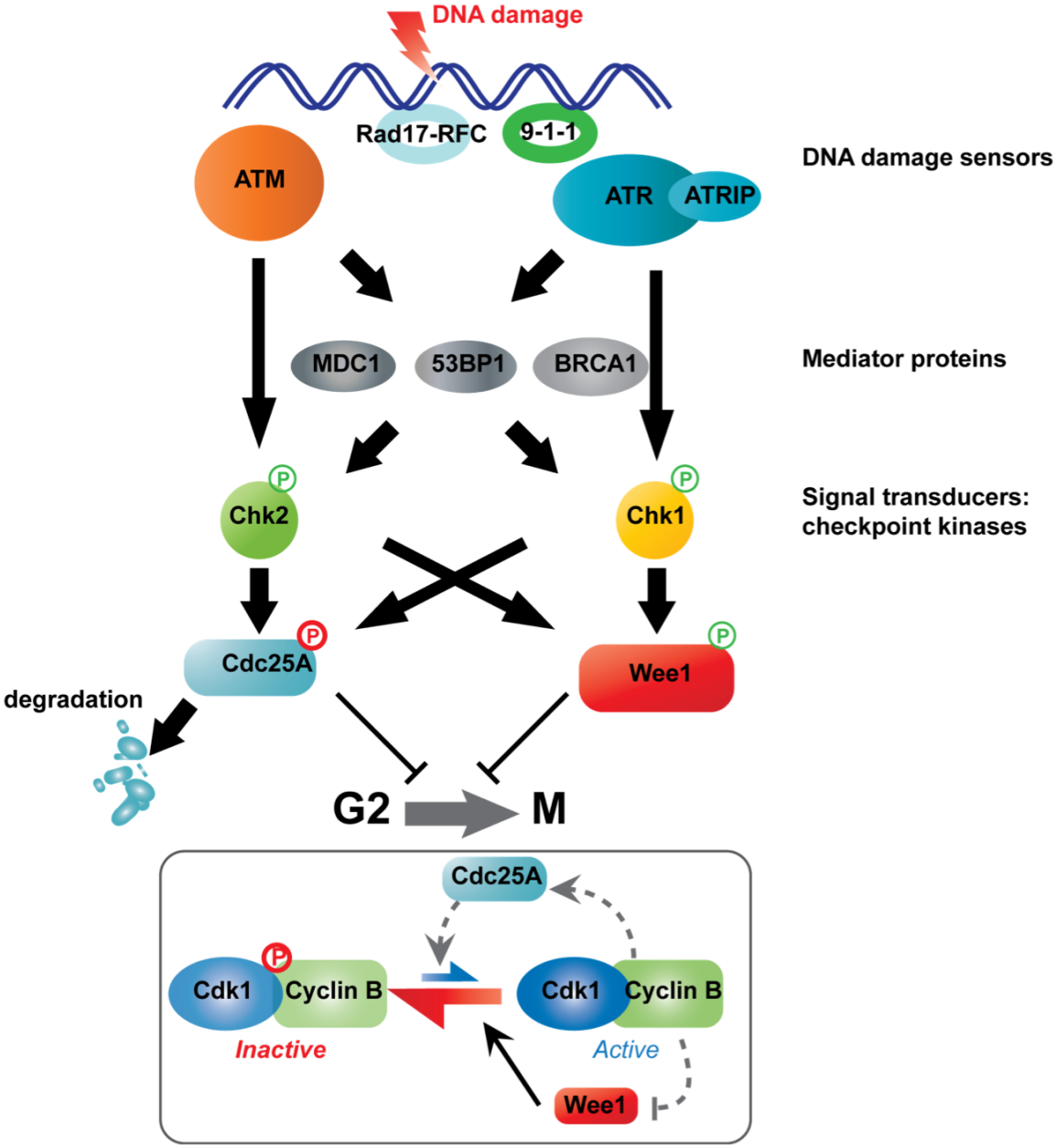

Figure 4 The G2/M DNA damage checkpoint inhibits activation of Cdk1

This figure is adapted from Sancar et al. (Sancar et al., 2004). DNA damage in G2 activates DNA damage sensor kinases ATM and ATR, which phosphorylate and activate Chk2 and Chk1 kinases respectively. Rad17-RFC (replication factor C) and the heterotrimeric 9-1-1 complex, which consists of Rad9-Rad1-Hus1, are also recruited to sites of DNA damage where they promote checkpoint activation. The checkpoint kinases Chk1 and Chk2 phosphorylate and activate Wee1 kinase and inactivate Cdc25A phosphatase, leading to prevention of mitotic entry. Checkpoint signalling is amplified by mediator of DNA damage checkpoint 1 (MDC1), p53 binding protein 1 (53BP1), and breast cancer type 1 susceptibility protein (BRCA1). The grey box indicates the roles of Cdc25A and Wee1 in the activation and inhibition of Cdk1, respectively. Green 'P' indicates activatory phosphorylation. Red 'P' indicates inhibitory phosphorylation

DNA repair pathways

The purpose of cell cycle stalling in response to DNA damage is to allow time for repair of DNA lesions. Many different proteins are involved in DNA repair and exactly which proteins are involved depends on the type of DNA lesion. In response to abasic sites, base excision repair (BER) proteins carry out the process of removing the abasic site using an endonuclease to cut the sugar-phosphate DNA backbone, polymerase to fill in the gap, and ligase to join the resulting nicked DNA stand, reviewed in Sancar *et al.* (Sancar et al., 2004). Nucleotide excision repair (NER) is required for moving bulky DNA lesions; first dual incisions are made surrounding the lesion by a nuclease then the resulting single strand DNA fragment (ranging from 24 to 32 nucleotides in mammals) is removed. The gap is filled by DNA synthesis and the single strand nicks are then ligated (Sancar et al., 2004).

The repair of DNA double strand breaks (DSBs) can occur by two different pathways: non-homologous end joining (NHEJ) or homologous recombination (HR) (Sancar et al., 2004). NHEJ is an error-prone pathway that results in loss of genetic information since the DNA ends at the break are cut back then ligated together. First of all, Ku70, Ku80, and DNAPKcs recognise DNA DSB ends and the Mre11/Rad50/Nbs1 complex (MRN) carries out resection of the DNA ends. The two double strand DNA ends are then ligated by the Ligase4/XRCC4 heterodimer.

HR provides a mechanism for conserving genetic information providing that there is a homologous chromosome from which to copy. For HR to occur, the double strand DNA ends must first be resected to produce single strand 3’ overhangs, which then form base pair interactions with the complementary strand in the homologous chromosome in a process called strand invasion. This process results in a DNA structure containing two 4-way junctions (Holliday junctions). The MRN complex carries out resection of DNA ends and the resulting 3’ overhang single strand DNA is coated by Rad51 polymer, which is required for strand invasion into the homologous duplex DNA. Double Holliday junctions are structures in which the to DNA double helices are topologically

linked and they can be resolved by GEN1, which cleaves the two Holliday junctions, resulting in either cross-over or non-crossover products. Double Holliday junction dissolution can occur by the action of BLM helicase (Bloom syndrome helicase) along with its interacting partners TopoIIIα, RMI1, and RMI2, which exclusively results in non-crossover products, reviewed by Mimmitou *et al.* (Mimitou and Symington, 2009). BRCA1 and BRCA2 are also important for HR repair (Boulton, 2006). Since NHEJ is error-prone, homologous recombination is the predominant pathway used by cells in S-phase or G2, when a homologous chromosome is present.

1.1.3 The Spindle Assembly Checkpoint

In order to ensure equal segregation, replicated "sister" chromatids are attached to opposite poles of the mitotic spindle and progression to anaphase is prevented until all pairs of sister chromatids are properly attached to spindle microtubules. Important factors for the equal segregation of sister chromatids are the cohesion between sister chromatids and the attachment of spindle microtubules from opposite spindle poles to sister chromatids via the kinetochore, which is a large multi-layered protein complex that forms at centromeres (Cheeseman and Desai, 2008). Surveillance of kinetochore to spindle microtubule interaction is carried out by the spindle assembly checkpoint (SAC). The SAC holds cells at metaphase by inhibition of the APC/C. When the SAC is satisfied, the APC/C becomes active and causes degradation of cyclin B and cleavage of cohesin, the protein responsible for sister chromatid cohesion (figure 5).

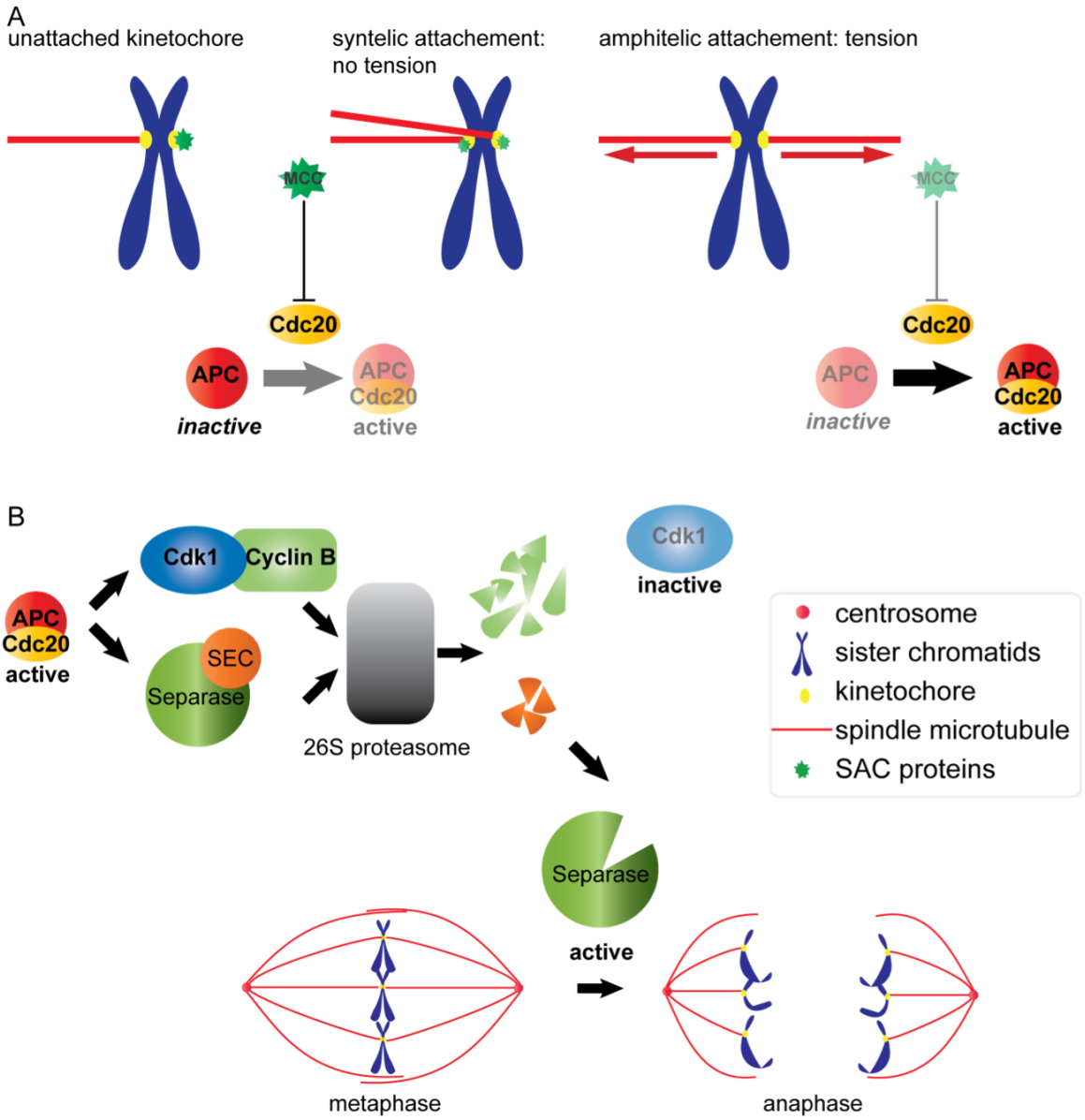

Figure 5 The spindle assembly checkpoint (SAC)
(A) The SAC is activated when sister chromatids are not attached to the mitotic spindle in a bipolar fashion. Spindle checkpoint proteins are recruited to unattached kinetochores, which leads to the formation of a soluble mitotic checkpoint complex (MCC), which binds and inactivates Cdc20 and thus inhibits APC/C activity (left). Kinetochores that are occupied, but not under tension, also result in formation of the MCC to inhibit APC/C (middle). When sister chromatids are bound by microtubules from opposite spindle poles, the kinetochores occupied and under tension and the SAC is satisfied (right). (B) When the SAC is satisfied the E3 ubiquitin ligase APC/C-Cdc20 becomes active and targets its mitotic substrates for degradation by the 26S proteasome. Substrates include Cyclin B, required for the activity of the mitotic Cdk (Cdk1), and securin (SEC), which holds the enzyme separase inactive. Activated separase cleaves cohesin, a protein responsible for sister chromatid cohesion.

SAC Activation

The spindle assembly checkpoint monitors the binding of spindle microtubules to kinetochores in two ways: detection of unattached kinetochores and kinetochores that are not under tension (Musacchio and Salmon, 2007). If all sister chromatids are attached to microtubules from opposite spindle poles, all kinetochores are occupied and under tension from the force of spindle microtubules moving towards spindle poles, and the SAC is satisfied. Detection of kinetochores that are not under tension is important in the case of syntelic attachment of chromosomes to the spindle, where both sister chromatids are attached to the same spindle pole.

Activation of the SAC prevents anaphase and allows time for all kinetochores to become attached to microtubules. Therefore the SAC is active during every prometaphase/metaphase. Furthermore, the SAC promotes destabilisation of kinetochore-microtubule attachments that do not generate tension, allowing the formation of correct, bipolar attachment.

Evidence that the inhibitory signal that prevents anaphase onset is generated by unattached kinetochores comes from work following anaphase onset after laser ablation of unattached kinetochores (Rieder et al., 1995). Importantly, the presence of one unattached kinetochore is sufficient to activate the SAC and arrest cells in metaphase. Furthermore, when the unattached kinetochore on the last mono-oriented chromosome in a cell is destroyed, anaphase onset occurs in the presence of the mono-oriented chromosome. These experiments show that SAC inhibition is dependent on the presence of unattached kinetochores. Also, the presence of one mono-oriented chromosome, i.e. lack of tension across one kinetochore, was not sufficient to maintain SAC activity. However, a study of micromanipulation of chromatids in spermatocytes shows that tension across kinetochores is important for inactivation of the SAC (Li and Nicklas, 1995). Furthermore, the SAC is activated in HeLa cells that have all chromosomes bi-oriented and all kinetochores occupied, but lack of tension in spindle microtubules (Skoufias et al., 2001).

SAC components

There are many components required for the precise regulation of the SAC, but here I will describe only the key players. SAC components are comprehensively reviewed in Musacchio *et al*. (Musacchio and Salmon, 2007).

In response to unattached kinetochores, spindle checkpoint proteins Mad1 and Mad2 are recruited to the outer kinetochore. These proteins remain at the kinetochore and catalyse the conformational change of a highly dynamic pool of Mad2. This model for the conformational change and consequent activation of Mad2 is called the Mad2 template model, which provides an explanation of how the signal can be amplified from the kinetochore such that only one unattached kinetochore is sufficient for preventing anaphase onset (Musacchio and Salmon, 2007). Inhibition of the APC/C is carried out by the mitotic checkpoint complex (MCC), which consists of the spindle checkpoint proteins Mad2, Bub3 and BubRI, and the co-activator of APC/C, Cdc20. The MCC renders the APC/C inactive by preventing interaction with its cofactor Cdc20, which is required for the mitotic activity of APC/C. The precise mechanism of MCC inhibition of the APC/C is unclear: either the MCC binds and sequesters Cdc20 or the MCC acts as a pseudo-substrate for the APC/C and acts as a competitive inhibitor (Musacchio and Salmon, 2007).

SAC kinases MPS1, Bub1, BubR1, Plk1, NEK2, MAPK and Aurora B are also important for SAC signalling. Aurora B is important for sensing kinetochore tension. It is responsible for destabilising kinetochore-microtubule interactions that do not generate tension, which promotes new binding events and therefore promotes chromosome bi-orientation (Musacchio and Salmon, 2007). The current model proposes that stretching of the kinetochore moves Aurora B substrates in the outer kinetochore out of reach of Aurora B kinase, which is tethered to the centromere (the region of chromatin upon which the kinetochore forms). Thus, lack of tension results in the close proximity of Aurora B and its substrates, but upon the formation of intra-kinetochore tension, its substrates are moved out of reach of the kinase and the SAC is satisfied

(Maresca and Salmon, 2009, Uchida et al., 2009). Aurora B kinase activity either activates the SAC directly or Aurora B-dependent destabilisation of the kinetochore-microtubule interaction causes activation of the SAC via the resulting unattached kinetochore (Maresca and Salmon, 2010).

Interestingly, the checkpoint kinase, Chk1, is also required for SAC function (Zachos et al., 2009). Chk1 deficient DT40 chicken lymphoblast cells are not able to maintain mitotic arrest when incubated in the microtubule-stabilising drug, taxol, due to their inability to recruit BubR1 to kinetochores. However, both BubRI recruitment and mitotic arrest were efficient when cells were treated with the microtubule depolymerising drug, nocodazole, which indicates the importance of Chk1 in the detection of kinetochores that are not under tension. Interestingly, Chk1 kinase activity is required for its function in the SAC and BubR1 is a target of Chk1 kinase.

1.1.4 The mitotic spindle

Microtubules

Mitotic spindles are made up from three main groups of microtubules: k-fibres, interpolar microtubules, and astral microtubules, all of which have the minus ends held at the spindle pole (figure 6). In higher eukaryotes, each kinetochore binds to multiple spindle microtubules, which together form k-fibres. K-fibres are responsible for moving and aligning mitotic chromosomes. Interpolar microtubules overlap with microtubules from the opposite spindle pole and are required for pushing the poles apart. Astral microtubules migrate in all directions from the centrosomes to the cell cortex and are involved in spindle positioning within the cell.

Microtubules are large polymers of α- and β-tublin heterodimers. GTP-bound subunits are incorporated into the plus (+) end of microtubules. GTP hydrolysis is stimulated by microtubule binding, so the majority of a microtubule consists of GDP-bound tubulin monomers. The plus end is the most dynamic end of the microtubule: addition of GTP-

tubulin to the plus end results in microtubule growth. However, if the rate of GTP hydrolysis is faster than new tubulin subunit addition, the microtubule shrinks. Microtubules *in vitro* and *in vivo* change rapidly and unpredictably between growth and shrinkage. This property of microtubules is called dynamic instability, which is regulated by many proteins during mitotic spindle assembly in the cell (Kline-Smith and Walczak, 2004).

Spindle Assembly

Although mitotic spindles are formed in a centrosome dependent manner in most cell types, spindle assembly can occur in the absence of centrosomes. A series of studies using *Xenopus laevis* mitotic egg extracts showed that bipolar spindles form around DNA coated beads by the nucleation of microtubules around the DNA (Heald et al., 1996). In this system, centrosomes are not present, yet spindle poles are able to form due the activity of a minus end-directed microtubule motor protein, dynein (Heald et al., 1997). Importantly, dynein inhibition inhibits pole formation, but does not affect the bipolar array of microtubules around chromatin, which indicates that it is the polarity of the microtubules themselves and activity of other microtubule motor proteins that are responsible for bipolarity. During acentrosomal spindle assembly, microtubules nucleate around chromatin due to the presence the GTP-bound form of a small GTPase, Ran (Carazo-Salas et al., 1999). In fact, addition of constitutively active Ran-GTP, which is unable to hydrolyse GTP, causes microtubule nucleation in *Xenopus* mitotic egg extracts, whereas mutant Ran with low affinity for GTP or GDP cannot. The high local concentration of Ran-GTP at chromatin is due to the chromatin localisation of its GEF (guanine nucleotide exchange factor), RCC1.

The most striking evidence for the lack of requirement for centrosomes in mitotic spindle assembly and cell division is the fact that DSas-4 null flies, which lack centrioles, and therefore centrosomes, grow to adulthood as long as there is a maternal complement of DSas-4 (and centrosomes) for the initial embryonic divisions (Basto et al., 2006). In these flies spindle assembly occurs normally, although at a slower rate.

About 30% of asymmetric cell divisions, important in brain development, are abnormal (see section 1.2.4). Centrosomes are, however, essential for embryonic cell divisions, as shown in *Xenopus laevis* (Klotz et al., 1990).

Although centrosomes are not required for mitotic spindle assembly, they are dominant over chromatin-dependent microtubule nucleation such that presence of a single centrosome causes the formation of a monopolar spindle (Heald et al., 1997). Indeed, centrosomes provide a nucleation site for microtubules, which increases efficiency of nucleation: purified centrosomes incubated with purified tubulin can nucleate microtubules at much lower tubulin concentrations than spontaneous microtubule formation (Mitchison and Kirschner, 1984). Microtubules nucleated by centrosomes form a radial array, which is called an aster, consequently, microtubules that radiate from the centrosome to the cell cortex are called astral microtubules (figure 6). Microtubule nucleation by the centrosome is described further in 1.2.2. Nucleation of microtubules in the vicinity of chromatin, where Ran-GTP levels are high, also contributes to spindle assembly in centrosome-containing cells (Tulu et al., 2006). Chromatin microtubule nucleation is dependent on the Ran-dependent spindle assembly factor TPX2 (Tulu et al., 2006). Preformed k-fibres are incorporated into the spindle by recruitment of their minus ends to centrosomes by the action of minus end directed motor proteins, such as dynein (Khodjakov et al., 2003, Tulu et al., 2006).

There are four main groups of motor proteins that are important for spindle assembly and spindle pole focussing: Kinesin-5, Dynein, Chromokinesins, and Kinesin-14 (figure 6) (Kline-Smith and Walczak, 2004). Kinesin-5 is a bipolar motor protein, which is plus end directed and is important for microtubule cross-linking required for spindle pole separation. Dynein has a motor domain at one end of the molecule, which is minus end directed; the other end of the molecule can bind microtubules or other proteins. Dynein is important for microtubule minus end clustering at spindle poles and attachment of astral microtubules to the cell cortex. Chromokinesins, kinesin-4 and -10, contain a plus end directed motor domain and a DNA binding domain. These proteins bind mitotic chromosomes and promote their attachment to the plus ends of microtubules. Kinesin-

14 contains a motor domain at one end of the molecule, which is minus end directed; the other end of the molecule can bind microtubules. Kinesin-14 is important for microtubule cross-linking and minus end clustering at spindle poles (Tanenbaum and Medema, 2010, Gatlin and Bloom, 2010).

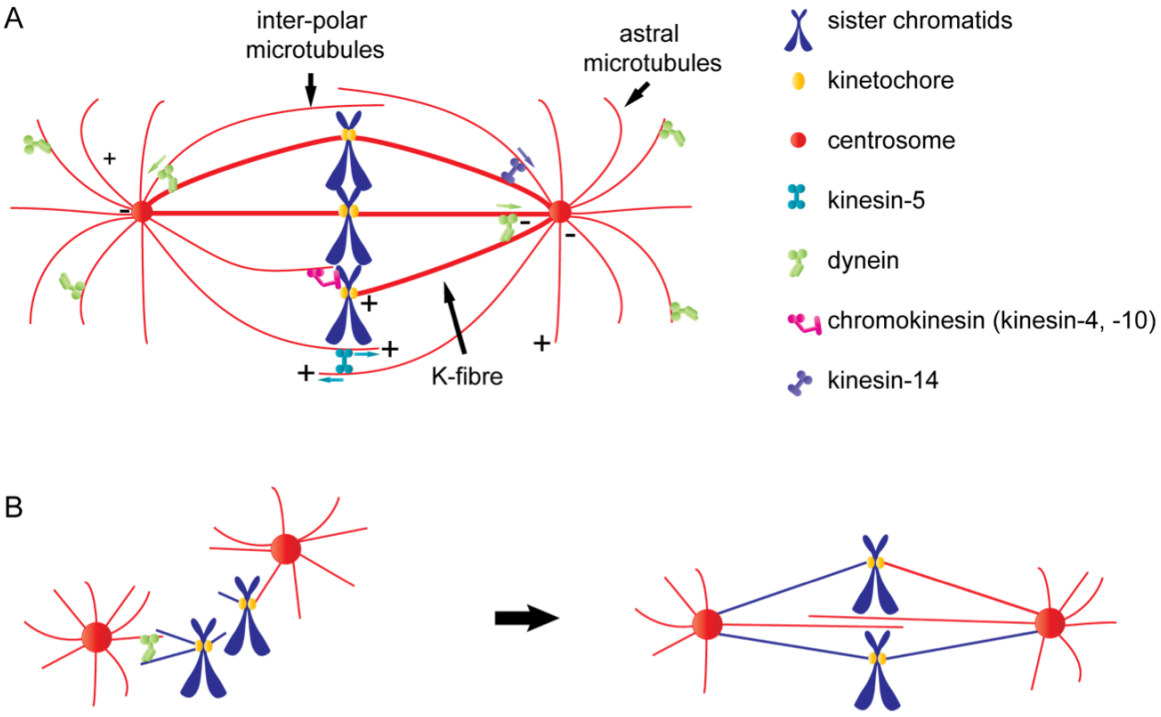

Figure 6 Spindle assembly: the role of motor-proteins
(A) Adapted from Kline-Smith *et al.* (Kline-Smith and Walczak, 2004) and Morgan, 2007. The spindle is composed of three types of microtubule. Microtubule minus ends (-) are anchored at spindle poles, to centrosomes. K-fibres (kinetochore fibres) consist of multiple microtubules that connect the centrosome to the kinetochore ; interpolar microtubules come from opposite poles and overlap; and astral microtubules attach the centrosome to the cell cortex. Motor proteins are required for organisation for microtubules into a biopolar array around chromosomes: kinesin-5 associates with inter-polar microtubules and causes them to move apart, kinesins-4 and 10 connect microtubules to chromatin. Dynein and kinesin-14 are involved in spindle pole clustering. Dynein also plays an important role in attaching astral microtubules to the cell cortex via binding to proteins located at the cortex. (B) Adapted from Tulu *et al.* (Tulu et al., 2006). The contribution of chromatin-nucleated microtubules (blue) to spindle assembly in the presence of centrosomes.

1.2 The centrosome

Centrosomes consist of a pair of centrioles surrounded by pericentriolar material (PCM). Centrosomes are the primary microtubule organising centre (MTOC) in somatic cells: in dividing and post-mitotic cells. However, microtubule nucleation can occur at non-centrosomal sites and centrosome nucleated microtubules can also be released and maintained elsewhere in differentiated cells (Keating and Borisy, 1999, Abal et al., 2002). The centrosome has many different functions in different cell types, such as cell motility, adhesion, cell polarity, and spatial organisation as well as organisation of mitotic spindle poles (Nigg and Raff, 2009). Furthermore, centrosomes have non-microtubule associated functions in cell cycle regulation (1.2.2.2). In addition to their role in the formation of centrosomes, centrioles can also form cilia, which have functions in cell signalling in dividing cells, and sensory signalling and movement in differentiated cells. Here I will introduce centrioles with respect to their role as part of the centrosome.

1.2.1 Centrosome structure

Centrioles are cylindrical arrays of triplet microtubules with 9-fold symmetry (figure 7) (Paintrand et al., 1992). Centrioles are not symmetrical along their length. Serial sectioning electron microscopy studies show that there are 9 sets of triplet microtubules (A to C, figure 7) at the proximal end of the centriole, but 9 sets of doublet microtubules at the distal end. Nine-fold symmetry is established at the beginning of centriole biogenesis by the organisation of the centriolar Sas-6 protein, which is recruited early in centriole biogenesis and oligomerises to forms a cartwheel shaped structure with 9-fold symmetry (Kitagawa et al., 2011). Centrioles within a centrosome are linked by a long bundle of thin filaments, which are visible by electron microscopy (EM) (Paintrand et al., 1992). This structural link is maintained during centriole duplication in interphase and is abolished upon entry into mitosis (1.2.3). The centrioles within a centrosome are not equal: their structure is determined by their age. The mother centriole has two sets of 9 appendages: distal and sub-distal (figure 7a and b), which are involved in

anchoring microtubules and docking of centrioles at the plasma membrane for ciliogenesis (Bettencourt-Dias and Glover, 2007).

In a G1 cell, there is one centrosome, which contains two disengaged centrioles, a mother and a daughter. Formation of new centrioles occurs at the proximal end of existing centrioles. New centrioles are formed perpendicular to the existing parent centriole and are tightly linked (engaged). During mitosis, the mother centriole acquires appendages and daughter centrioles acquire the ability to organise PCM and act as an MTOC, although they cannot act as an MTOC until they are disengaged from their mother centriole. The steps of centriole duplication and the regulation of centriole duplication are discussed further in 1.2.3 (reviewed in (Nigg, 2007)). Importantly, centrioles are required for PCM organisation and centrosome duplication. Upon disruption of centriole structure, centriole and centrosome (PCM) markers disappear (Bobinnec et al., 1998).

PCM is responsible for the nucleation of microtubules: it is composed of a matrix of proteins that allows recruitment of γ-tubulin, which exists as part of the γ-tubulin ring complex (γ-TuRC), required for microtubule nucleation (Bettencourt-Dias and Glover, 2007) (1.2.2). Two predominant members of the PCM are coiled coil domain containing proteins AKAP450 and pericentrin, which form a lattice that allows docking of components required for microtubule nucleation. AKAP450 and pericentrin are recruited to the centrosome themselves via a non-coiled coil region of around 90 amino acids that is conserved between the two (Gillingham and Munro, 2000). Fusion of this domain to other proteins causes their localisation to the PCM. PCM surrounds the mother centriole in interphase and mitotic cells. Furthermore, it has been shown that only centrioles that have acquired mitosis-specific modifications can organise the PCM (Wang et al., 2011) (1.2.3).

There is a distinct compartment of the PCM, the PCM tube, which is closely associated with the centriole, possibly due to association of microtubule binding proteins that bind the polyglutamylated tubulin of the centriole walls as well as tubulin minus end binding

proteins that bind the proximal end of the centriole (Bornens, 2002). The PCM tube is visible by immunofluorescence with autoimmune serum that recognises multiple different PCM components (Ou and Rattner, 2000). Correlative electron microscopy and immunofluorescence of the same cell shows that the PCM tube surrounds the centriole wall (Ou et al., 2003). PCM components pericentrin, ninein and γ-tubulin localise to different regions within the PCM tube (Ou et al., 2003) (figure 8).

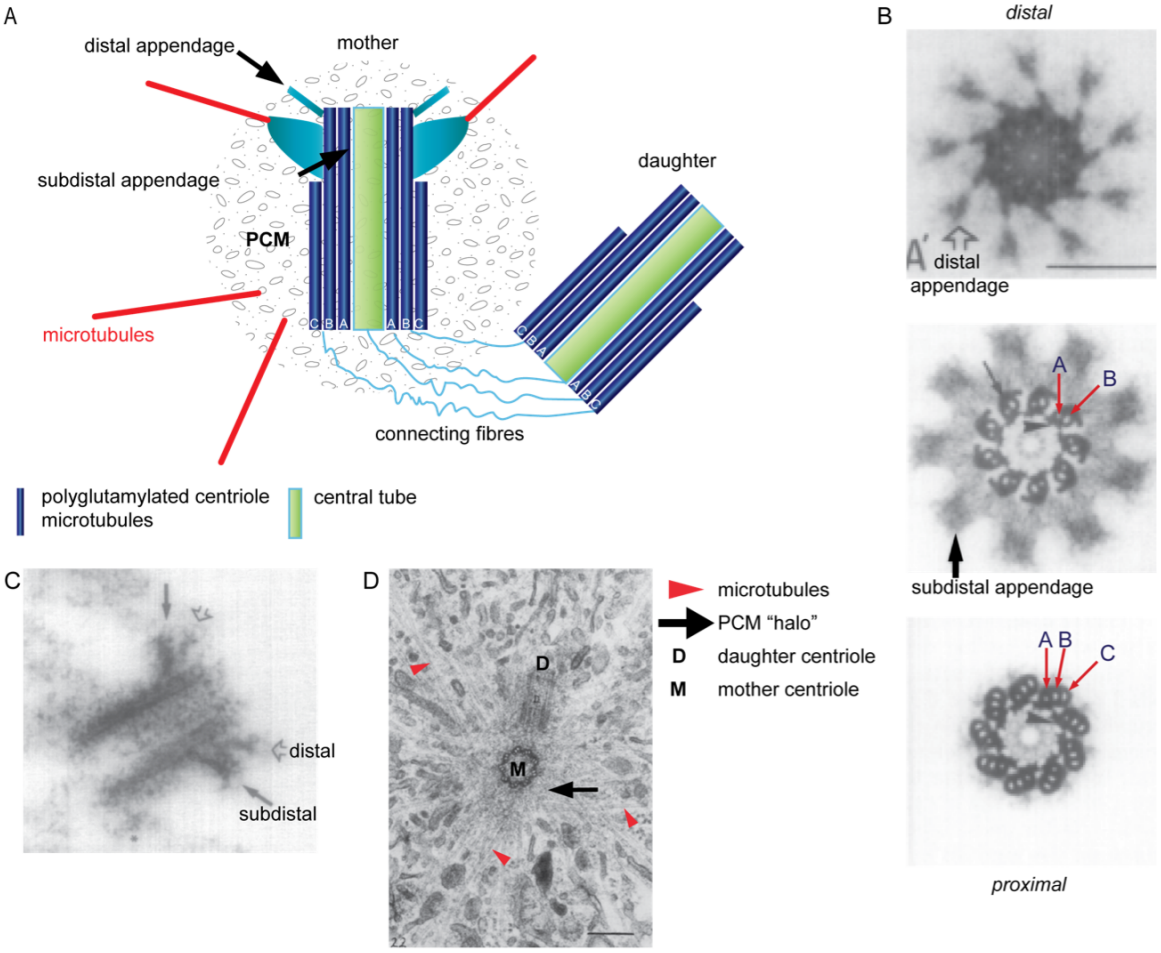

Figure 7 Centrosome structure
(A) Adapted from Sluder (Sluder, 2005). A G1 centrosome: mother and daughter centrioles are disengaged, but still linked together by fibres. Diagrammatic representation of longitudinal sections: triplet microtubules are represented in blue and the central tube in green. The mother centriole has distal and subdistal appendages and is surrounded by pericentriolar material (PCM), which contains the necessary components for nucleation of microtubules (red). (B) Three averaged EM sections from a mother centriole taken from Paintrand *et al.* (Paintrand et al., 1992). Scale bars are 0.2 µm. The 9 triplet microtubules can be seen at the proximal end (tubules labelled A, B, and C, red arrows) and 9 doublet microtubules (A, B, red arrows) are seen in a more distal section. Distal appendages are marked with an open arrow (top panel). Subdistal appendages are indicated by a short arrow (middle panel). (C) Electron micrograph of the longitudinal section through a mother centriole taken from (Paintrand et al., 1992). The distal (open arrows) and subdistal appendages (black arrows) can be seen. (D) Electron micrograph of an *in situ* prophase centrosome taken from (Vorobjev and Chentsov Yu, 1982). The mother centriole (M) is seen in cross section and the daughter (D) in longitudinal section. The electron dense PCM can be seen surrounding the mother centriole (black arrow) and microtubules (red arrowheads) can be seen emanating from the PCM.

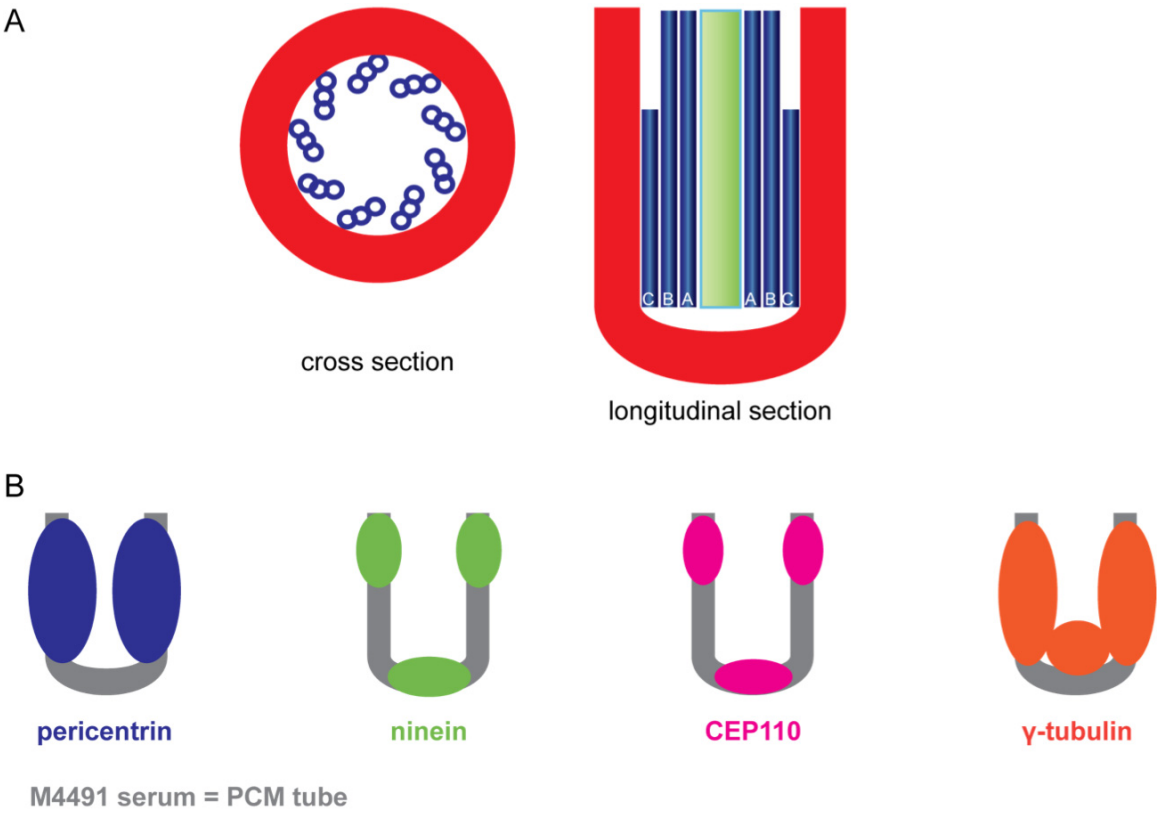

Figure 8 The PCM tube
(A) Diagram adapted from Ou *et al*. (Ou et al., 2003). The PCM tube (red) surrounds centriole walls and proximal ends. A cross section and longitudinal representation of the PCM tube with respect to centriole triplet microtubules (blue) are shown. (B) Diagram showing the localisation of PCM proteins pericentrin (blue), ninein (green), CEP110 (pink), and γ-tubulin (orange) relative to the PCM tube, as visualised by immunofluorescence by Ou *et al*. (Ou and Rattner, 2000, Ou et al., 2003). All four of these proteins localise to different regions of the PCM tube and γ-tubulin can also be observed in the lumen of the PCM tube as it is a component of the centriole at the proximal end where it caps centriole microtubule minus ends.

1.2.2 Centrosome-dependent microtubule organisation

The microtubule nucleation capacity of the centrosome changes with progression through the cell cycle. At the G2/M transition many proteins required for microtubule nucleation are recruited to the centrosome, including γ-tubulin containing complexes, so the PCM becomes larger and the microtubule nucleating capacity of the centrosome increases dramatically (Wiese and Zheng, 2006). This process is called centrosome maturation. Centrosome maturation is dependent on the polo-like kinase, Plk1 (Lane and Nigg, 1996). Plk1 modifies centrioles during mitosis, such that both mother and daughter centrioles in the subsequent G1 phase are able to recruit PCM components and act as MTOCs (Wang et al., 2011). Without this mitotic Plk1-dependent modification, daughter centrioles inherited by the resulting G1 cells are unable to recruit γ-tubulin or act as MTOCs whether the daughter centrioles are engaged or disengaged from the mother centriole. This mitosis-dependent modification means that duplicated centrioles contain only one centriole (the mother) that is MTOC competent. Plk1 is also required for the recruitment of γ-tubulin complexes to the PCM of MTOC-competent centrioles (Haren et al., 2009b).

Microtubule nucleation at the centrosome occurs via the γ-tubulin containing γ-tubulin ring complex (γ-TuRC) and via γ-TuRC independent pathways (Wiese and Zheng, 2006) (figure 9).

γ-TuRC dependent microtubule nucleation

The γ-TuRC consists of γ-tubulin and cap subunits GCP2-6 and GCP-WD (also called NEDD1) (Raynaud-Messina and Merdes, 2007). The γ-TuRC forms a template for tubulin α/β dimer binding and therefore provides a kinetic advantage for the nucleation of microtubules. Although a γ-tubulin protofilament model was first put forward as the mechanism for nucleation of microtubules by γ-tubulin (Erickson et al., 1996), more recent evidence from analysis of γ-TuRC immuno-staining by EM favours the γ-TuRC template model where γ-TuRC forms a template that caps the minus ends of

microtubules (Keating and Borisy, 2000). Plk1 activity is required for γ-TuRC recruitment to centrosomes, and so CDK11p58 kinase also plays an important role by facilitating recruitment of Plk1 and Aurora A to centrosomes in mitosis (Petretti et al., 2006). GCP-WD is essential for the recruitment of the γ-TuRC to centrosomes and it's recruitment is dependent on Plk1, which phosphorylates GCP-WD in mitosis (Luders et al., 2006). Plk1-dependent recruitment of GCP-WD to the centrosome may be direct, in part, but it is also mediated via recruitment of centrosome proteins Cep192, CDK5RAP2/Cep215, Kizuna and pericentrin (Haren et al., 2009b){Oshimori, 2006 #505}. Indeed, pericentrin is also required for γ-TuRC subunits GCP2 and GCP3 (Zimmerman et al., 2004).

Constitutive centrosomal proteins PCM-1 and Nudel are important for the centrosomal localisation of pericentrin, and consequently they are important for γ-TuRC as well (Dammermann and Merdes, 2002, Guo et al., 2006). Pericentrin recruits the γ-TuRC to the centrosome via dynein-dependent transport along microtubules, mediated by pericentrin-dynein interaction (Young et al., 2000). Thus, inactivation of dynein or its adaptor protein, dynactin, results in reduced levels of pericentrin and γ-tubulin at the centrosome and spindle disruption. Although microtubule depolymerisation has been shown to decrease pericentrin and γ-tubulin levels at mitotic centrosomes (Young et al., 2000), there is also evidence that γ-tubulin is recruited to the same extent in the presence and absence of microtubules (Khodjakov and Rieder, 1999). Therefore, parallel pathways exist for the recruitment of pericentrin and γ-TuRC to the centrosome in mitosis, as discussed by Young *et al.* (Young et al., 2000).

In addition to pericentrin, the PCM protein AKAP450 is also required for efficient localisation of γ-tubulin to the centrosome and microtubule nucleation from the centrosome via centrosome proteins Cep72 and Kizuna (Oshimori et al., 2009).

Microtubule organisation independent of γ-tubulin complexes

In addition to the proteins described above, there are proteins required for proper mitotic spindle assembly that function independently of γ-tubulin. In fact, depletion of γ-tubulin doesn't completely inhibit microtubule nucleation (Wiese and Zheng, 2006). Transforming acid coiled coil proteins (TACCs) and tumor overexpressed genes (TOGs) promote microtubule aster formation at the centrosome independently of γ-tubulin recruitment (Wiese and Zheng, 2006).

Proteins that function to stabilise microtubules and anchor the minus ends of microtubules at the centrosome include NuMA, AKAP450, CDK5RAP2, CAP350, FOP, EB1, and Cep135. Firstly, NuMA (Nuclear Mitotic Apparatus) is a nuclear protein during interphase, but localises to spindle poles during mitosis (Haren et al., 2009a). Experiments in which the mitotic localisation of NuMA is disrupted, but the interphase functions remain unaffected, show that NuMA is essential for anchoring the spindle pole to the centrosome and focussing spindle poles, but not for initial microtubule nucleation (Silk et al., 2009). NuMA functions by recruiting dynein-dynactin to spindle poles (Merdes et al., 2000). Furthermore, cohesin, which is required for linking replicated sister chromatids, also has a distinct function in spindle assembly, which is mediated by interaction with NuMA (Kong et al., 2009). NuMA also interacts with poly (ADPribose) (pADPr), which localises to centrosome asters and Ran-induced asters in *Xenopus laevis* egg extracts where it is required for proper spindle assembly (Chang et al., 2009). Interestingly, translocations between NuMA and the retinoic acid receptor alpha (RARα) genes are found in a small percentage of acute promyelocytic leukaemia (APL), where aberrant functions of RARα and aberrant functions of NuMA may play a role in the disease (Piazza et al., 2001). Translocations between RARα and nucleophosmin (NPM, described in section 1.3.2) are also found in certain cases of APL.

CDK5RAP2 interacts with AKAP450 and targets it to the centrosome and AKAP450, in turn, interacts with the dynactin subunit p150glued (Barr et al., 2010). AKAP450 also

interacts with the small GTPase, Ran, which is required for nucleation of microtubules around chromatin (section 1.1.6) (Keryer et al., 2003). When the AKAP450-Ran interaction is disrupted γ-tubulin still localises to the centrosome, yet asters do not form efficiently in microtubule re-growth assays indicating that γ-tubulin independent pathways are important for microtubule nucleation from centrosomes (Keryer et al., 2003).

The centrosomal protein complex consisting of CAP350, FOP, and EB1 is also required for maintenance and stabilisation of microtubule minus ends at the centrosome via the interaction between EB1 and dynactin p150glued (Yan et al., 2006). Another constitutive centrosome protein, Cep135, contributes to the recruitment of the dynactin complex to centrosomes, via interaction with the p50 subunit, dynamitin (Ohta et al., 2002, Uetake et al., 2004).

In addition to the proteins described above with characterised functions, there are other proteins that have been shown to be involved in microtubule organisation, but their molecular functions have yet to be characterised. *Drosophila melanogaster* abnormal spindle protein Asp is required for spindle pole focussing and organisation of spindle structure (Wakefield et al., 2001). Asp has a human homologue, ASPM, which also localises to spindle poles, but its function has not yet been specified. Additionally, cAMP dependent protein kinase (PKA) might be involved in spindle assembly as it binds and localises to the centrosome with pericentrin (Diviani et al., 2000).

Aurora A in microtubule organisation

Aurora A kinase is a key player in centrosome maturation and spindle assembly (Brittle and Ohkura, 2005). It is important for the chromatin-dependent microtubule nucleation pathway via TPX2; the accumulation of PCM proteins required for microtubule nucleation in mitosis; and centrosome-dependent microtubule stabilisation via TACC proteins. Aurora A kinase is required for the recruitment of *Drosophila melanogaster* centrosomin (Cnn) to the centrosome, which is required for efficient γ-tubulin complex

recruitment (Ducat and Zheng, 2004). The Cnn homologue in humans is CDK5RAP2/Cep215 (mentioned above) and paralogue, myomegalin (Gomez-Ferreria and Pelletier, 2010). Aurora A also promotes full recruitment of *C. elegans* and *D. melanogaster* SPD-2, which in turn recruits the γ-TuRC and *C. elegans* Zyg-9 (a TOG protein) (Ducat and Zheng, 2004). The human SPD-2 homologue, Cep192, is required for recruitment of PCM components γ-tubulin, GCP-WD, and pericentrin during centrosome maturation (Zhu et al., 2008). Furthermore *X. laevis* Cep192 is essential for activation of Aurora A kinase specifically at the centrosome by promoting Aurora A dimerisation, which leads to strong activation of the kinase and microtubule assembly (Joukov et al., 2010). CDK11p58 kinase is also required for localisation of Aurora A to the centrosome (Petretti et al., 2006). Aurora A inactivation leads to decreased accumulation of PCM components during centrosome maturation, a lower density and reduced length of centrosome-derived microtubules, and a failure to maintain centrosome separation (Ducat and Zheng, 2004).

In summary, there are redundant pathways for microtubule nucleation and spindle pole maintenance, some of which are centrosome-dependent; others are centrosome independent. Centrosome-derived microtubule nucleation and maintenance involves many different proteins that function in redundant pathways, which indicates the importance of the fidelity of chromosome and centrosome segregation in mitosis for genome stability. The roles of proteins involved in centrosome-dependent microtubule nucleation discussed here are summarised in figure 9.

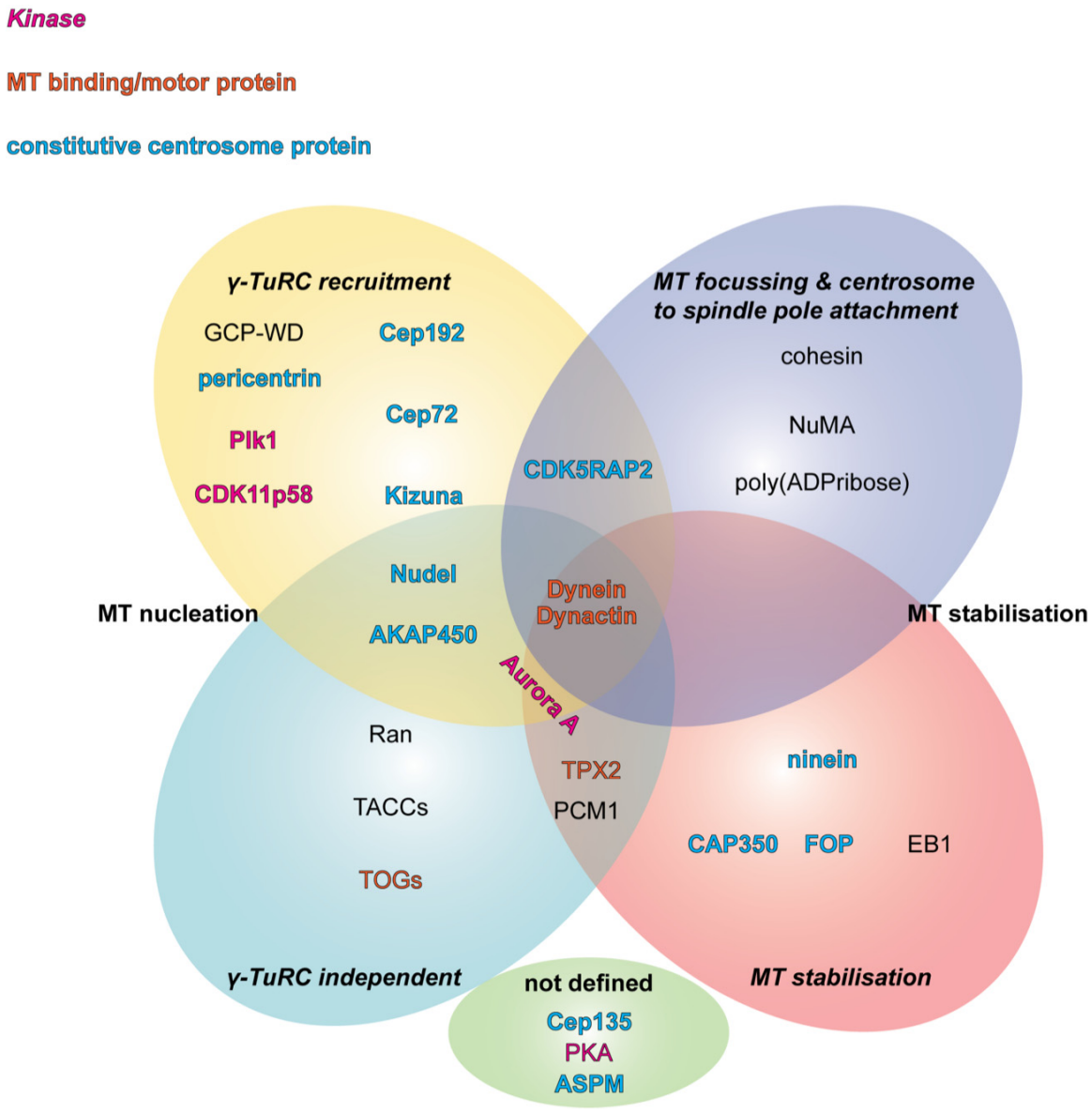

Figure 9 Centrosome dependent microtubule organisation
Proteins involved in centrosome dependent microtubule (MT) organisation are categorised by function. Proteins that are involved in multiple MT organisation functions are present in the overlapping regions of the appropriate function areas. Proteins that are involved in centrosome dependent MT organisation, but have no defined function are also shown. Proteins are coloured with respect to their molecular function, if known.

1.2.3 The centrosome in cell cycle regulation

The structure and function of the centrosome changes during the cell cycle (section 1.3), but the centrosome also influences cell cycle phase transitions by acting as a docking site for cell cycle regulatory proteins (Doxsey et al., 2005).

Activation of the key mitotic regulator, Cdk1-cylin B initially occurs at the centrosome before it moves to the nucleus (Jackman et al., 2003). In fact, proteins that regulate the activation of Cdk1-cyclin B have been shown to localise to the centrosome by immunofluorescence or Western blot of purified centrosomes (Doxsey et al., 2005). Cdk1 requires the action of phosphatase Cdc25 for full activation of its kinase activity. Cdc25 removes inhibitory phosphorylation at Tyrosine 15 (Y15) of Cdk1. Antibodies that specifically detect phospho-Cdk1 Y15 stain the centrosome and cytoplasm in G2 and levels reduce as cells progress to metaphase (Lindqvist et al., 2005). Interestingly, RNAi depletion of Cdc25A or B resulted in high levels of Cdk1 Y15 phosphorylation and cell cycle arrest pre-mitosis, whereas depletion of Cdc25C did not affect the ability of cells to enter mitosis (Lindqvist et al., 2005). However, Cdc25C has also been shown to localise to centrosomes during mitosis and its overexpression causes an increased percentage of cells that enter mitosis at a specific time after release of cells from synchronisation (Bonnet et al., 2008). Conversely, expression of a Cdc25C phosphatase mutant caused a decrease in cells entering mitosis, which shows that Cdc25C also has a role in Cdk1-cyclin B activation at the centrosome.

As Cdk1-cyclin B and its activator Cdc25 phosphatase localise to the centrosome during G2, so do the regulators of Cdc25 phosphatase activity. Aurora A phosphorylates Cdc25B, which contributes to Cdc25 activation and subsequent G2 to M transition, and both active Aurora A (phospho-T288) and Aurora A phosphorylated Cdc25B (phospho-S353) localise to the centrosome (Dutertre et al., 2004, Cazales et al., 2005). Furthermore, Aurora A contributes to the accumulation of cyclin B to the centrosome (Hirota et al., 2003). There is also evidence for positive regulation of cyclin B by Polo-like kinase, Plk1, at centrosomes (Petronczki et al., 2008).

Chk1 is a well-characterised DNA damage checkpoint kinase that is known to prevent mitotic entry by preventing activation of Cdk1-cyclin B by phosphorylating and inhibiting Cdc25 (Sancar et al., 2004). Chk1 is also present at centrosomes during an unperturbed cell cycle where it phosphorylates Cdc25B on S280, which results in Cdc25B inactivation (Schmitt et al., 2006). The Cdc25B phospho-S280 epitope is present at centrosomes in G2, prophase and early prometaphase, but disappears during prometaphase indicating activation of Cdc25B. Mutation of S280 to inhibit Chk1 phosphorylation of Cdc25B causes premature mitotic entry (Cazales et al., 2005). Furthermore, Chk1 activity at the centrosome leads to the presence of inactive Cdk1 phospho-Y15 at the centrosome (Löffler et al., 2007). Centrosome proteins microcephalin (MCPH1), pericentrin, and CDK5RAP2 are important for centrosomal localisation of Chk1 (Tibelius et al., 2009, Barr et al., 2010). These findings are summarised in figure 10.

Further to the presence of Chk1 DNA damage kinase at the centrosome, other DNA damage kinases including ATM, ATR, DNA-PK, ATRIP and Chk2 have also been visualised at the centrosome (Zhang et al., 2007). Chk2 localises to the centrosome in the absence and presence of DNA damage (Tsvetkov, 2003, Golan et al., 2010), although its function at the centrosome has not been confirmed.

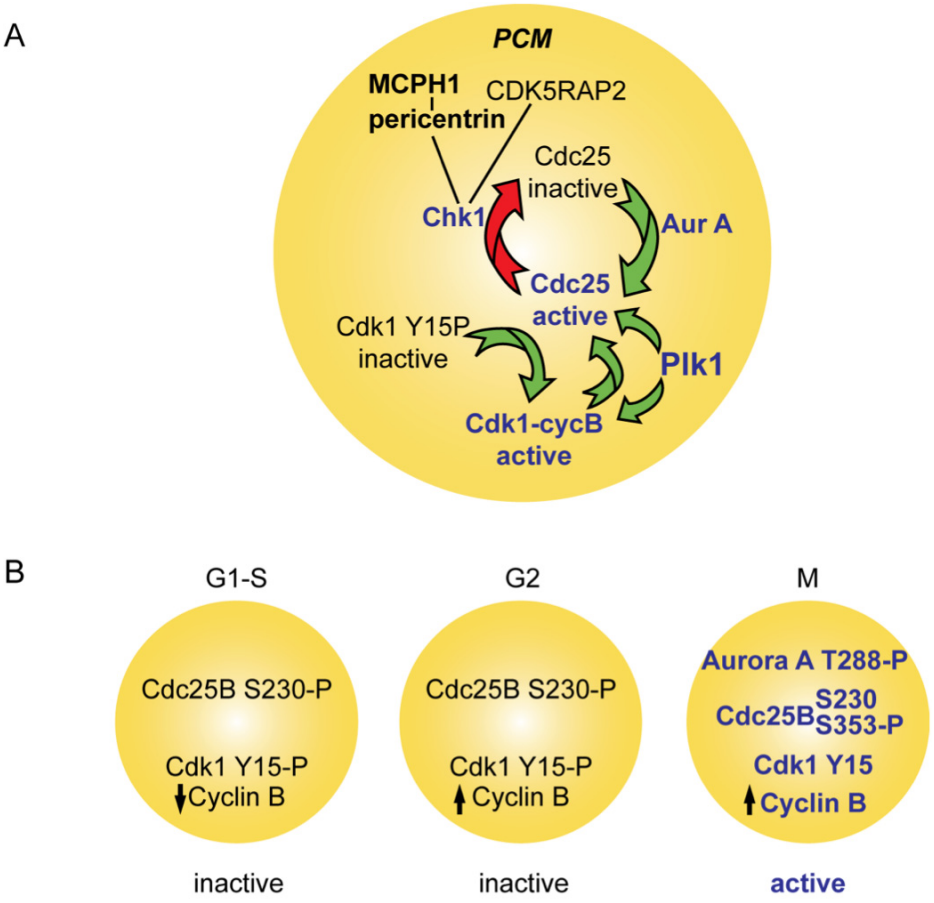

Figure 10 Activation of Cdk1-cyclin B at the centrosome
(A) Diagram of cell cycle regulatory proteins that localise to the centrosome and their activities that have been shown at the centrosome. PCM proteins microcephalin (MCPH1), pericentrin and CDK5RAP2 recruit Chk1 to the centrosome. Chk1 holds Cdc25 phosphatase inactive, preventing mitotic entry. Upon entry into mitosis, Cdc25B is dephosphorylated. Aurora A further activates Cdc25B and promotes Cyclin B recruitment to the centrosome. Plk1 further activates Cdc25C that has already been phosphorylated by Cdk1-cyclin B. (B) Summary of the different immunofluorescence signals detected at the centrosome during the cell cycle.

The influence of centrosomes on the G2 to M cell cycle transition can be seen in *Xenopus laevis* eggs: injection of centrosomes activates MPF (maturation promoting factor, or Cdk1-cyclin B) and advances mitotic entry relative to eggs without centrosomes (Perez-Mongiovi et al., 2000). However, eggs without centrosomes are able to enter mitosis, with a delay. This phenomenon has also been observed in human tissue culture cells: centrosomes promote, but are not required for, mitotic entry (Doxsey et al., 2005). Perhaps this is due to redundancy, so centrosomes have a dominant effect on the G2/M transition, but the transition can occur by activation of Cdk1-cyclin B away from the centrosome. Alternatively, centrosomes *per se* might not be required, but in the absence of a centrosome, PCM components might associate and recruit cell cycle regulatory proteins with no requirement for the presence of centrioles.

1.2.4 Centrosomes and microcephaly

Microcephaly (small brain) is a common feature of genetic diseases MCPH (autosomal recessive primary microcephaly); MOPD II (Majewski osteodysplastic primordial dwarfism type II); and Seckel syndrome. MCPH patients have a head circumference at least 4 standard deviations below average, but have normal stature (Woods et al., 2005). MOPD II and Seckel syndrome patients have microcephaly in combination with growth retardation and their clinical features can be hard to distinguish (Piane et al., 2009). Microcephaly is defined by head circumference, which is a measure of brain size. In microcephaly, the overall structure of the brain is normal, but the cerebral cortex is smaller due to reduced numbers of neurons produced during development (Woods et al., 2005).

All known cases of primary microcephaly, MCPH, have been mapped to 7 regions of the genome, designated MCPH1-7. All MCPH mutations have now been mapped to genes within these regions, all of which are involved with centrosome or mitotic spindle pole function (table 1) (Megraw et al., 2011).

MCPH gene	Gene name	Centrosome (C) or spindle pole (SP)	DNA damage response
MCPH1	Microcephalin	C	Yes
MCPH2	WDR62	SP	ND
MCPH3	CDK5RAP2, Cep215	C	Yes
MCPH4	Cep152	C	ND*
MCPH5	ASPM	SP	Yes
MCPH6	CPAP, CENPJ, Sas-4	C	ND
MCPH7	STIL, Sas-5	SP	ND

Table 1 MCPH genes
Table adapted from Megraw *et al.* (Megraw et al., 2011). If there is evidence for a gene in the DNA damage response at any stage, it is indicated "Yes". If there is no evidence, the gene is marked "ND" (not determined). * Kalay *et al.* concluded that DNA damage signalling was altered in cells from Cep152 MCPH4 patients, but the evidence presented does not support the conclusion; see text (Kalay et al., 2011).

Due to the heterogeneity of MCPH, different mutations in different genes, the resulting cellular phenotypes are varied. Consequently, a common biological cause for MCPH has not yet been defined. It is clear that MCPH is a disease caused by centrosome abnormalities, but which centrosome function is crucial for properly regulated neurogenesis and full cerebral cortex growth? Is it due to the role of the centrosome in mitotic spindle assembly and spindle positioning; or the role of the centrosome in DNA damage signalling; or the role of centrosome asymmetry in asymmetric cell divisions; or perhaps it is the role of primary cilia in cell signalling pathways? There is evidence for each of these explanations, which is reviewed in Megraw *et al*. (Megraw et al., 2011) and summarised below.

It is important to note that MCPH genes are expressed in the developing cerebral cortex at the stage of development when neurogenesis occurs, as determined by *in situ* hybridisation of mouse or human embryo brain sections or cDNA analysis (Jackson et

al., 2002) (Bilguvar et al., 2010, Yu et al., 2010, Bond et al., 2005, Guernsey et al., 2010, Bond et al., 2002, Kumar et al., 2009).

MCPH1 microcephalin

MCPH1 deficient cells show similarities to cells from ATR-Seckel patients, which have defective ATR-dependent DNA damage signalling pathways. MCPH1 patient cells have been well characterised alongside ATR-Seckel patient cells: they share common phenotypes of nuclear fragmentation, supernumerary mitotic centrosomes and defective G2/M checkpoint in response to UV (Alderton et al., 2006). The G2/M checkpoint is defective due to inefficient Chk1 signalling via Cdc25A: after UV irradiation, phospho-Chk1 (active) levels are the same as control cells, but Cdc25A is not degraded and thus Cdk1-cyclin B is still activated, which could be explained by the finding that microcephalin and pericentrin are required for Chk1 localisation to the centrosome (Tibelius et al., 2009). For the same reason, Cdk1-cyclinB is activated prematurely in an unperturbed cell cycle in MCPH1 patient cells, causing premature chromatin condensation (PCC). However, mitotic entry and progression occurs with the same kinetics as wild type cells. MCPH1 null mice have a reduced birth rate and slow growth; brain size was not examined. In addition MCPH1 mice are hypersensitive to γ-irradiation and show male infertility due to arrest and apoptosis of spermatocytes during meiosis (Liang et al., 2010).

MCPH2 WDR62

The WDR62 protein localises to the nucleus in interphase, to spindle poles from prophase to telophase and to the central spindle in anaphase (Bhat et al., 2011, Nicholas et al., 2010) but its molecular function is yet to be characterised.

MCPH3 CDK5RAP2

CDK5RAP2 localises to the centrosome throughout the cell cycle, but it is enriched on the centrosome during prophase to metaphase and levels decrease again during anaphase and telophase (Bond et al., 2005). Mice with homozygous deletions of the conserved first centrosomin domain (CNN1) have microcephaly as well as infertility, aneuploidy, radiation sensitivity, anaemia and cancer predisposition (Lizarraga et al., 2010). Examination of the developing cortex shows that, in the absence of CDK5RAP2 function, there is misalignment of mitotic spindles in neural precursors and a loss of neural progenitors. Neural progenitor loss is coincident with premature cell cycle exit and elevated apoptosis (Buchman et al., 2010). *In utero* RNAi of CDK5RAP2 leads to premature cell cycle exit, loss of apical progenitors and an increase in basal progenitors and differentiated neurons during the three-day experiment (Buchman et al., 2010). These studies show evidence for the lack of control of mitotic spindle positioning as a potential cause of microcephaly and the loss of neural progenitors due to inefficient cell cycle regulation.

At the cellular level, CDK5RAP2 localisation to centrosomes is required for maintaining the link between centrosomes and mitotic spindle poles (Barr et al., 2010). CDK5RAP2 interacts with AKAP450 and is required for the localisation of AKAP450 and the dynactin subunit p150glued to the centrosome. Additionally, CDKRAP5 and AKAP450 are required for centriole cohesion during interphase: to prevent mother and daughter centrioles disengaging before mitosis. CDK5RAP2 is also required for efficient G2/M checkpoint activation in response to γ-IR, which is likely due to recruitment of Chk1 to the centrosome (Barr et al., 2010).

MCPH4 Cep152

Cep152 mutations have been identified in MCPH4 patients and in Seckel patients (Guernsey et al., 2010, Kalay et al., 2011). Cells from MCPH4 patients have not yet been analysed, but a cell line from one Cep152-Seckel patient shows multiple different sized nuclei and centrosomes, micronuclei, misaligned chromosomes in mitosis as well

as monopolar spindles and multipolar spindles (Kalay et al., 2011). The authors of this study also conclude that there is enhanced Chk2 phosphorylation and increased γ-H2AX foci formation in response to hydroxyurea (HU) induced replication stress in Cep152 Seckel cells relative to wild type. However, the data presented in the paper do not support these conclusions. Thus, whether Cep152 is involved in DNA damage signalling remains to be shown.

Cep152 has been characterised by RNAi studies in human cell lines: it is required for centriole duplication (section 1.3), but there is no evidence of impaired centrosome maturation or microtubule nucleation (Blachon et al., 2008, Dzhindzhev et al., 2010b, Cizmecioglu et al., 2010, Hatch et al., 2010b).

MCPH5 ASPM

ASPM mutations are the most common MCPH mutations, with a variety of different truncation mutations (Nicholas et al., 2009). Even a small C-terminal truncation of 120 amino acids (from 3477 amino acids) causes microcephaly (Bond et al., 2003). ASPM contains an N-terminal putative microtubule binding domain followed by multiple calmodulin binding IQ domains. Interestingly, the number of IQ repeats increases with brain complexity in evolution: the *C. elegans* protein has 2 IQ domains; *Drosophila* have 24; mouse has 61 and humans have 74. Deletion of the C-terminus and only 6 IQ domains is sufficient to cause microcephaly (Bond et al., 2002). The function of the IQ domain is not known.

Murine Aspm is required for maintaining symmetric cell divisions during early neurogenesis (Fish et al., 2006). In the developing cerebral cortex, early divisions of neuroepithelial cells are symmetric such that each of the daughter cells maintains contact with the apical membrane and both daughters maintain proliferative potential (figure 11). During this stage of development, Aspm is found at the mitotic spindle poles of all cells, whereas Aspm levels at spindle poles decrease at later developmental stages where asymmetric cell divisions are more common (Fish et al., 2006).

Asymmetric divisions result in one daughter cell that maintains contact with the apical membrane and retains its proliferative potential and one daughter cell that loses apical basal polarity and becomes a terminally differentiated neuron. RNAi of Aspm in the developing cerebral cortex results in an increased proportion of asymmetric cell divisions, due to spindle rotation, at a developmental stage where symmetric cell divisions are predominant. Thus, depletion of Aspm causes an increase in the production of neurons at an early stage of brain development, which reduces the neurogenic capacity at later developmental stages. The Drosophila orthologue, Asp, is required for spindle pole focussing and functions by cross-linking microtubule minus ends (do Carmo Avides and Glover, 1999, Wakefield et al., 2001).

MCPH6 CPAP

CPAP (also called CENPJ) localises to the centrosome during interphase and to spindle poles during mitosis and CPAP antibody disrupts centrosome induced microtubule nucleation *in vitro* (Bond et al., 2005, Hung et al., 2000). CPAP RNAi results in multipolar mitoses in human cell lines, which is likely due to centrosome splitting since interphase cells do not contain multiple centrosomes (Cho et al., 2006). Furthermore, CPAP regulates centriole length (Kohlmaier et al., 2009, Schmidt et al., 2009, Tang et al., 2009), see section 1.3. Interestingly, CPAP and Cep152 interact and Cep152 is required for recruitment of CPAP to the centrosome (Cizmecioglu et al., 2010).

MCPH7 STIL

STIL localises to spindle poles in mitosis and it is required for proper bipolar spindle assembly in human cells and in zebrafish (Pfaff et al., 2007). Sil (mouse orthologue of STIL) null mice die after embryonic day 10.5 and show arrest of neural tube closure (Izraeli et al., 1999). There are fewer cells in the neural fold due to apoptosis rather than a defect in proliferation.

STIL (SIL) null mouse embryonic fibroblasts (MEFs) show slow growth, low mitotic index and have no detectable centrosomes (Castiel et al., 2011). STIL null cells have high levels of E3 ubiquitin ligase Chfr, which negatively regulates entry into mitosis by targeting Plk1 for degradation, resulting in a delay in Cdk1-cyclin B activation.

In summary, there is no consensus for the molecular cause of microcephaly, although there are common themes of deregulation of centrosome MTOC function, mitotic spindle assembly and DNA damage checkpoint signalling. Seckel patients have defective ATR-dependent DNA damage checkpoint signalling and also have microcephaly. Interestingly, some instances of Seckel syndrome are caused by mutations in pericentrin (PCNT), which results in defective Chk1 phosphorylation in response to ATR-dependent DNA damage signalling (Griffith et al., 2008). Thus, pericentrin-Seckel, MCPH1 (microcephalin) and MCPH3 (CDK5RAP2) patient cells share a common phenotype of defects in the ATR-dependent G2/M checkpoint, but all have a range of other non-overlapping phenotypes. Pericentrin and microcephalin interact at the centrosome where they are required for centrosomal localisation of Chk1 (Tibelius et al., 2009). Furthermore, CDK5RAP2 also interacts with pericentrin (Buchman et al., 2010).

Figure 11 shows the effect of symmetric versus asymmetric neuroepithelial cell division. Changes in the control of symmetric versus asymmetric are controlled by the precise spindle orientation, which can be affected by centrosome amplification, loss of spindle pole to centrosome association, or loss of astral microtubule nucleation. All of these are phenotypes observed in subsets of microcephaly cells, but there are other possible explanations for reduced number of neuroepithelial cells in microcephaly models. Some models of microcephaly show loss of neuroepithelial cells due to inappropriate exit from the cell cycle and/or apoptosis (MCPH1 and CDK5RAP2).

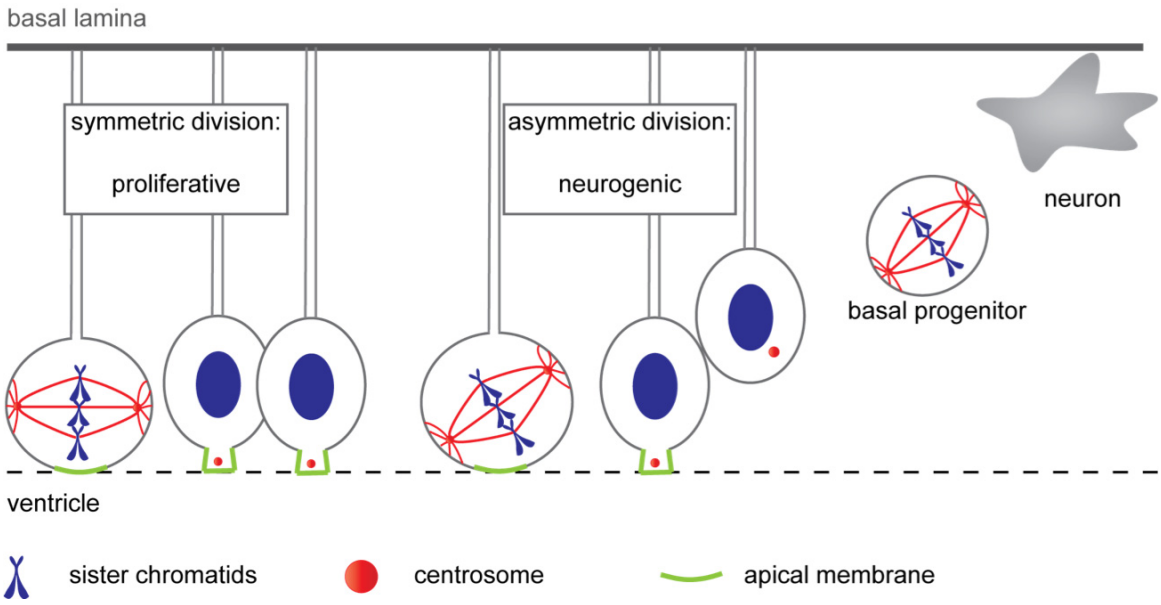

Figure 11 Symmetric and asymmetric neuroepithelial cell divisions
Adapted from Thornton *et al.* (Thornton and Woods, 2009). Neuroepithelial cells span from the basal lamina to the ventricle, but only undergo mitosis at the ventricular (apical) surface. Before the onset of neurogenesis, the mitotic spindle aligns perpendicular to the ventrical surface and symmetric cell divisions result in two daughters, both with apical determinants and both with self-renewing capacity. During neurogenesis, or when the spindle is rotated, asymmetric cell divisions give rise to one daughter with apical determinants and self-renewing capacity and one daughter that becomes a non-polarised basal progenitor or fully differentiated neuron. If spindle orientation is not tightly controlled, spindle rotation can cause asymmetric cell divisions before the onset of neurogenesis, which can lead to a depleted pool of neural progenitors for subsequent neurogenesis.

1.3 The centrosome cycle

G1 cells contain one centrosome with two centrioles: a mother and a daughter, which are disengaged and licensed to duplicate, but still attached to each other via a flexible linker between their proximal ends. During S phase, a new daughter procentriole is formed at right angles to the mother centriole at the proximal end of the mother. Mother and daughter centrioles are tightly engaged during S, G2 and mitosis. During G2, new centrioles elongate and the younger mother centriole (a daughter in the previous cell cycle) fully matures and acquires appendages. At the G2 to M transition, the flexible linker between the two centrosomes is broken and centrosomes separate to allow mitotic spindle assembly, see figure 12 and (Nigg, 2007).

During S and G2 phases there are three different generations of centrioles present: the grandmother and mother centrioles (mother and daughter from G1) and their new daughter centrioles. In order to reach full maturity, a daughter centriole has to pass though mitosis to acquire MTOC capacity and the ability to form a new centriole (licensing) then in the following G2 phase it becomes fully mature and acquires appendages at its distal end.

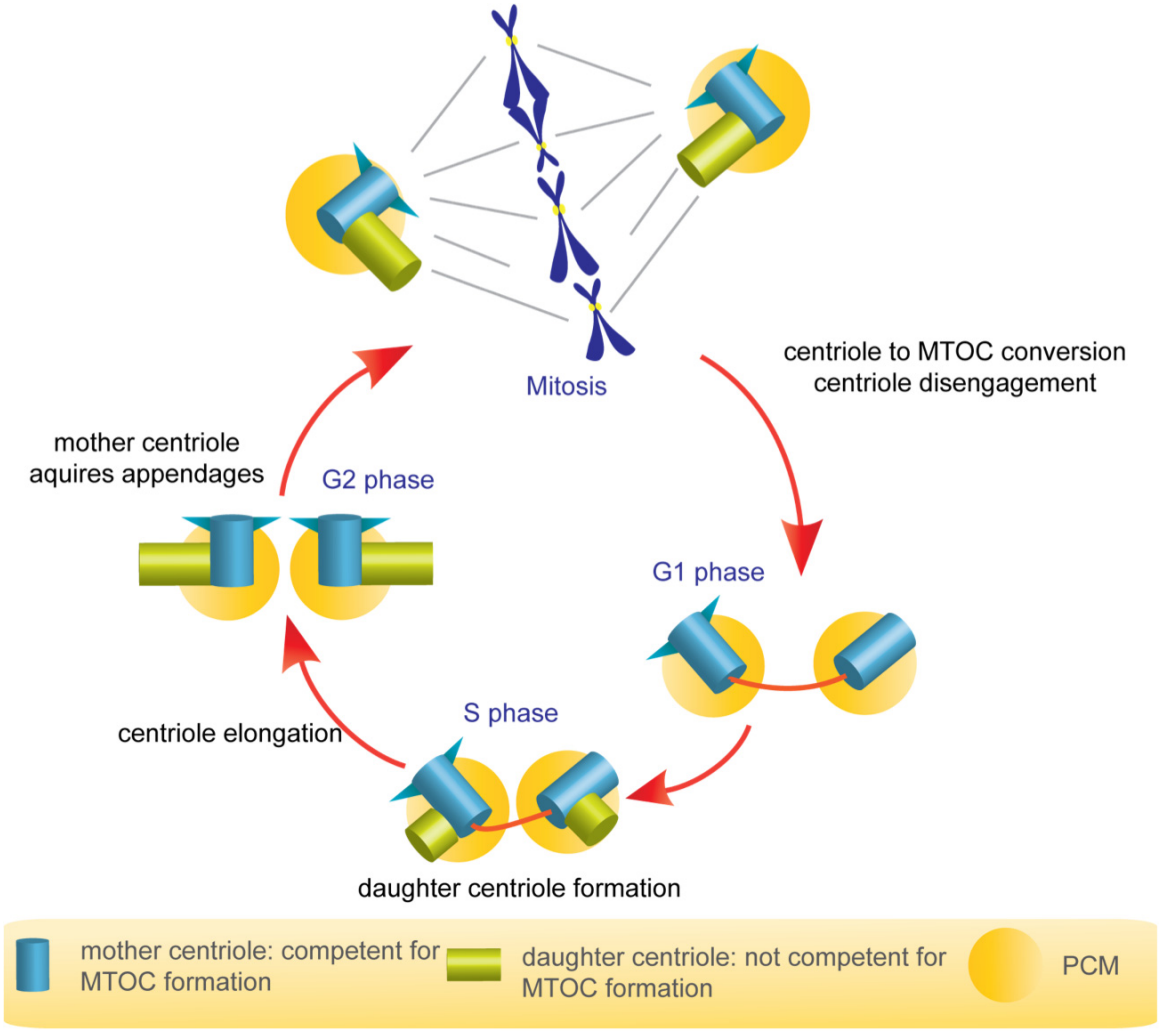

Figure 12 The centrosome duplication cycle
Centrioles are disengaged and licensed for duplication upon exit from mitosis (blue). During G1 and S centrioles are attached to each other by flexible fibres (orange). Upon passage through mitosis, daughter centrioles become competent to organise PCM (yellow) and duplicate. New procentrioles are formed during S phase and remain tightly attached "engaged" to mother centrioles until exit from mitosis. Procentrioles elongate in G2 then the younger mother centriole acquires appendages and the fibrous link between mother centrioles is severed. Upon entry into mitosis, centrosomes segregate and localise to the spindle poles. Centrioles disengage during mitotic exit or early G1 to allow another round of centriole duplication.

1.3.1 Centriole formation

Polo like kinase Plk4 is required for the recruitment of core centriole components hSas-6, Cep135, CPAP, and CP110 to the newly forming daughter centriole (Kleylein-Sohn et al., 2007) (figure 13). The first component observed at the site of procentriole formation is hSas-6, which forms the cartwheel structure with 9-fold symmetry onto which centriole microtubules assemble (Leidel et al., 2005, Kitagawa et al., 2011). HSas-6, CPAP, Cep135 and γ-tubulin are all dependent on each other for localisation to the centrosome (Kleylein-Sohn et al., 2007). CPAP is concentrated in the proximal lumen of the procentriole and is required for centriole formation and elongation (Cho et al., 2006, Tang et al., 2009). The *C. elegans* CPAP orthologue, SAS-4, is required for attachment of the first and innermost centriole microtubule (the A tubule, figure7). CPAP and γ-tubulin interact, indicating that CPAP might play the same role in human cells (Hung et al., 2000). The A tubule nucleates from a γ-TuRC cap at its minus end and the subsequent formation of the B and C tubules appear to form from the side of the A tubule, and B tubule respectively, in a bidirectional manner with no minus end cap (Azimzadeh and Marshall, 2010). Recruitment of the γ-TuRC is essential for centriole duplication (Haren et al., 2006) (Kleylein-Sohn et al., 2007). Cep135 is also essential for centriole formation, but its role in centriole formation is not well characterised. The *Chlamydomonas* Cep135 orthologue, Bld10p, regulates the length of the radial spokes of the cartwheel structure and consequently, centriole diameter (Azimzadeh and Marshall, 2010). CP110 lies downstream of CPAP, Cep135, and γ-tubulin, and forms a cap at the distal end of the procentriole, under which α/β-tubulin dimers polymerise to elongate the centriole (Kleylein-Sohn et al., 2007).

Cep192 is also required for centriole duplication but it remains to be determined if Cep192 carries out a similar function to its *C. elegans* orthologue SPD-2, which is required for Plk4 localisation to the centrosome (Zhu et al., 2008, Carvalho-Santos et al., 2010). Cep152 lies upstream of the proteins described above: it is required for centriole duplication due to its role in recruitment of Plk4 and CPAP to the centrosome (Blachon et al., 2008, Dzhindzhev et al., 2010a, Cizmecioglu et al., 2010, Hatch et al., 2010b). Although depletion of Cep152 does not lead to complete depletion of Plk4 from

the centrosome, Cep152 depletion results in reduced recruitment of Plk4 to the centrosome and centriole duplication failure (Cizmecioglu et al., 2010). Additionally, Centrosome proteins SPICE and Cep120 are both required for centriole duplication and Cep120 functions downstream of hSas-6 recruitment to the procentriole (Archinti et al., 2010, Mahjoub et al., 2010).

Centrins are conserved proteins that are present in the distal lumen of centrioles, although their localisation is not restricted to the centrosome (Paoletti et al., 1996). Centrin is required for spindle pole body duplication in yeast, but the requirement for centrins in higher eukaryotes remains controversial (Azimzadeh and Marshall, 2010). Studies in *Xenopus* embryos show a requirement for centrins 2 and 3 in centrosome duplication and successful embryo cleavage (Paoletti et al., 1996, Middendorp et al., 2000). Centrin 2 is has also been shown to be required for centriole duplication in HeLa cells (Salisbury et al., 2002). However, several studies show that centriole duplication occurs in the absence of centrins (Dantas et al., 2011, Yang et al., 2010).

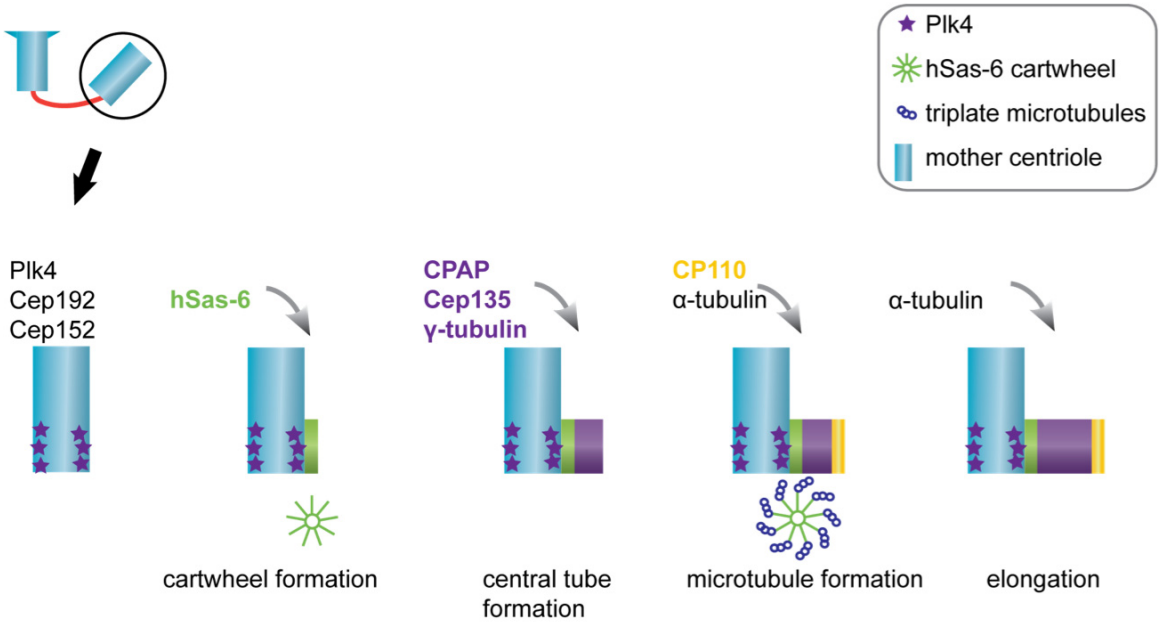

Figure 13 Centriole formation
Adapted from Kleylein *et al.* and Azimzadeh *et al.* (Kleylein-Sohn et al., 2007, Azimzadeh and Marshall, 2010). Centriole biogenesis is dependent on Plk4 kinase and structural components of the centriole: hSas-6, CPAP, Cep135, γ-tubulin and CP110. Procentriole formation begins with the recruitment of hSas-6, which forms a cartwheel structure with 9-fold symmetry that determines the position of centriole microtubules. CPAP, Cep135 and γ-tubulin are then recruited to the central tube and α/β-tubulin dimers are then recruited and polymerised to form the centriole triplet tubules. CP110 forms a cap at the distal end of the centrioles and defines the centriole length.

During G2, centrioles elongate by the extension of centriole microtubules. CPAP and CP110 act antagonistically to regulate centriole length, with CPAP promoting centriole elongation and CP110 restricting elongation (Schmidt et al., 2009, Kohlmaier et al., 2009). The daughter centriole protein, centrobin, is also important for centriole elongation. Centrobin is recruited to the daughter centriole in a hSas-6 dependent fashion and its interaction with tubulin is required for the stabilisation of centriole microtubules (Gudi et al., 2011). Along with elongation, daughter centrioles acquire markers of maturation including hPOC5 at their distal end beginning in G2 and continuing during mitosis (Azimzadeh et al., 2009). HPOC5 and centrin levels increase throughout G2 and mitosis and consequently, mother centrioles can be distinguished from procentrioles due to increased centrin levels.

At the end of G2, the younger mother centriole (that was a daughter in the previous cell cycle) reaches full maturity and acquires distal appendages, which consist of proteins Ofd1, Cep164, ninein, Cep170, ε-tubulin, ODF2 and cenexin (Azimzadeh and Marshall, 2010). At this time the fibrous linker between the two centrosomes is broken, which allows centrosomes to separate in mitosis. The linker between the proximal ends of the two mother centrioles consists of C-Nap1 and Rootelin, which interact with each other and are both essential for linking the two centrosomes in interphase (Mayor et al., 2000, Bahe et al., 2005, Yang et al., 2006). The linker is broken at the G2/M transition by Nek2 kinase via β-catenin (Bahe et al., 2005, Bahmanyar et al., 2008).

Centriole duplication is tightly regulated such that only one procentriole can form at each mother centriole and the duplication process can only occur once per cell cycle. Procentrioles form in tight association with the mother centriole, but *de novo* centriole formation can occur: the presence of a mother centriole "template" is not essential but likely acts to concentrate the required factors and thus speed up the kinetics of centriole formation in comparison with *de novo* formation (Khodjakov et al., 2002). The presence of one daughter centriole per mother prevents the formation of additional procentrioles: removal of the daughter centriole allows formation of another (Loncarek et al., 2008). Importantly, it is a centrosome-intrinsic property that prevents reduplication since G2

cytoplasm is permissive for duplication of centrioles from G1 cells and centrosomes form G2 cells cannot duplicate in the presence of S phase cytoplasm (Wong and Stearns, 2003). Furthermore, *de novo* centriole formation only occurs in the absence of any centrioles and during *de novo* centriole formation there is no restriction on the number formed (La Terra et al., 2005).

Centriole duplication is coordinated with the chromosome duplication cycle. In order for a centriole to duplicate it must have passed through mitosis and it must be disengaged from its partner centriole, which occurs after the metaphase to anaphase transition. Since both the mitosis specific modification and disengagement processes are not active during S or G2, centriole duplication is restricted to once per cell cycle.

1.3.2 Centriole duplication licensing

From centriole formation in S phase through to the metaphase-anaphase transition mother and daughter centrioles remain tightly held together in orthogonal arrangement (engaged). Upon metaphase to anaphase transition the protease separase becomes active due to the destruction of its inhibitor, securin, as described previously (figure 5). Separase cleaves cohesin, which is involved in holding mother and daughter centrioles together, and is therefore essential for centriole disengagement (Tsou and Stearns, 2006, Tsou et al., 2009, Schockel et al., 2011) (figure 14). Importantly, disengagement is not sufficient for centrioles to be competent for duplication: Plk1 activity during mitosis is also required (Tsou et al., 2009, Wang et al., 2011). Plk1 is required for efficient cleavage of cohesin by separase, perhaps by modifying cohesin and thus making it a better substrate for separase cleavage. However, aside from the role of Plk1 in centriole disjunction, it has a role in modifying centrioles during mitosis in an unknown manner, which primes them for duplication in the subsequent S-phase. When centrioles are pushed through mitosis in the absence of Plk1 activity, the resulting centrioles remain engaged due to the role of Plk1 in centriole disjunction. However, if single centrioles, formed *de novo*, are put through the same process they cannot duplicate during the subsequent S-phase even though they are not engaged (Wang et al., 2011). Therefore,

both centriole disjunction and Plk1-dependent modification of centrioles are required for duplication. It is important to note that separase activity is not absolutely required for centriole disengagement: without separase, centriole disengagement is delayed, but still occurs in a Plk1 dependent fashion (Tsou et al., 2009).

Centriole duplication is temporally separated from disengagement and licensing, as DNA replication is separated from replication origin licensing, which prevents multiple rounds of licensing and duplication/replication in one cell cycle. Cdk2-cyclin E and Plk2 are active in S phase and promote centriole duplication by removal of nucleophosmin from the centrosome (Okuda et al., 2000, Krause and Hoffmann, 2010). Nucleophosmin is phosphorylated by these two kinases on distinct sites and its subsequent removal from the centrosome is required for centriole duplication. Nucleophosmin is recruited back on to centrosomes at mitosis and remains there during G1 to inhibit centriole duplication when licensing is ongoing. Furthermore, Cdk2-cyclin E dependent phosphorylation of Mps1 stabilises Mps1 at the centrosome where its kinase activity is required for centriole duplication (Fisk and Winey, 2001, Fisk et al., 2003). Intriguingly, NPM mutations are found in lymphomas and leukaemia, either as translocations with other genes, including the RARα gene found in APL as mentioned previously, or as aberrant NPM proteins, which can result in aberrant localisation of NPM and its interacting partners to the cytoplasm (Meani and Alcalay, 2009, Falini et al., 2007).

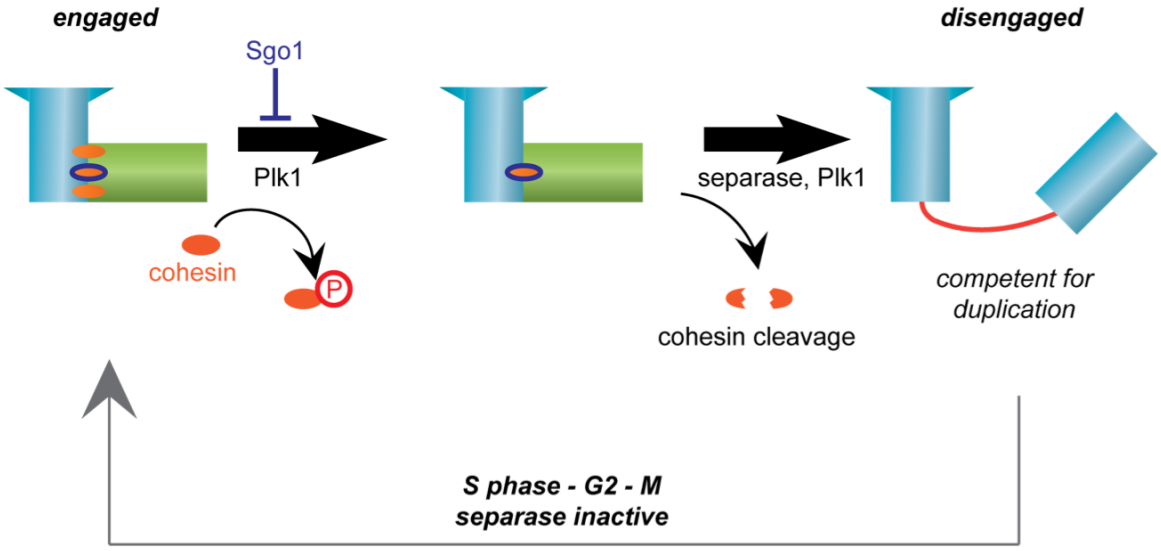

Figure 14 Centriole disengagement
Adapted from Schöckel *et al.* (Schockel et al., 2011). Plk1 leads to removal of a phosphatase-sensitive fraction of cohesin during prophase, but a sugoshin 1 (Sgo1, blue oval) protected pool of cohesin remains (orange encased in blue). Furthermore, Plk1 primes cohesin, probably by direct phosphorylation, for cleavage by separase. When separase becomes active at the metaphase to anaphase transition, it cleaves the remaining cohesin and centriole engagement is abolished. The centrioles inherited by G1 cells are disengaged and both competent for PCM recruitment, microtubule organisation, and duplication. Plk1 activity is essential for centriole disjunction/disengagement.

1.3.3 Control of centriole copy number

The mechanisms restricting the formation of daughter centrioles to one per mother centriole are not fully understood, but Plk4 regulation plays an important role in this process. Plk4 is absolutely required for centriole duplication and the precise regulation of Plk4 protein levels is essential for controlled centriole duplication: Plk4 overexpression causes the formation of multiple daughter centrioles per mother centriole in a flower-like arrangement (Habedanck et al., 2005). Both its localisation to the centrosome and its kinase activity are required for centriole duplication. Importantly, Plk4-induced centriole "flower" formation is only observed in S phase or G2 cells, suggesting that Plk4-induced centriole formation is subject to cell cycle regulation (Kleylein-Sohn et al., 2007).

Proteolysis is essential for restricting centriole copy number to one per mother centriole. Inhibition of the proteasome leads to centriole flower formation, which is dependent on Plk4 (Duensing et al., 2007). Plk4 is subject to proteasome-mediated degradation following Plk4 trans-autophosphorylation, which leads to ubiquitination by the $SCF^{Slimb/\beta\text{-}TrCP}$ ubiquitin ligase (Guderian et al., 2010, Holland et al., 2010). Plk4 over-expression causes centriole flower formation to a lesser extent than proteasome inhibition. Cdk2-cyclin E over-expression enhances Plk4-induced centriole flower formation to levels seen using the proteasome inhibitor. Although Cdk-cyclin E is not required for centriole over-duplication (Duensing et al., 2007), it is a positive regulator of duplication and it needs to be regulated in order to prevent the formation of multiple daughter centrioles. Along with Plk4, Cdk2-cyclin E levels are regulated by proteolysis (Duensing et al., 2007). Furthermore, the Cdk inhibitor p21 is required to prevent the formation of more then one daughter centriole per mother (Duensing et al., 2006), and Cyclin E is regulated by Orc1 (origin recognition complex subunit), which prevents cyclin E dependent centriole reduplication (Hemerly et al., 2009). Depletion of Orc1 leads to an increase in cyclin E levels and centriole reduplication.

Plk4 induced centriole duplication is dependent on factors that are required for formation of the centriole structures: hSas-6, CPAP, Cep135, and CP110. Depletion of any of these factors does not affect Plk4 centrosomal localisation, but these proteins are all structural components of the procentriole (hSas-6, CPAP, Cep135) or the growing centriole (CP110) and are therefore necessary for daughter centriole formation (Kleylein-Sohn et al., 2007).

HSas-6 recruitment to the centrosome is the essential first step in procentriole formation and its levels are tightly regulated by proteolysis. Over-expression of hSas-6 also leads to the formation of centriole flowers (Strnad et al., 2007). Localisation of hSas-6 to the centrosome is dependent on Plk4 (Strnad et al., 2007), and hSas-6 is targeted for degradation by the SCF-FBXW5 ubiquitin ligase at the end of mitosis such that hSas-6 is absent from the cytoplasm and centrioles of G1 cells, but protein levels begin to accumulate at the G1/S transition allowing pro-centriole formation (Puklowski et al., 2011). FBXW5 itself is cell cycle regulated by the APC/C, which keeps levels of FBXW5 low at the end of mitosis and during G1. At the beginning of S phase the APC/C becomes inactive and FBXW5 protein levels peak. However, Plk4 phosphorylates and inactivates FBXW5 allowing hSas-6 levels to rise (Puklowski et al., 2011). As mentioned above, Plk4 is responsible for its own down-regulation, so as S phase proceeds and Plk4 activity decreases, FBXW5 becomes active and targets hSas-6 for degradation (figure 15).

CP110, is also regulated by proteolysis; it is ubiquitinated by SCF-cyclin F, and targeted for degradation (D'Angiolella et al., 2010). Cyclin F levels peak in G2 and therefore prevent centriole reduplication by limiting the amount of CP110. CP110 is also negatively regulated by Cep76, which interacts with CP110 and specifically prevents centrosome reduplication rather than normal duplication (Tsang et al., 2009). Cep76 specifically inhibits centriole duplication induced by DNA replication stalling agents, but has no effect on the formation of multiple daughter centrioles around one mother centriole induced by overexpression of Plk4.

As Plk4 kinase is a positive regulator of centriole duplication, the phosphatase Cdc14B is an important negative regulator, although its substrates at the centrosome are not yet known. Cdc14B activity at the centrosome prevents centriole reduplication caused by cell cycle arrest with replication stalling agents, or by proteasome inhibition (Wu et al., 2008). Since proteasome inhibition leads to centriole reduplication in a Plk4 dependent manner it seems likely that Cdc14B may dephosphorylate Plk4 targets involved in centriole duplication.

In summary, multiple mechanisms ensure that centriole numbers are strictly regulated so that cells enter mitosis with only 2 centrosomes, each containing a pair of engaged centrioles. The mechanisms described above are summarised in figure 15. There is a plethora of evidence for the role of centrosome amplification in the formation of multipolar spindles, aneuploidy and genome instability (Nigg and Raff, 2009, Acilan and Saunders, 2008). As centriole duplication is tightly regulated, so is centriole elongation during G2, and maturation and separation of centrosomes at the G2/M transition, which is reviewed in (Azimzadeh and Marshall, 2010).

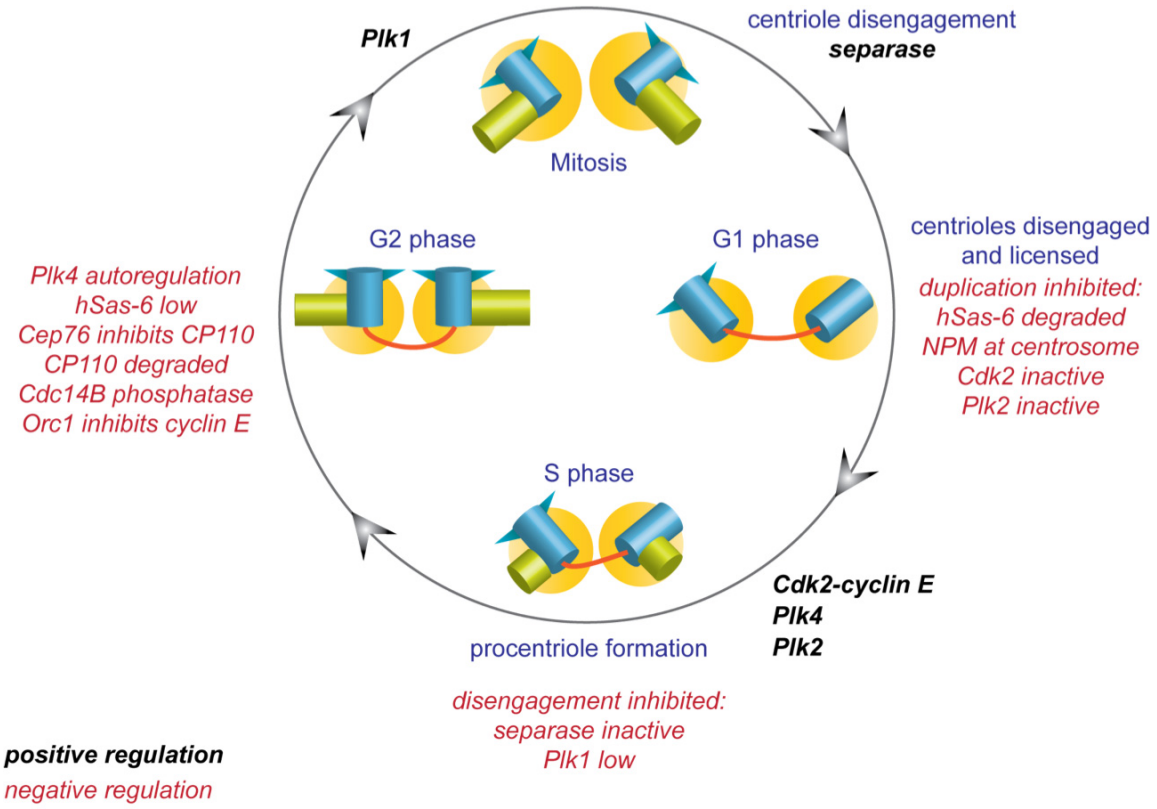

Figure 15 Regulation of centriole duplication
Centrioles are disengaged at the end of mitosis by the combined activities of Plk1 and separase. In G1 centrioles are licensed for duplication, but duplication does not take place until S phase when the S phase Cdk-cyclin kinase is active. Cdk2-cyclin E, Plk4 and Plk2 activity promotes daughter centriole formation. Centriole reduplication is prevented in G2 by mechanisms that restrict daughter centriole formation to one per mother centriole and prevent disengagement and licensing of centrioles before the next cell cycle.

1.3.4 Centriole reduplication

The formation of multiple procentrioles per mother centriole in a flower-like arrangement described previously, caused by overexpression of Plk4, hSas-6 or inhibition of the proteasome is due to abolishment of "copy number" control. However, centriole reduplication can also occur when cell cycle regulation of centriole duplication is deregulated. Reduplication of centrioles upon treatment of the human osteosarcoma cell line, U2OS, with replication stalling agents such as hydroxyurea (HU) or aphidicolin (Aph) is well known (Cizmecioglu et al., 2008). This phenomenon is also apparent in Chinese hamster ovary cells (CHO) (Balczon et al., 1995, Kuriyama et al., 2007), but does not occur in other cancer cell types such as HeLa or in non-transformed cells. Treatment of U2OS cells with HU or Aphidicolin to arrest them in S phase results in centrosome reduplication caused by multiple rounds of duplication and disengagement of mother and daughter centrioles as determined by the fact that centriole diplosomes and individual centrioles are formed, rather than mother centrioles surrounded but daughter centriole flowers (figure 16). Treatment of cells with γ-IR also results in centrosome duplication in the same way: uncoupling of the centriole duplication cycle from the cell cycle.

Centrosome reduplication after DNA damage is due to a prolonged G2 phase, which is dependent on the DNA damage induced G2/M checkpoint (Dodson et al., 2004). Centrosome amplification in G2 following DNA damage is due to a centrosome intrinsic signal that allows centriole disengagement (Inanç et al., 2010). Inanç and colleagues performed cell fusion experiments between human and chicken cells in order to distinguish between centrosomes that came from cells that had been irradiated and those that had not been irradiated. Only centrosomes from irradiated cells undergo amplification in G2. Recent experiments have shown that centrosome reduplication in HU-arrested U2OS cells also actually occurs in G2 rather than S phase, as previously thought (Loncarek et al., 2010). HeLa cells treated with HU, arrest with duplicated centrioles, which are engaged with procentrioles shorter than their mother and lacking the maturation marker hPOC5. However, U2OS cells in the same condition contain procentrioles that are as long as their mothers and also have hPOC5 staining at their

distal end. These mature procentrioles disengage from their mothers and multiple rounds of centriole duplication occur. Importantly, Cdk1 inhibition, which causes both HeLa and U2OS cells to arrest in late G2 phase, causes centriole disengagement and reduplication in both cell lines. Thus, the previously unknown difference between the effect of S phase arrest on centriole duplication in these two cell lines is not due to a difference in their centriole duplication mechanisms, rather a difference in the stringency of the S phase arrest. Centrosome disengagement, and therefore reduplication, during G2 is dependent on active Plk1 at the centrosome (Loncarek et al., 2010). During an unperturbed S phase, Plk1 activity is low and centriole disengagement cannot occur; therefore multiple rounds of centriole duplication cannot occur. During G2, Plk1 becomes active at the centrosome; centrioles can disengage and undergo another round of duplication if they are held in G2 for long periods of time. In accordance with this, centrosome amplification also occurs in CHO and DT40 cells upon inhibition of Cdk1, which causes G2 arrest (Steere et al., 2011).

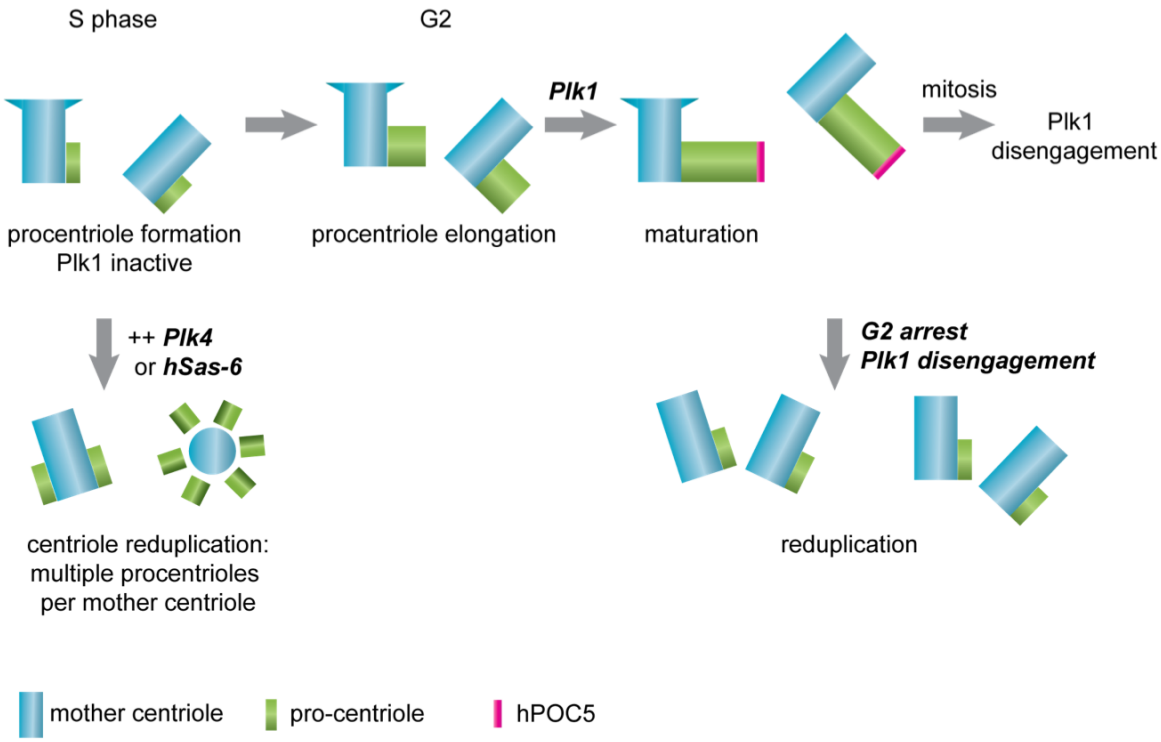

Figure 16 Centriole reduplication
Centriole duplication can occur due to abrogation of centriole copy number control by overexpression of Plk4, for example (left) or due to prolonged G2 arrest (right). In late G2, Plk1 becomes active at centrosomes, which promotes procentriole maturation and disengagement during arrest in G2, therefore licensing them for another round of duplication.

1.4 Cep63

Cep63 was identified as a centrosome protein in a mass spectrometry analysis of purified centrosomes (Andersen et al., 2003), also verified by (Jakobsen et al., 2011). *Xenopus laevis* Cep63, herein referred to as XCep63, was identified in the laboratory of Dr. Costanzo as a novel ATM substrate in *Xenopus* egg extracts (Smith et al., 2009). XCep63 localises to the centrosome in *Xenopus* tissue culture cells and to the centrosomes associated with sperm nuclei when incubated in *Xenopus* egg extracts. Depletion of XCep63 from *Xenopus* CSF (cytostatic factor arrested) extracts results in defective spindle assembly induced by the addition of purified sperm nuclei (and their associated centrosomes). Interestingly, XCep63 depletion does not affect the formation of chromatin-induced spindles upon the addition of DNA coated beads to CSF extract, which indicates that XCep63 plays a role specifically in centrosome-dependent spindle assembly (Smith et al., 2009).

In the presence of DNA damage in CSF extract, ATM is activated and DNA damage signalling leads to disruption of mitotic spindle assembly induced by the addition of purified sperm nuclei. XCep63 is phosphorylated by ATM in response to DNA damage on serine 560 and consequently delocalises from centrosomes. Addition of recombinant XCep63 mutated in the ATM target sequence, S560A, rescues the defect in spindle assembly resulting from DNA damage signalling. Furthermore, XCep63 S560A remains localised to the spindle poles in the presence of DNA damage, when the endogenous protein delocalises. Additionally, caffeine, an inhibitor of ATM and ATR kinases, also rescues spindle formation in the presence of DNA damage (Smith et al., 2009).

DNA damage in mitosis has been studied, but the effects on mitotic progression are varied. Upon DNA damage during mitosis, cells either die after a prolonged mitotic arrest or progress to G1 without delay (Nitta et al., 2004, Mikhailov et al., 2002); or revert to a G2-like phase without passing through mitosis (Chow et al., 2003).

Importantly, many of these studies show a cell line and DNA damage dose-specific response (Mikhailov et al., 2002, Nitta et al., 2004, On et al., 2011).

In response to extensive DNA damage, cells arrest in mitosis in a spindle assembly checkpoint (SAC) dependent manner due to disruption of kinetochore function (Mikhailov et al., 2002, Royou et al., 2005). In this situation, SAC activation is independent of ATM/ATR signalling. Smaller amounts of DNA damage that result in double strand DNA breaks, but not kinetochore damage, result in mitotic progression without delay (Mikhailov et al., 2002) or mitotic delay due to Chk1 dependent signalling (Royou et al., 2005). The extent of mitotic catastrophe in response to mitotic DNA damage is affected by the extent of SAC signalling and mitotic delay (On et al., 2011). Abrogation of SAC signalling prevents mitotic delay and mitotic catastrophe after DNA damage (Mikhailov et al., 2002, Nitta et al., 2004, On et al., 2011).

In conclusion, the effects of DNA damage signalling on mitotic cells is varied, depending on the cell type, efficiency of the SAC, dose and type of DNA damage. It is clear that the SAC is required for the mitotic delay in many different cell types, but the extent to which DNA damage signalling kinases are required varies. In *Xenopus laevis* egg extracts, XCep63 function in spindle assembly is inhibited by ATM dependent phosphorylation in response to DNA damage, which leads to disruption of spindle structure and, likely, activation of the SAC and mitotic delay (Brown and Costanzo, 2009).

1.4.1 Aims

Study of XCep63 indicates that it is an extremely interesting candidate for involvement in the maintenance of genome stability. The reasons for this are twofold: XCep63 is a target of DNA damage signalling kinases and it is involved in formation of bipolar mitotic spindles. Due to the potential for Cep63 to promote genome stability, future study of this protein may have important implications for cancer research.

The aim of my thesis is to characterise the function of human Cep63, which at the beginning of this project was unknown. Two approaches are taken to identify the role of Cep63 in human cell lines. Firstly, pull down of Cep63 and identification of binding partners will indicate pathways or processes in which Cep63 may play a role. Secondly, RNA interference (RNAi) to deplete Cep63 protein levels in cells will allow detection of any abnormalities in cell cycle progression or spindle assembly. Since Cep63 is a centrosome protein and an ATM target, there is potential for Cep63 to be involved in the regulation of cell cycle phase transitions. Furthermore, if the ATM-dependent phosphorylation of Cep63 is conserved between *Xenopus* and human, study of Cep63 may lead to a better understanding of mitotic DNA damage signalling. Perhaps Cep63 and potential associated partners might be the link between DNA damage checkpoint activation and activation of the spindle assembly checkpoint. As XCep63 is required for bipolar spindle assembly and maintenance, it will be interesting to see if this centrosomal function is conserved in humans. Perhaps Cep63 plays a role in maintaining microtubule minus ends at the centrosome, or mediating the link between spindle poles and the centrosome. As a centrosome protein, Cep63 has potential to be involved in many different pathways that regulate the duplication of the centrosome itself; the transition from one cell cycle phase to the next; and spindle assembly and mitotic progression.

Outline of aims

- Study the cellular localisation of Cep63.
- Produce and validate an antibody to allow study of human endogenous Cep63.
- Validate Cep63 siRNAs.
- Identify Cep63 interacting proteins.
- Investigate the function of Cep63 in human cell lines using RNAi.
- Ascertain if human Cep63 is phosphorylated by ATM, as XCep63 is.
- Set up a Cep63 gene-trap mouse model to allow study of Cep63 at the level of the whole organism and cell based studies.

Chapter 2. Materials and Methods

2.1 Chemicals and solutions

2.1.1 Suppliers of reagents

Unless stated, all chemicals were obtained from Sigma-Aldrich, BDH Laboratory Supplies (UK) or Fisher Scientific (UK). All restriction enzymes were purchased from New England Biolabs (NEB).

Standard solutions of 0.5 M EDTA, pH 8.0; 1M Tris-EDTA (TE), pH8.0; 1M Tris-HCl, pH7.5; 1M $MgCl_2$; 5M NaCl; Phosphate Buffered Saline (PBS); and Tris Borate EDTA (TBE) were prepared by Cancer Research UK London Research Institute (LRI) Central Services. All other stock solutions were made according to standard methods (Sambrook *et al*.).

Ultrapure agarose was obtained from Invitrogen; ammonium persulfate (APS), N,N,N,N'-tetra-methyl-ethylenediamine (TEMED), Tween 20, formaldehyde 36.5%, Igepal, Triton X-100 and bovine serum albumin (BSA) were obtained from SIGMA. Ethidium bromide, 40% Acrylamide/Bis 37.5:1, 1.5 M Tris HCl pH8.8, 0.5 M Tris HCl pH 6.8 and Laemmli sample buffer were obtained from Biorad. Sodium dodecyl sulfate (SDS), DMSO and β-mercaptoethanol were obtained from Fisher Scientific. Ultra Pure 30 % Acrylamide and Ultra Pure 2% Bisacrylamide were obtained from National Diagnostics (UK). Complete protease inhibitor cocktail tablets were obtained from Roche (UK). All primers were produced by Sigma-Genosys (UK).

2.1.2 Medium for bacteria

Luria-Bertani Broth (LB): 1% w/v bacto-tryptone (DIFCO), 0.5% w/v yeast extract (DIFCO), 0.1 M NaCl. pH adjusted to 7.

LB agar: LB broth + 2 % (w/v) Bacto agar

SOC: 2% w/v bacto-tryptone, 0.5% w/v yeast extract, 10mM NaCl , 2.5mM KCl, 10mM $MgCl_2$, 10mM $MgSO_4$, 20mM glucose. pH adjusted to 7.

2.1.3 Solutions

PBS (Phosphate Buffered Saline) and PBS-Tw: 0.13 M NaCl, 7 mM Na_2HPO_4, 3 mM NaH_2PO_4, pH adjusted to 7.5 with HCl. Routinely, a 10x stock solution was prepared and diluted in water before use. 0.1% Tween-20 was added for PBS-Tw

TBS (Tris Buffered Saline) and TBS-Tw: 10mM Tris-base, 150mM NaCl, pH adjusted to 7.5 with HCl. Routinely, a 10x stock solution was prepared and diluted in water before use. 0.1% Tween-20 was added for TBS-Tw

TE (Tris-EDTA): 1mM Tris-Cl pH 7.5, 0.1mM EDTA, pH 8.0. Routinely, a 10x stock solution was prepared and diluted in sterile water before use.

10 x Tris-Glycine: Trizima base 30.3 g/l, Glycine 144 g/l.

2.1.4 Bacterial strains

From Invitrogen

MAX Efficiency DH5α Competent Cells

One shot TOP10 Chemically competent cells

One shot BL21(DE3) pLysS

From Stratagene

BL21 Codon Plus (DE3-RIL)

XL1-Blue Supercompetent Cells

2.1.5 Bacterial storage

E. coli strains were stored at 4°C on solid medium containing the appropriate antibiotic for up to 1 week. For long term storage, glycerol stocks were made by mixing an overnight culture with 30% sterile glycerol and freezing in a dry ice/ethanol bath before storing at -80°C.

2.2 Molecular biology techniques

2.2.1 Plasmid preparation

For plasmid preparation a QIAGEN Miniprep or Maxiprep kit was used according to the manufacturer's instructions.

2.2.2 Restriction digests and ligation reactions

DNA was digested in a final volume of 20 µl at 37°C for 1 h. All restriction enzymes were from New England Biolabs (NEB), and digestions were performed in the appropriate NEB buffer. All digestions were analysed by agarose gel electrophoresis.

Ligation reactions were performed using Quick T4 DNA ligase (New England Biolabs) as recommended by the manufacturer:

10 µl 2X Quick Ligation Buffer

50 ng vector DNA

3X molar excess of insert DNA

1µl of Quick T4 DNA Ligase

Double distilled (dd) H_2O to 20 µl

Ligation was carried out for 5 minutes at room temperature (approximately 23 ˚C).

2.2.3 Agarose gel electrophoresis

Horizontal agarose gels were routinely used for the separation of DNA fragments. All agarose gels were 1% w/v agarose in 1xTBE, except for fragments being separated for band excision and extraction of the DNA, for which 0.6% agarose gels were used. Samples were loaded in 1x loading dye (6x stock: 0.25% bromophenol blue; 0.25 xylene cyanol FF; 30% v/v glycerol). Gels also contained 1µg/ml ethidium bromide to allow visualisation of DNA under UV light. Gels were run at ~6V/cm of the distance between the two electrodes. 1Kb ladder (New England Biolabs) was used for determination of fragment size. Visualisation of DNA fragments by UV light was carried out with a Geldoc trans-illuminator (Biorad).

2.2.4 Purification of DNA from agarose gels

Following agarose gel electrophoresis, DNA gel slices were excised using UV light to visualise the position of the fragment. DNA was extracted from the agarose gel using a Qiagen gel extraction kit as directed by the manufacturer's protocol.

2.2.5 DNA sequencing

Sequencing reactions were carried out using the BigDye Terminator v.3.1 Cycle Sequencing Kit (Applied Biosystems) according to the manufacturer's instructions. The Cancer Research UK Sequencing Service was used for analysis of the reactions. Sequences were analysed using Sequencher v4.5 software (Genecodes).

2.2.6 Transformation of *E. coli* with plasmid DNA

Plasmid transformation of *E. coli:*

50 µl of chemically competent cells (TOP10, Invitrogen) were mixed with DNA and incubated on ice for 30min. The cells were then subjected to heat shock at 42°C for 30 sec, and cooled on ice for 2 minutes. 0.25 ml of SOC was then added and the tubes were

incubated at 37°C with shaking for 1 hour. Cells were then plated on LB agar plates with the appropriate antibiotic.

2.2.7 Conventional Cloning

Conventional cloning was carried out by polymerase chain reaction (PCR) using appropriate primers that incorporated convenient restriction enzyme sites for the expression vector to be used.

Pfu Ultra polymerase (Stratagene) was used as follows:

5 µl 10x *Pfu* buffer

5 µl DMSO

0.4 mM of each dNTP

125 ng forward primer

125 ng reverse primer

1 µl *Pfu turbo* Polymerase

50 ng DNA template

dH_2O to 50 µl

For the amplification of Cep63 cDNA, PCR reactions were usually performed with the following cycling parameters:

1 cycle: 5 min at 95°C

30 cycles: 30 sec at 95°C

30 sec at the primer annealing temperature (50 – 60 ˚C)

2 min at 72°C (or 1 min per kb of DNA to amplify)

1 cycle: 10 min at 72°C

Blunt end PCR products were then checked by agarose gel electrophoresis to visualise the size of the fragment and to detect the presence of potential off-target products. PCR reactions generating only one product were used in a Topo cloning reaction to insert the fragment into the pCR-BluntII TOPO vector (Invitrogen) using the kit as per manufacturer's instructions. Topo vectors were amplified in TOP10 *E. coli* and DNA was prepared by miniprep (Qiagen). Topo vectors were checked by restriction digest to select clones containing the correct fragment size, and then positive clones were sequenced. Vectors containing the correct inserts were digested with the appropriate restriction enzymes and DNA fragments were purified by agarose gel electrophoresis and gel extraction. Expression vectors were digested and purified in the same way. Cut fragment and vector were ligated as described above and then amplified in TOP10 *E. coli* (Invitrogen).

For cloning into the pMAL-c4x expression vector, Cep63 was amplified by PCR using a forward primer with a BamHI restriction site and a reverse primer with the SalI site. These restriction sites were also included in the primers used for the generation of Cep63 fragments. The same procedure, using the same restriction enzyme sites, was also carried out with the *Xenopus* Cep63 sequence.

For cloning into the pIRES puro 3 GFP-Flag mammalian expression vector, Cep63 was amplified with primers containing AgeI and NotI restriction sites. The same restriction sites were used for the cloning of Cep152 N and C terminal halves. I was unable to generate TOPO clones with the full-length human Cep152 sequence.

For cloning *Xenopus laevis* Cep152 (XCep152) proteins (full length, N-terminal half and C-terminal half) into pcDNA3, forward primers contained BamHI restriction sites and reverse primers contained NotI sites.

2.2.8 Gateway cloning

Gateway cloning was carried out as described by the Gateway manual (Invitrogen). PCR primers were designed to include *att*B sites and the IMAGE clones listed below were used as templates. PCR reactions were checked by agarose gel electrophoresis to ensure that only one product was made and the PCR reaction was then used directly in the BP reaction with pDONR221. *E. coli* were then transformed with the BP reaction and amplified pDONR plasmids were checked by restriction digest and sequencing. Correct pDONR plasmids were used for LR reactions to produce Destination vectors with the desired insert.

LR reactions were performed with the following destination vectors:

pcDNA5 Dest FRT/TO Flag

pcDNA5 Dest FRT/TO YFP

both kind gifts from Zuzanna Horejsi.

2.2.9 Colony PCR

Colony PCR was used to screen large numbers of colonies for the presence of inserts during conventional and Gateway cloning protocols for Cep152 (human) cDNA.

Preparation of colonies

Single colonies were picked and resuspended in 100 µl ddH_2O, vortexed, then incubated for 10 minutes at 100 °C followed by centrifugation at 16,000 x g for 5 minutes. The resulting DNA suspension was used in the PCR reaction.

PCR reaction

5 µl DNA suspension

5 µl 10 x buffer

5 µl DMSO

4 µl 25 mM $MgCl_2$

0.4 µl 25 mM dNTP mix

2 µl of primer mixture (100 pmol/µl stocks; each diluted 1:10)

0. 25 µl Simple Red Taq polymerase (Thermo Scientific)

For reactions with primers spanning the full length Cep152 an extension time of 5 minutes was used. For reactions containing primers for the C-terminal half of Cep152 and extension time of 2 minutes was used. Annealing temperature was 50 – 55 °C.

2.2.10 Cep63 and Cep152 templates

XCep63: XCEP63 BC088974 *Xenopus laevis* hypothetical LOC496369. Coding sequence 1947 bp.

Cep63: CEP63 transcript variant 2 Homo sapiens centrosomal protein 63kDa IMAGE:5951988 complete cds. Coding sequence 1626 bp.

XCep152: *Xenopus laevis* hypothetical protein LOC446951 IMAGE:5084879. Coding sequence 4992 bp.

Cep152: Hs CEP 152kDa, mRNA IMAGE:40125733 complete cds. Coding sequence 4965 bp.

2.2.11 Cep63 cloning

The human Cep63 protein sequence was divided as follows to produce truncated forms of the protein. These truncated sequences were cloned into the pMAL-c4x vector for expression of MBP-tagged proteins in *E. coli.* Gateway cloning, as described above, was used to clone the same truncation sequences into vectors for expression in mammalian cells.

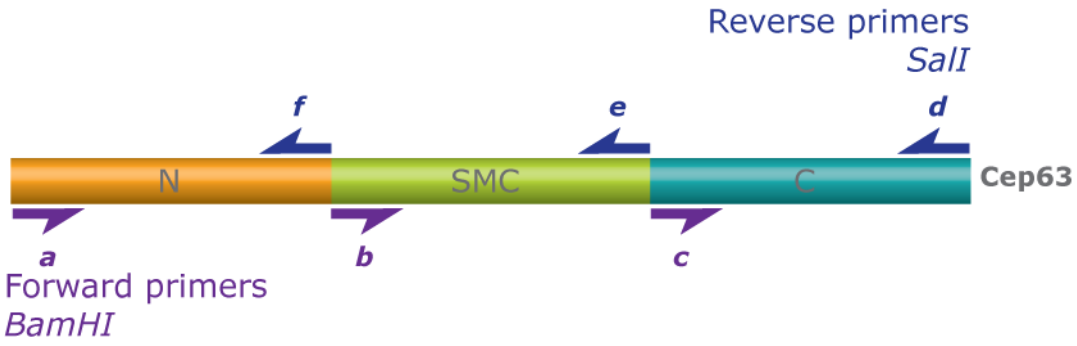

	Sequence 5' – 3' (pMAL-c4x)	Sequence 5' – 3' (Gateway)
a	GGATCCGAGGCTTTGTTAGAAGGAATAC	GGGG**ACAAGTTTGTACAAAAAAGCAGGCT**TCGAGGCTTTGTTAGAAGGAATAC
b	GGATCCTCTGAAATTGAGAGGTTAACTGC	GGGG**ACAAGTTTGTACAAAAAAGCAGGCT**TCTCTGAAATTGAGAGGTTAACTGC
c	GGATCCTTACATCAGCGAGATATCACTATTG	GGGG**ACAAGTTTGTACAAAAAAGCAGGCT**TCTTACATCAGCGAGATATCACTATTG
d	GTCGACCTACTTTAAGGCTGTGAATTGTCTC	GGGG**ACCACTTTGTACAAGAAAGCTGGGT**CCTACTTTAAGGCTGTGAATTGTCTC
e	GTCGACCTATAACTCCTGAGTTAGATGGGAG	GGGG**ACCACTTTGTACAAGAAAGCTGGGT**CCTATAACTCCTGAGTTAGATGGGAG
f	GTCGACCTACCGATCTTCCCTGTGATTTTTG	GGGG**ACCACTTTGTACAAGAAAGCTGGGT**CCTACCGATCTTCCCTGTGATTTTTG

Bold letters indicate the *attB* recombination site required in the first step of Gateway cloning. Red letters highlight the stop codon.

No.	Domain	Start-end nt	primers	Size bp	Start-end aa	Size kDa	Size +MBP
1	N-term	1-408	a/f	408	1-135	16	60
2	SMC-like	409-1272	b/e	864	136-424	33	77
3	C-term	1273-1626	c/d	357	425-841	14	58
4	N-SMC	1-1272	a/e	1272	1-424	49	93
5	SMC-C	409-1626	b/d	1218	136-841	47	91
6	Full	1-1626	a/d	1626	1-841	63	107

Table 2 Human Cep63 truncation proteins

Cep63 full length was also cloned into pIRESpuro3GFP-Flag (a kind gift from Tohru Takaki), for mammalian expression and generation of stable cell lines, using AgeI and NotI restriction sites and primers as follows:

Cep63 Forward AgeI

ACCGGTGAGGCTTTGTTAGAAGGAATAC

Cep63 Reverse NotI

GCGGCCGCCTACTTTAAGGCTGTGAATTGTC

2.2.12 Cep152 cloning

Xenopus Cep152 full length sequence was cloned into the pMAL-c4x vector for expression in *E. Coli* using BamHI and SalI restriction sites. Primer sequences are as follows:

Forward BamHI

5′ GGATCCTCTATCGACTTTGATAGTG 3′

Reverse SalI

5′ GTCGACTTAGTTGAAGTTATTTAAG 3′

Human Cep152 was cloned using the Gateway system to generate vectors for mammalian cell expression using the following primers:

Forward

5′ GGGG**ACAAGTTTGTACAAAAAAGCAGGCT**TCTCATTAGACTTTGGCAGTG 3′

Reverse

5′ GGGG**ACCACTTTGTACAAGAAAGCTGGGT**CTTAGTCTAGATTAACAAATG 3′

Bold letters indicate the ***attB*** recombination site required in the first step of Gateway cloning.

Human Cep152 N- and C-terminal halves were cloned into a pIRESpuro3GFP-Flag vector also for mammalian expression using AgeI and NotI restriction sites and primers as follows:

	Forward primer *AgeI*	Reverse primer *NotI*
N	ACCGGTTCATTAGACTTTGGCAGTGTGGCAC	GCGGCCGCTTAAACATCACTGGTGGTTACTTGGT
C	ACCGGTATTTCCAAGAAAGAGATGGCA	GCGGCCGCTTAGTCTAGATTAACAAATGGGC

C152 truncation	Start-end nt	bp	Start-end aa	Size kDa
N-terminal half	1-2409	2409	1-803	93
C-terminal half	2410-4965	2556	804-1654	96
full length	1-4965	4965	1-1654	189

Table 3 Human Cep152 truncation proteins

During cloning of all Cep152 constructs, many colonies were screened at each step by colony PCR due to low efficiency of Cep152 cloning. This was the case for conventional and Gateway cloning.

2.2.13 Expression vector gifts

pEGFP-Cep152 was a kind gift from Ingrid Hoffmann (German Cancer Research Center, DKFZ, Heidelberg). Flag-Plk2 and Myc-Plk4 constructs were also gifts from Ingrid Hoffmann's lab.

pIRESpuro3 vector modified with an N-terminal GFP-Flag tag was generated by Tohru Takaki (Petronczki lab, Clare Hall). pcDNA5Dest FRT/TO-Flag and YFP vectors were generated by Zuzanna Horejsi (Boulton lab, Clare Hall).

2.2.14 Site directed mutagenesis (SDM)

Point mutations in the Cep63 and Cep152 ORFs were introduced by using the QuikChange site-directed mutagenesis kit (Qiagen), Pfu Turbo DNA polymerase and a temperature cycler following manufacture's instructions. Presence of the point mutation(s) was then confirmed by DNA sequencing.

pIRES puro3 GFP-Flag-Cep63 was used as a template for SDM to mutate the site targeted by siRNA 63-2. The SDM reaction was carried out with the following primers:

Wobble 2 F	GAGGAATTCCGTCAAAAGAGCTTAGATTGGGAGAAGCAACGCTTG
Wobble 2 R	CAAGCGTTGCTTCTCCCAATCTAAGCTCTTTTGACGGAATTCCTC

Table 4 Cep63 mutagenesis primers

For SDM of pEGFP-Cep152, the following primers were used:

Q265P F	AAAGTTAAATGAAAGTGAACGTCCAATTCGATATCTGAATCACCAGC
Q265P R	GCTGGTGATTCAGATATCGAATTGGACGTTCACTTTCATTTAACTTT
R987X F	ACCGGCAATTTTTAGATGATCACTGAAATAAAATTAATGAGGTGCTT
R987X R	AAGCACCTCATTAATTTTATTTCAGTGATCATCTAAAAATTGCCGGT

Table 5 Cep152 mutagenesis primers

2.2.15 Reverse transcription-PCR (RT-PCR)

RNA extraction was carried out using the RNeasy kit (Qiagen). RT-PCR reactions were carried out using a one-step RT-PCR kit (Qiagen) with the primers shown on the next page. 2 μg RNA was used per 50 μl reaction.

Name	Sequence	product length, bp (Cep63 variant)
2F	GTTGCCAAAACAAAGGGGATTTGGTG	1493 bp (1&2); 1355 bp (3&4)
2R	CTCATGTAAACCCAATTCCAATTTC	
4F	AAACCAACACACAGCAGAAC	483 bp (variant 1)
4R	CTTTAAGGCTGTGAATTGTC	
5F	AGTTGGATGTGACACATAAG	548 bp (all variants)
5R	CTGCTGCTCCTGTAGGACAG	
6F	CATACATGAGGCCAGAATAC	347 bp (1&2); 209 bp (3&4)
6R	GTTCTTTCAACTTCTTAATC	
G1F	CTGCACCACCAACTGCTTAG	GAPDH 111 bp control
G1R	ACAGTCTTCTGGGTGGCAGT	
G2F	TTCACCACCATGGAGAAGG	GAPDH 104 bp control
G2R	TTCACACCCATGACGAACAT	

Table 6 Cep63 RT-PCR primers

2.3 Protein Expression

2.3.1 Expression of recombinant proteins

MBP tagged recombinant proteins

MBP tagged Cep63, XCep63 and XCep152 proteins and truncations were expressed in BL21 Codon Plus (DE3-RIL) cells (Stratagene) and purified on amylose resin and eluted with maltose according to manufacturer's protocol (MBP purification protocol, NEB). *E. coli* were grown at 37 °C until an optical density (OD) at 600 nm of 0.5 was reached, then cultures were shifted to 16 °C and induced with 0.3 mM IPTG for 2-4 hours. Cells were collected by centrifugation at 4,000 x g for 20 minutes at 4 °C and pellets were resuspended in column buffer (20 mM Tris HCl pH 7.5, 200 mM NaCl, 1 mM EDTA, 1 mM DTT) plus Complete protease inhibitors. Cells were passing through a cell disruptor twice then incubated with amylose resin for 2 hours at 4 °C. Washes and elution were carried out in a glass column with diameter 2.5 cm. Resin was washed with 12 column volumes of column buffer and bound protein was eluted in column buffer

containing 10 mM maltose. Fraction size was 1/5 of the column volume; 20 fractions were collected. Proteins were dialysed to remove maltose before use in experiments.

2.3.2 *In vitro* transcription-translation

^{35}S-methionine (Promix, Amersham) labelled recombinant proteins were generated using a SP6 or T7 quick-coupled transcription- translation reticulocyte lysate (TNT, Promega). XCep63 was under the control of an SP6 promoter. Reactions were set up as follows:

TNT SP6 master mix, 40 µl

DNA, 400 ng

Promix ^{35}S-Methionine, 3 µl

ddH_2O to 50 µl

Reactions were incubated for 90 minutes at 30 °C.

2.3.3 Quantification of proteins

Protein concentrations were determined using the Bradford method (Bradford, 1976).

Protein samples were mixed with Bradford's reagent (Biorad) and the absorbance at 595 nm was measured on a spectrophotometer. Protein absorbance measurements were converted to concentration using standard curve readings from a range of known bovine serum albumin (BSA) concentrations.

2.4 Protein Techniques

2.4.1 SDS Poly Acrylamide Gel Electrophoresis (SDS-PAGE)

SDS-PAGE gels were poured using the Biorad Protean mini-gel apparatus unless otherwise stated. Stacking gels were made using 40% Acrylamide/Bisacrylamide 37.5:1

(Biorad) and resolving gels were made using Ultra Pure 30 % Acrylamide and Ultra Pure 2% Bisacrylamide (National Diagnostics UK). SDS-PAGE gels were run at 100 V, constant voltage. Biorad Precision Plus dual colour protein markers were used as molecular weight standards.

SDS-PAGE running buffer: 1 x Tris-glycine, 0.1% SDS

Resolving gel	7.5%	10%	15%	Stacking gel	4%
30% Acrylamide	2.5	3.34	5	40% Acryl/Bis	1
2% Bisacrylamide	0.97	0.65	0.43		
1.5 M Tris-HCl, pH 8.8	2.5	2.5	2.5	0.5 M Tris-HCl pH 6.8	2.5
10% SDS	0.1	0.1	0.1	10% SDS	0.1
ddH2O	3.8	3.3	1.9	ddH2O	6.3
APS	0.1	0.1	0.1	APS	0.1
TEMED	0.01	0.01	0.01	TEMED	0.01
Total volume (ml)	*10*	*10*	*10*	*Total volume (ml)*	*10*

Table 7 SDS-PAGE gel recipes

Phos-tag™ SDS-PAGE gels were prepared with Phos-tag™ AAL-107 (NARD Institute Ltd., Japan) and 40% Acrylamide and 2% Bisacrylamide from Biorad. Phos-tag gels were cast using the Biorad Protean mini-gel apparatus and run for 20 mA, constant mA, per gel. Before transfer to nitrocellulose membrane, Phos-tag gels were washed twice for 15 minutes in transfer buffer containing 10 mM EDTA, then once in transfer buffer alone.

	Phos-Tag 20 µM
40% Acril	1.88 ml
2% BisAcril	0.49 ml
1.5 M Tris-Cl, pH 8.8	2.5 ml
5 mM Phos-Tag	40 µl
10 mM $MnCl_2$	40 µl
10% SDS	100 µl
10% APS	100 µl
TEMED	10 µl
ddH_2O	4.80 ml
Total volume (ml)	*10*

Table 8 Phos-tag acrylamide gel recipe

Other SDS-PAGE gels used include Nupage Novex Bis-Tris 4-12% or tris-acetate 7% mini gels (Invitrogen). These gels were run using MOPS or MES buffer (Invitrogen) at 100 V. 7% Tris-acetate gels were used when carrying out a Western blot for ATM phospho-Serine 1981 since ATM is a large protein, which migrates slower that 250 kDa.

Coomassie blue staining: After separation of loaded protein samples, polyacrylamide gels were incubated in Coomassie blue stain (0.5% Coomassie blue, 45% methanol, 10% acetic acid) for 5 minutes and incubated with destain solution (25% methanol, 7% acetic acid) overnight.

Sypro Ruby staining: as per manufacturer's instructions (Invitrogen).

2.4.2 Western blotting

Transfer buffer: 1 x Tris-Glycine (TG), 0.01% SDS, 20% methanol

Proteins were transferred from SDS-PAGE gels to Protran nitrocellulose membrane (Whatman) for 2 hours to overnight at 100 mA using Biorad wet transfer apparatus for mini-gels. Transfer buffer with 2 x TG was used when detection of large proteins was required; routinely used for Cep152 and ATM phospho-Serine 1981 Western blots.

Membranes were blocked for 30 minutes in 5% (w/v) non-fat powder milk in PBS-Tw (PBS + 0.1% Tween) at room temperature. Antibodies were prepared at dilutions indicated in table 9 in 5% milk in PBS-T unless stated otherwise. Membranes were incubated overnight at 4°C with primary antibodies, followed by 3 washes in PBS-Tw. Primary antibodies were detected using HRP-conjugated secondary antibodies (dilution indicated in Table) in 5% milk PBS-Tw. Membranes were washed 3 times and antibody complexes detected using ECL substrate (GE Healthcare), and visualised on Hyperfilm ECL (GE Healthcare). TBS-Tw (TBS, 0.1% Tween 20) was used for Western blotting with antibodies directed specifically against phosphorylated-protein antigens.

Membrane stripping and re-probing:

For re-probing membranes, bound antibodies were removed by incubation with stripping buffer (100mM ß-mercaptoethanol, 2% SDS, 62.5 mM Tris-HCl, pH6.7) for 10 minutes at 55°C. The membranes were washed three times for 10 minutes in PBS-Tw, followed by blocking and probing as described above.

2.4.3 Preparation of cell lysates for Western blot

Cells were washed in PBS, collected in 5 ml PBS using a cell lifter (Corning) and collected by centrifugation. Cell pellets were resuspended in RIPA buffer plus either Complete or LPC protease inhibitors. Cells were incubated on ice for 5 minutes then sonicated for 10 seconds, three times. Insoluble material was collected by centrifugation at 16,000 x g and the resulting supernatant was retained. For analysis of histone proteins (phospho-histone H3 and γH2AX) by Western blot, cells were lysed directly in Laemmli buffer, boiled and sonicated.

RIPA buffer: 150 mM NaCl, 1% Igepal, 0.1% SDS, 0.5% sodium deoxycholate in MilliQ water.

2.4.4 Pull-down of tagged proteins from cell lysates

Flag IP buffer: 50 mM Tris HCl, pH 7.4, 150 mM NaCl, 1 mMEDTA, 1% Triton X100

Flag immuno-precipitations were carried out using anti-Flag M2 affinity gel (SIGMA A2220). All experiments were carried out according to the manufacturer's instructions. Small-scale experiments for analysis by Western blot were carried out using one 10 cm plate and approximately 1 mg of total protein (whole cell lysates). Proteins were eluted by boiling the resin in Laemmli buffer.

For large-scale experiments for analysis of Flag-Cep63 binding proteins by mass spectrometry, 20 litres of 293 Flag-Cep63 or Flag-Empty cells were used. This volume of cells (grown by cell services in suspension) gave 15 ml cell pellets. Cell pellets were resuspended in 50 ml Flag lysis buffer and sonicated 5 times for 1 minute on ice. The lysates was centrifuged in a Sorval centrifuge with the SS34 rotor at 16,000 x g for 30 minutes at 4 °C. A Bradford assay was performed on the cleared cell lysates in order to equalise the amount of protein in the control and experimental samples; 1300 mg cell lysates was used for each sample. First the lysates was incubated with 500 µl protein A-agarose beads for 1 hour at 4 °C with agitation. Agarose beads were pre-washed three times with 10 ml TBS. Agarose beads were removed by centrifugation at 500 x g and the supernatant was passed through a 10 ml column (Biorad) to remove residual beads . The resulting lysates was incubated with 500 µl of anti-Flag M2 resin for 4 hours at 4 °C. Flag resin was washed 3 times with 10 ml TBS before use. Flag resin was then washed four times with 15 ml TBS 0.1% Triton X100, then 3 times with 15 ml TBS. Bound proteins were eluted in three elution steps, each with 500 µl of 0.5 mg/ml Flag peptide solution. For analysis by Western blotting; 5 µl of pre-cleared whole cell lysates and each elution fraction was mixed with Laemmli buffer and loaded on a SDS-PAGE gel. For mass spectrometry analysis 75 µl of each fraction was separated by SDS-PAGE

on a NuPAGE 4-12% Bis-Tris gel. The first elution fraction of each sample (Flag-Empty and Flag-Cep63) was sent for mass spectrometry analysis. The gel was stained using Sypro Ruby (Invitrogen) and visualised with a fluorescence scanner. The resulting picture was printed and the gel aligned on a glass plate on top. The entire lane of each elution fraction was cut into approximate 1 mm bands and put in a 96-well plate and sent to the mass spectrometry facility (Mark Skehel, Protein Analysis & Proteomics, London Research Institute Clare Hall Laboratories).

This protocol was repeated with cells incubated in the presence (or absence) of 0.2 mg/ml Phleomycin for 2 hours before collection.

2.4.5 Cell fractionation

Solutions

Sucrose buffer: 10 mM Hepes, pH 7.9, 340 mM sucrose, 3 mM $CaCl_2$, 2 mM magnesium acetate, 0.1 mM EDTA. Add Complete protease inhibitors fresh.

Nuclear Lysis buffer: 20 mM Hepes, pH 7.9, 150 mM KCl, 3 mM EDTA, 1.5 mM $MgCl_2$, 10% glycerol. Add Complete protease inhibitors fresh.

Nuclease Incubation buffer: 150 mM Hepes, pH 7.9, 1.5 mM $MgCl_2$, 10% glycerol.

All centrifugation steps were carried out in a bench top microcentrifuge at 4 °C.

293 FlpIn cell lines stably expressing Flag-Empty or Flag-Cep63 (one 15 cm plate each) were trypsinised, washed in PBS and resuspended in 2 ml sucrose buffer + 0.5% Igepal and incubated on ice for 10 minutes. Nuclei were collected by centrifugation at 3,900 x g for 20 minutes. The resulting supernatant was removed and kept on ice (this was the cytoplasmic fraction). The nuclear pellet was resuspended in sucrose buffer without detergent, and then centrifuged at 3,900 x g for 20 minutes. The supernatant was discarded and pellets were resuspended in 1 ml nuclear lysis buffer and incubated on a rotating wheel at 4 °C for 30 minutes. Centrifugation was then carried out at 16,000 x g for 30 minutes and the supernatant was removed and kept as the nucleoplasmic fraction.

The insoluble pellet was incubated in 300 µl nuclease incubation buffer with 5 µl benzonase (25U/µl stock, Novagen) for 1 hour at room temperature. Insoluble material was then sedimented by centrifugation at 16,000 x g for 30 minutes and the supernatant was removed and kept as the chromatin fraction. Fractions were analysed by SDS-PAGE and Western blotting.

2.4.6 Centrosome preparation from cultured cells

Purification of centrosomes from KE37 human lymphoblast cells was carried out using a protocol based on the paper Structural and Chemical Characterization of Isolated Centrosomes (Bornens et al., 1987). Centrifugation steps were carried out at 4 °C for 5 minutes at 1,200 x g for all cell collection and washing steps and all other steps were carried out on ice with pre-chilled solutions.

Solutions

Lysis buffer: 1 mM Tris-HCl pH 8.0, 0.1% β-mercaptoethanol, 0.5% Igepal, 0.5 mM $MgCl^2$. Complete protease inhibitors added fresh.

DNase incubation buffer: 0.5 M K-PIPES pH 7.2, 1 mM EDTA.

Sucrose gradient buffer: 10 mM K-PIPES pH 7.2, 1 mM EDTA, 0.1% β-mercaptoethanol, 0.1% Triton X-100.

2 x 10^8 KE37 cells were incubated for 1 hour in 0.2 µM nocodazole then collected by centrifugation. Cells were washed twice in 50 ml PBS and once in 8% sucrose in 10 times diluted PBS. Cells were resuspended gently in 25 ml of lysis buffer by pipetting with a 10 ml pipette with a 2 mm hole. The tube was inverted 3 times and incubated for 5 minutes. Swollen nuclei were sedimented at 1,200 x g for 10 minutes and the supernatant was filtered through a 70 µm Nylon cell strainer (BD Falcon). The filtered lysates was then incubated for 30 minutes with 600 U of benzonase in 0.5 ml DNase incubation buffer. The supernatant was then poured gently on top of a discontinuous sucrose gradient in a SW28 centrifuge tube (Beckman, Ultraclear) as follows: 3 ml 70%

(w/w) sucrose, 2 ml 50% sucrose and 4 ml 40% sucrose prepared in sucrose gradient buffer. Centrifugation was carried out at 26,000 rpm for 1 hour in an SW28 swing rotor in a Beckman Ultracentrifuge. The gradient was collected from the bottom using a 19-gauge needle to pierce the tube and fractions were collected by hand. The first 1.5 ml were discarded and 15 x 0.5 ml fractions were collected subsequently. For Western blot analysis, 50 µl of each fraction was resuspended in 1 ml 10 mM K-PIPES pH 7.2 then centrifuged at 16,000 x g for 15 minutes at 4 °C. Liquid was removed and the remaining centrosome pellet (invisible) was resuspended in 20 µl 1 x Laemmli buffer. Samples were analysed by SDS-PAGE and Western blotting on a 10% Anderson gel.

For immunofluorescence analysis 20 µl of each fraction was resuspended in 3 ml 10 mM K-PIPES, pH 7.2 and centrifuged onto a poly-L-Lysine (0.01%, Sigma) coated glass coverslip at 20,000 x g for 10 minutes in a HB-6 swing rotor (Sorvall). Glass coverslips were positioned on top of a Perspex disc supported by a fixed solid support in modified 15 ml glass Corex tubes (homemade). Coverslips were removed and post-fixed in -20 °C methanol and rehydrated with three 5 minute washes in PBS 0.1% Trition X100. Immunofluorescence was carried out as described for immunofluorescence of cultured cells. Typically, most centrosomes were found in fractions 5 and 6.

Centrosome preparation from 3T3 MEFs was carried out using the solutions and the protocol described above, but the starting number of cells was 3 x 10^7 per sample.

2.4.7 Analytical gel filtration of cell lysates

Gel filtration was carried out using a Superdex 200 10/300 GL column (GE Healthcare) with eluent buffer (50 mM Phosphate buffer pH7.0, 150 mM NaCl). An AKTA FPLC (Amersham – now GE Healthcare – model UPC900) was used and set to a flow rate of 0.5 ml/minute. A sample size of 500 µl was used.

Calibration was carried out using 500 µl Blue dextran (2 mg/ml). Elution was at 15 minutes, which determined the void volume of the column as 7.5 ml. Protein standards (Sigma) were dissolved in 500 µl phosphate buffer at the following concentrations:

Thyroglubulin 0.8 mg/ml and Albumin 1 mg/ml

β-amylase 0.8 mg/ml and carbonic anhydrase 0.6 mg/ml

Apoferritin 1 mg/ml and alcohol dehydrogenase 0.5 mg/ml

Elution volume (V_e) was divided by void volume (V_0) and a standard curve was drawn using semi-logarithm graph paper.

Three 10 cm plates of 293 cells stably expressing YFP-Cep63 (clone 10) were trypsinised and the cytoplasmic fraction was prepared as described above. Before loading on the column, the salt concentration of the extract was adjusted to 150 mM NaCl. Ten mg was loaded in 500 µl. Fractions 1 to 6 were 1 ml and the subsequent fractions were 0.5 ml. Fractions 1 to 12 were analysed by SDS-PAGE; 10 µl of each fraction was loaded. Estimations of protein complex size were drawn from the standard curve.

2.4.8 Antibodies

Cep63

Cep63 antibodies 47 and 49 were produced by Millipore. GST-tagged Cep63 (isoform b) was injected into rabbits and serum from the test bleeds and final bleeds were pooled and affinity purified using the recombinant protein. I generated the pDONR221-Cep63 vector, and from here on Millipore carried out the protein expression and purification, and the immunisation of rabbits. I tested serum throughout the immunisation process and gave feedback to Millipore. Millipore then affinity purified (AP) the antibodies using recombinant GST-Cep63.

Millipore immunisation protocol

Date	Procedure
17-Nov-2009	Pre-Bleed
17-Nov-2009	Injection
08-Dec-2009	Injection
29-Dec-2009	Injection
19-Jan-2010	Injection
01-Feb-2010	Bleed
09-Feb-2010	Injection
22-Feb-2010	Bleed
25-Feb-2010	Bleed
01-Mar-2010	Shipping
02-Mar-2010	Injection
09-Mar-2010	Bleed
30-Mar-2010	Injection
07-Apr-2010	Bleed
12-Apr-2010	Bleed
15-Apr-2010	Exsang

Cep63 47AP and 49AP antibodies were used 1:1000 to 1:5000 for immunofluorescence and at the same dilutions for Western blotting.

Cep152

Cep152 antibody no. 9 was produced by immunisation of rabbits with peptides a and b (below) (Pettingill technology Ltd., PTL). Affinity purification was carried out using 5 mg of a 1:1 mixture of peptides *a* and *b* conjugated to a Sulfolink column (Pierce). 10 ml of final bleed serum was passed through the column. The column was then incubated with 5 ml of the serum for 4 hours at 4 °C with agitation, then the other 5 ml was incubated with the column overnight. The column was washed with 12 ml coupling buffer (Pierce) and antibody was eluted with 0.1 M Glycine-HCl, pH2.5. Eight 1 ml fractions were collected and each neutralised with 100 µl Tris-HCl, pH8.0. Cep152 9AP4 (affinity purified fraction 4) was used at a dilution of 1:100 for Western blotting.

Cep152 peptide a: *C*EYDEEDYEREKELQ (N-terminal peptide)

C added for KLH (Keyhole Limpet Hemocyanin) conjugation.

Cep152 peptide b: CGHPSRHKADRLKSDFKK (C-terminal peptide)

PTL 77 day rabbit immunisation protocol

Day	Date	Technique
0	26-Nov-09	Pre-bleed (10ml) + Immunisation in Complete Freunds Adjuvant
14	10-Dec-09	Boost 1 in Incomplete Freunds Adjuvant
28	24-Dec-09	Boost 2 in Incomplete Freunds Adjuvant
35	31-Dec-09	TEST BLEED 1 (10ml)
42	07-Jan-10	Boost 3 in Incomplete Freunds Adjuvant
49	14-Jan-10	TEST BLEED 2 (10ml)
56	21-Jan-10	Boost 4 in Incomplete Freunds Adjuvant
63	28-Jan-10	TEST BLEED 3 (10ml)
70	04-Feb-10	Boost 5 in Incomplete Freunds Adjuvant
77	11-Feb-10	TERMINAL BLEED

2.4.9 Commercial Antibodies

Primary antibody	source	company	catalogue no.	IF	WB
ATM PSer1981	rabbit	Rockland	200-301-400		1:1000
α-tubulin	mouse	SIGMA	T6199	1:10,000	1:10,000
Cdk1	mouse	Julian Gannon	clone A17	1:500	1:1000
Centrin 20H5	mouse	Millipore	64-1624	1:500	
Centrin 2	rabbit	Santa Cruz	sc-27793-R	1:500	
Centrin 3	mouse	abcam	ab54531		1:1000
Cep152-479	rabbit	Bethyl	A302-479A	1:1000	1:1000
Cep152-480	rabbit	Bethyl	A302-480A		
Cep63 PTG	rabbit	PTG Lab	16268-1-AP		1:1000
CPAP	rabbit	P. Gönczy	gift	1:1000	1:1000
Cyclin B	mouse	Julian Gannon	V152		1:1000
FLAG M2 AI	mouse	SIGMA	F3165	1:1000	1:5000
GFP	rabbit	Julian Gannon		1:1000	1:1000
GFP	mouse	Roche	11814460001	1:1000	1:1000
γ-tubulin	mouse	SIGMA	T5326	1:10,000	1:10,000
γ-tubulin	rabbit	SIGMA	T3559	1:1000	
ninein	rabbit	Abcam	ab4447	1:1000	
pericentrin	rabbit	Covance	PRB-432C	1:1000	
Phospho-Chk1 Ser 345	rabbit	Cell Signaling	2341		1:1000
Phospho Histone H3	mouse	Cell Signaling	9706	1:1000	1:1000
Phospho histone H3	rabbit	Upstate	06-570	1:1000	1:1000
Phospho-p53 Ser15	rabbit	Cell Signaling	9286		1:1000
Phospho-(Ser/Thr) ATM/ATR Substrate	rabbit	Cell Signaling	2851		1:1000
γ-H2AX clone JBW301	mouse	Millipore	05-636	1:1000	1:1000
γ-H2AX clone	rabbit	Upstate	07-164	1:1000	1:1000
SAS-6	mouse	Santa Cruz	81431	1:1000	1:1000
53BP1	rabbit	Sigma	B4436	1:1000	1:1000

Table 9 Commercial primary antibodies

Secondary antibody	source	Company	catalogue no.	IF	WB
Alexa Fluor 488 anti-rabbit (H+L)	goat	Invitrogen	A11008	1:400	
Alexa Fluor 488 anti-mouse IgG_1	goat	Invitrogen	A21121	1:400	
Alexa Fluor 594 anti-rabbit (H+L)	goat	Invitrogen	A11012	1:400	
Alexa Fluor 594 anti-mouse (H+L)	goat	Invitrogen	A11005	1:400	
Alexa Fluor 350 anti-mouse (H+L)	goat	Invitrogen	A21049	1:200	
anti-rabbit-HRP	goat	Dako	P0448		1:10,000
anti-mouse-HRP	goat	Dako	P0447		1:10,000

Table 10 Commercial secondary antibodies

2.5 *Xenopus laevis* egg extract

Xenopus laevis eggs were laid in MMR (see below) and extract was prepared in the absence of calcium ions in order to maintain the cytostatic factor (CSF) mediated arrest in metaphase of meiosis II.

2.5.1 Solutions for making CSF extract

10 x MMR: 1 M NaCl, 20 mM KCl, 10 mM MgCl2, 20 mM CaCl2, 1 mM EDTA, 50 mM Hepes, pH 7.8.

10 x XB: 0.1 M HEPES, pH 7.8*,* 0.5 M sucrose

20 x salt solution: 2 M KCl, 0.1 M EGTA, 40 mM $MgCl_2$

10 x XB and 20 x salt solution were filter sterilised, kept at 4 °C and diluted on the day of use.

50 x Energy mix: 375 mM creatine phosphate, 50 mM ATP, 10 mM EGTA, 50 mM $MgCl_2$

LPC Protease inhibitors: 30 mg/ml each of Leupeptin, pepstatin and chymostatin in DMSO.

Cytochalasin B: 10 mg/ml in DMSO

Energy mix, protease inhibitors and Cytochalasin B were aliquoted and stored at -20 °C.

2M sucrose for freezing extract: filtered and stored at 4 °C.

Solutions to be made on the day of use (quantities for 2 lots of eggs):

2% Cysteine solution: make 1 litre Cysteine in MilliQ water, adjust pH to 7.8 with NaOH.

XB wash buffer: make 1 litre 1 x XB, 1 x salt solution in MilliQ water. Check pH is 7.8. Chill on ice before use.

2.5.2 CSF extract preparation

Eggs were laid and collected in MMR solution. All was steps were carried out at room temperature (approximately 22 °C); all centrifugations were carried out at 4 °C and all steps after crushing of the eggs were carried out on ice. During all wash steps care was taken not to pour solutions onto the eggs directly, but on the side of the beaker. White or miscoloured eggs were removed using a 1.5 ml Pasteur pipette during all wash steps as and when necessary.

MMR solution was poured off and cysteine solution added to the eggs (approximately 200 ml at a time). Cysteine washes were repeated 3 times and the total incubation time was not longer than 10 minutes, in most cases eggs were completely de-jellied in 5 minutes. Eggs were then washed 3 times with XB wash buffer. XB wash buffer was then poured off and 14 µl of 10 mg/ml Cytochalasin B (in DMSO) and 14 µl of LPC protease inhibitors were added and the eggs were poured into a 15 ml polypropylene round-bottomed tube (Falcon 2059). Eggs were then packed by centrifuging for 1 minute at 300 x g in a swing bucket rotor (rotor 4250, Beckman Allegra X-22R). Excess liquid on top of the packed eggs was removed and the eggs were crushed by centrifugation in a swing rotor at 22,500 x g for 20 minutes (Beckman; rotor JS 13.1 12,000 rpm). The resulting cytoplasmic extract (middle golden yellow layer) was removed by puncturing the side of the tube with a 19-gauge needle and slowly removing the cytoplasmic layer with a 2 ml syringe. This extract was placed in a 5 ml

polypropylene round-bottomed tube (Falcon 2063). Energy mix was added (1:50 dilution) and LPC and Cytochalasin B were added (1:1000 dilution). The extract was then mixed gently using a 1.5 ml Pasteur pipette and then centrifuged at the same conditions for a further 15 minutes. In order to fit the 5 ml tubes in the JS 13.1 rotor, they were placed inside a 15 ml Falcon tube with 1 ml water to act as a cushion. The resulting extract was also removed by needle and syringe as above, and the extract placed in a fresh tube ready for use. Extract was kept on ice until use and was incubated at 23 °C during assays.

For long term storage the extract was mixed with 2 M sucrose (10% in the extract) and frozen in liquid N_2 in 20 µl aliquots, which form small balls when added to the liquid N_2.

2.5.3 Checking the CSF arrest of egg extracts

10 µl samples of extract were incubated at 20 °C with 3000 sperm nuclei per µl in the presence or absence of 0.4 mM $CaCl_2$. At times 0, 20, 30, 45 and 60 minutes after calcium addition; 1 µl of each extract was taken and mixed with 1 µl fixative including Hoechst on a glass slide and a coverslip placed on top. Slides were then analysed with a fluorescence microscope. The sample without $CaCl_2$ should contain mitotic shaped nuclei throughout the incubation, but extract activated with $CaCl_2$ should start forming round nuclei with a nuclear membrane between 30 and 60 minutes.

Fixative (1.5 ml): 0.5 ml EB buffer, 150 µl formaldehyde (37%), 3 µl Hoechst (1 mg/ml), 0.75 ml glycerol, up to 1.5 ml with ddH_20. Stored at -20 °C.

EB buffer: 100 mM KCl, 2.5 mM $MgCl_2$, 50 mM Hepes pH 7.5.

2.5.4 Activation of ATM in CSF extract

In order to activate ATM and the downstream DNA damage signalling cascade, including phosphorylation of XCep63, DNA double strand breaks were added to the extract. Poly A and poly T 70 nucleotide oligomers were annealed by denaturing at 95 °C and gradual cooling of 5 °C every 5 minutes for 18 cycles. These pA/pT double stranded annealed oligos were stored at -20 °C and used at a concentration of 5 ng/µl in the extract.

2.5.5 MBP-protein pull down assays in *Xenopus* CSF extract

MBP-XCep152 pull-down

Amylose resin was washed 3 times with EB buffer, then 75 µl packed resin was incubated with approximately 5 µg MBP or MBP-XCep152 in 500 µl EB on a rotating wheel at 4 °C for 2 hours. Resin was then washed 3 times with EB + 0.25% Igepal then 3 times with EB. Packed resin bound to MBP or MBP-XCep152 (25 µl per sample) was then incubated with CSF containing either ^{35}S-labelled XCep63 or ^{35}S Luciferase. For each reaction, 150 µl of CSF plus 15 µl TNT reaction mix was used. Another set of MBP or MBP-XCep152 bound resin was incubated with 10 µl of the TNT mix without extract, diluted to 200 µl in EB buffer. Samples were incubated with gentle agitation for 1 hour at 4 °C. Resin was then washed 6 times with PBS + 0.25% Igepal. All proteins were eluted by boiling the amylose resin in Laemmli buffer for 2 minutes. All centrifugation steps were carried out at 100 x g in a bench top microcentrifuge at 4 °C. TNT reactions were set up as described previously (2.3.2). Samples were separated by SDS-PAGE on a 10% Anderson gel. The gel was then dried and an autoradiography film was exposed to the gel overnight to detect ^{35}S-labelled proteins.

For interaction studies using phosphorylated XCep63, the procedure was carried out as outlined above, but extract was first incubated with the TNT mix containing XCep63 and 5 ng/µl pA/pT for 15 minutes at 22 °C.

2.6 Cell culture

HeLa, HeLa Kyoto, U2OS and 293 FlpIn cells (Invitrogen) were obtained from the London Research Institute Cell Services and were grown in DMEM (+ 4.5 g/l glucose + Glutamine + Pyruvate, GIBCO) with 10% foetal bovine serum (FBS, PAA Laboratories GmbH) heat inactivated by incubation at 56 °C for 30 minutes. A trypsin and versene mixture was used to detach cells from cell culture plates. The mixture was obtained from LRI cell services and diluted 1 in 5 in PBS before use. Cells were washed in PBS, then incubated in 1 x trypsin/versene for 5 to 10 minutes then collected in pre-warmed growth medium. Cells were collected by centrifugation for 5 minutes at 300 x g and resuspended in medium and diluted appropriately. Cells were counted using an improved Neuberger haemocytometer.

5 x Trypsin/Versene (1 litre): Trypsin 2.5 g, NaCl 8.0 g, Na_2HPO_4 1.15 g, KH_2PO_4 0.2 g, Versene (EDTA) 1.0 g, Phenol Red (1%) 1.5 ml, Double distilled water (ddH2O) to 1 litre. The pH of the solution was then adjusted to 7.2 using NaOH and aliquots were stored at -20 °C.

The U2OS GFP-Centrin 1 stable cell line was obtained from Stefan Duensing (University of Pittsburgh Cancer Institute) with the permission of Michel Bornens (CNRS-Institut Curie). U2OS cells expressing HA-Plk2 under a tetracycline regulated (Tet-off) promoter were obtained from Ingrid Hoffmann (DKFZ, Heidelberg). U2OS HA-Plk2 cells were grown in DMEM low glucose (1 g/l glucose, Gibco) with 10% heat inactivated FBS and 2 µg/ml doxycyline. For induction of HA-Plk2 expression cells were trypsinised and resuspended in tetracycline and doxycycline-free medium containing 10% certified tetracycline-free FBS (PAA Laboratories GmbH).

2.6.1 Freezing cells for storage

Cells were frozen down for long term storage by trypsinisation of a 70% confluent 10 cm plate with 1 ml trypsin and resuspension in 4 ml of 10% DMSO in FCS. The resulting 5 ml was split between 4 cryo-tubes and the tubes were wrapped in thick layered tissue paper and kept at – 80 °C. Cells were kept at – 80 °C for at least 3 days before being moved to a liquid nitrogen storage tank.

Cells were thawed in a 37 °C water bath then mixed drop wise with 5 ml pre-warmed culture medium. Cells were collected by centrifugation and gently resuspended in culture medium and plated in a 10 cm plate. The medium was changed approximately 12 hours after plating.

2.6.2 Generation of stable cell lines

HeLa Kyoto cells stably expressing either GFP or GFP-Cep63 were generated by transfection with pIRES(puro3)-GFP-Flag (Empty vector) or (Cep63) using Effectene transfection reagent (Qiagen). For each 10 cm tissue culture plate transfected, 2 μg plasmid DNA and 60 μl Effectene. Transfection complexes were removed the day after transfection and selection with puromycin was started 2 days after transfection. Cells were maintained in 0.3 μg/ml puromycin for 2 weeks, by which time untransfected control cells were dead. Clones were generated by trypsinisation and isolation of individual colonies using cloning rings. Cells were maintained in medium containing puromycin throughout.

293 FlpIn stable cell lines expressing Flag or YFP tagged proteins were generated by transfecting pDestFRT/TO vectors with the pOGG44 recombinase vector. For each 10 cm tissue culture plate a total of 6 μg of DNA was transfected with 18 μl Fugene transfection reagent. A ratio of 3:1 pcDNA5 Dest FRT/TO Flag-Cep63 to pOG44 was used (i.e. 4.5 μg Flag-Cep63 and 1.5 μg pOG44 per plate). Cells with integrated Flag-

Cep63 were selected using 100 µg/ml Hygromycin B (Roche) 3 days after transfection. Clones were isolated by diluting cells to a density of 1 cell per 200 µl medium and plating 100 µl per well in a 96-well plate.

2.6.3 RNA interference (RNAi)

Transfection of siRNAs was carried out using Lipofectamine RNAiMax (Invitrogen). For RNAi of Cep63 and Cep152 siRNAs were transfected at a concentration of 50 nM using 7.5 µl RNAiMax reagent and 0.5 ml Optimem (Invitrogen) per well in a 6-well plate (total volume of medium and transfection complexes was 2.5 ml per well). First a reverse transfection was carried out, where cells were collected by trypsinisation and plated on top of transfection complexes. After 24 hours, a second transfection was carried out by adding transfection complexes to the cells on the plate (forwards transfection). For RNAi of Cep63 or Cep152, cells were collected 4 days after the first transfection unless otherwise stated.

Target gene	Target Sequence	Company	Name
Cep63	GAGUUACAUCAGCGAGAUA	Dharmacon	63-1
Cep63	CGUCAGAAAUCGCUGGACU	On-Target plus	63-2
Cep63	GGAGUCAGUUGGAUGUGACACAUAA	Invitrogen	63-3
Cep152	GAGCAAGAUUACCGGCAAU	Dharmacon	152-1
Cep152	AAAUGAAAGUGAACGUCAA	On-Target plus	152-2
Cep152	GCAUUGAGGUUGAGACUAA		152-3
Cep152	GACCAGAGUCGUAGAGAAU		152-4
Control	Medium GC content	Invitrogen	Control
Mad2	HSS106243	Invitrogen	Mad2

Table 11 siRNA sequences

2.6.4 Reduplication assays

First, U2OS cells were transfected with siRNAs as described above. At the time of the second transfection 1.9 μg/ml Aphidicolin was added to the medium and cells were collected 3 days later. Reduplication assays carried out using hydroxyurea (HU) were carried out as described, but with 2 mM or 4 mM HU in place of Aphidicolin. HU powder (Sigma) was dissolved in water to a concentration of 1 M, fresh before each use. Aphidicolin powder (Sigma) was dissolved in DMSO to a concentration of 5 mg/ml and stored in aliquots at -20 °C.

2.6.5 Cell synchronisation

Double thymidine block for HeLa Kyoto cells was carried out as follows:

- 2.5 mM thymidine (Sigma) 23 hours
- Release 8 hours
- 2.5 mM thymidine 14 hours
- Release and collect samples at varying time points

Mouse embryonic fibroblasts (MEFs) were incubated with 100 ng/ml nocodazole (Sigma) for 7 hours then released in the presence of 10 μM MG132 (proteasome inhibitor, Calbiochem) for 1 hour to enrich the percentage of mitotic cells.

All drugs were washed out using one wash with PBS followed by two washes with medium. Nocodazole powder was dissolved in DMSO to a stock concentration of 10 mg/ml and kept at 4 °C. MG132 was purchased in solution (DMSO 1 mg/ml). Thymidine powder was dissolved in Optimem medium (Gibco) to a stock concentration of 100 mM and stored at -20 °C.

2.6.6 DNA damaging agents for cell culture

Cells were irradiated using a Caesium 137 irradiator with 2Gy or 10 Gy as indicated. UV irradiation was carried out using a Stratalinker (Stratagene): cells were first washed with PBS and PBS was removed before irradiation. Phleomycin was used at a final concentration of 100 μg/ml in culture medium. Cells were incubated with Phleomycin for one hour, then the drug was washed out and cells were collected 1 hour later.

2.7 Fluorescence activated cell sorting (FACS)

All FACS analyses were carried out by the LRI FACS laboratory (Head of Department: Derek Davies). Cells were collected by trypsinisation, resuspended in complete medium and centrifuged to collect the cell pellet. Cells were then washed in PBS, collected by centrifugation then resuspended by drop wise addition of ice cold 70% ethanol while vortexing. The subsequent steps were carried out by cell services: for analysis of DNA content, cells were first treated with ribonuclease (100 μg/ml) then stained with 50 μg/ml propidium iodide (PI).

For quantification of mitotic index, cells were stained with phospho-histone H3 (Serine 10) antibody (Cell Signaling) and an anti-mouse fluorescent secondary antibody, as follows. After fixation in ethanol cells were washed twice in PBS then permeabilised in blocking solution (PBS, 0.1% BSA, 0.2% Tween20) for 15 minutes at room temperature. Cells were then collected and resuspended in 50 μl of phospho-H3 antibody diluted 1:1000 in the above blocking solution. Cells were then washed in blocking solution then incubated with a secondary anti-mouse red fluorescent antibody for 30 minutes at room temperature. Cells were then washed in PBS, treated with ribonuclease and stained with PI, as above.

Samples were analysed using a FACScan or FACSCalibur analytical cytometer (Becton Dickinson).

2.8 Immunofluorescence

12 mm diameter glass coverslips were washed in 70% ethanol then PBS then added to tissue culture plates and washed with medium before plating cells. Upon collection coverslips were washed in 37 °C PBS, 1 mM EGTA then fixed in -20 °C Methanol for 30 minutes minimum. Cells were then rehydrated by 3 washes with PBS 0.01% Triton X100 (TX). Permeabilisation was carried out with a 20 minute incubation in PBS 0.2% TX, then coverslips were washed 3 times, each for 5 minutes, with PBS-0.01% TX. Blocking was carried out at room temperature for 30 minutes in PBS, 1% BSA, 2% HI FCS. All antibody incubations were also carried out with antibodies diluted in this blocking solution. Primary antibody incubations were either carried out at room temperature for 1 hour or overnight at 4 °C. Coverslips were inverted onto a 100 µl drop of primary antibody solution on parafilm and the incubation was carried out in a wet chamber. After primary antibody incubation coverslips were rinsed once with PBS-0.01% TX then washed 3 times for 5 minutes with PBS-0.01% TX. Secondary antibody incubations were carried out as for primary incubations, but at room temperature for 30 minutes. Washes were carried out as above and for samples with DAPI staining, an additional 5 minute incubation in 0.1 µg/ml DAPI in PBS 0.01% TX was carried out. Coverslips were then rinsed in PBS then ddH_2O before mounting on pre-cleaned glass slides with Vectashield (Vector Laboratories). Coverslips were sealed with nail varnish. GFP and YFP fusion proteins were viewed by direct fluorescence unless indicated otherwise.

2.8.1 Co-staining Cep63 and Centrin-2

For immunofluorescence using both Cep63 and Centrin-2 antibodies (both rabbit) coverslips were first incubated with anti-Centrin-2 (1:500 dilution) overnight at 4 °C. Coverslips were then washed 3 times for 5 minutes with PBS-0.01% TX and incubated with Alexa Fluor (AF) 594 anti-rabbit secondary antibody (1:400) for 30 minutes. Coverslips were then washed extensively (minimum 10 washes) in PBS-0.01% TX then incubated with anti-Cep63 49AP (1:5000) for 1 hour; if a mouse antibody was also used, it was included during this incubation; washed 3 times in PBS-0.01% TX then

incubated in AF488 anti-rabbit (1:1000) for 30 minutes. Final wash steps and mounting were carried out as above.

2.9 Microscopy

All microscopy was carried out using a Delta Vision RT inverted fluorescence microscope with Softworx software, unless stated otherwise. For all experiments requiring the visualisation of centrosomes, an Olympus UPlanSApo 100 x/1.4 oil objective was used. A COOLSNAPHQ / ICX285 CCD camera was used. Z-stacks were acquired at 0.2 μm intervals and z-stacks were then projected by maximum intensity to a flat image. Deconvolution was performed using Softworx with the "enhanced ratio (aggressive)" setting and noise filtering set to medium for 10 cycles. Deconvolution was not carried out for all pictures and is indicated in the figure legends.

Fluorescence filters:

DAPI	Excitation 360 nm	Emission 457 nm
FITC	Excitation 490 nm	Emission 528 nm
RD-TR-PE	Excitation 555 nm	Emission 617 nm

Softworx data inspector was used to measure fluorescence intensities. A circle of 20 x 20 pixels was used to measure fluorescence intensities at the centrosome. Fluorescence intensities were measured as a ratio; relative to the intensity of γ-tubulin staining. Local background was subtracted. Measurements were taken from the flattened R3D files without deconvolution.

Live cell images in figure 18 (chapter 3) were taken with a Zeiss Axiovert 200M microscope with a Zeiss 10 x Ph1 Plan Neo FL objective using an Axiocam MRm camera and Axiovision 3.1 software. Pictures were collected for one z position only. Pictures in figure 46 (chapter 4) were taken with a Zeiss Axio Imager M2 microscope with a Zeiss Plan Apochrome 63 x objective and a Hamamatsu digital camera

(C10600), using Volocity software. Images of primary MEFs in figures 66 and 68 (chapter 5) were taken using a Leica microscope in Dr Travis Stracker's lab.

Time-lapse microscopy in figure 53 (chapter 4) was carried out using a Zeiss Axio Observer Z1 microscope with a Zeiss 10 x objective, Hamamatsu digital camera (C8484), a motorised Nanodrive stage and Simple PCI 6 software. Cells were grown in a 6-well plastic tissue culture plate in CO_2 medium without phenol red and 10% HI FCS. Cells were kept at 37 °C throughout imaging. Images were taken in 9 different fields: 3 field for each different RNAi treatment and pictures were taken every 5 minutes at one z position only.

2.10 Mass spectrometry

Mass spectrometry was carried out on gel slices form Flag-Cep63 pull down elutes (as described previously). Liquid chromatography mass spectrometry was carried out by the Protein Analysis & Proteomics laboratory at London Research Institute Clare Hall Laboratories, headed by Dr Mark Skehel.

Polyacrylamide gel slices (1-2 mm) containing the purified proteins were prepared for mass spectrometric analysis using the Janus liquid handling system (PerkinElmer, UK). Briefly, the excised protein gel pieces were placed in a well of a 96-well microtitre plate and destained with 50% v/v acetonitrile and 50 mM ammonium bicarbonate, reduced with 10 mM DTT, and alkylated with 55 mM iodoacetamide. After alkylation, proteins were digested with 6 ng/µL Trypsin (Promega, UK) overnight at 37 °C. The resulting peptides were extracted in 2% v/v formic acid, 2% v/v acetonitrile. The digest was analysed by nano-scale capillary LC-MS/MS using a nanoAcquity UPLC (Waters, UK) to deliver a flow of approximately 300 nL/min. A C18 Symmetry 5 µm, 180 µm x 20 mm µ-Precolumn (Waters, UK), trapped the peptides prior to separation on a C18 BEH130 1.7 µm, 75 µm x 100 mm analytical UPLC column (Waters, UK). Peptides were eluted with a gradient of acetonitrile. The analytical column outlet was directly interfaced via a modified nano-flow electrospray ionisation source, with a hybrid linear

quadrupole fourier transform mass spectrometer (LTQ Orbitrap XL/ETD, ThermoScientific, San Jose, USA). Data dependent analysis was carried out, using a resolution of 30,000 for the full MS spectrum, followed by eight MS/MS spectra in the linear ion trap. MS spectra were collected with an automatic target gain control of $5x10^5$ and a maximum injection fill time of 100 ms over a m/z range of 300–2000. MS/MS scans were collected using an automatic gain control value of $4x10^4$ and a threshold energy of 35 for collision induced dissociation. LC-MS/MS data were then searched against a protein database (UniProt KB) using the Mascot search engine programme (Matrix Science, UK) (Perkins et al., 1999). Database search parameters were set with a precursor tolerance of 5 ppm and a fragment ion mass tolerance of 0.8 Da. One missed enzyme cleavage was allowed and variable modifications for oxidized methionine, carbamidomethyl cysteine, pyroglutamic acid, phosphorylated serine, threonine and tyrosine were included. MS/MS data were validated using the Scaffold programme (Proteome Software Inc., USA) (Keller et al., 2002). All data were additionally interrogated manually.

2.11 Mouse Techniques

2.11.1 Cep63 gene trap targeting construct

ES cells containing a gene trap between exons 1 and 2 of the Cep63 gene were purchased from EUCOMM (European Conditional Mouse Mutagenesis Program; Cep63 MGI 2158560; clone ID EUCE0251_H11). This was a clone that has lost its 3' LoxP site and is consequently not conditional. The structure of the gene trap construct is outlined below.

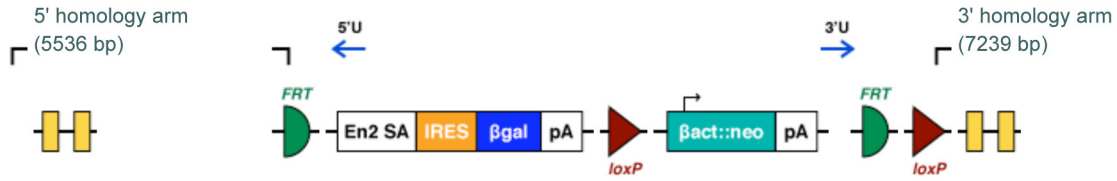

The 5' homology arm, or sequence tag, is in the intron following Exon1 and the 3' sequence tag is in the intron before Exon2.

5’ sequence tag (5’ to 3’):

TAGTATGAGAGGTGCGGAAATGTGGCGGGAACCCCTGATGGCAGGGGAATTGCAGATGGCTTCACGCTTT
CAAGTCAAGCATAGGAAACAAGATTGGTGGAGTGAAAGTTTGGAAAGGGGAATTCCACAACAGCGCTTTC
ACGCGGAGACACTTGACAGTGAATGGGCTTTTGTCCTTTACAAAATCGTGGAGTTAGTGCATTCTGATGT
CAGACCTAGTTTTCATTTACAGACTGTAGACTTGTTGCCAAAAGTGCTCCCCATTCTCCCCAACT

3’ sequence tag (5’ to 3’):

GCTATGATCTGGAACTTGCAGTGTAGACCAGGCTGGCCTCAAACTCAGAGATGGGCCTACCTATGTCTCC
TAATTAAGGATCCGCGCCACCTCGCCTGGCTTTCTTGAGGCCAATTTAGAGTTTCAAAAATGTATTACTT
TATTATAGCTCTTTGTACAACTCGAATATTTGTATTTTATATTTTGTATGTAAGTCAGAGATCAATGGCT
ATAGTTATCTT

2.11.2 ES cell culture

E14 Medium:

500 ml Knockout™ DMEM (Gibco 10829)

50 ml FBS (PAA Laboratories GmbH)

5 ml 100X L-Glutamine (Gibco)

5 ml 100X beta-mercaptoethanol (360 microliters/500 ml PBS; filtered, stored at -20°C)

Murine LIF (Leukemia inhibitory factor, ESGRO, Millipore ESG1107, dilute 1000 x)

Freezing Medium: Add dimethylsulphoxide (DMSO) (Sigma # D2650) to E14 medium to a final concentration of 10% (v/v) and filter sterilise. Make fresh before use.

PBS: Dulbecco’s phosphate-buffered saline (PBS) without calcium and magnesium (Invitrogen # 14190-094)

Trypsin: 500ml PBS (Gibco), add 0.1g EDTA and 0.5g D-glucose. Filter sterilize (0.22 µm). Add 5ml Chicken Serum (Gibco), 10ml 2.5% Trypsin (Gibco), and store in 20 ml aliquots at -20°C

Tissue culture plates were coated with gelatin before use by adding a 0.1% solution of gelatin in sterile water (2% gelatin stock, Sigma) at least 10 minutes then aspirating the liquid off before plating cells. ES cells were grown in E14 medium at 37 °C and 5% CO_2. Initially, cells were brought up in the LRI Transgenics Unit in a mycoplasma-free facility and early passage cells were frozen for microinjection and sent to Dr Travis Stracker (IRB, Barcelona).

2.11.3 Checking ES cells for gene trap insertion

Confirmation of gene trap position by PCR

Genomic DNA from Cep63 gene trap (gt) ES cells or wild type (wt) ES cells was extracted using a genomic DNA extraction kit (Qiagen). PCR reactions were carried with Simple Red Taq polymerase using 100 ng of genomic DNA as a template and the primers listed below.

Name	Sequence	product size (bp)
Ms C63 5'P1	AACCGACCGCATGCCCCAAAGAC	1532
Ms C63 5'P2	GTAGGACCAGGCCTTAGCGTTAG	1225
Ms C63 5'P3	CAGGTGCTTCGGCCTGCGGGAG	1314
B32	CAAGGCGATTAAGTTGGGTAACG	reverse primer in gt
Ms C63 3'P4	TGGTGGCGCACGCCTTTAATC	1931
Ms C63 3'P5	TGAAACTTCAGCATATACAC	2164
Ms C63 3'P6	CAATTCATTGCTGTAGTCTG	3433
GT 2	GGGAGGATTGGGAAGACAAT	forwards primer in gt

Table 12 Mouse Cep63 gene-trap PCR primers

The 5' Cep63 forward primers were used in combination with the B32 reverse primer whose binding sequence is in the β-galactosidase gene of the gene trap. The 3' Cep63 reverse primers were used with the GT2 forwards primer whose binding sequence is in the 3' end of the gene trap.

2.11.4 Southern blotting

Southern blotting was used on genomic DNA digests from wt and gt ES cells in order to confirm that the targeting construct was only inserted in one location.

Solutions

Alkaline transfer buffer: 0.4 N NaOH, 1.5 M NaCl

Neutralisation buffer: 0.5 M Tris-HCl pH 7.2, 1 M NaCl

Pre-hybridisation buffer: 45% formamide, 4 x SSC, 100 mM sodium phosphate, pH 6.5, 10 x Denhardt's solution (Sigma), 2% SDS, 0.25 mg/ml Herring sperm DNA (Sigma).

Hybridisation buffer: 45% formamide, 4 x SSC, 100 mM sodium phosphate, pH 6.5, 1 x Denhardt's solution, 0.4% SDS, 0.1 mg/ml Herring sperm DNA, 10% Dextran sulphate and ^{32}P α- dATP labelled probe.

Wash solution: 0.1 x SSC, 0.1% SDS

20 x SSC: 175.32 g/l NaCl, 88.25 g/l Tri-sodium Citrate

Genomic DNA was extracted from ES cells and 10 µg was used per reaction; with 5 U/µl ApaI, DraI or NcoI restriction enzymes. DNA digests were incubated overnight at the appropriate reaction conditions in a total of 50 µl. The resulting DNA fragments were separated by electrophoresis on a 0.7% agarose gel without ethidium bromide. Electrophoresis was carried out at 60 V for 11 hours and the gel was post-stained with ethidium bromide to visualise DNA by UV light. The DNA fragments were transferred by chromatography overnight to a Hybond N+ membrane (positively charged nylon membrane, Amersham – now GE Healthcare) using alkaline buffer. The membrane was then incubated in neutralisation buffer for 15 minutes at room temperature, then pre-hybridisation buffer for 7 hours at 42 °C; all membrane incubations were carried out in a sealed glass tube on a rotating rack in a hybridisation oven. Hybridisation was carried out at 42 °C overnight in hybridisation buffer containing a radio-labelled DNA probe (see below). The membrane was washed at 48 °C using 8 volumes of pre-warmed was

solution. The membrane was then wrapped in Saran wrap and exposed to autoradiography film (GE Healthcare) at – 80 °C for one week.

2.11.5 Generating a probe for Southern blotting

Vectors B1 and SK+Tag3 (from Ian Rosewell, LRI Transgenics Unit) were digested with BamHI and PstI respectively to isolate a 1 kb (B1) and 780 bp and 200 bp fragments (SK+) that code for the Neomycin resistance gene. The digest was carried out using 2 µg vector DNA. DNA fragments were separated by agarose gel electrophoresis and once separated the bands were visualised a square of agarose gel was removed from in front of the band of interest and this hole was filled with 0.5 % low melting point agarose (Seaplaque, Lonza). The gel was put back in the electrophoresis chamber and run until the band of interest was in the low melting point agarose square. This agarose was then cut from the gel and boiled for 5 minutes with 100 µl ddH_2O then placed immediately on ice; 10 µl of this DNA solution was used per 50 µl Prime-It random primer labelling reaction (Stratagene). The reaction was carried out as per manufacturer's instructions using 5 µl α-^{32}P dATP (Easytides, Perkin Elmer) to label the DNA probe. The reaction was carried out at 37 °C for 30 minutes, then 2 µl stop mix (Stratagene) was added and DNA was purified by passing through a G25 column (GE Healthcare). The probe was then boiled and added directly to the warmed hybridisation solution.

2.11.6 Generation of mouse embryo fibroblasts (MEFs)

MEF media

DMEM high glucose (Gibco, Invitrogen)

1X glutamax (Gibco, 100X stock)

15% Fetal bovine serum (Hyclone)

Penicillin/Streptomycin (100X stock, Gibco)

All breeding and MEF generation was carried out by Dr Travis Stracker (IRB, Barcelona).

Breeding animals were set up and plugs were checked the following morning. (Before 10 am is optimal). Plugged females were separated and sacrificed at day E13.1 using CO_2 asphyxiation in animal facility. Embryo sacs were dissected out in a tissue culture hood and transfer to PBS, as follows:

- Use sterile scissors and tweezers for incision of each skin layer.
- Tease apart yolk sacs to release the embryos and carefully transfer to fresh sterile PBS.
- Using tweezers, remove the tail and transfer to an eppendorf tube for genotyping.
- Remove all of the red tissue (heart, liver, spleen) delicately with tweezers.

The embryos were then transferred to 5 ml cold trypsin-EDTA overnight then incubated at 37 °C for 20 minutes to digest tissue. Excess trypsin was removed and the tissue was homogenised by pipetting with fresh media. Large tissue pieces were left to settle for 3 minutes and the remainder was plated to three 10 cm cell culture plates. The following day, cells were washed twice with PBS to remove non-fibroblast cells and debris. The 3T3 protocol was carried out by plating 1 million cells to a 10 cm plate. Early passage cells were frozen in 10% DMSO, 50% FBS, 40% MEF media. Genotyping of embryos was carried out by Travis Stracker. Primary cells and 3T3 cells were split every two to three days to 0.5×10^6 cells per 10 cm plate or 1.8×10^5 per 60 mm plate.

Chapter 3. Cep63 is a constitutive centrosome protein that interacts with Cep152

The aim of this project was to characterise the human Cep63 protein, herein referred to as Cep63. Cep63 was originally identified as a centrosome protein in a centrosome purification and mass spectrometry screen to identify novel components (Andersen et al., 2003). Previous work carried out in the Costanzo lab confirmed that *Xenopus laevis* and chicken Cep63 also localise to the centrosome (Smith et al., 2009). Although extensive work has been carried out on XCep63 in *Xenopus laevis* cell free extract as described in introduction 1.4, the function and characteristics of the human protein were unknown. Firstly, localisation of exogenous Cep63 to the centrosome when expressed in human cell lines was confirmed. Secondly, in order to determine the function of Cep63, a biochemical approach was used to identify Cep63 binding partners by mass spectrometry.

3.1 Exogenous Cep63 localises to the centrosome throughout the cell cycle

Human embryonic kidney cell lines (293) were generated stably expressing Flag-tagged Cep63 using the FlpIn system from Invitrogen (figure 17). 293 FlpIn cells from Invitrogen include only one copy of an FRT recombinase site in the genome. 293 FlpIn cells were transfected with Flag-Cep63 or YFP-Cep63 vectors containing the FRT sites, along with a vector containing the recombinase enzyme and carried out antibiotic selection to isolate positive clones. Flag or YFP vectors with no insert (empty) were used as negative controls for all experiments. Both Flag-Cep63 and YFP-Cep63 co-localised with centrosome components γ-tubulin and pericentrin (figure 17 and 18). Flag-Cep63 was visualised using an anti-Flag antibody, which stained centrosomes in 293 Flag-Cep63 cells, but not in Flag-Empty 293 cells, indicating that centrosomal staining with the Flag antibody was due to detection of Flag-Cep63, rather than the Flag antibody recognising a centrosome epitope. YFP-Cep63 was observed by direct fluorescence in fixed cells (figure 18a and c) and live cells (figure 18d), to confirm that

Cep63 localisation was not affected by the fixation process. Positive clones were identified by checking for localisation of the tag (Flag or YFP) at the centrosome and checking for the presence of tagged-Cep63 at the appropriate size on Western blots of whole cell lysates. Examples of positive Flag and YFP clones are shown in figure 17 and 18 respectively. Flag-Cep63 migrated to approximately 63 kDa and YFP-Cep63 to around 90 kDa on SDS-PAGE gels (figures 17b and 18b). Flag-Cep63 293 stable clones expressed less Flag-Cep63 than 293 cells collected one day after transfection, which was likely due to the stable clones containing only one copy of the expression construct per genome (figure 17, loading control not shown but equal loading was confirmed by Ponceau staining of the membrane). Cells that were not selected for stable integration of the construct were likely to contain multiple expression constructs per cell, which would lead to higher expression levels.

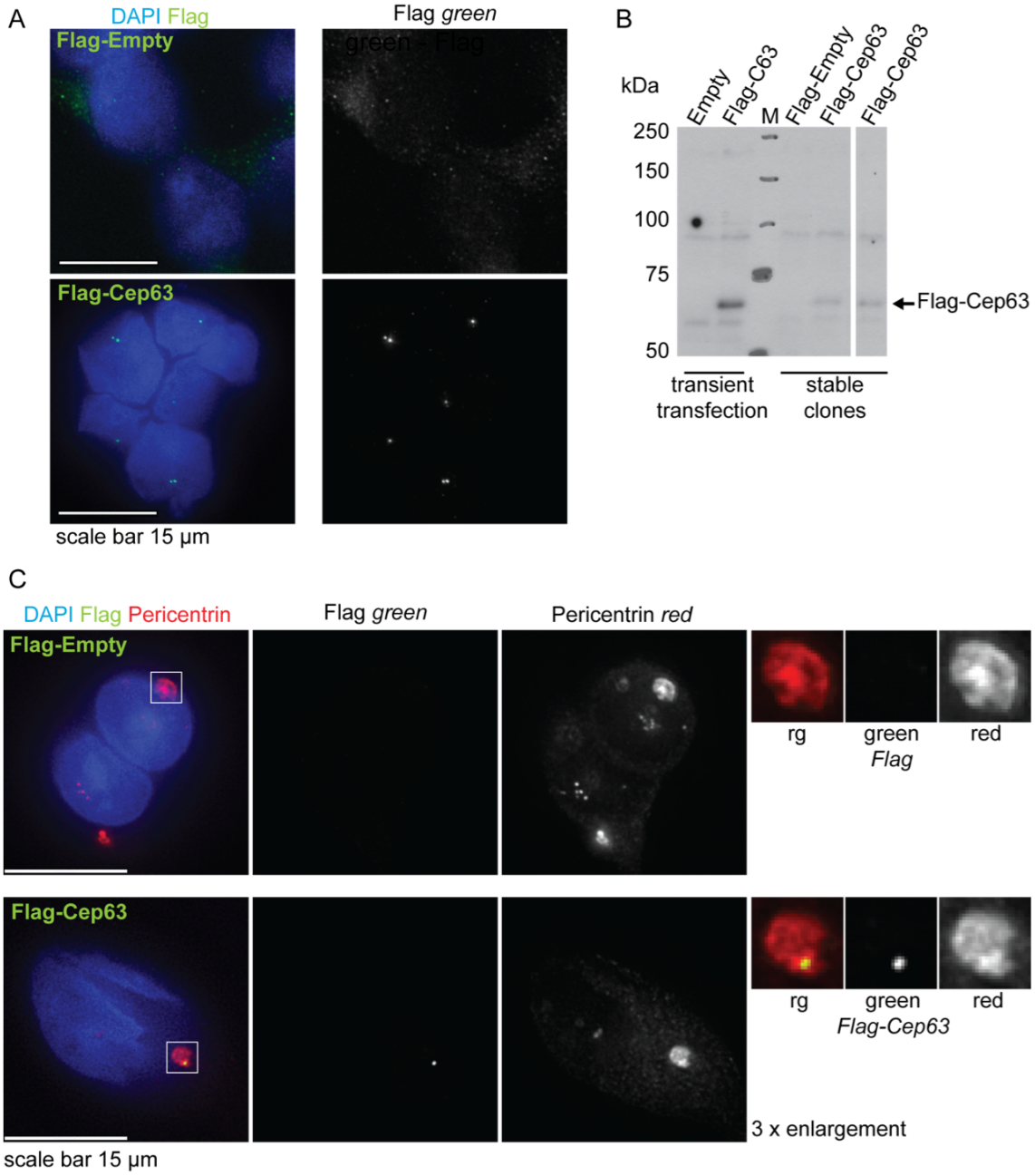

Figure 17 Flag-Cep63 localises to the centrosome
(A) 293 FlpIn cells stably expressing Flag-Cep63. Flag-Cep63 293 cells (pool of cells after antibiotic selection) fixed and stained with anti-Flag M2 antibody and DAPI. (B) Western blot of 293 cell lysates, separated by SDS-PAGE on a 10% gel, with anti-Flag M2 antibody. 293 cells transiently expressing Flag or Flag-Cep63 and collected after 24 hours (first two lanes) were used for comparison with Flag and Flag-Cep63 293 stable clones. (C) Flag-Cep63 or Flag-Empty 293 cells (clones) fixed and stained with anti-Flag M2 (green) and anti-pericentrin (red) antibodies and DAPI (blue). Small panels show the boxed region enlarged three times (C). Images are maximum projections of deconvolved z-sections.

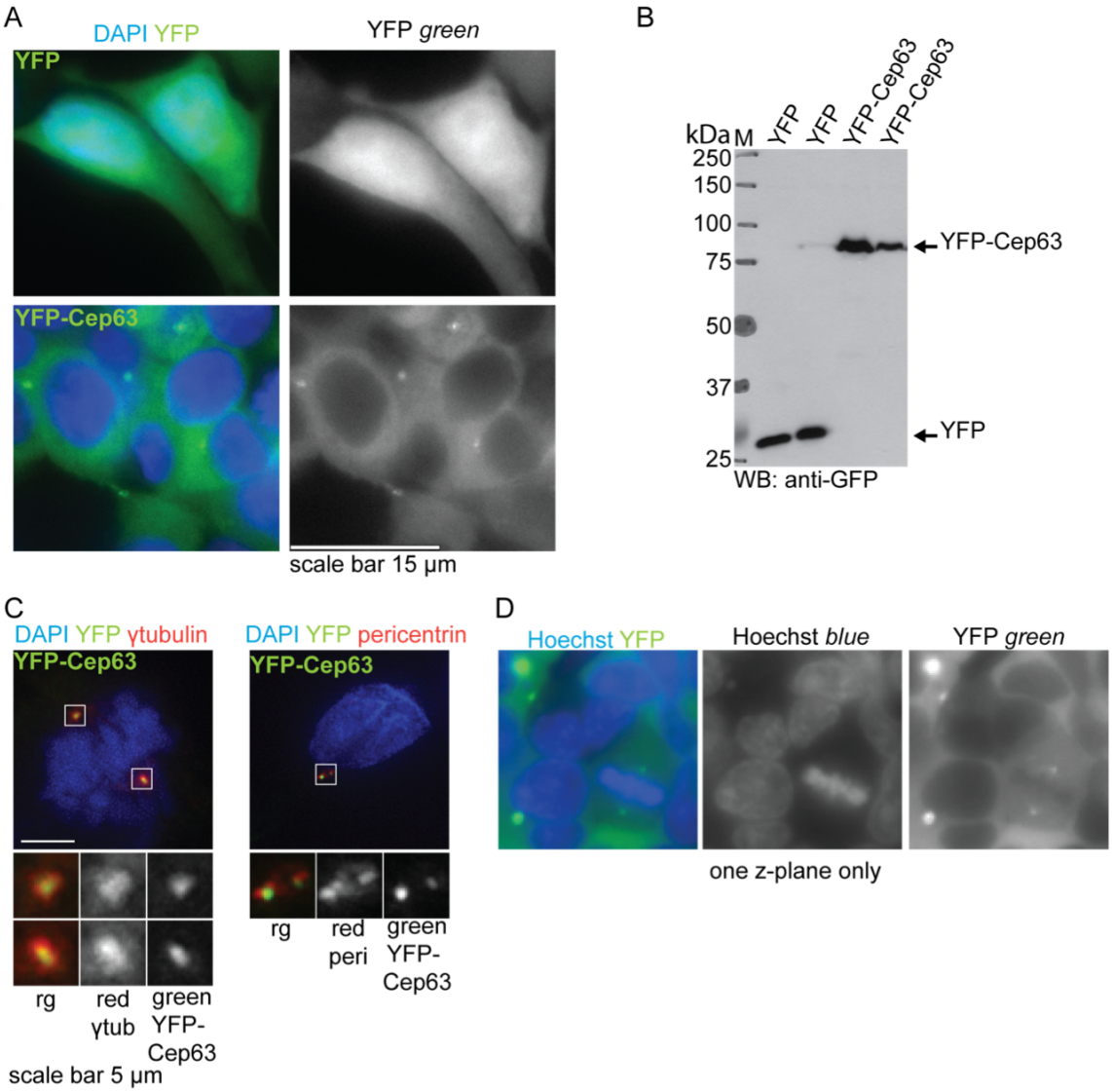

Figure 18 YFP-Cep63 localisation at the centrosome
(A) 293 FlpIn cells stably expressing YFP-Cep63. YFP-Cep63 cells (pool of cells after selection) were fixed and stained with DAPI. (B) Western blot of 293 YFP and YFP-Cep63 stable cell lysates separated by SDS-PAGE on a 15% gel and blotted with anti-GFP antibody. (C) YFP-Cep63 293 cells stained with DAPI (blue) and anti-pericentrin or anti-γ-tubulin (red). Lower panels are enlargements of the boxed areas. Images are maximum projections of deconvolved z-sections. (D) Images of YFP-Cep63 293 live cells incubated with Hoechst: two images were taken in quick succession with the blue filter (to visualise Hoechst) and the green filter (to visualise YFP). YFP-Cep63 localises to the centrosome in interphase and mitotic cells. Live cell images show only one focal plane without deconvolution.

To examine the subcellular localisation of YFP-Cep63, cell fractionation of 293 YFP-Cep63 cells was performed. Fractionation experiments showed that YFP-Cep63 was cytoplasmic, as would be expected for a centrosome protein (figure 19a). Gel filtration of 293 YFP-Cep63 cell lysates showed that the elution peak of YFP-Cep63 (fraction 4) partially overlapped with the elution peaks of known centrosome components γ-tubulin and Centrin-3 (fraction 3, figure 19b).

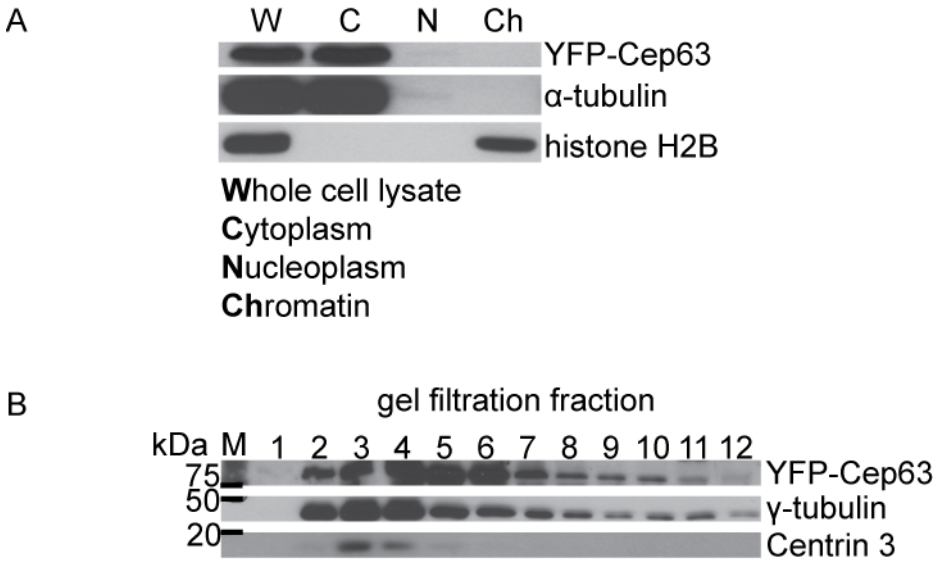

Figure 19 YFP-Cep63 is cytoplasmic
(A) 293 YFP-Cep63 cells were fractionated and whole cell lysates, cytoplasmic, nuclear and chromatin fractions were separated on a 15% SDS-PAGE gel and analysed by Western blotting with anti-GFP; anti-α-tubulin to mark the cytoplasm and anti-histone H2B to mark the chromatin. (B) 293 YFP-Cep63 cell lysate was separated by gel filtration and fractions were analysed by SDS-PAGE on a 15% gel and Western blotting with anti-GFP, anti-γ-tubulin and anti-Centrin 3. Protein standards are marked in (B).

These findings were further confirmed in HeLa Kyoto cells, a human cervical cancer cell line. HeLa cells stably expressing GFP-Flag-Cep63 using a bicistronic pIRES expression vector with a puromycin resistance gene were generated. It was important to generate these additional cell lines because HeLa cells are much more amenable to microscopy when compared to 293 cells, which detach easily from the coverslip or plate making it more difficult to follow mitotic cells. Furthermore, 293 cells are considerably more 3-dimensional and therefore less amenable to live cell imaging in which fewer z-sections are optimal. Larger, flatter HeLa cells stay attached to the coverslip or plate throughout the cell cycle and therefore provide a better system for microscopy based studies.

GFP-Flag-Cep63 (hereafter called GFP-Cep63) also localised to the centrosome in HeLa cells (figure 20 and 21). GFP-Cep63 was visualised at the centrosome throughout the cell cycle and it was not visible at any other cellular location (figure 20b). All immunofluorescence analysis was carried out on clonal cell populations due to the variation in levels of overexpression between clones. Analysis of GFP-Cep63 HeLa cells by immunofluorescence showed that GFP-Cep63 colocalised with pericentriolar material (PCM) components γ-tubulin, pericentrin and Cep152. Colocalisation with γ-tubulin and pericentrin was incomplete, such that GFP-Cep63 resides in a smaller area than that covered by these two PCM proteins (figure 21a and b). All of GFP-Cep63 localised within the PCM, but GFP-Cep63 was only present in part of the area covered by γ-tubulin and pericentrin. Colocalisation of GFP-Cep63 with Cep152, on the other hand, was complete (figure 21d).

Centrin-3 is a centriole protein and staining with this antibody marks the position of the distal end of the centrioles (Strnad et al., 2007). GFP-Cep63 is located between the Centrin-3 foci in G2 or mitotic cells (figure 21d) and adjacent to the single centrin focus in G1 cells that have separated, but not yet duplicated their centrioles (figure 21e). This pattern of localisation suggests that Cep63 localises to the PCM surrounding the proximal end of the centriole.

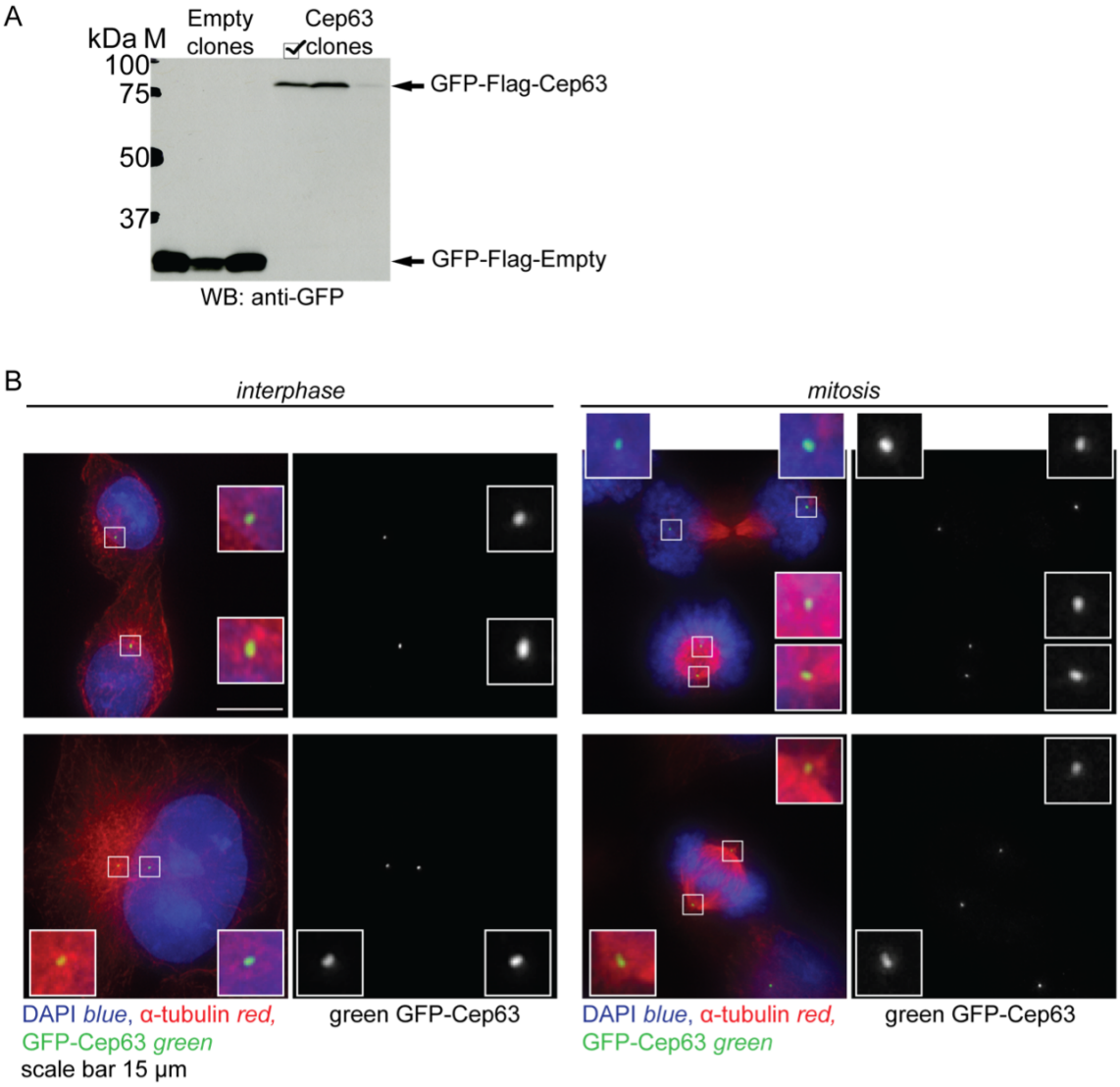

Figure 20 GFP-Cep63 localises to the centrosome throughout the cell cycle
(A) Western blot of HeLa GFP-Empty or GFP-Cep63 clone lysates with anti-GFP antibody. Lysates were separated on a 15% SDS-PAGE gel. Lane marked with a tick shows the clone that was used for further immunofluorescence experiments. (B) HeLa cells stably expressing GFP-Cep63 were fixed and stained with anti-α-tubulin antibody (red) and DAPI (blue). GFP-Cep63 localised to the centrosome at all stages of the cell cycle: examples shown are G1 cells (top left), S-phase or G2 cell (bottom left), prophase and late anaphase (top right) and metaphase (bottom right). Inserts show 3.75 x enlargements of the boxed areas. Images are maximum projections of deconvolved z-sections.

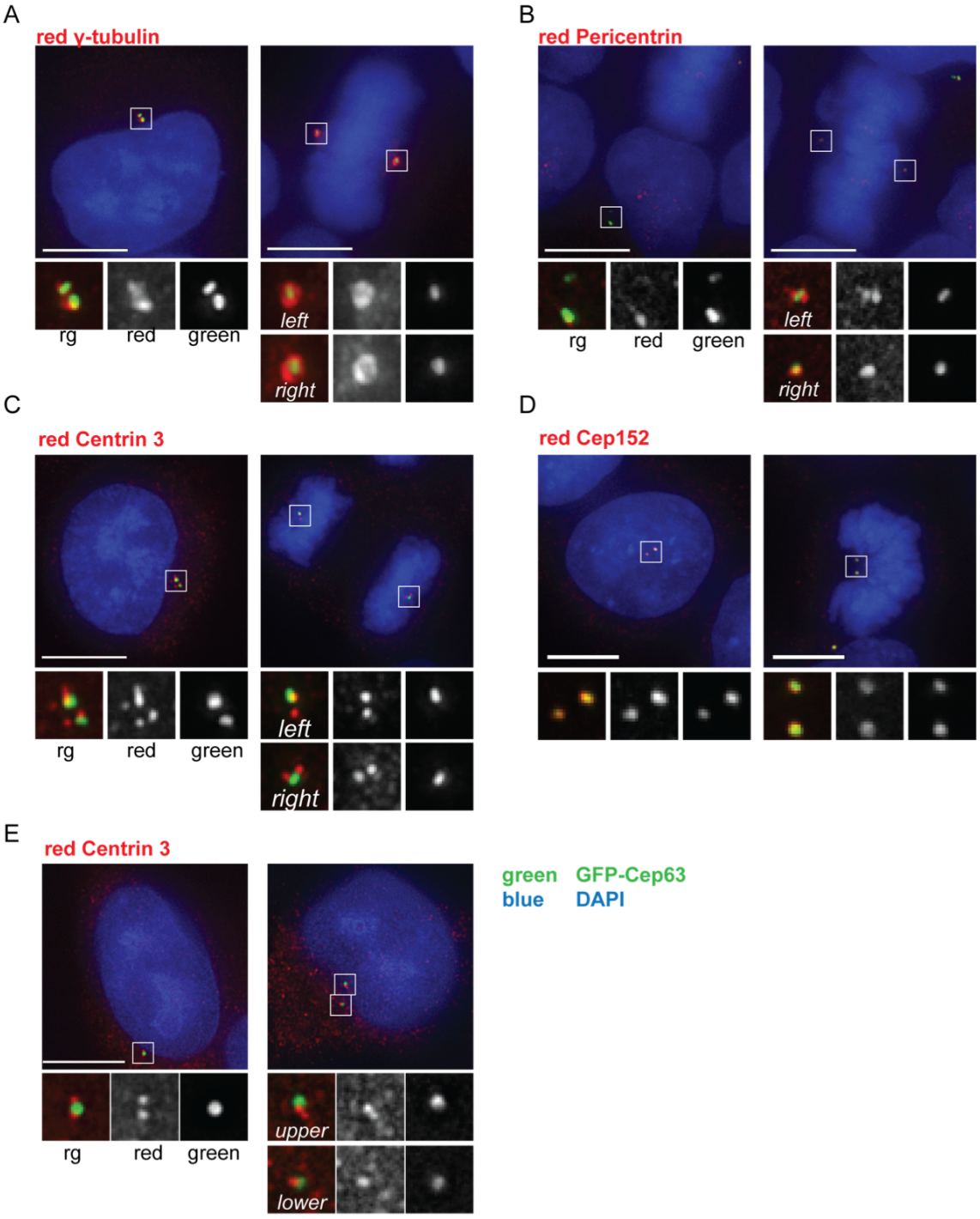

Figure 21 GFP-Cep63 colocalises with pericentriolar material (PCM) proteins
HeLa GFP-Cep63 stable cells were fixed and stained with γ-tubulin (A), Pericentrin (B), Centrin-3 (C,E) and Cep152 (D) (red) and DAPI (all). GFP-Cep63 was visualised by direct fluorescence. Left hand panels show interphase cells with 2 centrosomes and right hand panels show mitotic cells (A-D). GFP-Cep63 showed exact colocalisation with Cep152 (D) and overlap with γ-tubulin and pericentrin (A and B). GFP-Cep63 localised between pairs of Centrin-3 foci, and adjacent to single Centrin-3 foci (E). Scale bar is 15 μm in A,B,C and E; 10 μm in D. Lower panels are 3x enlargements of the boxed areas. Images are maximum projections of deconvolved z-sections.

3.2 Cep63 interacts with Cep152

To investigate the function of Cep63, anti-Flag immunoprecipitation (IP) experiments using FLAG-Cep63 were performed. The eluted proteins from immunoprecipitation were sent for analysis by mass spectrometry. Identification of Cep63 interacting proteins was a starting point for highlighting cellular processes in which Cep63 could be involved. Using the Flag-Cep63 and Flag-Empty cell lines described in 3.1, large-scale Flag IPs were performed using anti-Flag M2 affinity gel (Flag M2 antibody immobilised on agarose beads, Sigma). The Flag IP was carried out on equal amounts of Flag-Empty or Flag-Cep63 293 whole cell lysates and bound proteins were eluted using a peptide with 3 Flag repeats (Sigma). Eluted proteins were separated by SDS-PAGE on a 4-12% Bis-Tris gel (NuPage, Invitrogen) and stained with Sypro Ruby (Invitrogen) to visualise total protein with a blue fluorescent light scanner (figure 22b). Flag-Cep63 was visible in the eluate on the Sypro Ruby stained gel (arrow, figure 22b), but there were no other visible bands present only in the Flag-Cep63 eluate and not in the Flag-Empty control.

A small fraction of each sample was analysed by Flag or Cep63 Western blot in order to check that Flag-Cep63 was indeed present in the eluate (figure 22a). Both lanes of the Sypro Ruby stained gel were cut into bands and sent for analysis by mass spectrometry. The proteins were eluted from the gel, subjected to tryptic digestion and analysed by LC-MS as described in materials and methods (2.10). Figure 22c shows the two highest scoring proteins, with respect to number of peptides identified, that were present in the Flag-Cep63 eluate, but absent from the control. Mass spectrometry analysis confirmed that Cep63 was present in the Flag-Cep63 eluate and Cep152 was the most abundant interacting protein identified.

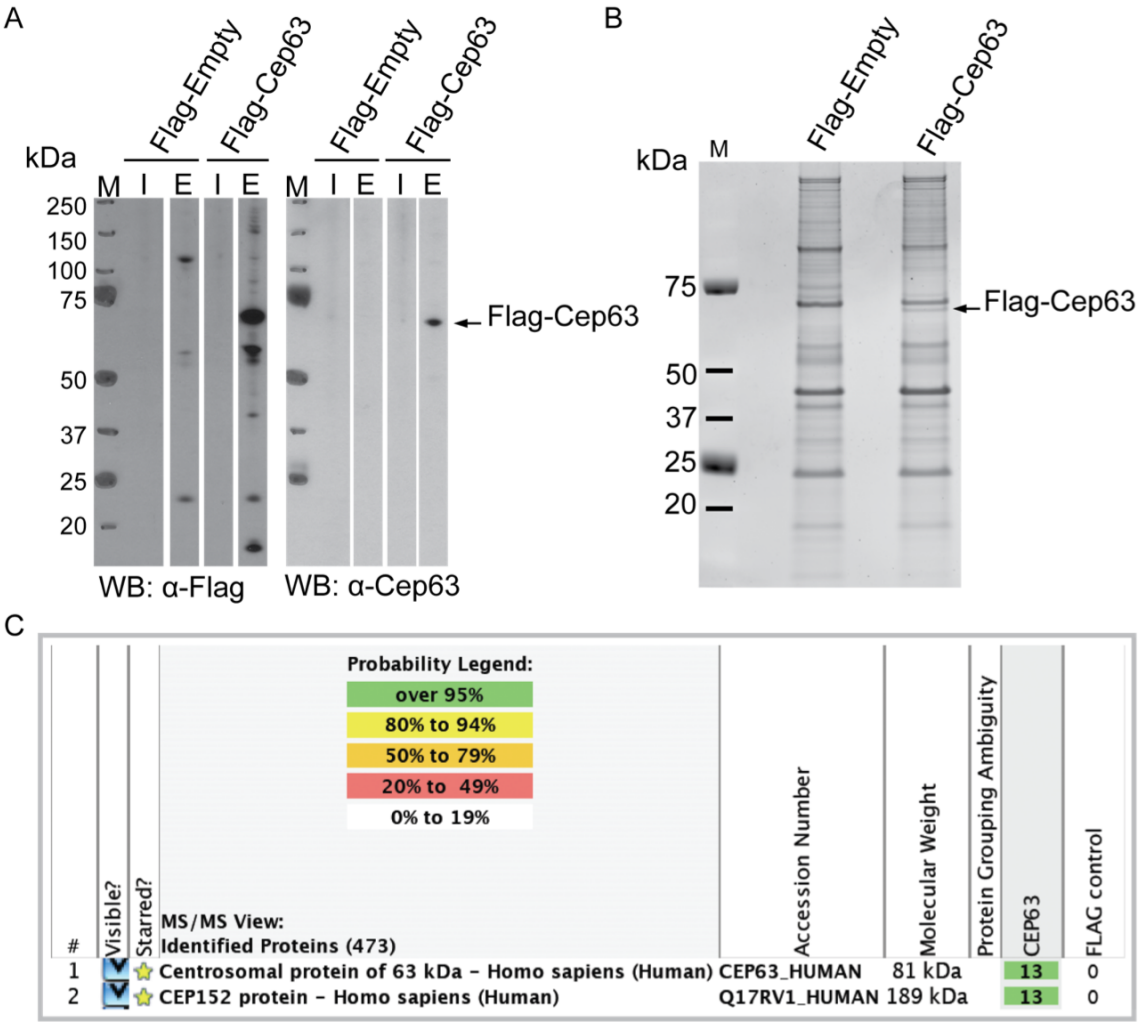

Figure 22 Identification of Cep152 as a Flag-Cep63 interacting protein
An anti-Flag IP experiment was performed with cell lysates from 293 cells stably expressing Flag-Cep63 or the empty vector. Input (I) and eluate (E) fractions were separated by SDS-PAGE on a 4-12% Bis-Tris gel and analysed by Western blotting with Flag M2 mouse antibody (A, left) or Cep63 rabbit (A, right). Eluted proteins were separated by SDS-PGE on a 4-12% Bis-Tris gel, stained with Sypro Ruby and visualised using a fluorescence scanner (B). Both lanes were cut into 1 mm fragments and sent for analysis by mass spectrometry (Protein Analysis and Proteomics Laboratory, Clare Hall). (C) The two highest scoring proteins identified in the Flag-Cep63 eluate that were absent in the control: Cep63 and Cep152.

Cep152 is a centrosome protein, which was also identified in the centrosome purification screen (Andersen et al., 2003). Cep152 has also been identified as a Plk4 interacting partner and it has been shown to be involved in the regulation of centrosome duplication (Cizmecioglu et al., 2010, Hatch et al., 2010b, Dzhindzhev et al., 2010a) as described in Introduction 1.3. Mammalian Cep152 was uncharacterised when this result was obtained. Literature on the mutants of the *Drosophila melanogaster* orthologue, *asterless* (Varmark et al., 2007, Blachon et al., 2008) demonstrate that *asterless* flies have severe problems with spermatogenesis due to an inability to form asters, and hence proper bipolar spindles, causing unequal segregation of chromatids (Varmark et al., 2007), which made Cep152 a very interesting candidate to focus my attention on.

Blachon *et al.* showed that *Asl* is required for centriole duplication in *Drosophila* and that the vertebrate homologue of Cep152 plays the same role in zebrafish (Blachon et al., 2008). Experiments were undertaken to confirm the Cep63-Cep152 interaction via several methods prior to investigating a role for Cep63 in this process.

A *Xenopus* Cep152 orthologue (XCep152) was identified by sequence homology using the NCBI BLAST database search tool using the human Cep152 nucleotide sequence as reference. Henceforth I will refer to human Cep152 as Cep152 and *Xenopus* Cep152 as XCep152. The sequence identified for XCep152 was hypothetical *Xenopus laevis* protein LOC446951; the complete coding sequence for this and for human Cep152 were available as IMAGE clones (IMAGE:5084879 and IMAGE:40125733 respectively) and used as a starting point for cloning.

Xenopus cell free egg extract provides a useful *in vitro* system for biochemical studies and as such it was important to validate the Cep63-Cep152 interaction in both *Xenopus* egg extract and human cell systems. A maltose binding protein (MBP) tag was added at the N-terminus of a XCep152 expression construct and the MBP fusion protein was expressed in *E. coli* at 16°C since the protein was completely insoluble at higher temperatures. Expression and solubility were low, but it was possible to purify sufficient MBP-XCep152 for *in vitro* binding experiments from bacterial cell lysate

using an amylose resin column. It was not possible to obtain pure MBP-full length protein as the preparation always contained a series of what appeared to be either MBP-XCep152 degradation products or, perhaps, products of premature translation termination (figure 23c). It was not possible to remove these smaller degraded proteins either by anion exchange or by gel filtration (not shown). Therefore, pull down assays were performed using preparations that contained shorter truncation, or degradation, products.

Either ^{35}S-labelled Luciferase or XCep63 was mixed with *Xenopus laevis* CSF extract before incubation with MBP or MBP-XCep152 bound to amylose resin. ^{35}S-XCep63 and ^{35}S-XCep152 were generated by adding the appropriate expression vectors to a rabbit reticulocyte *in vitro* transcription translation system, supplemented with ^{35}S labelled methionine (see 2.3.2 and 2.5.5). XCep63 was present in MBP-XCep152 eluate, but not in the MBP eluate (figure 23). Luciferase was used as negative control and was absent in both eluates, which showed that MBP-XCep152 was not just binding all proteins in the reaction.

Importantly, in the reaction without CSF extract, MBP-XCep152 and XCep63 were able to interact, which shows that the interaction was likely to be direct. The amount of XCep63 in the eluate from the reaction containing XCep152, without extract, was lower than the reactions carried out with extract, but this was due to a lower amount of MBP-XCep152 being bound to the amylose resin (figure 23c). This *in vitro* experiment was carried out using XCep63 that was produced using rabbit reticulocyte lysate, so all proteins in the lysate were also present and there is a possibility that they could have mediated the interaction. In order to confirm the direct interaction an *in vitro* experiment in the absence of any other proteins would be necessary. Both Cep63 and Cep152 recombinant proteins are insoluble. Adding an MBP tag to Cep63 promotes solubility, but MBP-Cep152 is still mainly insoluble. In order to carry out this validation it will be necessary to generate soluble recombinant Cep152 with a tag other than MBP. Another option would be expression of the recombinant proteins together using a bicistronic expression vector. I predict that this would promote their solubility

due to the recombinant proteins being able to interact upon expression and improve solubility in a chaperone-like manner.

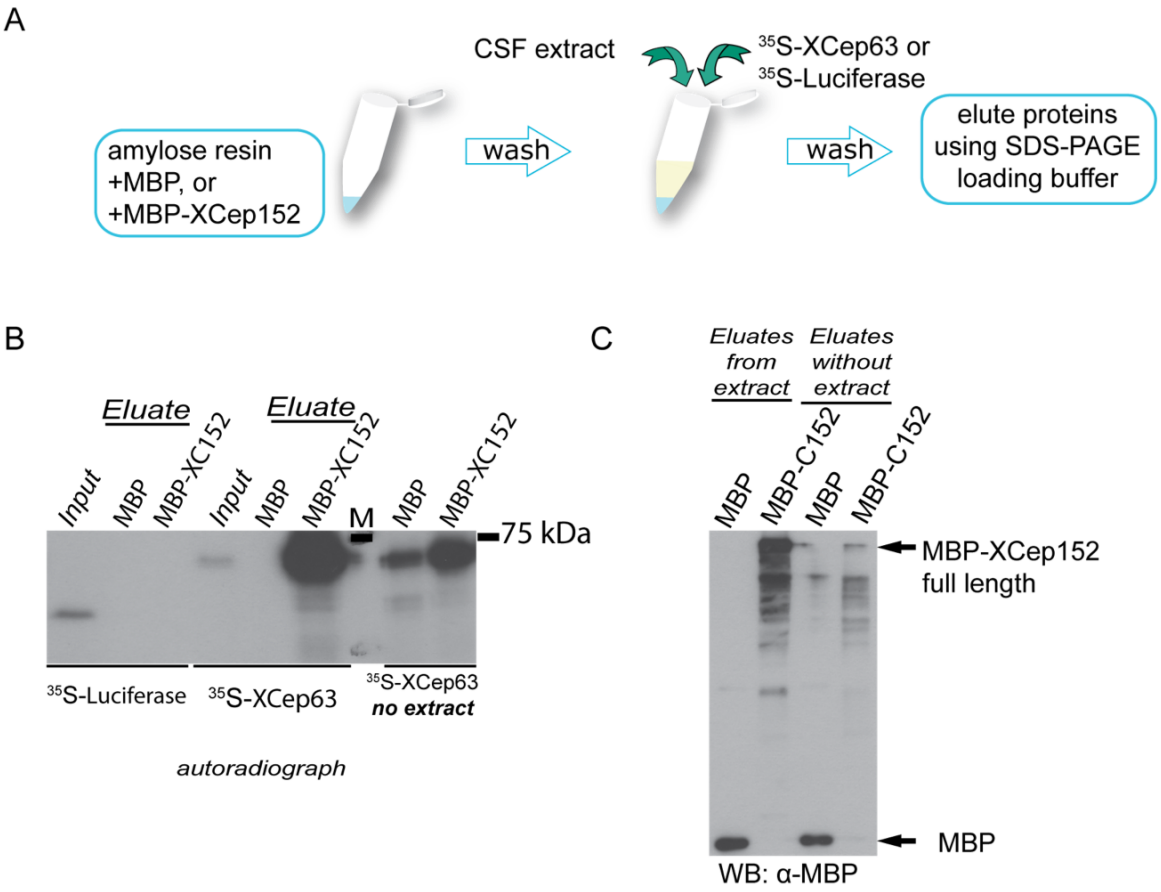

Figure 23 Xenopus Cep63 and Xenopus Cep152 recombinant proteins interact
(A) Schematic diagram of the MBP pull down experiment performed. Either ^{35}S-labelled Luciferase or XCep63 was mixed with *Xenopus* CSF extract before incubation with MBP or MBP-XCep152 bound to amylose resin. (B) Autoradiograph of input (CSF extract mixed with ^{35}S labelled protein) and MBP or MBP-XCep152 eluate samples. Eluate samples from MBP or MBP-XCep152 and ^{35}S-XCep63 incubated without extract are also shown (right hand side). (C) Anti-MBP Western blot showing MBP or MBP-Cep152 in the eluate fractions with or without CSF extract as indicated.

In order to study the Cep63-Cep152 interaction in human cells, human Cep152 was cloned into a Flag destination vector using the Gateway system and 293 stable cell lines were subsequently generated using the FlpIn system, as with Flag-Cep63 (figure 24). Flag-Cep152 localised to the centrosome in these cell lines, as expected (figure 24a). To validate the interaction a Flag IP was carried out after transient transfection of Flag-Cep152 in YFP-Empty or YFP-Cep63 cell lines (figure 8c). YFP-Cep63, but not YFP, was present in the Flag-Cep152 eluate and neither YFP nor YFP-Cep63 were present in the Flag-Empty eluate, which confirmed the mass spectrometry result. Exogenously expressed Cep63 and Cep152 interacted in human cells.

The reverse experiment was then carried out: to pull down exogenous Cep63 and blot for exogenous Cep152. While it was not possible to clone full length Cep152 by conventional cloning, the N-terminal half (amino acids 1-803, 93 kDa) and C-terminal half (amino acids 804-1654, 96 kDa) were successfully cloned into a pIRES expression vector with a N-terminal GFP-Flag tag. While these constructs were useful for other experiments, a full length Cep152 in a pEGFP mammalian expression vector was kindly provided by Ingrid Hoffmann (DKFZ, Mammalian Cell Cycle Control Mechanisms Group), whose group is also working on Cep152. The full length pEGFP-Cep152 was used for transient transfection in a 293 Flag-Cep63 stable cell line and Flag IP of Flag-Cep63 was performed (figure 25). Flag-Cep63 bound GFP-Cep152, but not GFP.

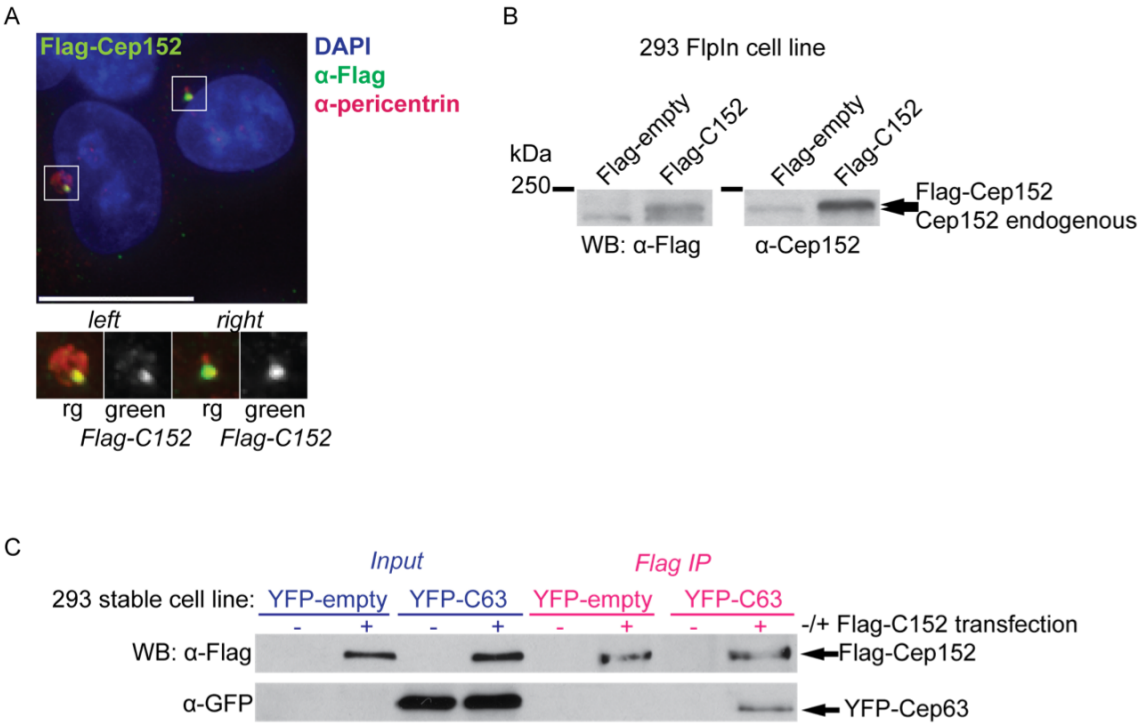

Figure 24 Flag-Cep152 localises to the centrosome and interacts with YFP-Cep63
(A) Flag-Cep152 293 cells stained with anti-Flag and anti-pericentrin antibodies and DAPI. Lower panels show 1.75x enlargements of the boxed areas. Scale bar 15 µm. This image is a maximum projection of deconvolved z-sections. (B) Western blot of cell lysates from Flag-Empty or Flag-Cep152 293 stable cell lines. Left panel shows a Western blot with anti-Flag antibody and the right shows that same membrane re-blotted with anti-Cep152 (479, Bethyl Labs). (C) YFP-Cep63 or empty vector control 293 cell lines were transfected with Flag-Cep152 (+) or empty vector control (-) and anti-Flag immunoprecipitation (IP) was carried out. *Input* cell lysates and eluted proteins (Flag IP) were analysed by SDS-PAGE on a 7.5% gel and Western blotting with anti-Flag antibody to visualise Flag-Cep152 and anti-GFP to visualise YFP-Cep63.

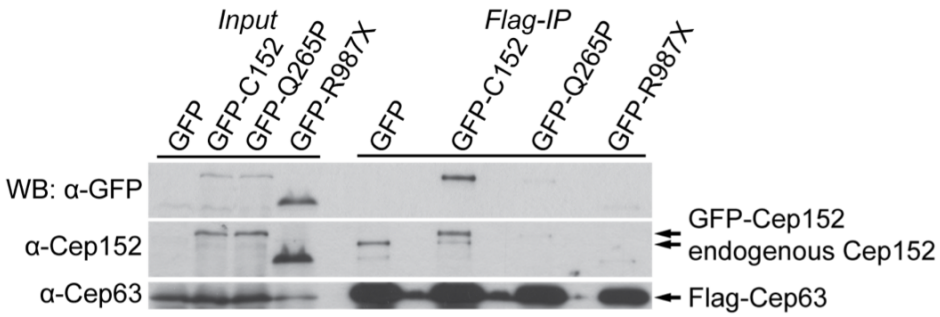

Figure 25 Flag-Cep63 interacts with GFP-Cep152
Flag IP with α-Flag M2 resin from 293 Flag-Cep63 cell lysates. Cells were transfected with pEGFP, pEGFP-Cep152, pEGFP-C152 Q265P or pEGFP-C152 R987X then collected after 48 hours. For Flag IP, 5 mg of cell lysate was used per sample. Bound proteins were eluted and separated on a 10% SDS-PAGE gel, then blotted with anti-GFP, anti-Cep152 479 (Bethyl Labs), or anti-Cep63 49AP (Millipore) antibodies to detect GFP-Cep152 proteins, GFP-Cep152 and endogenous Cep152, and Flag-Cep63. 100 μg whole cell lysate was analysed (*input*) samples.

Interestingly, work from Guernsey *et al*. has associated MCPH4 linked primary microcephaly in three patients to mutations in Cep152 (Guernsey et al., 2010). In this study, two patients were found to be homozygous for a single nucleotide change A to C at nucleotide 794 of Cep152. This was a non-conservative mutation causing a glutamine to proline change at amino acid 265 (Q265P). The third patient was heterozygous for Q265P as was one parent, but the patient was also found to be compound heterozygous with another Cep152 mutation from the other parent. This mutation was a single nucleotide change 2959 from C to T resulting in a premature stop codon at amino acid 987, instead of an arginine residue.

With the hypothesis that the Cep152 mutations described in patients with microcephaly may disrupt the interaction between Cep63 and Cep152, pEGFP-Cep152 vectors harbouring the described patient mutations were generated in order to study their ability to interact with Cep63. The pEGFP-Cep152 vector was used as a template for site directed mutagenesis, as described in 2.2.14, and the resulting constructs used for transient overexpression in Flag-Cep63 293 cells for subsequent Flag IP of Cep63 as described above (figure 25). Interestingly, although both of these mutants were expressed as efficiently (Q265P) or more efficiently (R987X) than the wild type protein, neither of them were as abundant in the Flag-Cep63 IP eluate as the wild type protein. This may have been expected to be the case for R987X, which does not localise to the centrosome (Guernsey et al., 2010), where both Cep63 and Cep152 normally localise. It is interesting to speculate that the pathology associated with mutations in Cep152 are a consequence of an inability of Cep152 to interact with Cep63.

The previously described GFP-Flag-Cep152 N and C terminal half constructs were employed for binding studies with Cep63. 293 cells were transfected with either of the truncation constructs of the pEGFP-Cep152 full length vector. Cell lysates were prepared from transfected cells and incubated with either MBP- or MBP-Cep63 bound amylose resin. Flag IP could not be used in this case since the Cep152 N and C constructs themselves contain a Flag tag. All three GFP-Cep152 proteins were expressed and the most efficient binding was seen between full length Cep152 and

Cep63. Although both the N and C-terminal halves could bind MBP-Cep63, binding was much more efficient with the C-terminal half (figure 26a). Importantly, MBP did not bind any of these Cep152 proteins (figure 26a) and, conversely, GFP did not bind either MBP or MBP-Cep63 (figure 26b).

Transfected 293 cells expressing either of the Cep152 truncations of full length protein were fixed for microscopy and DNA was counterstained with DAPI (figure 26c). Full length GFP-Cep152 localised to the centrosome as expected, as did the C-terminal half, the N-terminal half however did not. This data supports the finding that amino acid residues 1045 to 1290 are required for centrosome localisation of Cep152 (Hatch et al., 2010b) and that residues 1067 to 1654 (C-terminal end) of Cep152 are able to localise to the centrosome (Cizmecioglu et al., 2010). The C-terminal half truncation used covers residues 804 to 1654 and thus includes the residues necessary for centrosome localisation, while the N-terminal half does not. Since the interaction with Cep63 was stronger with the C-terminal half of Cep152, which includes the region required for centrosome localisation, it is interesting to speculate that the interaction with Cep63 may be required for centrosome localisation of Cep152. On the other hand, it could be the case that Cep63 and Cep152 are only able to interact if both are localised to the centrosome. However, since this experiment was carried out using MBP-Cep63 immobilised on amylose resin, it was likely that the interaction could occur without the need for both proteins to be located at the centrosome, as seen for the interaction study carried out in *Xenopus* egg extract where there were no centrosomes present (figure 23). The hypothesis that Cep63 has a role in localising Cep152 to the centrosome was investigated further and the results of these studies are presented in chapter 4.

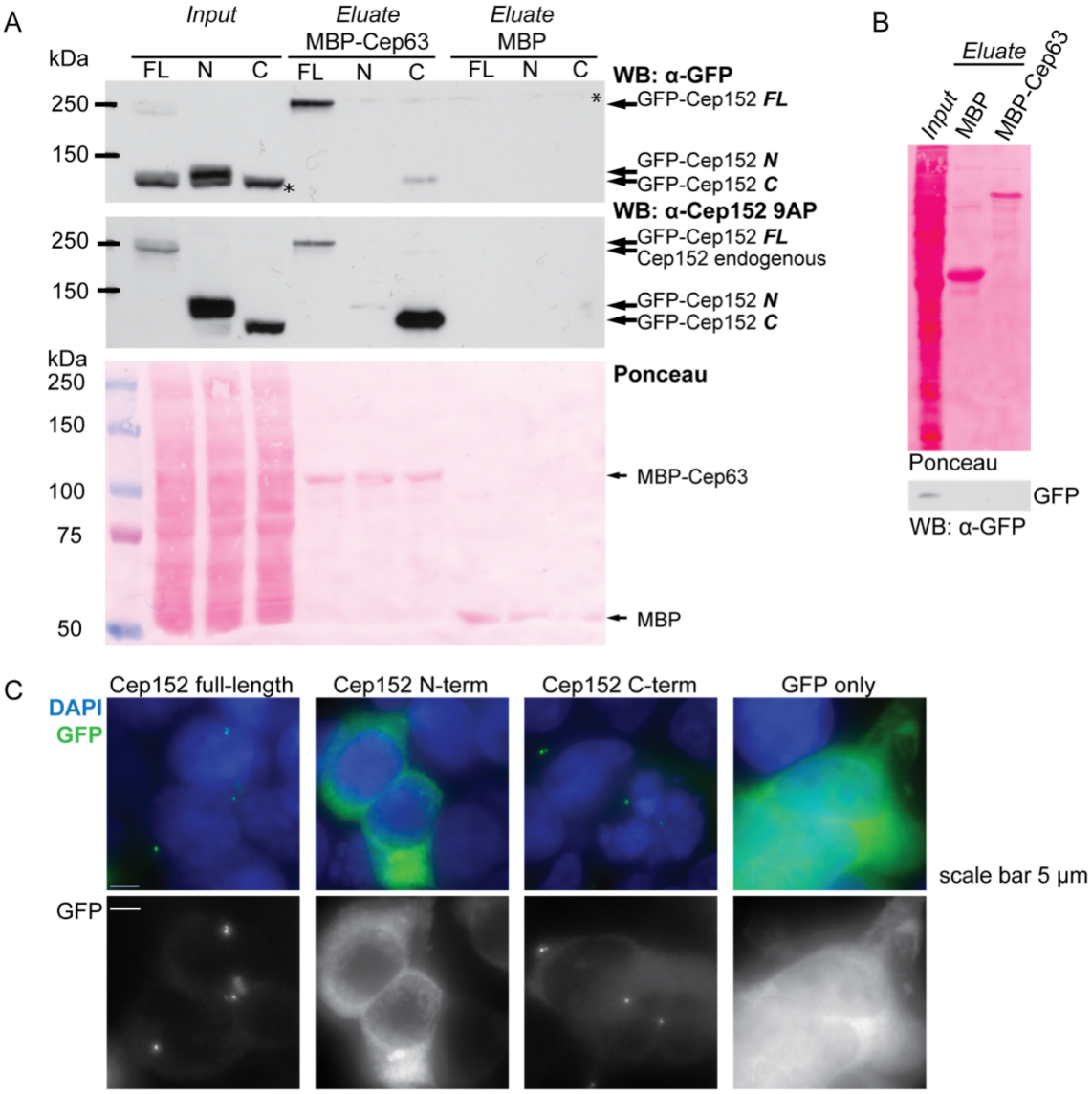

Figure 26 MBP-Cep63 interacts with the C-terminal half of Cep152
(A) Western blots of whole cell lysates (100 µg, *Input*) and eluates from amylose MBP or MBP-Cep63 pull downs carried out with 1 mg cell lysate from 293 cells transfected with GFP-Cep152 full length, N- or C-terminal expression vectors. 7.5% SDS-PAGE gel. Ponceau (bottom) stains total protein. Western blotting was carried out with anti-GFP (mouse) or anti-Cep152 9AP (rabbit) antibodies. * non-specific bands. (B) Western blot of *Input* (100 µg whole cell lysate) and eluates from amylose MBP or MBP-Cep63 pull downs carried out with 1 mg cell lysate from 293 cells transfected with GFP. 15% SDS-PAGE gel. Ponceau shows total protein on the membrane. (C) 293 cells used in the pull down experiment were fixed and stained with DAPI for microscopy. Images are maximum projections of z-sections.

3.2.1 Cep63 - Cep152 interaction is maintained in the presence of DNA damage

XCep63 is an ATM target, which is phosphorylated in response to DNA damage in *Xenopus* egg extract (Smith et al., 2009) and 1.4. XCep63 is a centrosome protein that is required for correct bipolar spindle assembly in CSF extracts. In the presence of DNA damage XCep63 is phosphorylated in an ATM/ATR dependent manner and it is subsequently de-localised from the centrosome. As a result, spindle formation and maintenance is disrupted. Addition of exogenous mutant XCep63 that cannot be phosphorylated by ATM/ATR, rescues spindle formation in the presence of DNA damage.

To address whether XCep63 was performing its function in spindle assembly in combination with XCep152 and whether the DNA damage dependent phosphorylation of XCep63 would have an effect on its interaction with XCep152, interaction studies were carried out in the presence of DNA damage. Exogenous XCep63 produced with the rabbit reticulocyte lysate *in vitro* transcription-translation system is completely phosphorylated in the presence of DNA damage signalling in *Xenopus* CSF extract, as determined by band shift (figure 27a and (Smith et al., 2009). DNA damage signalling in extract is stimulated, in this experiment, by the addition of short double stranded 70-mer fragments of DNA, created by annealing poly-A and poly-T 70-mer oligonucleotides (pA/pT). The experiment described in figure 23 was repeated in the presence of DNA damage. MBP or MBP-XCep152 was immobilised on amylose resin and CSF extract containing ^{35}S-labelled XCep63 was incubated with or without pA/pT double stranded DNA, then added to the amylose resin. Eluates were analysed by SDS-PAGE and autoradiography (figure 27a). ^{35}S-XCep63 was clearly phosphorylated in extract supplemented with pA/pT, as determined by SDS-PAGE band shift, and this phosphorylated form of the protein was still able to bind MBP-XCep152 with high efficiency.

To address the same question in human cells, a Flag IP was performed with Flag-empty or Flag-Cep63 cell lines incubated in the absence or presence of Phleomycin (0.2 mg/ml) for 2 hours prior to collection and lysis. Phleomycin is an antibiotic that causes double strand DNA breaks (Povirk, 1996) and thus causes activation of ATM and the downstream DNA damage signalling cascade. Activation of the DNA damage checkpoint after Phleomycin treatment was confirmed by Western blotting with anti-phospho-Serine 1981 ATM and γH2AX antibodies, which are direct and downstream markers of ATM activation, respectively (figure 27b). Flag IP eluates were separated by SDS-PAGE and bands were cut and sent to the Protein Analysis & Proteomics laboratory for mass spectrometry analysis. Cep152 was still present as the most abundant interacting protein in the Flag-Cep63 eluate with Phleomycin treatment; although this technique did not generate a quantitative result, it indicated that the presence of DNA damage signalling did not affect the stability of the Cep63-Cep152 interaction. It was unknown if human Cep63 was a target of ATM/ATR kinase activity. Cep63 does contain several ATM/ATR consensus sites, but the region of XCep63 that is phosphorylated is not conserved in the human protein (figure 55)(Smith et al., 2009)). The work presented in section 4.9 addresses the possibility that Cep63 might also be an ATM target in human cells.

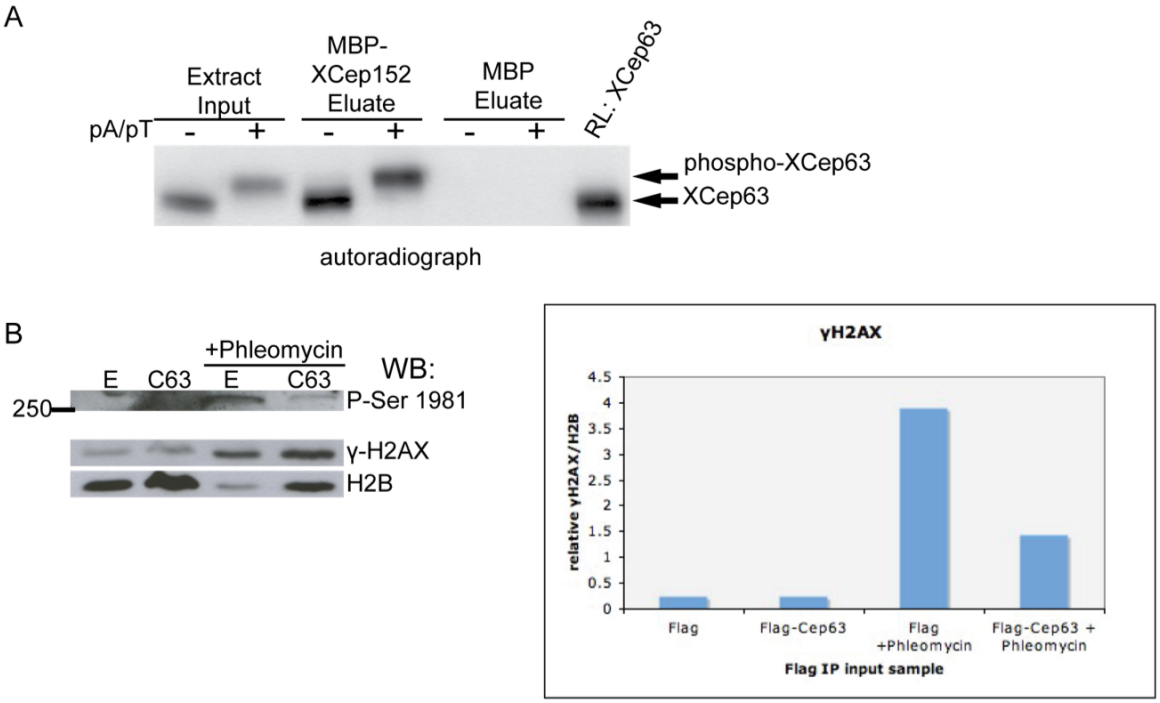

Figure 27 Cep63-Cep152 interaction is not disrupted by DNA damage
(A) MBP or MBP-XCep152 was immobilised on amylose resin and incubated with extract containing ^{35}S-labelled XCep63 in the absence (-) or presence (+) of 70-mer double stranded DNA molecules (pA/pT). XCep63 is phosphorylated in the presence of pA/pT, which activates ATM and the subsequent DNA damage signalling cascade, as detected by reduced electrophoretic mobility (phospho-XCep63 arrow). (B) Western blot of 293 cell lysates used in the Flag-IP assay untreated or treated with Phleomycin to induce DNA double strand breaks, with phospho-Ser 1981 ATM antibody, anti- γ-H2AX and anti-Histone H2B as a loading control for γ-H2AX. Cell lysates are from Flag-Empty (E) or Flag-Cep63 (C63) cells. Graph shows quantification of the γ-H2AX bands relative to the amount of histone H2B.

3.3 Western blotting of Cep63 and Cep152

The next step in confirming the interaction between Cep63 and Cep152 was to visualise the endogenous proteins by Western blotting.

3.3.1 Cep63 antibody validation by Western blotting

The Cep63 antibodies used in this thesis were generated in collaboration with Millipore. A Gateway donor vector containing the Cep63 sequence was prepared and sent to Millipore to generate GST-Cep63 full-length antigen for rabbit immunisation. The terminal bleeds of four rabbits were tested and two rabbits were identified as producing antibodies recognising Flag-Cep63 (47 and 49, figure 28). The resulting affinity purified antibodies were named Cep63 49AP and Cep63 47AP. These antibodies were generated using the same protocol, in two different rabbits. Antibodies 47AP and 49AP both specifically recognised over-expressed Flag-Cep63 by Western blotting (figure 28) and the endogenous protein by immunofluorescence (figures 34 and 35). A rabbit polyclonal Cep63 antibody was also purchased from Proteintech Group Inc. (designated Cep63 PTG in this thesis). The Cep63 PTG antibody recognised exogenous over-expressed Cep63 by Western blot and the endogenous protein by immunofluorescence (not shown).

All Cep63 antibodies were tested for Western blotting using whole cell lysates of cells untreated or transfected with Cep63 specific siRNAs. None of the bands detected by these antibodies, in whole cell lysate, appeared to be reduced or absent in RNAi treated cell lysates (one example is shown in figure 28b, Cep63 49AP). Cep63 RNAi did, however, reduce levels of GFP-Flag-Cep63 in a stable HeLa cell line (figure 28c). Cep63 RNAi validation was also carried out by detecting mRNA level and by immunofluorescence (section 3.4). Cep63 49AP and 47AP were able to recognise Cep63: throughout the immunisation process the serum recognised Flag-Cep63 whereas the pre-immune serum did not (figure 28a).

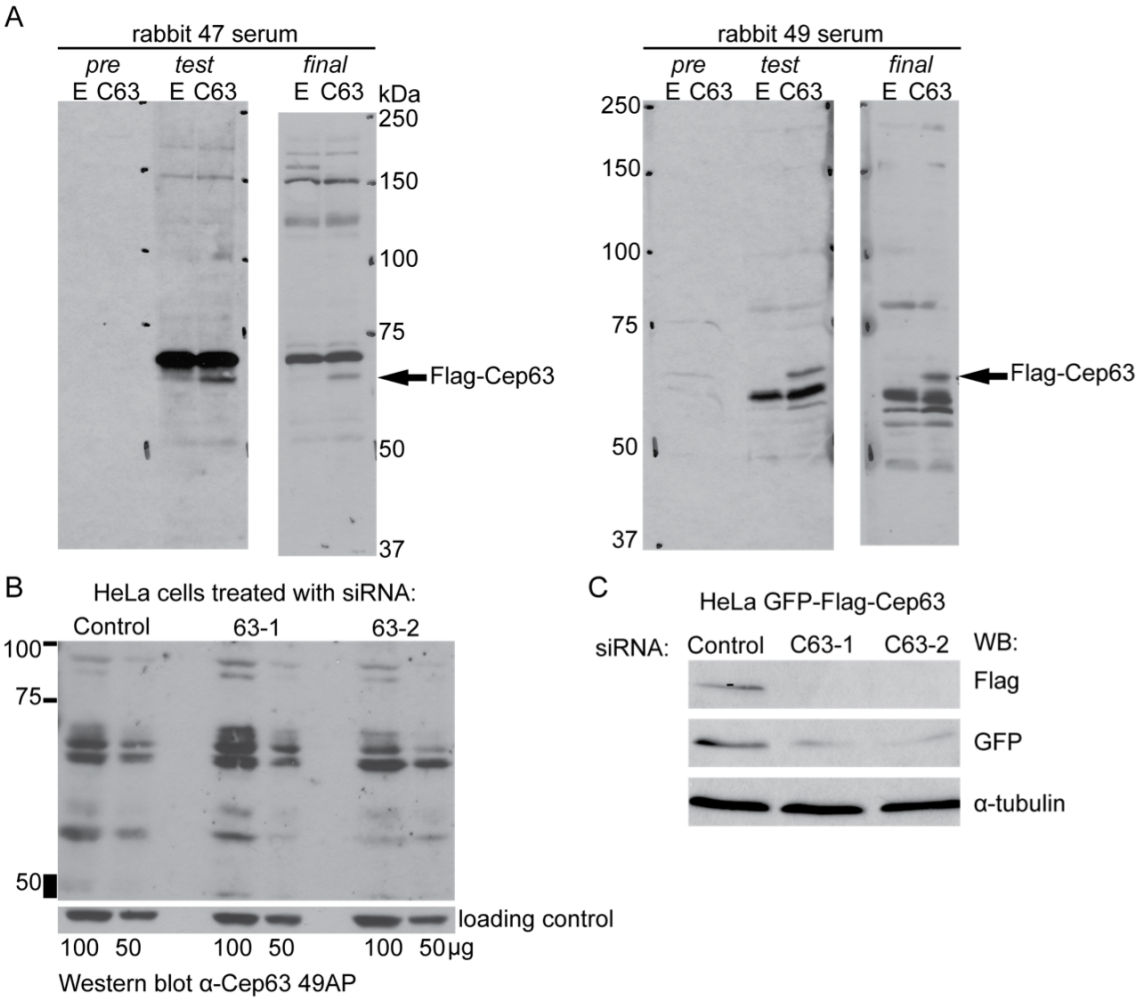

Figure 28 Cep63 antibody testing by Western blot
(A) Pre-immune (pre), third bleed (test) and final bleed (final) serum from two rabbits immunised with GST-Cep63 (rabbit no. 47 and 49) was tested by Western blot of whole cell extracts from 293 cells stably expressing Flag-Empty vector (E) or Flag-Cep63 (C63). Molecular weight markers are indicated in kDa. (B) Western blot of cell lysates from HeLa cells transfected with control or Cep63 specific siRNAs (63-1, 63-2), 100 and 50 µg of cell lysates were loaded. (C) Western blot analysis of HeLa cells stably expressing GFP-Flag-Cep63 treated with control or Cep63 RNAi (63-1 and 63-2). Anti-GFP and Flag antibodies were used to detect tagged Cep63 levels and α-tubulin was visualised as a loading control.

Cep63 RNA is alternatively spliced to give rise to 4 different variants that have been detected in expression profiles. There are 4 predicted protein isoforms a – d, which are 81, 63, 58 and 56 kDa in size. The isoform cloned and used for exogenous protein studies throughout this thesis is isoform b, 63 kDa. This was the protein identified in the mass spectrometry screen carried out by Andersen et al. (Andersen et al., 2003), and was the only full length coding sequence available from the IMAGE consortium. However it would be expected to see 4 Cep63 specific bands by Western blot.

Since the 49AP and 47AP antibodies specifically recognise over-expressed Cep63 by Western blot and endogenous Cep63 by immunofluorescence (figures 28 and 35), it was reasoned that they did not detect Cep63 specific bands in whole cell lysate due to very low expression of Cep63. To overcome this problem, experiments were carried out to enrich Cep63 (section 3.3.3).

3.3.2 Cep152 antibody validation by Western blot

A commercial Cep152 antibody (rabbit polyclonal, Bethyl Labs no. 479) that was generated using an N-terminal peptide, amino acids 50-100, as an antigen was tested for specificity using RNAi to deplete Cep152 before analysing cell lysates by Western blot (figure 29). Two anti-Cep152 reacting bands migrating between the 150 and 250 kDa protein marker on 7.5% SDS-PAGE gels were eliminated upon transfection with Cep152 siRNAs, which indicated that the Cep152 479 antibody was indeed specific to Cep152. Flag-Cep152 migrated to the same position as the larger endogenous protein (figure 29) and both Flag-Cep152 and YFP-Cep152 exogenous tagged proteins were also recognised by Cep152 479. Importantly, anti-Cep152 479 recognised a band of the same size in Flag-Cep63 Flag IP eluate (figure 30) and purified centrosome fractions (figure 31c). Another Cep152 antibody, Cep152 9AP also recognised two bands of the same size on Western blots of purified centrosomes (figure 31). It is possible that the faster migrating band represents an alternate splice variant that results in a smaller protein isoform.

The Bethyl Cep152 antibody was not available at the time Cep152 was identified as a Cep63 interacting protein. Consequently, rabbit polyclonal antibodies directed against N-terminal (amino acids 18-31) and C-terminal (amino acids1600-1617) Cep152 peptides were generated. The serum was affinity purified using both peptides and the resulting antibody, named Cep152 9AP, was able to detect full length, N-terminal and C-terminal halves of exogenously expressed Cep152 (figure 26a). Cep152 9AP was also able to recognise the endogenous protein in whole cell lysate and purified centrosomes (figure 31). However, no specific signal was detected when using this antibody for immunofluorescence (not shown), which indicated that the antibody either had low affinity for Cep152 or that it was only able to recognise the denatured form of the protein.

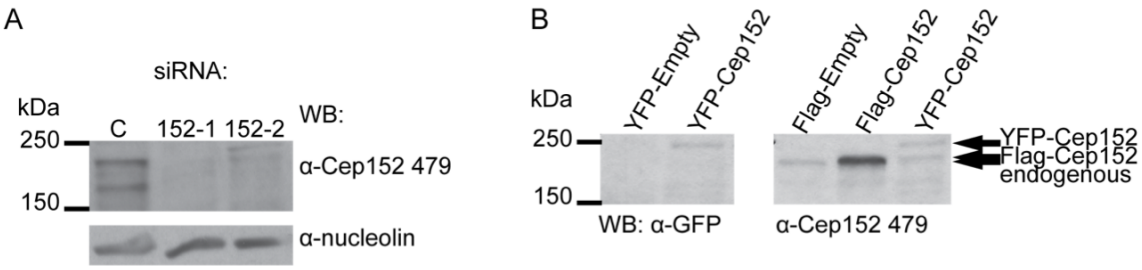

Figure 29 Cep152 antibody testing by Western blot

(A) Western blot of 293 cell lysates from cells transfected with control (C) or two different Cep152 siRNAs (152-1, 152-2) with anti-Cep152 479 antibody (Bethyl Labs). (B) Western blots of cell lysates from stable 293 Flag-Empty, Flag-Cep152 or YFP-Cep152 cell lines with anti-Cep152 479, shown for comparison. Cep152 479 recognises a band that migrates at the same position as Flag-Cep152 and which disappears upon Cep152 RNAi.

3.3.3 Cep63 enrichment for Western blotting

Using the 293 Flag-Cep63 and Flag-Cep152 cell lines, a Flag IP was performed followed by Western blot of the eluates using Cep63 and Cep152 antibodies in order to detect the endogenous proteins (figure 30). This experiment formed an important part of validating the Cep63 antibody.

Firstly, Cep152 could be seen in input samples from all cell lines and in eluates from Flag-Cep152 clonal and transiently transfected cells (this is Flag-Cep152, which runs at around the same molecular weight as endogenous Cep152 on the 7.5% gel used here). Endogenous Cep152 was clearly present in the Flag-Cep63 eluate (figure 30a, last lane), showing that Flag-Cep63 was able to specifically interact with endogenous Cep152. Flag-Empty eluates did not contain any Cep152 (second lane). Flag-Cep152 IPs, from clonal cells and from cells transiently over-expressing the protein, contained anti-Cep63 reacting bands that were absent from input cell lysate samples and from the Flag-Empty eluate (blue lines 1-4, figure 30). Band 1 indicates a band greater than 75 kDa that was present only in Flag-Cep152 eluates and could be Cep63 isoform a, which is predicted to be 81 kDa. The middle band 2, indicates a doublet, the upper of which migrated to the same position as Flag-Cep63. This doublet was not apparent in whole cell lysates or the Flag-Empty eluate, indicating that it could be Cep63 isoform b at 63 kDa. The lower doublet could be isoforms 3 and 4; it was present in Flag-Cep152 eluates, but not Flag-Empty eluates.

In summary, this experiment showed that Flag-Cep63 interacts with endogenous Cep152 and that Flag-Cep152 interacts with four anti-Cep63 reacting bands, which likely represent endogenous Cep63.

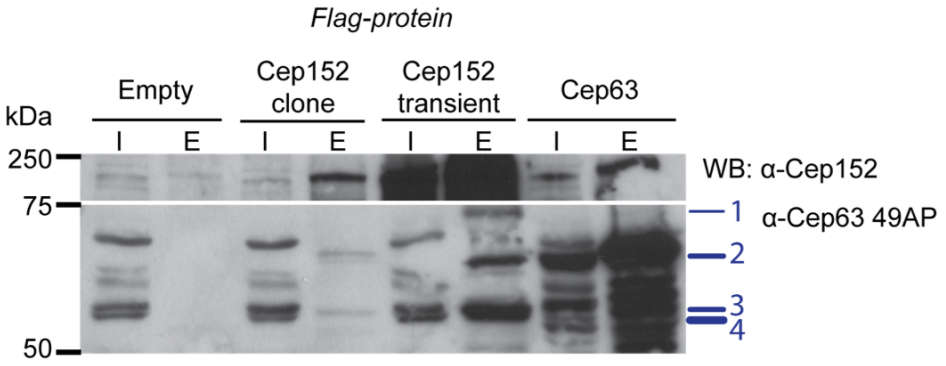

Figure 30 Flag-Cep63 interacts with endogenous Cep152 and Flag-Cep152 interacts with anti-Cep63 reacting proteins
Flag IPs were carried out using cell lysates from 293 stable cell lines expressing Flag-Empty, Flag-Cep152 or Flag-Cep63; or from 293 cells transiently over-expressing Flag-Cep152. Input (I) and eluate (E) samples were analysed by Western blotting with anti-Cep152 (479, Bethyl) and anti-Cep63 (49AP, Millipore) antibodies. Input samples are 100 µg cell lysate and IPs were carried out using 5 mg cell lysate. Proteins were separated on a 7.5% SDS-PAGE gel. Blue lines (1-4) indicate potential endogenous Cep63 bands, which are present in Flag-Cep152 eluate and the centrosome sample.

In order to enrich Cep63 by an alternative method, centrosomes were purified from a human lymphoblastoma cell line, KE37 according to the protocol described by Bornens *et al.* (Bornens et al., 1987). Specific details of the purification procedure can be found in 2.4.6. Fractions were examined by immunofluorescence and Western blot with antibodies against known centrosome proteins, γ-tubulin and Centrin 3, as well as the Cep63 49AP antibody (figure 31). Purified centrosomes assayed by immunofluorescence stained positive for Cep63 (figure 31a), which indicated that the protein should be enriched in these fractions. Analysis of fractions by SDS-PAGE on a 15% gel showed that γ-tubulin and Centrin 3, both known centrosome components, were present and Western blotting with Cep63 49AP antibodies revealed some anti-Cep63 interacting bands that were not apparent in the whole cell lysate (figure 31b). Fractions were then subjected to SDS-PAGE on a 7.5% gel in order to obtain better separation between the bands. Western blotting with Cep63 49AP (figure 31c), 47AP and Cep63 PTG antibodies (figure 31d) revealed the presence of 4 anti-Cep63 interacting bands. The same pattern of bands was seen with 3 different antibodies and these bands were absent (bands 1 and 2), or not abundant in whole cell lysate. The bands are labelled 1-4 in figure 31d. Band 1 migrated to a position that could be expected for Cep63 isoform a, 81 kDa. Band 2 migrated as a doublet, which could be isoform b, 63 kDa. Bands 3 and 4 could be isoforms c and d, which would presumably migrate close together due to the small difference in molecular weight (56 and 58 kDa).

Cep63 bands in a centrosome enriched sample and Flag-Cep152 eluate were compared directly, using a 10% SDS-PAGE gel and Western blotting (figure 31e). The same bands were present in the centrosome sample as in Flag-Cep152 eluate. Although these observations do not formally confirm that the identified bands were Cep63 there were few feasible options for further validation. RNAi of Cep63 led to no change in the pattern of bands in whole cell lysate (figure 28) and RNAi and subsequent centrosome purification would provide a way to verify that these bands are in fact Cep63, but this was not a viable option since the purification protocol requires 2 x 10^8 cells, for which an extremely large amount of siRNA and transfection reagent would be required. This purification could perhaps be scaled down for analysis of RNAi treated cells.

Alternatively, the generation of cell lines with stable expression of short hairpin RNAs (sh-RNAs) for stable knockdown of Cep63 could be used for large-scale experiments.

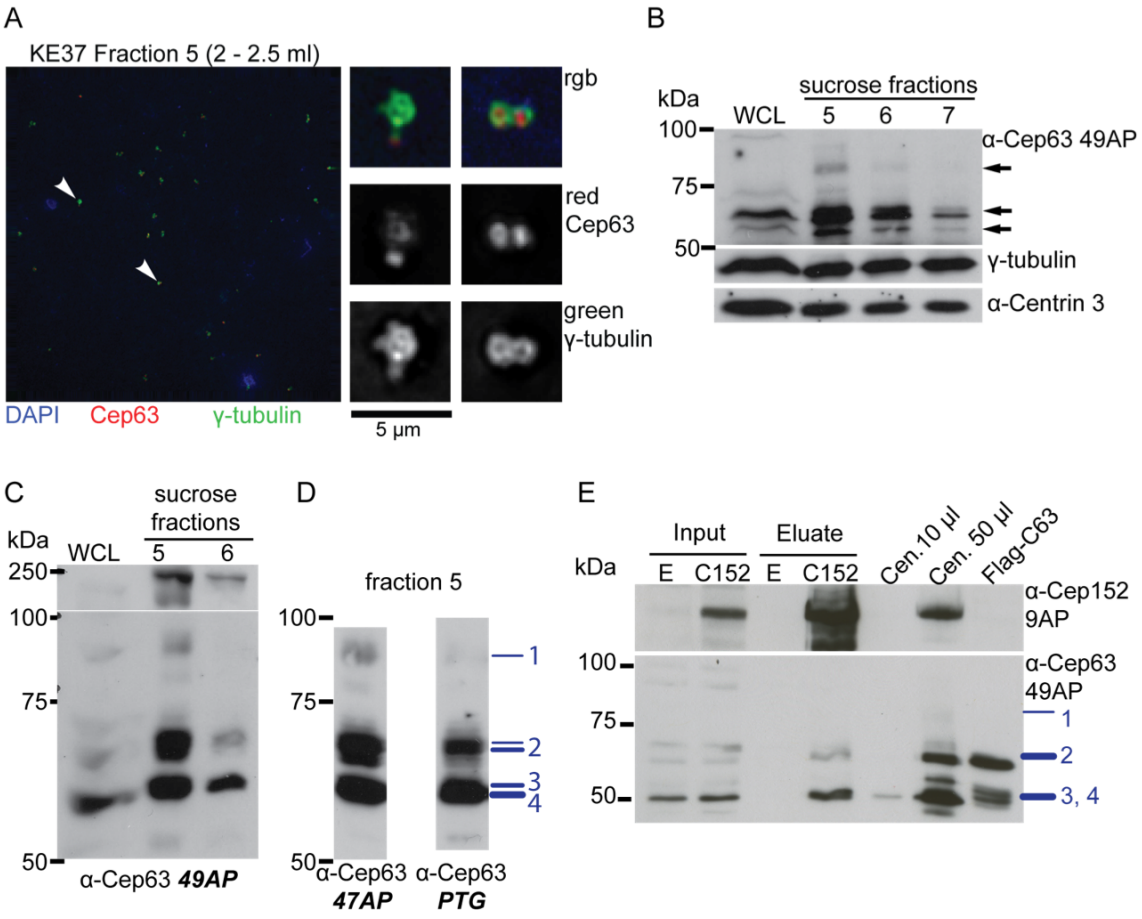

Figure 31 Centrosome purification from KE37 human cells

(A) Immunofluorescence of centrosomes from fraction 5 of the sucrose gradient using γ-tubulin (green) and anti-Cep63 49AP (red) antibodies. DAPI staining highlights that the centrosomes are not completely pure as DNA fragments are present in the fraction. Arrows indicate the two centrosomes enlarged in the right-hand panels. (B) KE37 whole cell lysate (WCL) and fractions 5-7 were analysed on a 15% SDS-PAGE gel and Western blotting with anti-Cep63 49AP, γ-tubulin and Centrin 3 antibodies. Arrows indicate Cep63 reacting bands that are not apparent in the WCL. Fractions 5 and 6 were separated on a 7.5% SDS-PAGE gel and Western blotting was carried out with anti-Cep63 49AP and anti-Cep152 479 (top panel, C) and anti-Cep63 47AP and PTG antibodies (D). (E) Western blot comparing Flag IP inputs (whole cell lysates) and eluates from Flag-Empty (E) or Flag-Cep152 (C152) 293 cells; two amounts of centrosome fraction 5 (Cen.); and Flag-Cep63 293 whole cell lysate. Anti-Cep152 Western blot (top panel) confirmed that Flag-Cep152 was present in the Flag-Cep152 eluate. Cep152 endogenous protein was also seen in centrosome fractions. Blue lines labelled 1-4 highlight the anti-Cep63 reacting bands present both in centrosome fractions and in Flag-Cep152 Flag IP eluate. Protein standard markers are indicated on the left of Western blots, sizes indicated are kDa.

3.4 Cep63 immunofluorescence and RNAi validation

Since endogenous Cep63 protein could not be detected by Western blotting of whole cell lysates, validation of Cep63 RNAi was performed by detecting Cep63 transcript levels by reverse transcriptase-polymerase chain reaction (RT-PCR) on purified RNA from untreated or Cep63 depleted cells using Cep63 primers (figure 32b and 33).

As previously mentioned, there are four predicted expressed splice variants of Cep63 (National Center for Biotechnology Information, NCBI). Since we could not predict which splice variants may be important in our assays it was important to ensure that all isoforms of the protein could be depleted. Three Cep63 siRNAs that were directed against exons included in all predicted Cep63 splice variants were used (figure 32a). For RT-PCR analysis four sets of primers were designed; two sets were designed to amplify regions that were identical in all variants (Cep63-2 and -5, figure 32) and two that were designed to differentiate variant 1 (Cep63-4) and variants 3 and 4 from 1 and 2 (Cep63-6). Variant 1 could be detected specifically using the primers Cep63-4 (482 bp product, figure 32b). These primer pairs did not allow differentiation between variants 1 and 2 or between 3 and 4. Variants 1 and/or 2 were present (1493 bp product Cep63-2; 347 bp product Cep63-6) and variants 3 and/or 4 were present (209 bp product Cep63-6). Importantly, all of these products were greatly reduced in cells treated with either of the Cep63 targeting siRNAs, 62-1 or 63-2, relative to control siRNA treated cells (figures 32b and 33). GAPDH specific primers were used as a control for the amount of RNA in each reaction and the PCR reaction itself (G1). Since this analysis was carried out, another group analysed Cep63 transcripts by quantitative PCR (qPCR) using primers that could identify the 4 variants specifically (Loffler et al., 2011). This study demonstrated that all variants are expressed in two different human cell lines, BJ and U2OS. Specifically, they identified variant 3 as the most abundant, followed in order by 2, 4 then 1 (Loffler et al., 2011).

Future RT-PCR analyses were carried out using primers Cep63-2 and -5 since they allowed visualisation of all transcripts. The RNAi experiment in figure 32b was carried out in HeLa Kyoto cells following 2 transfections with 20 nM siRNA carried out 24 hours apart. Cells were collected 4 days after the initial transfection. The same protocol was then carried out in U2OS cells (figure 33). The siRNAs depleted Cep63 in both U2OS and HeLa K cells with equal efficacy; in both experiments siRNA 63-2 appeared to be more effective, although this technique is not absolutely quantitative.

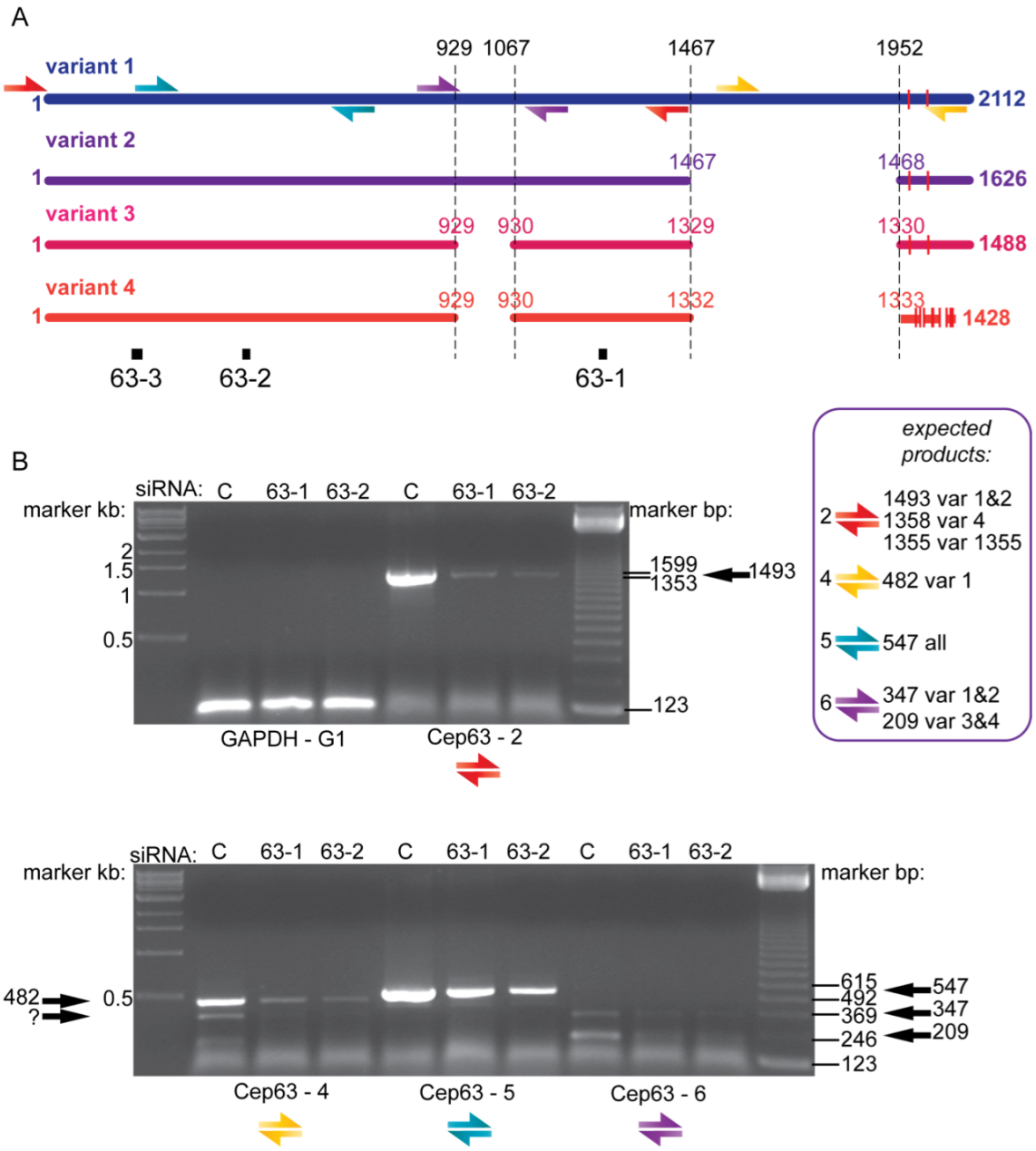

Figure 32 Cep63 splice variants and Cep63 RNAi
(A) Schematic showing the 4 published Cep63 splice variants and the position of the 3 siRNAs I used (black squares 63-1, 63-2, 63-3) and the 4 sets of primers used for RT-PCR (coloured arrows). (B) RT-PCR reactions carried out on RNA purified from HeLa K cells transfected with control (C) or Cep63 specific siRNAs (63-1, 63-2). Primers used are indicated below each panel. GAPDH-G1 primers were used as a control. RT-PCR products were separated by electrophoresis on a 1% agarose gel containing ethidium bromide to allow visualisation of DNA by UV illumination. 1 kb and 123 bp markers are indicated on the left and right of panels, respectively. Arrows indicate the estimated size of PCR products based on comparison with markers and the predicted product sizes. Purple box indicates variant specificity of the primer pairs.

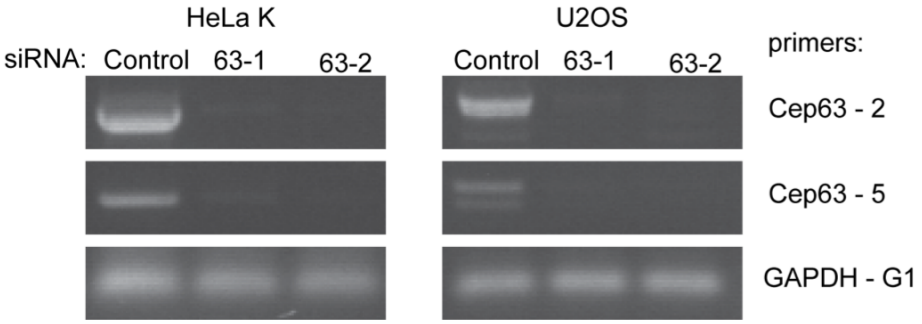

Figure 33 Cep63 RNAi depletes Cep63 mRNA
RT-PCR reactions carried out on RNA purified from HeLa K or U2OS cells transfected with control (C) or Cep63 specific siRNAs (63-1, 63-2), using primers Cep63-2, -5, or GAPDH-G1 as a control. RT-PCR products were separated by electrophoresis on a 1% agarose gel containing ethidium bromide to allow visualisation of DNA by UV illumination.

Cep63 antibodies were examined for their ability to stain endogenous Cep63 by immunofluorescence of fixed cells. Analysis of Cep63 47 and 49 pre-immune, third bleed, and final bleed serum by immunofluorescence is shown in figure 34. Pre-immune serum from both rabbits detected the centrosome (figure 34). However, after the immunisation program was complete, serum from both rabbits recognised the centrosome with much higher affinity and the staining covered a smaller and more defined region of the centrosome. Furthermore, Cep63 47 and 49 affinity purified antibodies (AP) also stained the same region of the centrosome, whereas other non-centrosomal cytoplasmic staining was lost.

In order to confirm that the purified antibody was reacting to Cep63 specifically and not alternate or additional centrosome proteins, immunofluorescence was performed with cells transfected with Cep63 siRNAs. Cep63 RNAi either eliminated or decreased Cep63 immunofluorescence at the centrosome confirming that Cep63 49AP was specific to Cep63 (figure 35). This is also shown and quantified in figure 49, chapter 4. These experiments also confirmed that it was possible to deplete Cep63 protein using Cep63 siRNAs. Throughout RNAi trials with Cep63 siRNAs and subsequent analysis with Cep63 immunofluorescence it became clear that it was necessary to carry out RNAi for a period of at least 4 days in order to obtain cells with no visible Cep63

staining. After 24 hours of knockdown all centrosomes still contained Cep63. From 72 hours, some centrosomes were depleted of Cep63, but cells often contained one Cep63 positive and one Cep63 negative centrosome. Therefore, all experiments were carried out using 2 transfections with 50 nM siRNA, 24 hours apart with subsequent cell harvest three days after the second transfection. Longer periods of knockdown lead to greatly reduced cell numbers.

Cep63 49AP localisation to the centrosome is dependent on Cep63. Furthermore, GFP and Flag tagged exogenous Cep63 proteins localise to the centrosome in 293 (figures 17 and 18), U2OS, and HeLa cells (figure 20). Cep63 49AP antibody exclusively stained the centrosome in the same region as that occupied by tagged Cep63 (figure 36). Cep63 antibody staining was present at the centrosome throughout the cell cycle; G1, G2 and mitotic examples are shown in figure 36. Cep63 appeared to adopt a bi-lobed shape, which was most apparent in mitotic cells, bottom panel figure 36. In other cells the shape was either bi-lobed or ring-doughnut shaped (top and middle panels).

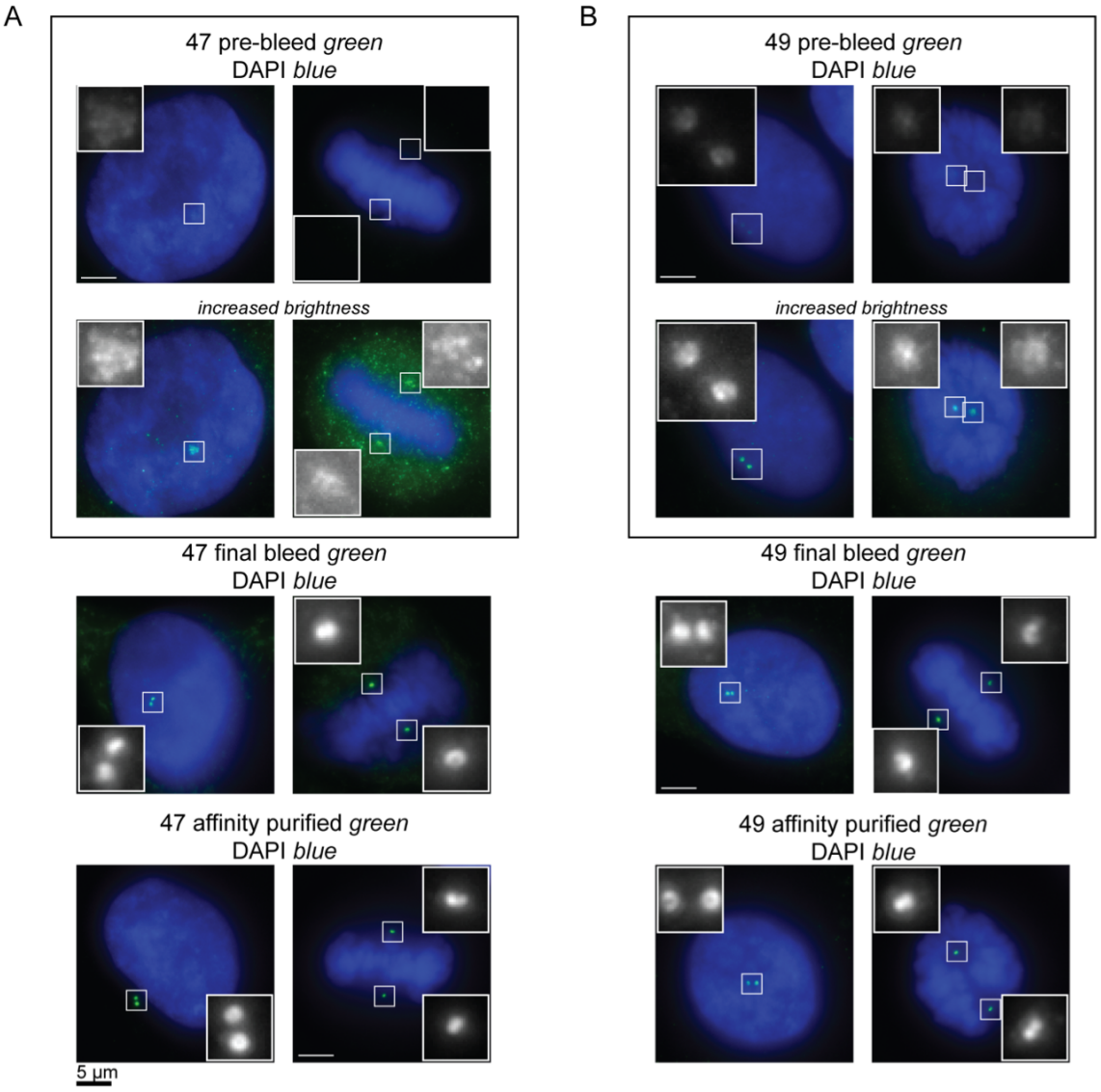

Figure 34 Cep63 antibody testing by immunofluorescence

HeLa cells were fixed and stained with pre-immune, final bleed (immune), and affinity purified Cep63 antibodies from rabbits 47 (A) and 49 (B) (green) and DAPI to visualise DNA. Images are maximum projections of z-stacks without deconvolution. The brightness was increased in the lower panels of the pre-immune pictures in order to illustrate the diffuse low-level staining seen in the centrosome region in these samples. Inserts show 5x enlargements of the boxed regions in each image. Pre-immune serum from both rabbits recognised centrosomal epitopes, but Cep63 immunisation resulted in the production of antibodies that recognised a very defined region of the centrosome, with much higher efficiency.

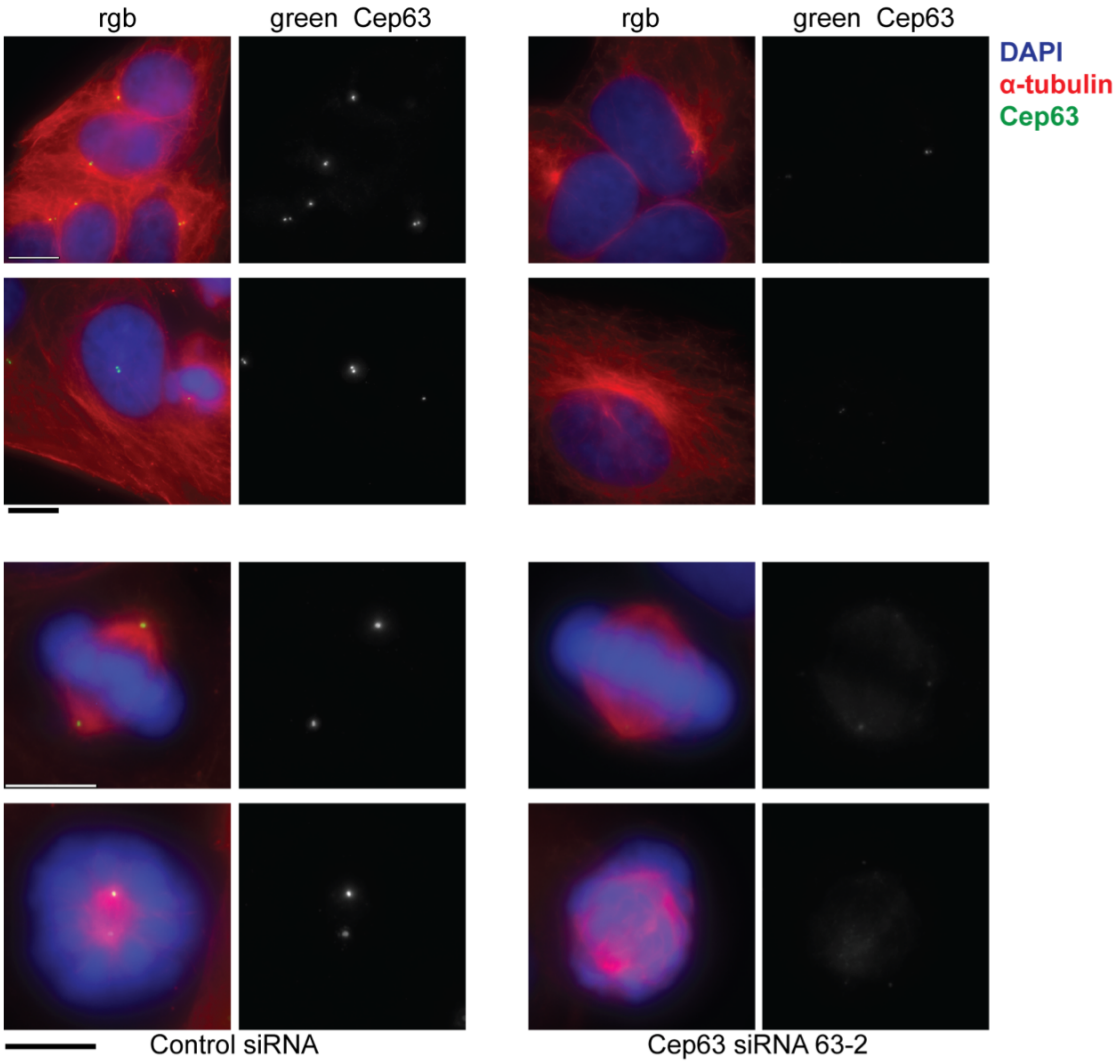

Figure 35 Cep63 immunofluorescence reduction after Cep63 RNAi
U2OS cells transfected with control siRNA (left) or Cep63 siRNA (63-2, right). Cells were stained with anti-Cep63 49AP (green) and α-tubulin (red) antibodies and DAPI. Cep63 staining is reduced in cells treated with Cep63 siRNAs. Images are maximum projections of z-sections without deconvolution. Scale bar 15 µm.

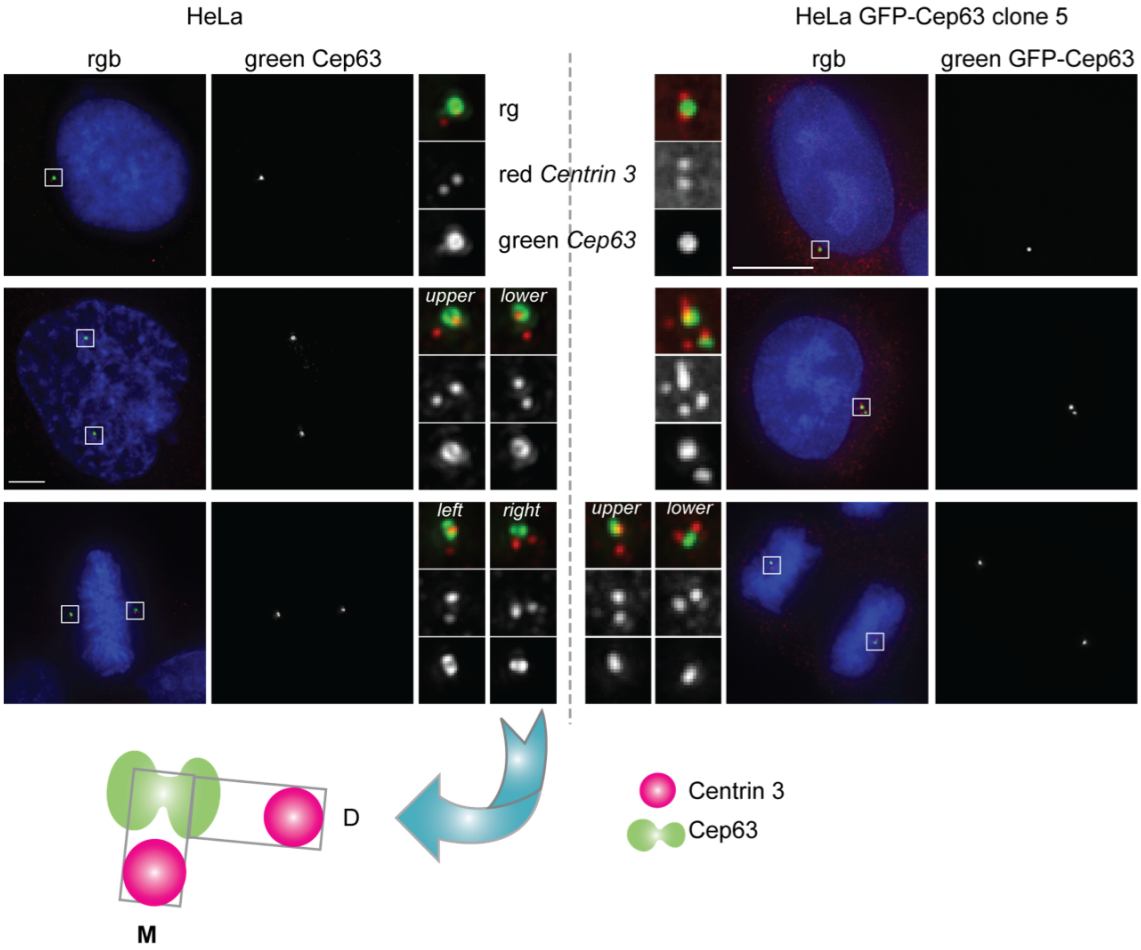

Figure 36 Centrosomal localisation of endogenous and exogenous Cep63
Left hand panels show HeLa K cells stained with anti-Cep63 49AP (green) and Centrin 3 (red) antibodies and DAPI to visualise DNA. Right hand panels show HeLa K GFP-Cep63 cells stained with Centrin 3 antibody (red) and DAPI; green shows direct GFP fluorescence. Small panels show three times enlargement of the boxed regions (centrosomes). Diagrams illustrate the Cep63 (green) and Centrin 3 (pink) staining with respect to the predicted centriole position (grey boxes). Images are maximum projections of deconvolved z-sections. Scale bars are 5 µm (left panels) and 15 µm (right panels).

3.5 Cep152 immunofluorescence

The anti-Cep152 rabbit polyclonal antibody from Bethyl Laboratories (no. 479) was used to study Cep152 localisation. This antibody recognised a band on Western blots of whole cell lysates, which was reduced or absent in Cep152 RNAi treated cells, indicating its specificity for Cep152 (figure 29). Cep152 479 antibody stained the centrosome in HeLa cells (figure 37a). Importantly, the signal was reduced or completely absent in centrosomes of cells treated with Cep152 siRNA-1, which indicated that the antibody was specific for Cep152. Furthermore, immunofluorescence in U2OS cells resulted in the same staining pattern, which was also abolished upon in cells transfected with two different Cep152 siRNAs (152-3 and 152-4, figure 37b). From these data, it was clear that anti-Cep152 479 recognised endogenous Cep152 by Western blotting of whole cell lysates and by immunofluorescence.

Cep152 localised to the PCM, as observed by colocalisation with γ-tubulin (figure 37). Specifically, it co-localised precisely with GFP-Cep63 (figure 21d) and appeared to take on a bi-lobed shape like Cep63, which was easiest to visualise in mitotic cells (figure 38). Cep152 localised adjacent to, but not overlapping with, Centrin 3, which fits with published data showing its localisation to the PCM at the proximal end of centrioles (Cizmecioglu et al., 2010). Cep152 showed the same localisation pattern relative to Centrin as Cep63 did. Anti-Cep152 479 antibody also stained the cytoplasm in a manner that resembled microtubule staining (figures 37 and 38). However, upon depletion of Cep152 by RNAi, this staining remained, while centrosomal staining was abolished, and was therefore assumed to be non-specific.

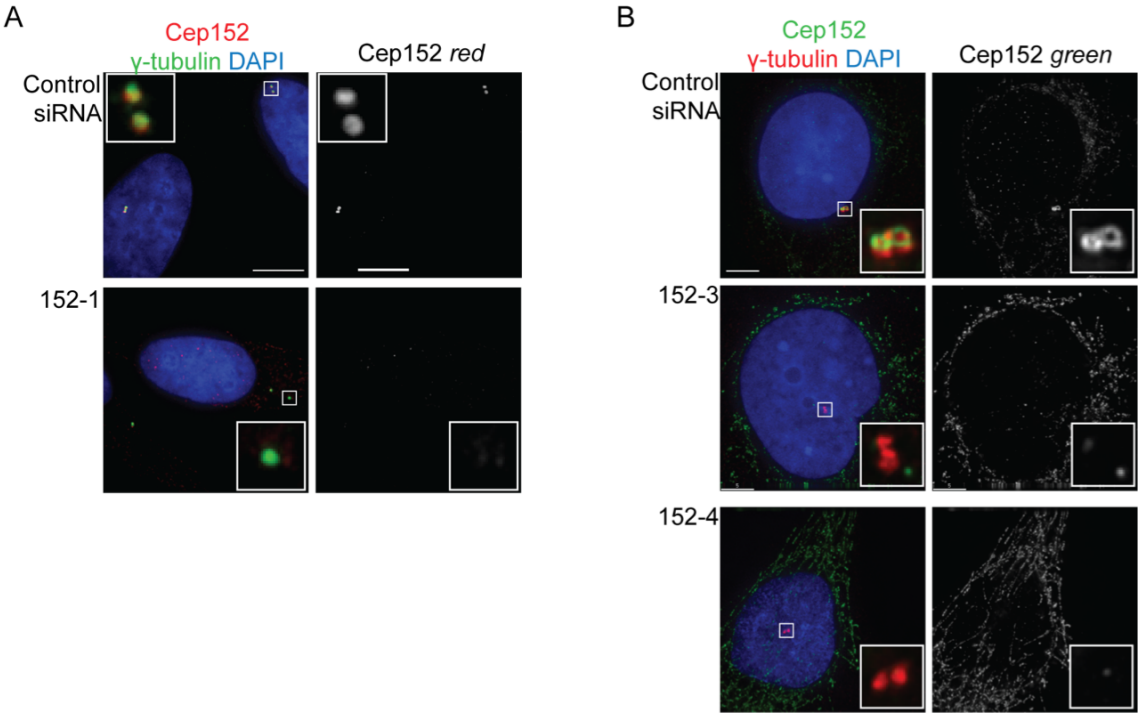

Figure 37 Visualisation of endogenous Cep152 by immunofluorescence
(A) HeLa cells transfected with control or Cep152 (152-1) siRNAs were stained with anti-Cep152 479 (red) and γ-tubulin (green) antibodies and DAPI (blue). Inserts show 3 times enlargements of the boxed regions. Scale bar 15 µm. (B) U2OS cells transfected with control or Cep152 (152-3 and 152-4) siRNAs were stained with anti-Cep152 479 (green) and γ-tubulin (red) antibodies and DAPI (blue). Inserts show 3 times enlargements of the boxed regions. Scale bar 10 µm. Images are maximum projections of deconvolved z-sections. Cep152 staining colocalises with γ-tubulin and is greatly reduced after Cep152 RNAi with different Cep152 siRNAs.

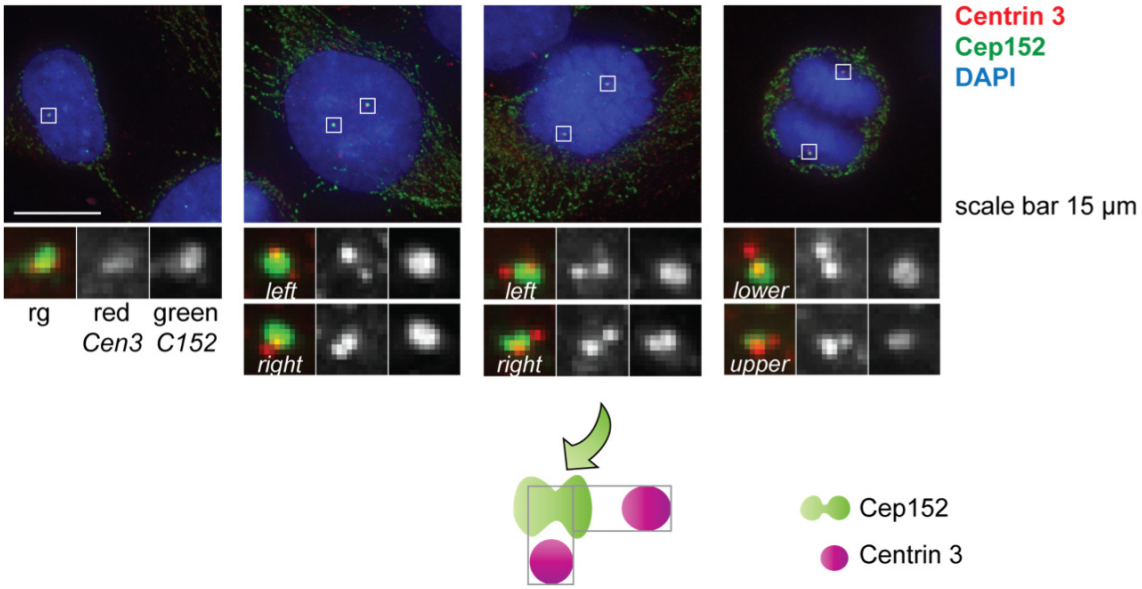

Figure 38 Cep152 localises to the PCM at the proximal end of centrioles
HeLa cells were stained with anti-Cep152 479 (green) and Centrin 3 (red) antibodies and DAPI (blue). Lower panels show 3 times enlargements of centrosomes marked by white boxes. Images are maximum projections of deconvolved z-sections. Diagram emphasises that Cep152 shows a bi-lobed appearance at the proximal end of centrioles, as seen previously for Cep63. Bi-lobed shape is most obvious in the right two panels, and Cep152 takes on the shape of a ring doughnut in the G2 cell shown (second panel).

3.6 Cep63 localisation during centrosome duplication

The Cep63 49AP antibody was used to study localisation of Cep63 throughout the cell cycle and, specifically, the kinetics of its recruitment to the new centriole during centriole duplication. Initially a U2OS cell line expressing a GFP-tagged exogenous copy of Centrin 1 was used; a kind gift from Stefan Duensing (University of Pittsburgh Cancer Institute) with permission from Michel Bornens (CNRS – Institut Curie). Centrin localises to the distal lumen of centrioles (Paoletti et al., 1996) and Cep63 localised adjacent to GFP-centrin 1 foci (figure 39a). This analysis confirmed previous experiments examining Cep63 and Centrin 3 immunofluorescence in HeLa cells (figure 36). In both experiments Cep63 immunofluorescence adopted a bi-lobed shape, which likely corresponds to the pericentriolar material (PCM) surrounding the outer centriole wall of the proximal end of the mother centriole, which organises PCM. Upon centriole disengagement in G1, Cep63 localised adjacent to each of the separated centrin foci, which is expected for a PCM protein as a daughter centriole is licensed to organise PCM upon passing through mitosis and upon disengaging from the mother centriole (simplified diagrams, figure 39). The same was observed when examining Cep63 co-staining with Centrin 2 and γ-tubulin to mark the distal ends of centrioles and the PCM, respectively (figure 39b). Cep152 localises to the PCM at the outer wall of the proximal end of centrioles (Cizmecioglu et al., 2010). Thus it is possible to infer that Cep63 also localised to the PCM surrounding the proximal ends of centrioles.

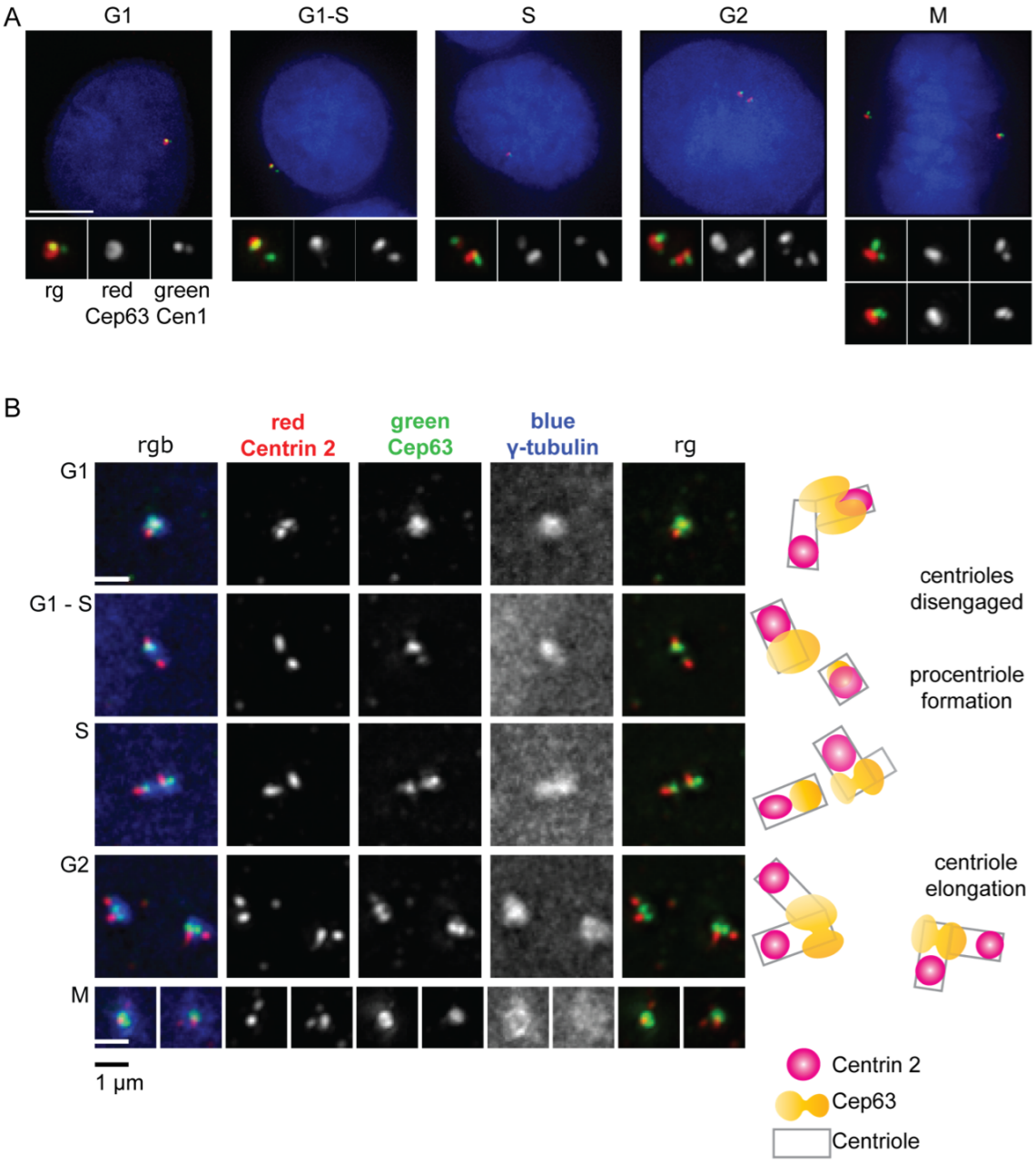

Figure 39 Cep63 localises to the PCM surrounding the proximal end of centrioles
(A) U2OS cells expressing GFP-Centrin 1 cells stained with anti-Cep63 49AP antibody (red) and DAPI. Green is direct GFP fluorescence. Scale bar 5 μm. (B) U2OS cells were stained with Centrin 2 (red), Cep63 (green) and γ-tubulin (blue) antibodies. Scale bar 1 μm. Diagrams indicate the predicted position of the centrioles (grey boxes) relative to Centrin and Cep63. All images are maximum projections of deconvolved z-sections.

In order to define the localisation of Cep63 further, Cep63 and Sas-6 (hSas-6) immunofluorescence was compared (figure 40). Sas-6 forms a cartwheel structure at the onset of procentriole formation and marks the proximal end of the newly formed centriole (Strnad et al., 2007) (Kitagawa et al., 2011). To test the specificity of the Sas-6 antibody, HeLa K cells were synchronised by double thymidine block then released for 9 to 12 hours to capture images of cells from metaphase through telophase to G1. Sas-6 protein is degraded at mitotic exit via the APC/C (Strnad et al., 2007). One Sas-6 focus per centrosome was observed throughout the cell cycle, which then disappeared during telophase, as expected (figure 40a). When centrioles disengaged during G1, Cep63 foci moved apart (figure 40b, middle panel). At this stage, Sas-6 staining was very weak, but not completely absent as in telophase cells. When Sas-6 was fully recruited, as observed by maximal fluorescence, Cep63 foci adopted a bi-lobed appearance again (figure 40a bottom panel). Triple staining with Centrin 2, Cep63 and Sas-6 antibodies showed that Cep63 is more proximal than Sas-6, which, in addition to the fact that it covers a larger area, indicated that Cep63 was indeed localised to the PCM surrounding the proximal end of the mother centriole in the pair of engaged centrioles, rather than being part of the centriole tube (figure 40c). In addition, Cep63 appears at the procentriole at or just before the time of full Sas-6 recruitment to the centrosome in G1. Sas-6 represents the earliest structural protein at the new procentriole, before centriole microtubule formation.

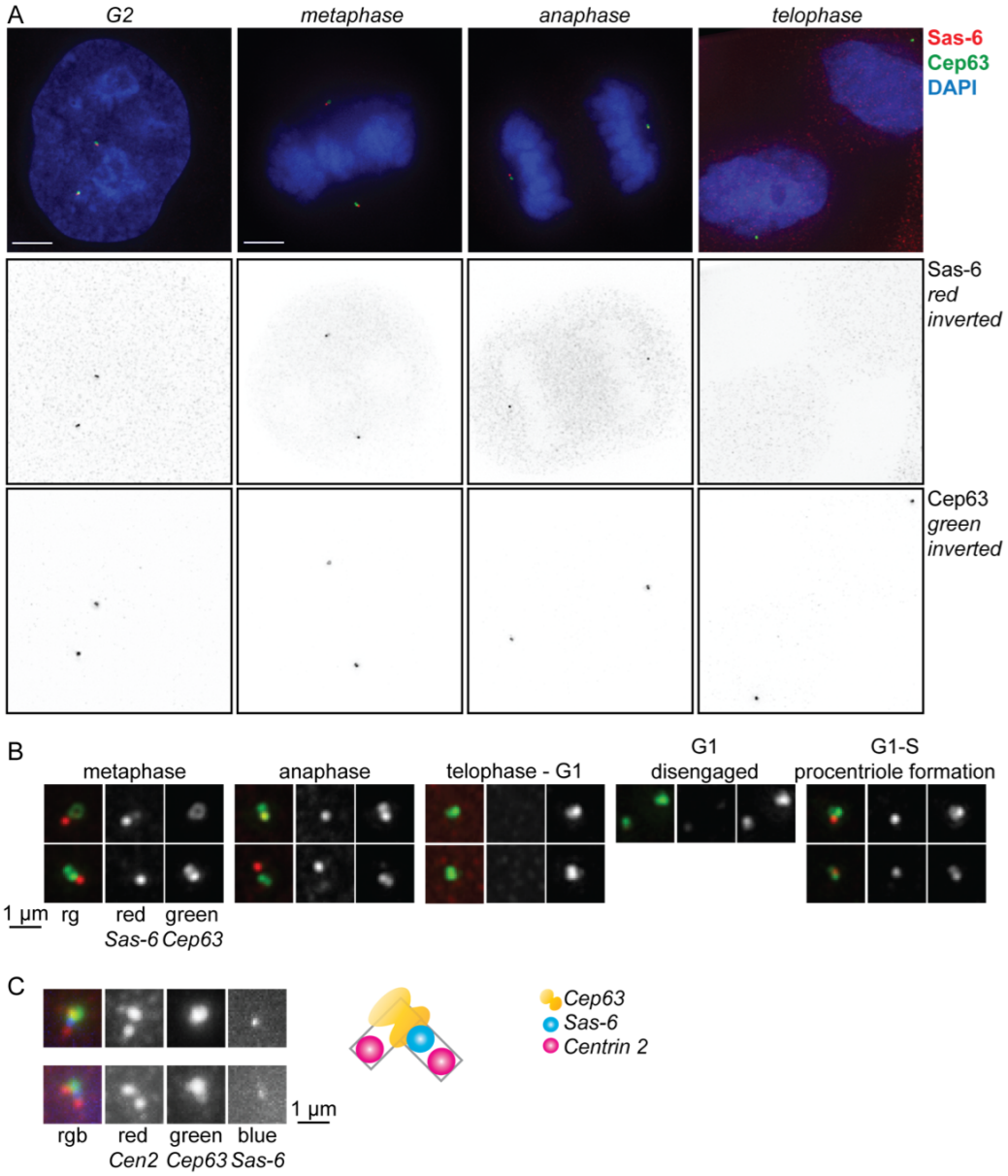

Figure 40 Cep63 localisation relative to pro-centriole component Sas-6
(A) HeLa K cells stained with Sas-6 (red), Cep63 (green) antibodies and DAPI (blue). Black and white pictures of the red and green channels are inverted for clarity. Sas-6 staining disappears after the metaphase to anaphase transition. Scale bar 5 µm. (B) Centrosomes from HeLa K cells stained as in (A). Examples are shown from cells in different stages of the centrosome duplication cycle (as indicated). (C) Centrosomes from a mitotic HeLa K cell stained with Centrin-2 (red), Cep63 (green) and Sas-6 (blue) antibodies. Diagram indicates positions of the proteins with respect to centrioles (grey boxes). All images are maximum projections of deconvolved z-sections.

3.7 Chapter 3 conclusions

Exogenous tagged Cep63 localises to the centrosome throughout the cell cycle and interacts with the essential centriole duplication factor Cep152. This study is the first demonstration of the interaction between Cep63 and Cep152. The Cep63-Cep152 interaction is also conserved in *Xenopus laevis* and it remains intact in the presence of DNA damage signalling. In this chapter I have also described the testing and validation of new Cep63 antibodies and the validation of a Cep152 commercial antibody. Cep63 rabbit polyclonal antibodies specifically recognise exogenous over-expressed Cep63 by Western blot, but they are not able to detect endogenous Cep63 by Western blot of whole cell lysates, likely due to a low abundance of endogenous Cep63 in whole cell lysates. However, Cep63 antibodies do specifically recognise endogenous Cep63 by immunofluorescence. Cep152 antibody (479 Bethyl) specifically recognises endogenous Cep152 by Western blot and immunofluorescence. The generation of another Cep152 antibody (9AP) was also carried out and this antibody was able to detect exogenous over-expressed Cep152 by Western blot and endogenous Cep152 on Western blots of centrosome enriched fractions, but it was not suitable for immunofluorescence.

Transfection of Cep63 siRNAs led to a decrease in Cep63 mRNA and protein levels, observed by RT-PCR and immunofluorescence, respectively. Cep152 siRNAs were proved efficient by Western blot and immunofluorescence analyses of transfected cells.

Immunofluorescence and direct fluorescence studies of Cep63 and Cep152 show that the two proteins localise to a specific region of the PCM surrounding the outer wall of the mother centriole at the proximal end such that fluorescent foci take on a bi-lobed or doughnut shaped appearance. This is the region in which daughter procentrioles are formed.

Chapter 4. Cep63 regulates centriole duplication

RNA interference (RNAi) using short-interfering RNAs (siRNAs) targeting Cep63 were employed to address the role of Cep63 in centriole duplication and cell cycle regulation in human cells. Cep63 interacts with the essential centriole duplication factor Cep152. So it follows that Cep63 may be involved in the same process. This chapter describes the involvement of Cep63 in centriole duplication and the study of the Cep63-Cep152 interaction and its function.

Cell cycle analysis of Cep63 cells treated with RNAi is detailed in section 4.5. These experiments pointed towards a role for Cep63 in the early stages of mitosis, RNAi mediated expression silencing of Cep63 resulted in the accumulation of cells in pro-metaphase to metaphase and a reduction of anaphase and telophase cells. However, the observed phenotype was not rescued upon expression of exogenous siRNA resistant Cep63. Attention was thus focused on the role of Cep63 in the centriole duplication cycle as detailed in the following sections.

4.1 Inhibition of centrosome reduplication by Cep63 RNAi

The requirement for Cep63 in centriole duplication was tested, initially, by carrying out centriole reduplication assays in the absence or presence of Cep63 siRNAs. Centriole duplication is regulated such that a new centriole can be formed only at the site of the original mother centriole and only once per cell cycle as discussed in 1.3 and reviewed in (Nigg, 2007). However, in some cell types including the human osteosarcoma cell line, U2OS, the regulation of centriole duplication can be uncoupled from the cell cycle (Balczon et al., 1995, Meraldi et al., 1999) .When these cells are incubated in the presence of a DNA replication stalling agent such as hydroxyurea (HU) or aphidicolin (Aph) for 2 to 3 days, centrioles go through multiple rounds of duplication and disengagement and multiple centrosomes form. This process will henceforth be referred to as centrosome reduplication.

The process of centrosome reduplication was followed in U2OS cells treated with control, Cep63 or Cep152 RNAi (figure 41). Two siRNA transfections were carried out 24 hours apart and a replication-stalling drug, HU or aphidicolin, was added at the time of the second transfection. Cells were collected for immunofluorescence after 48 or 72-hour drug incubations as indicated. Centrosomes were quantified by counting γ-tubulin foci by immunofluorescence: the percentage of cells with more than 2 centrosomes was scored.

Treatment of U2OS cells with 1.9 μg/ml aphidicolin causes centrosome re-duplication (Warnke et al., 2004). These conditions were used to carry out the first experiments in which 16% of cells showed centrosome reduplication after 48 hours and 35% after 72 hours incubation (figure 41). As expected, Cep152 RNAi reduced the number of cells with reduplicated centrosomes to 3% at 48 hours and 8% at 72 hours. Interestingly, Cep63 RNAi also reduced the number of cells with more than 2 centrosomes to 4% at 48 hours and 7% at 72 hours.

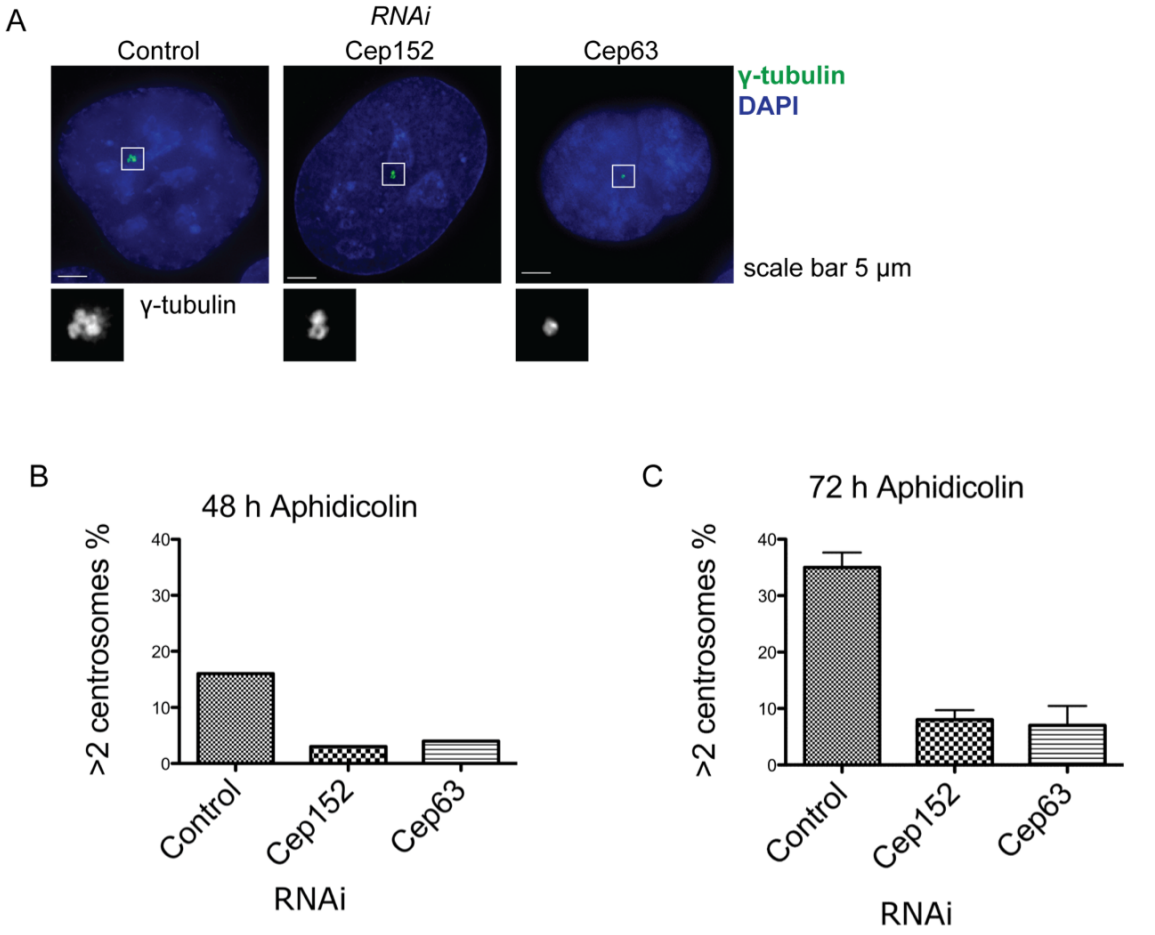

Figure 41 Cep63 or Cep152 RNAi prevents centrosome reduplication
U20S cells were transfected with control, 152-1 (Cep152) or 63-2 (Cep63) siRNAs and incubated for 48 hours (B) or 72 hours (A and C) with 1.9 μg/ml aphidicolin. Cells were stained with γ-tubulin antibody (green) and DAPI (blue) (A) and cells with greater than 2 γ-tubulin foci were scored (B and C). (B) One experiment shown; n >200 cells per sample. (C) 3 experiments n>150 cells per sample. Mean and standard deviation shown. Images are maximum projections of deconvolved z-sections.

Similar experiments were performed using hydroxyurea (HU) rather than aphidicolin. Incubation for 72 hours in 2 mM or 4 mM HU caused centrosome reduplication in U2OS cells transfected with control siRNAs. Reduplication was reduced by Cep63 or Cep152 RNAi (figure 42).

These experiments demonstrate that Cep63 RNAi inhibited centrosome reduplication when U2OS cells are arrested with replication stalling drugs to a similar extent as Cep152 RNAi. In order to confirm that it was the absence of Cep63 that was preventing centrosome reduplication in conditions of replication inhibition, I carried out Cep63 RNAi treatment using two different Cep63 siRNAs separately (63-1 and 63-2) in the presence or absence of siRNA resistant GFP-Cep63 (figure 43). U2OS cells stably expressing siRNA resistant GFP-Cep63 that was resistant to siRNA 63-2, but not 63-1 were generated. The experiment was carried out in parallel with GFP-Empty or GFP-Cep63 siRNA resistant (W) U2OS cell lines. Both Cep63 siRNAs led to a reduction in centrosome reduplication in cells treated with aphidicolin, relative to control siRNA (figure 43). Cep63 siRNA 63-1 depleted levels of GFP-Cep63 W and endogenous Cep63 but, siRNA 63-2 was not able to deplete GFP-Cep63 W although it depleted endogenous Cep63 (figure 43a). In the presence of GFP-Cep63 W, siRNA 63-2 did not cause a decrease in centrosome reduplication, indicating that Cep63 is specifically required for centrosome reduplication.

Interestingly, new γ-tubulin foci were able to form in the absence of detectable Cep63: arrows in figure 43d point to γ-tubulin foci with no visible Cep63 staining. In these cells there were low levels of Cep63 at one or two of the centrosomes, presumably the centrosome containing the grandmother centriole. This observation lead to the hypothesis that Cep63 is not required for formation of new centrioles in that it is not a structural component, but it is required for the regulation of centriole duplication. Altogether, these data lead to the conclusion that Cep63 plays a role in centrosome duplication, perhaps in partnership with its interacting partner Cep152.

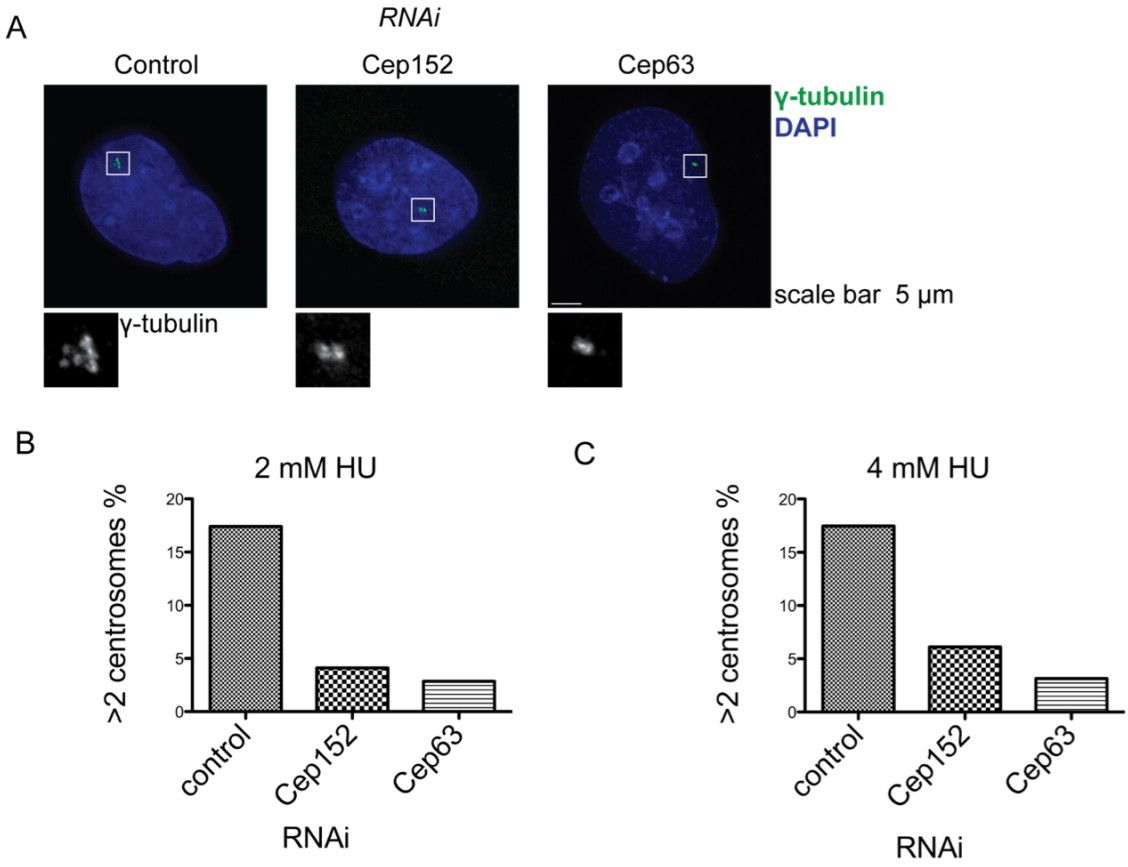

Figure 42 Cep63 or Cep152 RNAi prevents centrosome reduplication in response to HU-induced cell cycle arrest
U20S cells were transfected with control, 152-1 (Cep152) or 63-2 (Cep63) siRNAs and incubated for 72 hours with 2 mM (B) or 4 mM HU (A and C). (A) Cells were stained with γ-tubulin antibody (green) and DAPI (blue), lower panels show enlargements of the boxed areas. (B) & (C) cells with greater than 2 γ-tubulin foci were scored. One experiment shown: n >200 cells per sample. Images are maximum projections of deconvolved z-sections.

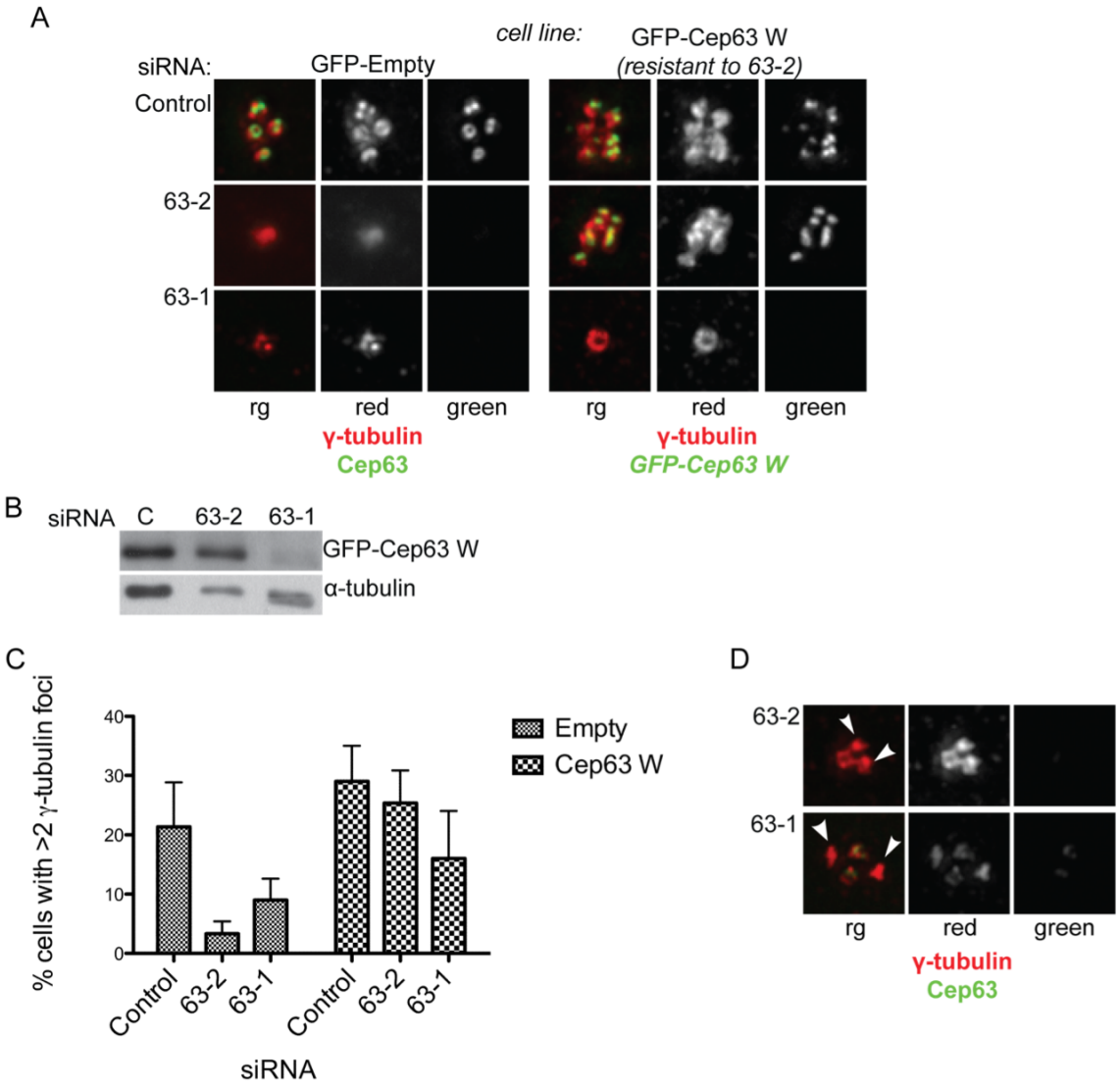

Figure 43 RNAi resistant GFP-Cep63 rescues centrosome duplication in Cep63 RNAi treated cells

U2OS cell lines expressing GFP-Empty or siRNA 63-2 resistant GFP-Cep63 (Cep63 W) were transfected with control or Cep63 siRNAs (63-1, 63-2) and incubated with 1.9 µg/ml aphidicolin for 72 hours. (A) Cells were stained with anti- γ-tubulin (red) and Cep63 (green, left panel) antibodies. GFP-Cep63 W was visualised by direct GFP fluorescence (A, right panel). (B) Western blot of cell lysates from GFP-Cep63 W cells treated with control (*C*) or Cep63 RNAi (*63-1, 63-2*). GFP-Cep63 W was visualised by blotting with anti-GFP antibody. α-tubulin was blotted as a loading control. (C) Cells with greater than 2 γ-tubulin foci were scored. Three experiments were carried out with n> 150 cells per sample: mean and standard deviation are shown. (D) Some cells with depleted Cep63 are able to duplicate their centrosomes: arrows point to γ-tubulin foci with no detectable Cep63 staining. Images are maximum projections of deconvolved z-sections.

Overexpression of Plk4 causes centriole over-duplication and overexpression of Plk2 can promote centrosome reduplication, reviewed in 1.3 (Warnke et al., 2004, Chang et al., 2010, Krause and Hoffmann, 2010, Habedanck et al., 2005, Kleylein-Sohn et al., 2007). Plk2 or Plk4 were over-expressed in Cep63 depleted cells in order to determine if Cep63 was involved in either one of these pathways specifically.

Initially, Cep63 expression was silenced using RNAi in U2OS cells expressing a HA-tagged exogenous copy of Plk2 regulated by the Tet-off system. U2OS HA-Plk2 Tet-off cells were a kind gift from Ingrid Hoffmann (German Cancer Research Center, DKFZ). U2OS cells were maintained in the presence of doxycycline. Three days prior to the first siRNA transfection, media was refreshed with doxycycline free medium to induce HA-Plk2 expression (figure 44a). Aphidicolin was added on the day of the second siRNA transfection; cells were collected 72 hours later and centrin foci were counted. HA-Plk2 overexpression in the presence of aphidicolin lead to 60% of cells containing over-duplicated centrioles (greater than 4 centrin foci, figure 44c). Cep63 RNAi prevented centriole reduplication, which indicated that it might function in the Plk2 pathway. However, since aphidicolin arrest-induced centriole reduplication is not solely Plk2 dependent, it was not possible to conclude at this stage. Further experiments would be required to examine centriole number in Cep63 depleted cells with or without Plk2 overexpression, with or without aphidicolin incubation, although overexpression of Plk2 in asynchronous cells causes only a mild centriole reduplication phenotype (Warnke et al., 2004).

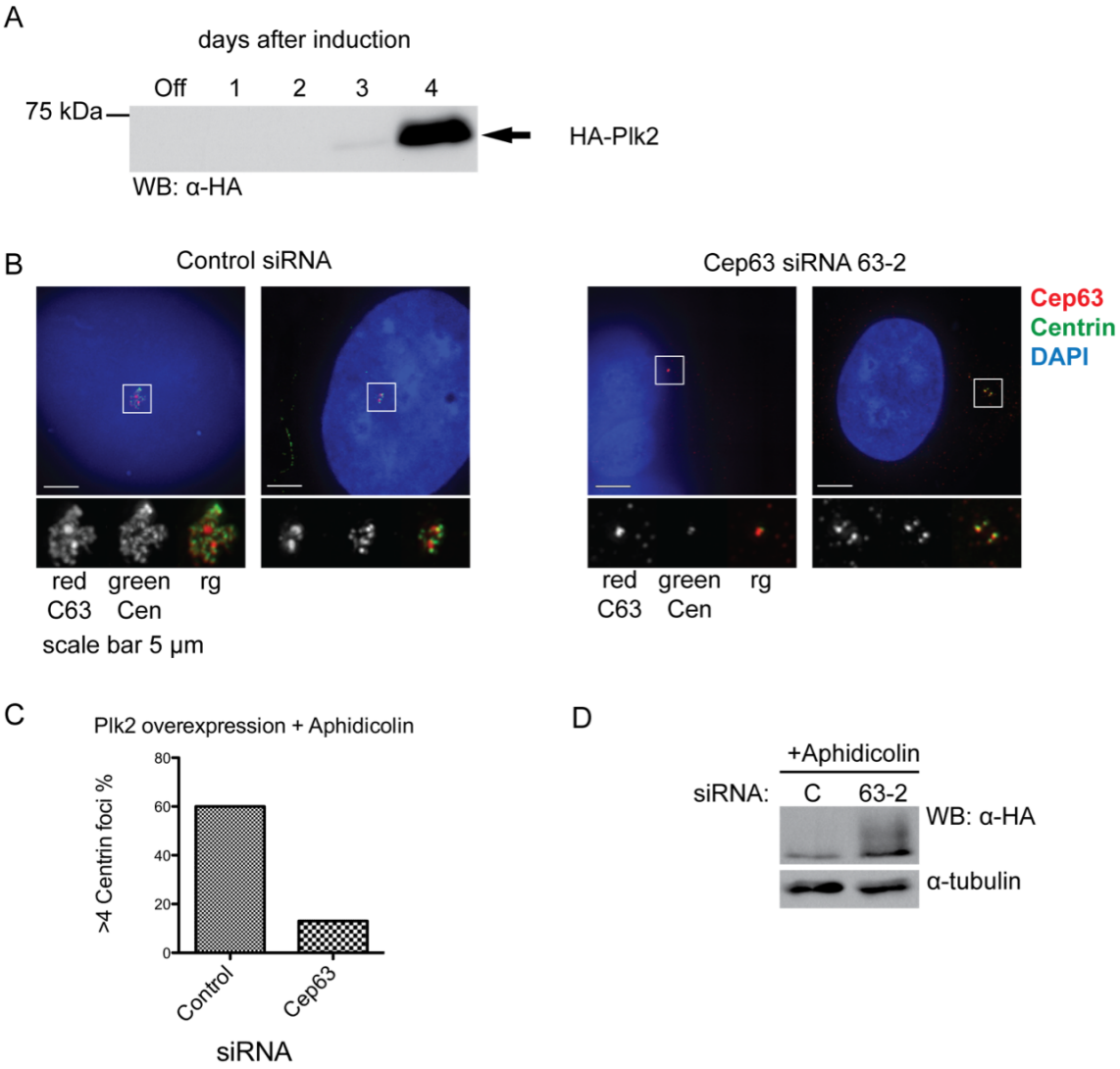

Figure 44 Plk2 and aphidicolin induced centriole reduplication is prevented by Cep63 RNAi

(A) Western blot of U2OS HA-Plk2 Tet off cells after the indicated number of days grown without tetracycline. HA-Plk2 was detected with anti-HA antibody. (B) Sample images of U2OS HA-Plk2 cells after HA-Plk2 induction, incubation with aphidicolin and transfection with control or Cep63 siRNAs. Cells were stained with anti-Cep63 49AP (red), anti-Centrin (20H5, green) antibodies and DAPI. Small panels show 2 times enlargement of the boxed areas. Scale bar 5 µm. (C) Cells with greater than 4 Centrin foci were scored, n> 150 cells. (D) Western blot of cell lysates from cells used in (B) and (C). HA-Plk2 is still being expressed at the end of the experiment in both samples. Images are maximum projections of deconvolved z-sections.

A Myc-Plk4 construct kindly donated by Ingrid Hoffmann (DKFZ) was used for Plk4-induced centriole reduplication. U2OS GFP-Centrin 1 cells (from Stefan Duensing) were subjected to Cep63 or Cep152 RNAi followed by transfection with the Myc-Plk4 construct and cells were collected after 48 hours. Due to cell death and a low number of cells with Myc-Plk4 positive centrosomes, a very low number of cells was available for analysis, but this preliminary experiment showed that Cep63 and Cep152 RNAi both reduced centriole over-duplication driven by Plk4 over-expression (figure 45). Cep152 has been shown to be involved in the Plk4 dependent centriole duplication pathway (Cizmecioglu et al., 2010, Hatch et al., 2010b) and it is interesting to speculate that Cep63 might also be a player in this pathway via interaction with Cep152. In U2OS cells overexpressing Myc-Plk4, Cep63 co-localised with the anti-Myc immunofluorescence (figure 45d). Colocalisation with Plk4 has already been shown for Cep152. In fact, Cep152 localisation to the centrosome is required for efficient localisation of Plk4 to the centrosome (Cizmecioglu et al., 2010). It would be interesting to see if Cep63 is also required for the centrosome localisation of Plk4, unfortunately due to time constraints this has not yet been investigated.

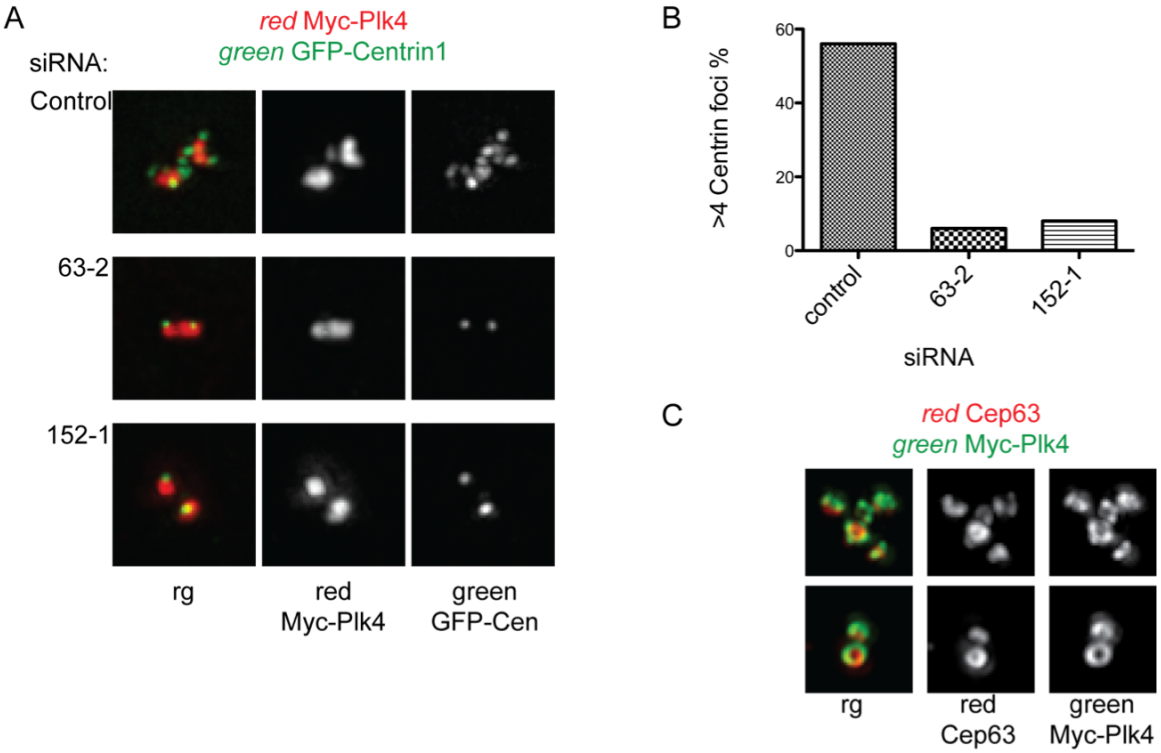

Figure 45 Plk4 induced centriole duplication is prevented by Cep63 or Cep152 RNAi

(A) Example images of U2OS cells transfected with Myc-Plk4 and control, Cep63 (63-2) or Cep152 (152-1) siRNAs. Cells were stained with anti-Myc 9E10 antibody and GFP-Centrin1 was visualised by direct fluorescence. (B) Cells with greater than 4 centrin foci were scored; n>15 cells. (C) Images from U2OS cells over-expressing Myc-Plk4; stained with anti-Cep63 49AP and anti-Myc 9E10 antibodies. Cep63 and Plk4 co-localised. Images are maximum projections of deconvolved z-sections.

4.2 Cep63 is required for efficient centriole duplication

RNAi experiments carried out in conditions that force centriole reduplication clearly showed that Cep63 and Cep152 are important in this process. To ascertain whether Cep63 might be involved in centriole homeostasis in unperturbed cells, centrioles were counted in asynchronous cells after Cep63 RNAi.

Knockdown of Cep63 or Cep152 by RNAi over 4 days in U2OS cells resulted in decreased centriole numbers relative to untreated cells (figure 46a and b). Centriole number was determined by staining with a Centrin 2 antibody and only mitotic cells were counted in order to eliminate cell cycle dependent variation in centriole number: all mitotic cells should contain 4 centrin foci. Mitotic cells were identified by DAPI staining and observation of mitotic chromosome condensation. Duplicate experiments scoring mitotic cells with centrin 2 staining showed that Cep63 RNAi samples contained significantly more cells with fewer than 4 centrioles ($p<0.05$) and significantly fewer cells with 4 centrioles ($p<0.01$, figure 46d). In most control cells, centrioles are duplicated before the onset of mitosis so that each mitotic cell contains two pairs of engaged centrioles, one pair in each centrosome; at each spindle pole. Cep63 RNAi samples contained cells with fewer than 4 centrin foci, which suggested that centrioles were not being duplicated in time for entry into mitosis. Figure 46a and c show examples of Cep63 depleted cells that contain single centrin foci at one spindle pole, or both. This pattern of centrin foci arrangement indicated that centrioles were able to disengage at the end of mitosis of the previous cell cycle and that either one or both of the centrioles were unable to duplicate. Centrosome separation at the beginning of mitosis appeared to be unaffected since cells were observed with well separated centrosomes, regardless of the number of centrioles they contained.

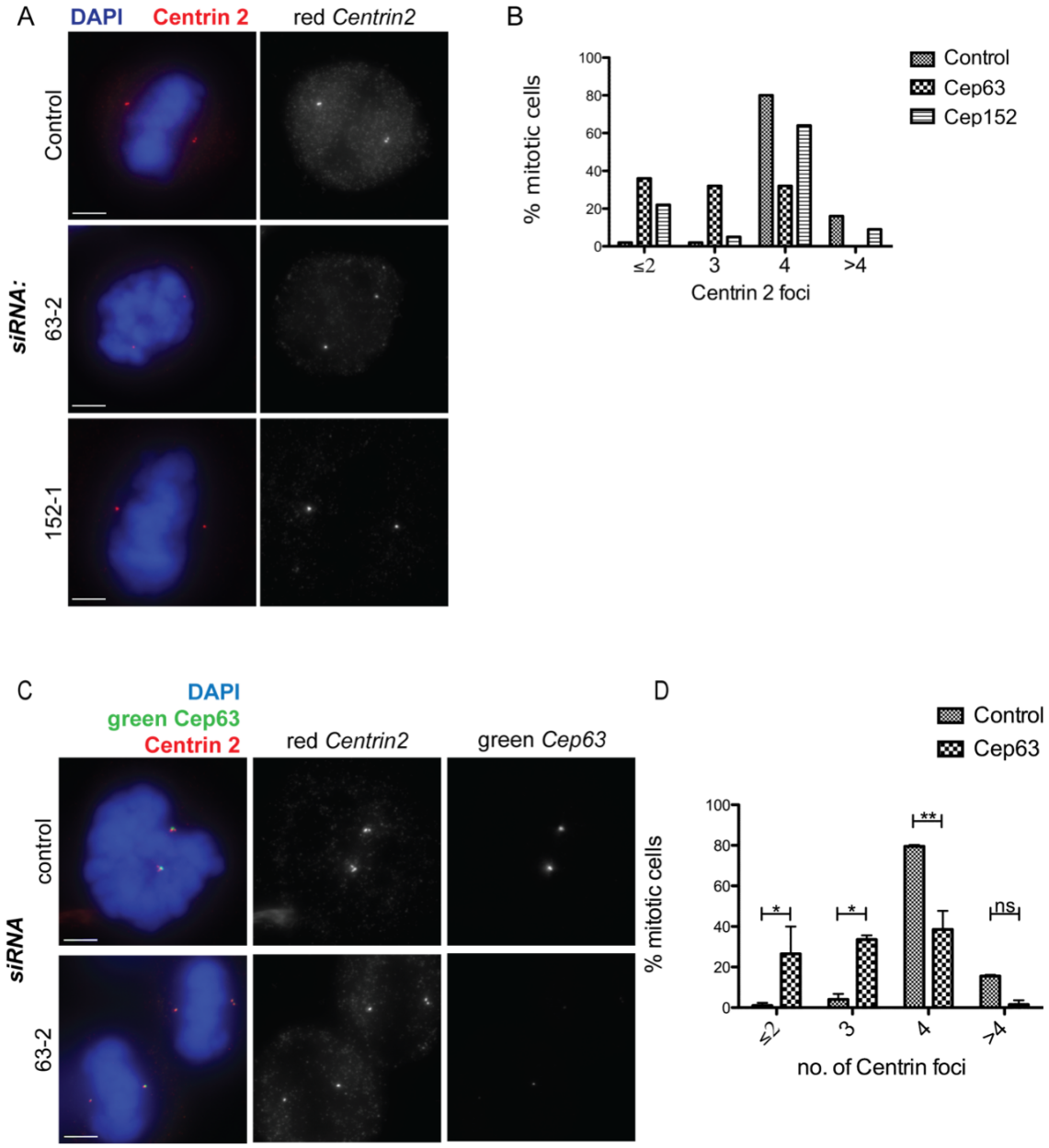

Figure 46 Centriole loss with Cep63 or Cep152 RNAi
(A) U2OS cells were fixed after 4 days of RNAi with control, Cep63 (63-2) or Cep152 (152-1) siRNAs and stained with anti-Centrin 2 antibody (red) and DAPI (blue). (B) Mitotic cells were scored for Centrin 2 foci number; n >100. (C) U2OS cells were fixed after 4 days of RNAi with control or Cep63 (63-2) siRNAs and stained with anti-Centrin 2 (red) and Cep63 49AP (green) antibodies and DAPI (blue). (D) Mitotic cells were scored for Centrin 2 foci number. Average from 2 experiments shown; n>60. Mean and standard deviation shown. * Significant difference with $p<0.05$; ** $p<0.01$; ns $p>0.05$. Images are maximum projections of z-sections with no deconvolution. Scale bars 5 μm.

In order to verify these results, an alternative method for scoring centriole number that does not rely on specific antibody staining was employed. U2OS GFP-Centrin 1 cells were used and GFP foci were counted by direct fluorescence (figure 47). Experiments in these cells showed the same pattern: Cep63 RNAi led to a decrease in centrin foci number. All cells were included in the analysis, then mitotic and interphase cells were separated into two data sets (figure 47b). As seen in experiments with Centrin 2 staining: Cep63 RNAi in U2OS GFP-Centrin 1 cells caused an increase in mitotic cells with 3 or fewer centrioles and a decrease in cells with 4 centrioles (figure 47b, left panel). Analysis of interphase cells showed that Cep63 RNAi increased the proportion of cells containing 2 or fewer centrioles and decreased the incidence of cells with 4 centrioles. Although a decrease in cells with 4 centrioles and concomitant increase in cells with 2 centrioles could be explained by a cell cycle defect resulting in an increase in G1 cells this was not the case for Cep63 RNAi: FACS analysis of DNA content of Cep63 RNAi treated U2OS did not show an increase in G1, but rather an increase in G2/M (section 4.5, figure 53). Also, data collected from mitotic cells clearly showed that reduced centriole numbers were due to a problem in centriole duplication rather than cell cycle arrest.

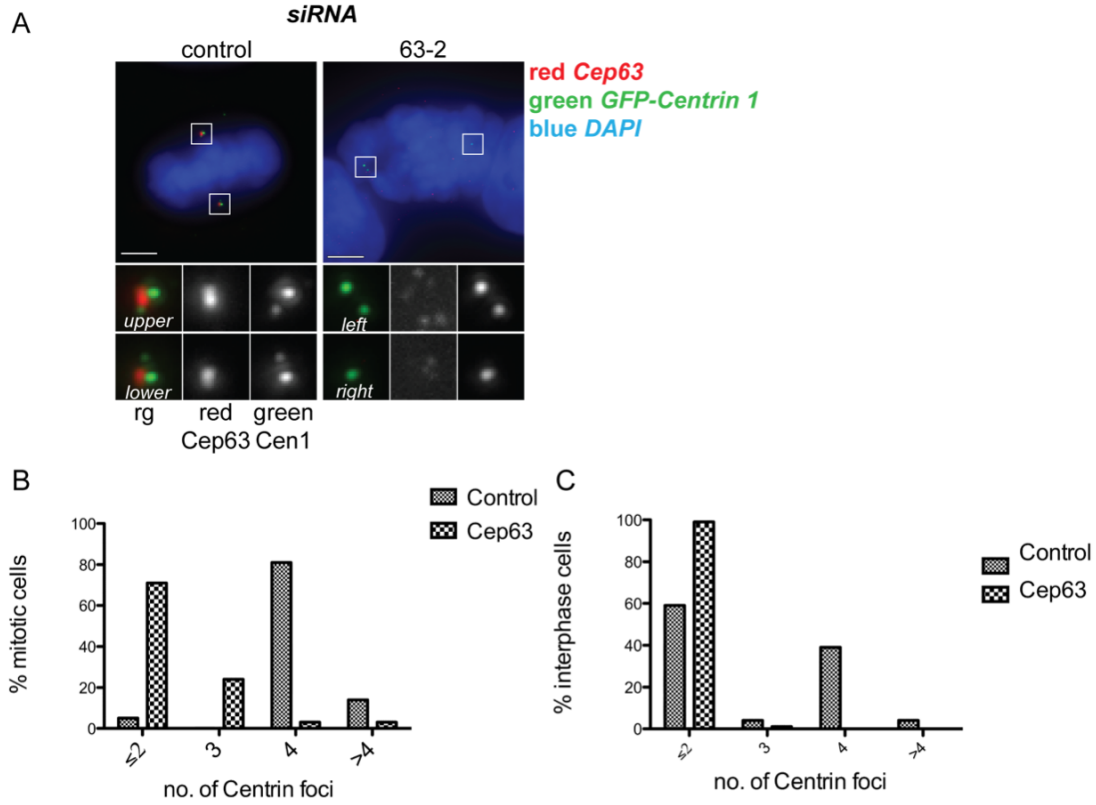

Figure 47 Centriole loss in GFP-Centrin 1 U2OS cells after Cep63 RNAi
(A) RNAi was carried out for 4 days in U2OS GFP-Centrin 1 cells using control or Cep63 specific (63-2) siRNAs. Cells were fixed for immunofluorescence with anti-Cep63 (red) anti-GFP (green) antibodies and DAPI (blue). Small panels show 3 times enlargements of the indicated boxed areas. Scale bar 5 μm. (B) GFP-Centrin 1 foci number was scored in mitotic cells, n>35. (C) GFP-Centrin 1 foci number was scored in interphase cells, n>75. Images are maximum projections of z-sections without deconvolution.

4.3 Cep63 RNAi leads to formation of extra γ-tubulin foci in mitosis – preliminary data

Cep63 depletion by RNAi caused an increase in mitotic cells with fewer centrioles, but when these cells were stained with γ-tubulin to visualise spindle poles, I noticed that many mitotic cells contained extra γ-tubulin foci (figure 48). Cells with extra γ-tubulin foci had foci not only at the major spindle poles, but also scattered throughout the cell. Most of these foci were not as large as the foci at spindle poles. Since the number of mitotic cells containing greater than 4 centrioles did not increase upon Cep63 RNAi, these extra γ-tubulin foci were probably devoid of centrioles. As observed for centriole number, this phenotype was present in only a small population of Cep63 depleted cells. The majority of mitotic cells contained 2 γ-tubulin foci; a small percentage contained only one and between 4 and 28% contained greater than 2 γ-tubulin foci (figure 48b and c). When 4 experiments were plotted together, the difference between the number of control and Cep63 RNAi cells with greater than 2 γ-tubulin foci was not significant (figure 48c). The same was true for the increased number of Cep63 RNAi treated mitotic cells with only one γ-tubulin focus.

These experiments were carried out with RNAi over 4 days, as described in 2.6.3. However, after 6 days of RNAi, both phenotypes became more pronounced: there were more cells with only one γ-tubulin focus in mitosis and more cells with extra smaller γ-tubulin foci in mitosis (figure 48a and b). The 6-day RNAi experiment must be repeated to confirm this interesting observation. This preliminary data suggests that there might be a role for Cep63 in maintenance of the mitotic spindle poles, either directly or indirectly by ensuring the correct complement of centrosomes are present. It is important to note that there were a small population of control cells that have multiple γ-tubulin foci in mitosis, which was lower or sometimes very similar to the proportion of Cep63 RNAi cells, depending on the individual experiment. This initial finding is potentially very interesting with respect to the *Xenopus* Cep63 work carried out previously: upon depletion of XCep63, the incidence of bipolar spindles is decreased in *Xenopus* CSF extracts supplemented with sperm nuclei (Smith et al., 2009).

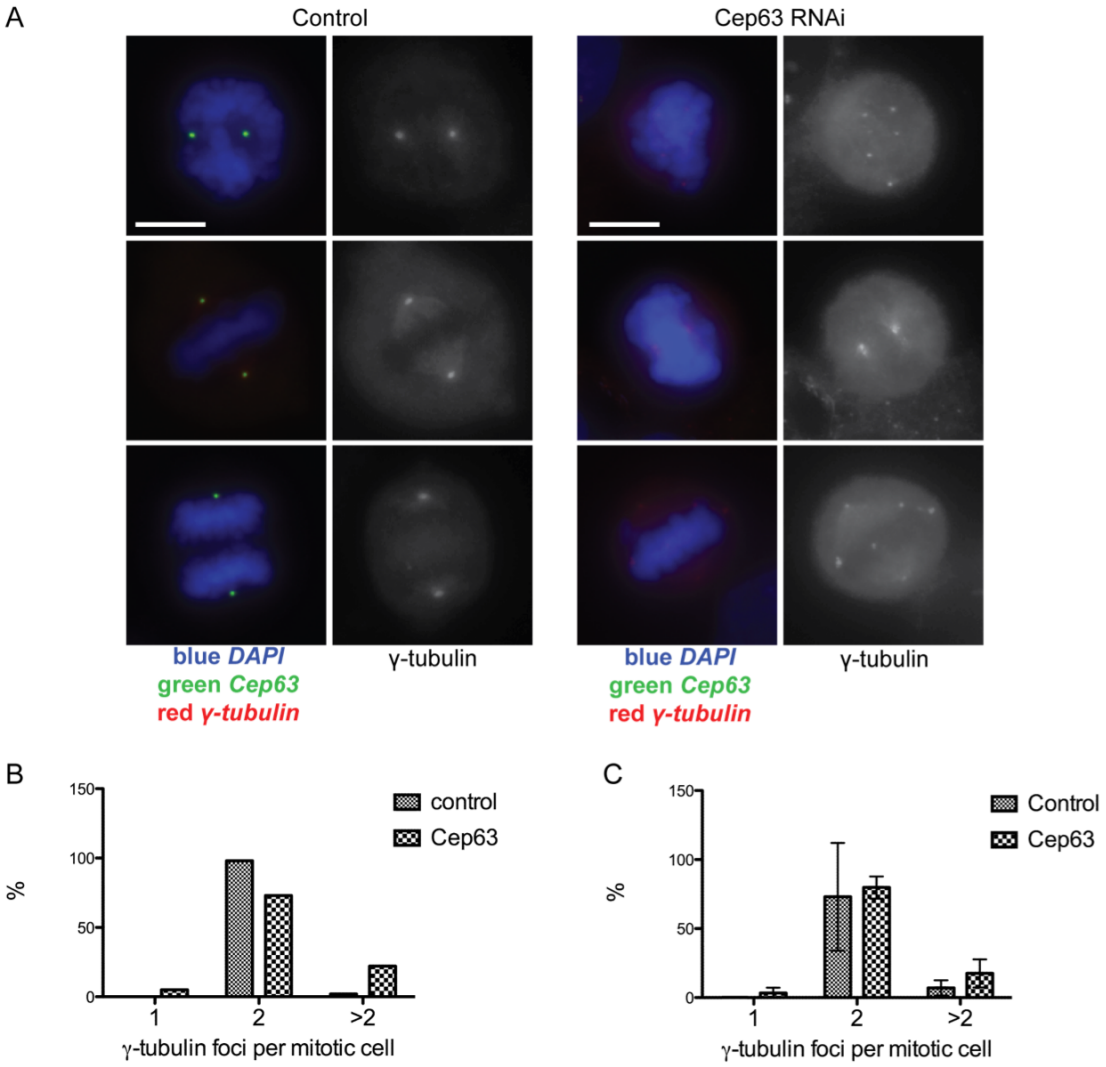

Figure 48 Extra γ-tubulin foci in mitosis in Cep63 RNAi treated cells
(A) U2OS cells were treated with control or Cep63 (63-2) RNAi over 6 days, and then cells were fixed and stained with anti-Cep63 (green) and γ-tubulin (red) antibodies and DAPI (blue). Three examples of mitotic cells are shown for each sample. Scale bar 10 μm. (B) Mitotic cells from this experiment were scored for the number of γ-tubulin foci, n>80, one experiment only. (C) Data from B was combined with 3 more experiments carried out with RNAi over 4 days. Graph shows the percentage of mitotic cells with 1, 2 or greater than 2 γ-tubulin foci. The mean and standard deviation are shown for each category. The difference between the means for control and Cep63 RNAi samples was not significant for any category.

4.4 Cep63 and Cep152 centrosome localisation is interdependent

Since Cep63 and Cep152 are interacting partners, as described in chapter 3, I decided to follow the localisation of each partner after RNAi of the other. U2OS cells were treated with RNAi over 4 days with 2 different Cep63 siRNAs (63-2 and 63-3) or two different Cep152 siRNAs (152-3 and 152-4) then cells were collected for immunofluorescence and stained with anti-Cep63 49AP and γ-tubulin, or anti-Cep152 479 and γ-tubulin antibodies. Images of approximately 30 cells per sample were collected and the fluorescence intensity of Cep63 or Cep152 at the centrosome was measured relative to the fluorescence intensity of γ-tubulin with local background subtraction (figure 49).

Cep63 RNAi led to a decrease in both Cep63 and Cep152 fluorescence at the centrosome. Conversely, Cep152 RNAi resulted in decreased Cep152 and Cep63 fluorescence at the centrosome (figure 49). This experiment was repeated in triplicate and the mean difference between the control sample and each RNAi sample was significantly different in each experiment (figure 49d and e). Importantly, Cep63 RNAi did not deplete the overall level of Cep152 protein as determined by Western blot (figure 49b). As endogenous Cep63 could not be visualised by Western blot of whole cell lysate, Western blot of U20S GFP-Cep63 cells treated with Cep152 siRNA, or Cep63 siRNA was carried out. Exogenous GFP-Cep63 protein levels were unaffected by Cep152 RNAi, but localisation to the centrosome was inhibited to a similar level as with Cep63 RNAi (figure 50).

In conclusion, Cep63 and Cep152 require each other for efficient localisation to the centrosome. Perhaps they bind to each other when translated in the cytoplasm and are incorporated into the PCM together. Therefore when one is depleted, the incorporation of the other to the PCM is inhibited.

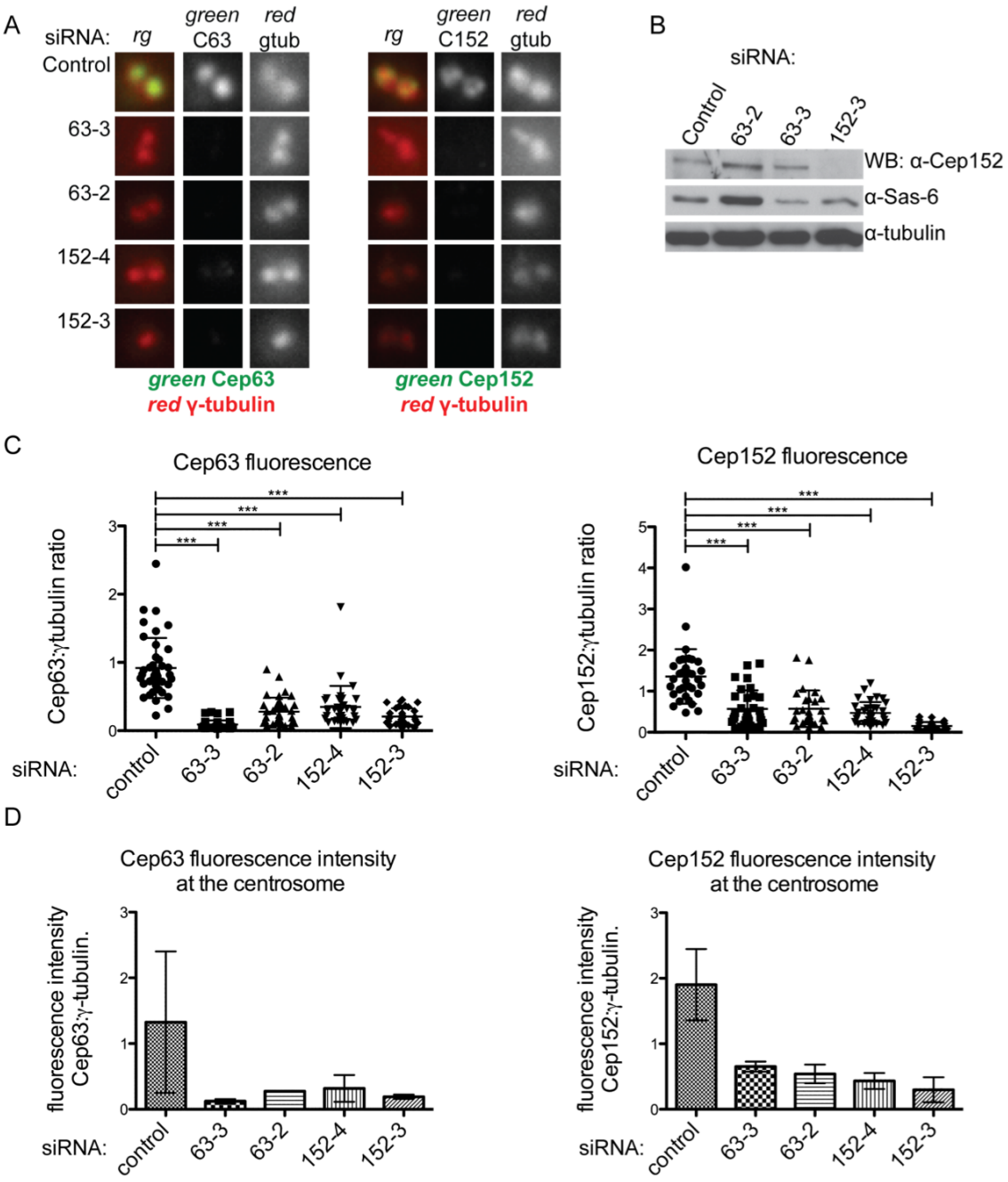

Figure 49 Cep63 and Cep152 centrosome localisation is interdependent
(A) Centrosomes from U2OS cells transfected with control, Cep63 (63-2, 63-3) or Cep152 (152-3, 152-4) siRNA and stained with anti-Cep63 (green) and γ-tubulin (red) or anti-Cep152 (green) and γ-tubulin (red) antibodies, as indicated. (B) Western blot of cell lysates with anti-Cep152 antibody. Sas-6 and α-tubulin Western blots are shown as loading controls. Cep63 RNAi did not affect Cep152 protein levels. (C) Fluorescence intensity measurements of Cep63 (left panel) or Cep152 (right panel) relative to γ-tubulin fluorescence for the experiment shown in A and B. Bars show the mean and standard deviation for each sample. *** Indicates a significant difference between samples; $p < 0.0001$. (D) Cep63 (left) and Cep152 (right) fluorescence measurements, relative to γ-tubulin, for three experiments. $N > 25$ measurements in each experiment. Mean and standard deviations are shown.

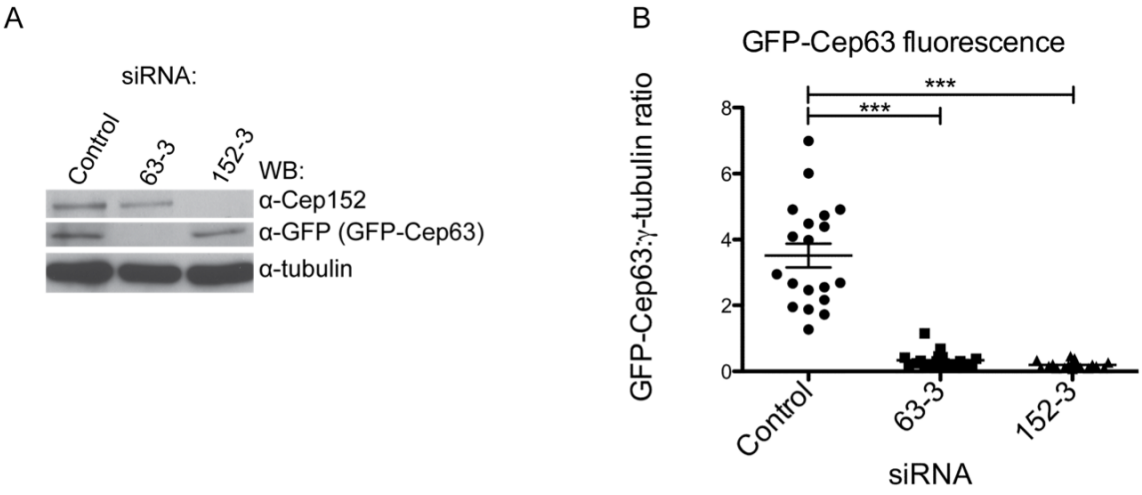

Figure 50 GFP-Cep63 centrosome localisation is dependent on Cep152
(A) Western blot of cell lysates from U2OS GFP-Cep63 cells transfected with control, Cep63 (63-3) or Cep152 (152-3) siRNAs. α-tubulin Western blot is shown as a loading control. (B) Graph shows fluorescence intensity measurements of GFP-Cep63 relative to γ-tubulin. Cep152 RNAi did not affect GFP-Cep63 protein level (A), but affected its localisation to the centrosome (B).

In order to investigate the function of the Cep63-Cep152 interaction further, Cep63 truncation proteins were generated. Cep63 was divided into three sections, N-terminus, SMC-like domain, and C-terminus. The SMC-like domain was predicted by searching the Conserved Domain Database using the NCBI interface (Marchler-Bauer et al., 2011). The region of Cep63 isoform b between amino acids 136 and 424 was predicted to be structurally similar to the SMC (structural maintenance of chromosomes) protein family. Recombinant proteins consisting of each domain (N, SMC or C); fusions N-SMC or SMC-C; and full length Cep63 were generated (figure 51c).

Initially, recombinant MBP-Cep63 truncation proteins were generated, which were bound to amylose resin then incubated with cell lysate from 293 cells over-expressing Flag-Cep152. Eluates from the amylose resin were analysed by Western blotting with anti-Cep152 antibody: Flag-Cep152 was present in eluates from full length (6) and C-terminal (3) MBP-Cep63 proteins (figure 51a). This experiment indicated that the C-terminal third of Cep63 was required for Cep152 binding since no Flag-Cep152 was observed in eluates from N-terminal (1), SMC (2) or N-SMC (4) MBP-Cep63 proteins.

However, there was also no detectable Flag-Cep152 in the eluate from MBP-Cep63 5, which contained SMC and C-terminal domains and therefore should have been able to bind Cep152. Upon further analysis, it appeared that although an equal amount of MBP-Cep63 5 was used in the experiment (Coomassie stained gel, figure 51a), this protein did not bind efficiently to amylose resin used for the pull down assay (Ponceau stained membrane, figure 51a). The experiment was repeated and the same problem occurred, which suggested that the MBP-tag in this protein was perhaps not sufficiently exposed to allow amylose resin binding.

Consequently, binding experiments were repeated using a different system. Flag-Cep63 truncation proteins (1 to 6) were stably expressed in 293 cells and anti-Flag IPs were carried out in cell lysates from these cell lines. Eluates were then analysed by Western blotting with anti-Cep152 antibody (figure 51b). Cell lysates were blotted for Cep152 to ensure that Cep152 protein level did not vary between Flag-Cep63 truncation cell lines. Cep152 was observed in eluates from Flag-Cep63 3 (C-terminal third), 5 (SMC – C-term) and 6 (full length) Flag IPs, which confirmed the MBP-Cep63 experiments: Cep63 C-terminus is necessary and sufficient for Cep152 binding. The presence of the Flag-Cep63 truncation proteins in cell lysates was confirmed by Western blot of whole cell lysates for all proteins except the N-terminal and C-terminal fragments (1 and 3). Flag-Cep63 N- and C-terminal fragments were not detectable in whole cell lysate, likely due to low expression level. Flag-Cep63 N-term was detected on the Western blot of Flag-IP eluates, but Flag-Cep63 C-term was not. The only evidence that Flag-Cep63 C-term was expressed was that Cep152 was present in the Flag IP from those cell lines. Flag IPs from 2 clones for each of Flag-Cep63 N-term and C-term truncations were performed due to the inability to robustly confirm the presence of the protein. Neither Flag-Cep63 N-term clone was able to bind Cep152 and both Flag-Cep63 C-term clones were able to pull down Cep152 in the Flag IP.

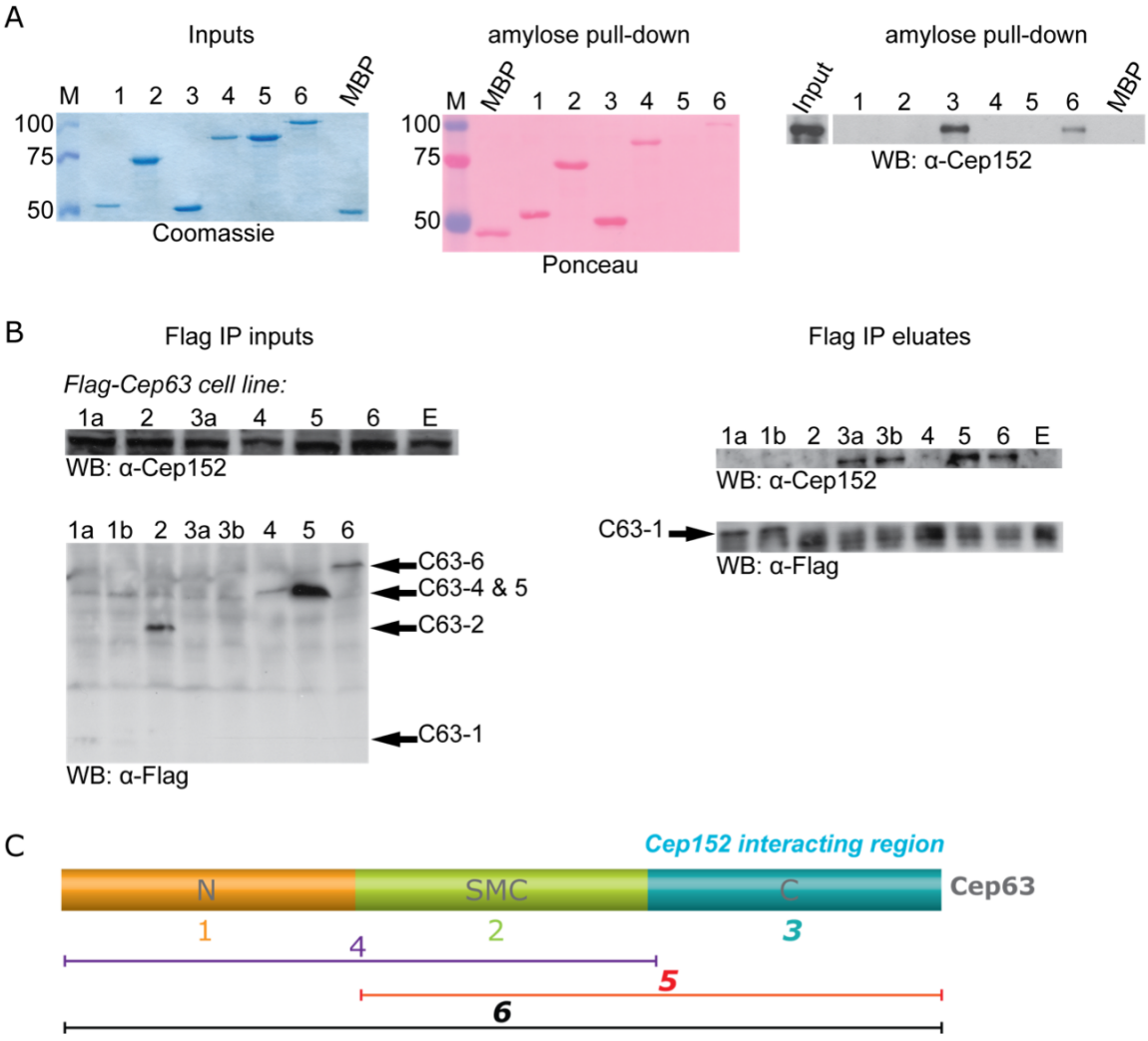

Figure 51 Cep63 C-terminal region interacts with Cep152
(A) MBP-Cep63 truncation proteins 1 to 6 and MBP alone were bound to amylose resin and incubated with Flag-Cep152 293 cell lysate. Input MBP proteins are shown on the Coomassie stained gel (left) and the MBP proteins present in the eluate are shown on the Ponceau stained membrane (middle). Eluates were also analysed by Western blotting with anti-Cep152 antibody (right). Flag-Cep152 was present in the eluate from MBP-Cep63 full length (6) and C-terminal domain (3). (B) 293 Flag-Cep63 truncation stable clones were used for a Flag IP experiment and the eluates were analysed by Western blotting for Cep152 (right, upper). Input cell lysates were analysed by Western blotting for Cep152 (left, upper) or Flag to visualise Cep63 truncation proteins (left, lower). Flag-Cep63 truncation 1 could only be observed in the Flag IP eluate (right, lower). Flag-Cep63 truncation 3 could not be visualised at all. 1a, 1b, 3a and 3b are different clones of the 293 stable cell lines, which were used in parallel in this experiment. (C) Diagram illustrates the regions of Cep63 contained in each Cep63 truncation protein, 1 to 6.

Next, YFP-Cep63 truncation proteins were expressed in U2OS cells in order to observe their localisation and their effect on Cep152 localisation (figure 52). The only protein to show robust localisation to the centrosome was full length Cep63 (full length), but there were also cells expressing YFP-Cep63 1 and 4 that showed YFP localisation at the centrosome (figure 52a and c). In comparison, there were no cells with detectable YFP at the centrosome in cells expressing Cep63 truncations 2, 3 or 5, or YFP alone. Since the experiment was carried out by transient transfection of the YFP-Cep63 vectors, the small number of examples of Cep63 1 and 4 localisation to the centrosome could have been due to low incidence of cells that were expressing the protein. Alternatively, localisation of these truncation proteins (1 and 4) may be reduced compared to the full-length protein, because the full length of the protein is required for efficient localisation. This hypothesis marries with the conclusion that Cep152 was required for proper localisation of Cep63 to the centrosome since the C-terminus of Cep63 was required for Cep152 binding. Without the C-terminus, and therefore without Cep152 binding, Cep63 localisation to the centrosome may be reduced.

To follow Cep152 localisation to the centrosome γ-tubulin immunofluorescence was used to locate the position of the centrosome (blue, figure 52a) in combination with Cep152 immunofluorescence (red, figure 52a). Interestingly, in cells over-expressing YFP-Cep63 3 or 5 (truncations containing the Cep152-binding C-terminal domain), Cep152 fluorescence was significantly reduced at the centrosome (figure 52a and c). Cep152 fluorescence was measured at the position of γ-tubulin foci, relative to γ-tubulin fluorescence. The level of Cep152 fluorescence in YFP-Cep63 1, 2, 4 or 6 cells was not significantly different from YFP-empty control cells (figure 52a and c). The expression of all of the YFP-Cep63 truncation proteins was confirmed by Western blotting of whole cell lysates with anti-GFP antibody (figure 52d). This experiment was repeated and the same pattern was found. Mean differences from YFP-Empty control cells for the two experiments are shown in figure 52e.

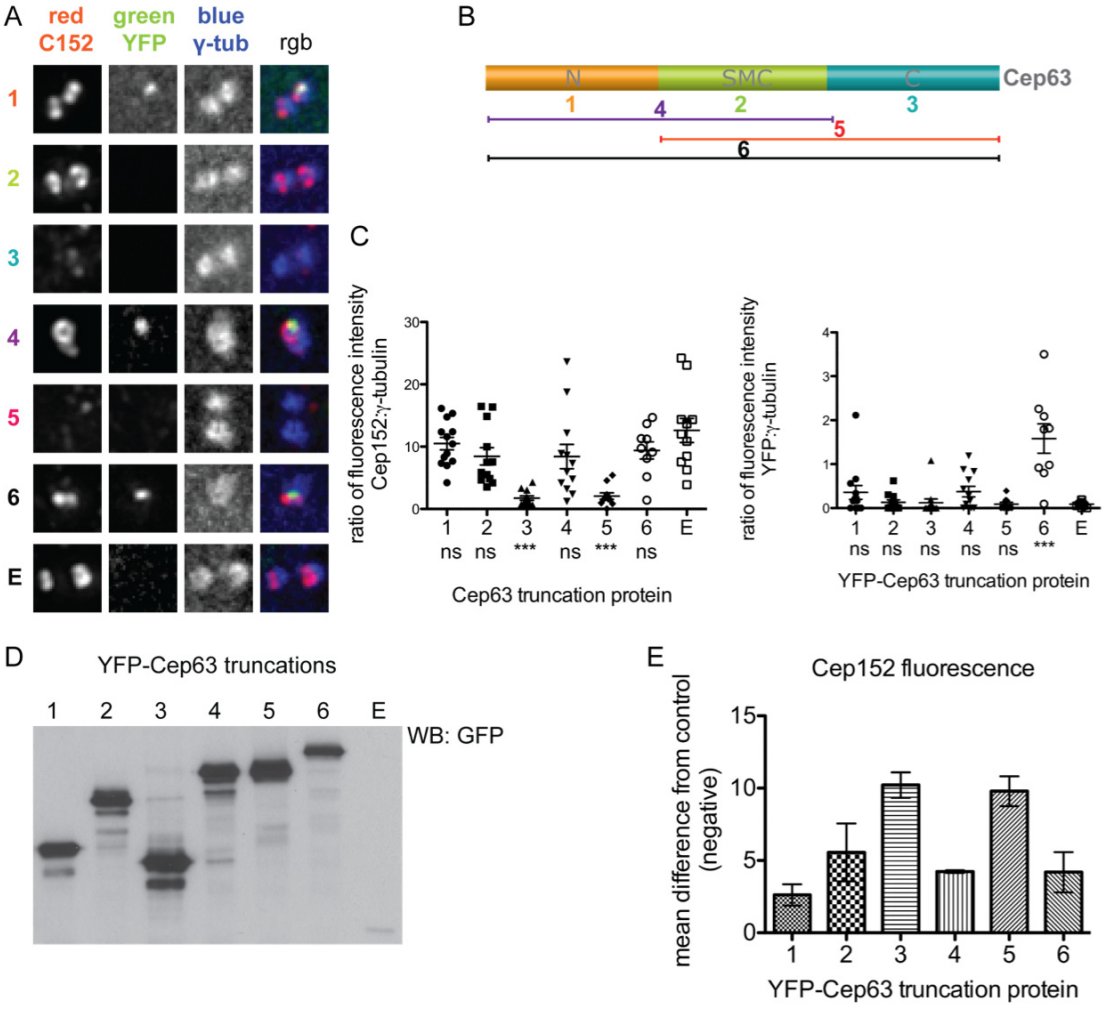

Figure 52 Cep152 is depleted from the centrosome upon overexpression of Cep63 C-terminal region

(A) Images of centrosomes from U2OS cells over-expressing YFP-Cep63 truncation proteins (1-5), full length Cep63 (6) or YFP only (E). Cells were stained with anti-Cep152 (red) and γ-tubulin (blue) antibodies and YFP was detected by direct fluorescence. (B) Schematic showing the domains present in Cep63 truncation proteins. (C) Fluorescence measurements of Cep152 (left) or YFP (right) relative to γ-tubulin fluorescence. Bars show mean and SEM. *** indicates a significant difference from control (E) $p<0.01$. ns: not significant. (D) Western blot of whole cell lysates from U2OS cells used in (A) and (C) with anti-GFP antibody. (E) Mean differences from control (YFP-Empty) of Cep152 fluorescence measurements from two experiments. Cep152 fluorescence was lower in all experimental samples compared with control, but the greatest differences were seen with Cep63 3 and 5 truncations. Mean and standard deviation are shown.

These data fit with the Cep152 literature: a C-terminal region of Cep152 (amino acids 1045-1290) is necessary and sufficient for its centrosome localisation (Hatch et al., 2010b, Cizmecioglu et al., 2010). In support of this, data presented here show that the C-terminal half of Cep152 interacted with Cep63 (figure 26). Localisation of endogenous Cep152 relied upon binding to full length Cep63 with both the N-terminal centrosome localisation domain and the C-terminal Cep152 binding domain. Overexpression of the C-terminal Cep152-binding domain of Cep63, which was not able to localise to the centrosome, resulted in depletion of Cep152 from the centrosome.

In conclusion, Cep63 is required for localisation of Cep152 to the centrosome since RNAi of Cep63 resulted in reduced levels of Cep152 at the centrosome while total protein levels remained constant. Furthermore, overexpression of the C-terminal domain of Cep63, which bound Cep152, but could not localise to the centrosome, acted in a dominant negative fashion such that Cep152 was depleted from centrosomes. However, the situation does not seem to be as simple as Cep63 being required for Cep152 localisation to the centrosome, perhaps acting as a chaperone or scaffold protein to bridge between Cep152 and another centrosome component, because Cep152 was also required for Cep63 localisation to the centrosome.

These data support the following hypothesis: Cep63 and Cep152 bind and form a complex upon translation in the cytoplasm. The Cep63-Cep152 complex forms an interface that is required for centrosome localisation, but each protein alone does not get efficiently incorporated into the PCM. The protein, or protein complex at the centrosome, to which Cep63-Cep152 binds is unknown. Cep152 RNAi leads to centriole loss due to its requirement for Plk4 and CPAP localisation to the centrosome (Cizmecioglu et al., 2010). Cep63 RNAi also led to centriole loss, most likely due to its requirement for efficient Cep152 localisation. Thus, if the hypothesis that Cep63 and Cep152 need to be bound to each other in order to localise to the centrosome is correct, it follows that Cep63 would also be required for efficient localisation of Plk4 and CPAP, which would explain how Cep63 is involved in centriole duplication. However,

this is purely speculative as a thorough investigation of Plk4 or CPAP localisation in Cep63 RNAi treated cells is yet to be completed.

4.5 Cep63 in mitosis – preliminary data

Studies using Cep63 RNAi led to the interesting observation of an increase in mitotic index in U2OS cells. FACS analysis of the cell population after RNAi showed this quantitatively (figure 53). Propidium iodide (PI) staining was used to score cells based on DNA content, which showed that Cep63 RNAi led to an increase in the G2/M population (figure 53a). In order to differentiate between G2 and mitotic cells, FACS analysis of cells stained with PI and anti-phospho-histone H3 serine 10 antibody, which specifically stains mitotic chromatin, was performed (P-H3, figure 53b). This analysis showed that the number of mitotic cells increased, which indicated that there was a delay or block during mitosis when Cep63 was depleted. The mean averages from 3 experiments were not significantly different, which was due to the large variation in the increase of mitotic index seen between experiments. The mitotic index for control cells was 1.11%, 1.17% and 1.59% for the three experiments and for Cep63 RNAi samples the mitotic index was 7.15%, 2.42% and 4.25%. There was always an increase in mitotic index in Cep63 RNAi treated cells, but the extent of the increase varied, perhaps due to the cell density used in each experiment and efficiency of transfection. The increase in mitotic index with Cep63 siRNA 63-1 was modest in comparison with that seen with 63-2, so further experiments were carried out using 63-2 since immunofluorescence showed that knockdown of Cep63 was much more efficient with 63-2 compared to 63-1 (not shown).

These data were extremely interesting since it resembled the XCep63 depletion phenotype. When XCep63 is depleted from *Xenopus* CSF extracts, centrosome-dependent mitotic spindle assembly is disrupted, such that fewer bipolar spindles form and the presence of disordered and aggregated spindle structures increases (Smith et al., 2009). U2OS cells treated with Cep63 RNAi were analysed by immunofluorescence to quantify the proportion of cells in different mitotic stages to see if there was a general

delay in mitosis or a delay in one particular stage (figure 54a). Cep63 RNAi led to an increase in cells in prophase to metaphase, but a decrease of cells in anaphase or telophase. This indicated that cells were delayed in mitosis due to activation of the spindle assembly checkpoint (SAC).

In order to find out if Cep63 RNAi induced mitotic delay was SAC dependent, cells were treated with Cep63 RNAi in combination with Mad2 RNAi, which abolishes SAC signalling, reviewed in chapter 1.1.3 and (Musacchio and Salmon, 2007). A decrease in mitotic index in Cep63 RNAi cells with a defective SAC was observed (Mad2 RNAi, figure 54b), which indicated that the increased mitotic index upon Cep63 RNAi was SAC-dependent. Mad2 RNAi alone caused a decrease in mitotic index compared to the control, as expected. This experiment was repeated twice and the same pattern was observed, a representative profile is shown.

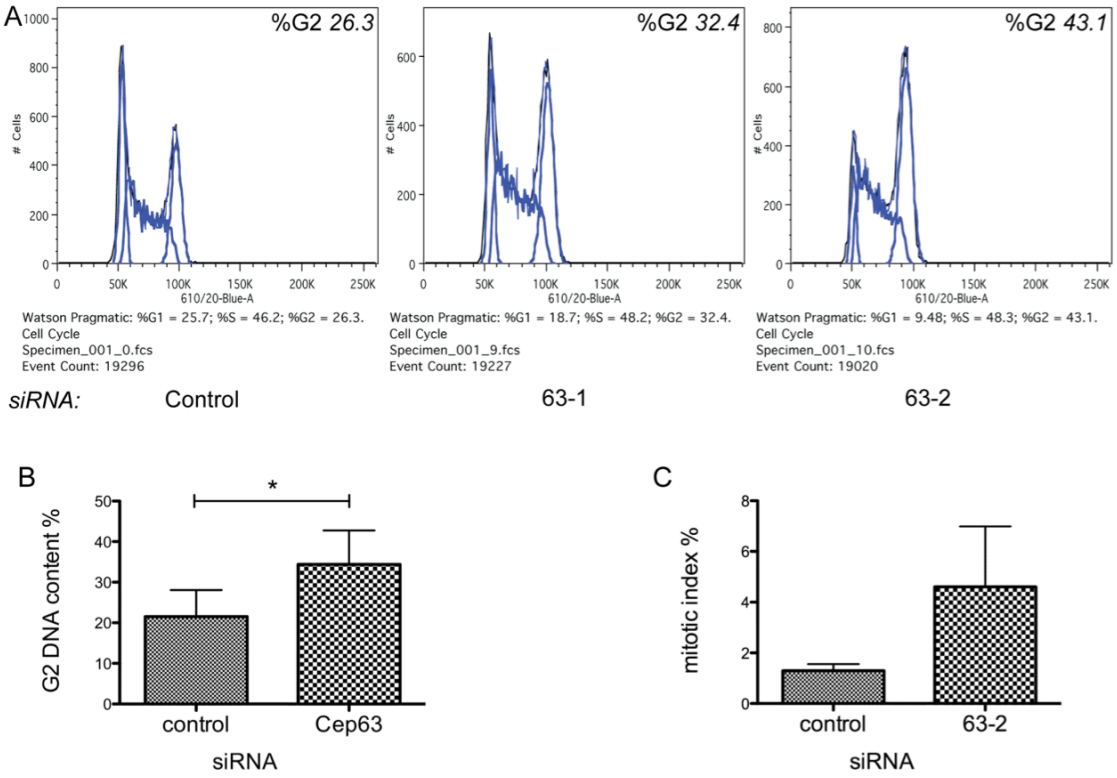

Figure 53 FACS analysis of U2OS cells after Cep63 RNAi
(A) U2OS cells were treated with control or Cep63 RNAi (63-1 and 63-2) for 4 days then fixed and stained with propidium iodide for FACS analysis of DNA content. (B) Percentage of cells with G2 DNA content from 4 experiments with control or Cep63 (63-2) RNAi. * Indicates that the means are significantly different $p<0.05$. (C) Mitotic index, as determined by the percentage of phospho-histone H3 positive cells, from 3 experiments with control or Cep63 (63-2) RNAi in U2OS cells. The means are not significantly different. Both histograms show the mean and standard deviation.

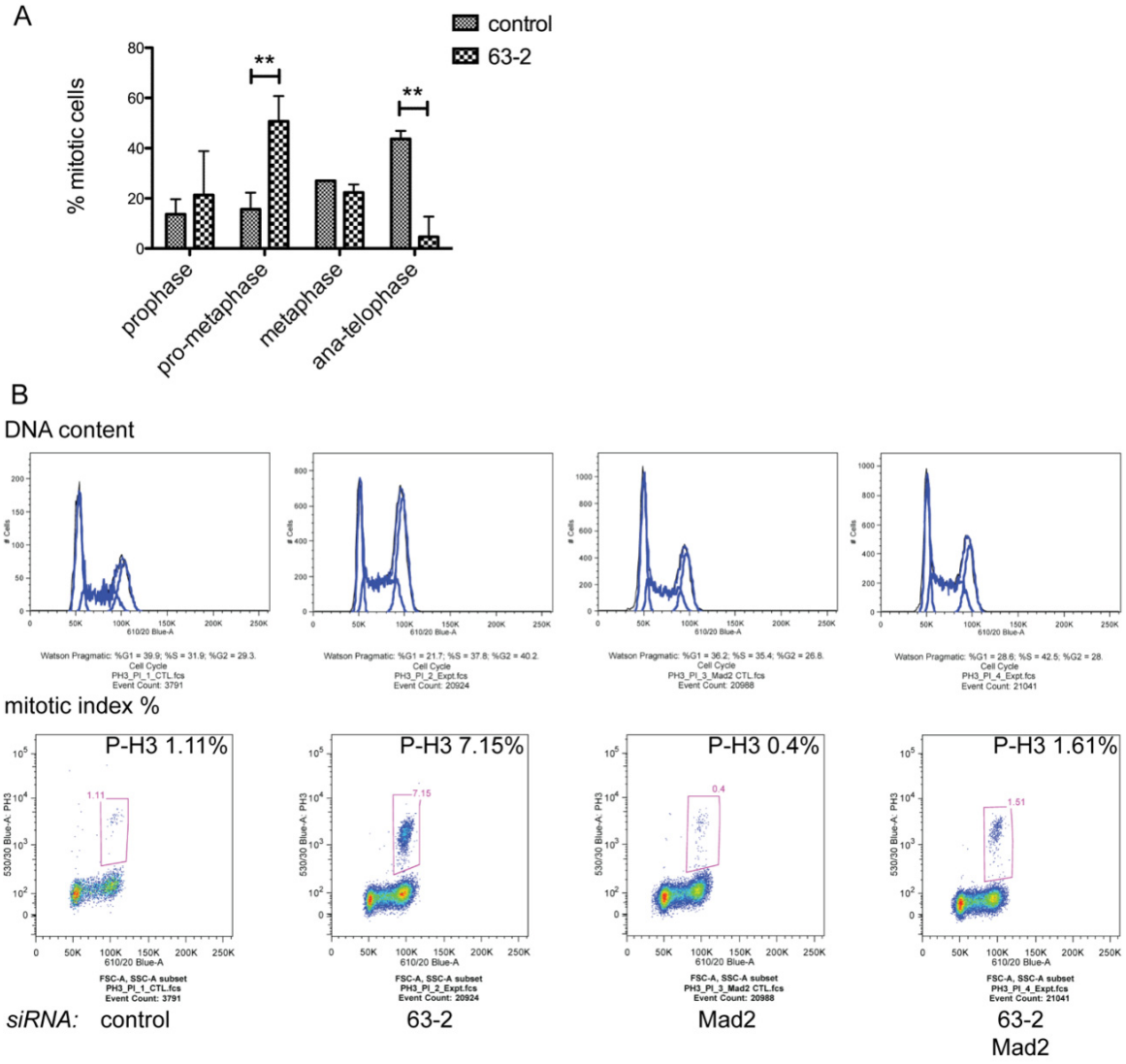

Figure 54 Increase in mitotic index after Cep63 RNAi is dependent on the SAC
(A) Mitotic stages were counted by microscopy in cells treated with control or Cep63 (63-2) RNAi. The average and standard deviation of 3 experiments is shown. N> 50 mitotic cells for each experiment. The differences in pro-metaphase cells and anaphase to telophase cells were significant, $p<0.01$ (**). (B) FACS analysis showing DNA content and mitotic index (% phospho-histone H3 positive cells) of U2OS cells treated with control, Cep63 (63-2), Mad2, or Cep63 and Mad2 RNAi.

Live cell imaging of U2OS cells treated with Cep63 RNAi was performed to see directly what happens when these cells enter mitosis (figure 55). The time from prophase, marked by cells rounding up, to anaphase onset was scored. Whereas all cells treated with control RNAi were able to complete the metaphase to anaphase transition within 60 minutes from prophase, the majority of Cep63 RNAi treated cells took 60 minutes or longer to satisfy the spindle assembly checkpoint and enter anaphase (figure 55b). The same experiment was also carried out with Cep152 RNAi, for which only a modest increase in prophase to anaphase timing was observed in comparison to the control. The majority of Cep152 RNAi treated cells were also able to complete the metaphase to anaphase transition within 60 minutes of the cells rounding up (figure 55b). Whereas 31% of control and Cep152 RNAi cells were able to proceed from prophase to anaphase in 30 minutes or less, only 1% of Cep63 RNAi cells were able to do the same. Furthermore, there was an increase in cells dying after rounding up in Cep63 RNAi samples. These cells may have been dying in mitosis due to prolonged SAC activation and the inability to proceed with cell division. However, this could also have been cell cycle independent cell death. There was no way to differentiate between these alternatives in this experiment. However, transfection with 63-2 siRNA also caused cell death in reduplication assays where the cell cycle was arrested for 3 days (not shown). This observation indicated that the cell death seen during time-lapse experiments was not exclusively due to problems in mitosis.

Analysis of prophase to anaphase timing showed that although the range of times for Cep63 RNAi cells was varied, the mean times for control and Cep63 RNAi were significantly different $p<0.0001$ (figure 55c). A possible reason for the variation in timing in Cep63 RNAi cells could be the extent of knockdown of Cep63 in different cells. The difference in the average time between control and Cep152 RNAi was not significant.

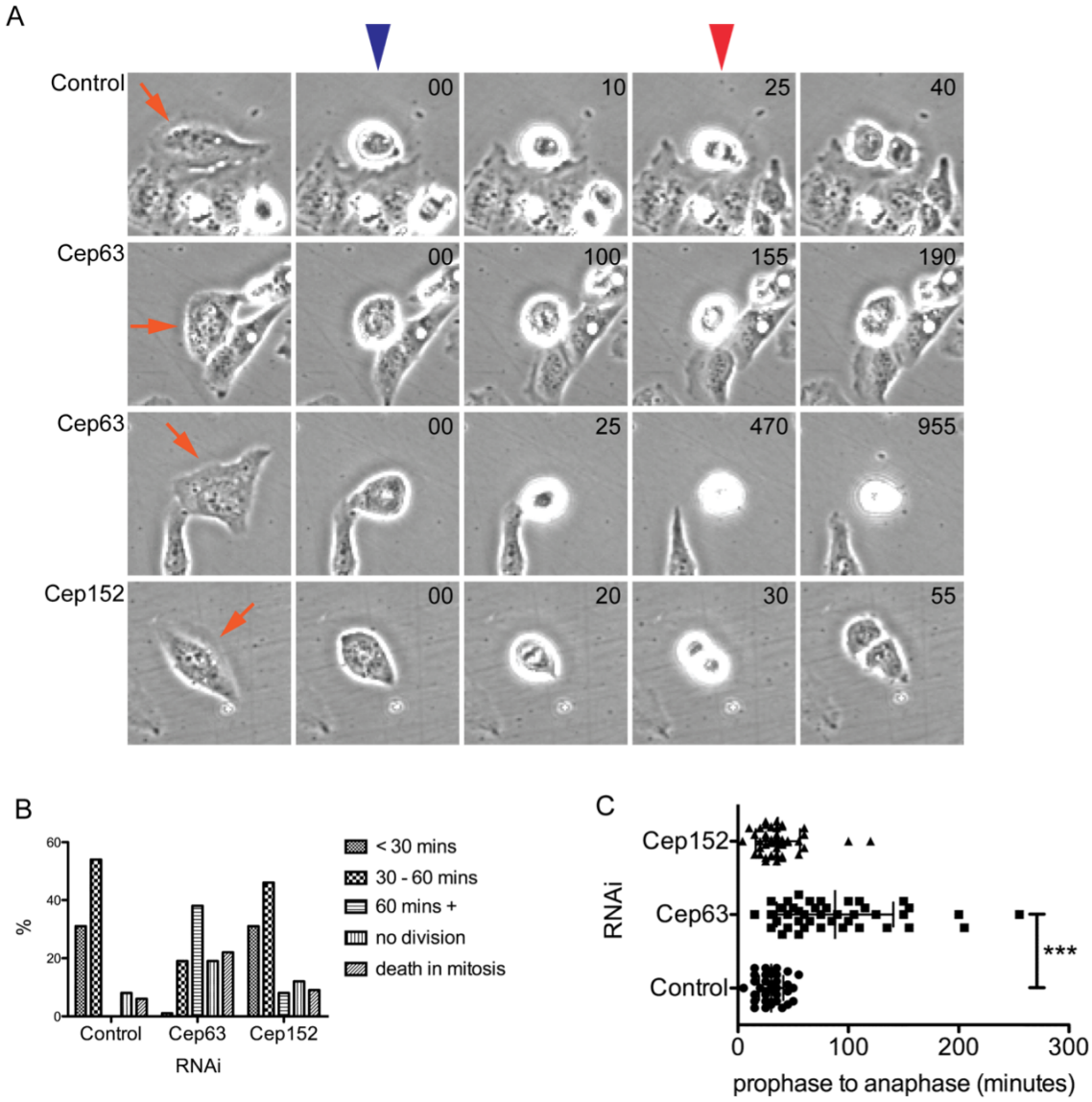

Figure 55 Live cell imaging of Cep63 RNAi treated U2OS cells
(A) Examples of U2OS cells going through mitosis, or dying (3rd row) after RNAi with control, Cep63 (63-2) or Cep152 (152-1) siRNAs. Blue arrowhead indicates cells rounding up, when timing was started. Red arrowhead points to cells showing the first indication of anaphase, when timing was stopped. Pictures were taken at 5 minute intervals. Orange arrows indicate the cell being recorded. (B) Cells were scored depending on their prophase to anaphase time; whether they died; or whether they did not divide at all. N>48. (C) Time of prophase to anaphase (blue to red arrowheads) was recorded. N>40. The difference between the mean times of control and Cep63 RNAi treated cells was significantly different (***) $p<0.0001$. The difference between Cep152 and control was not significant.

Cep63 RNAi using siRNA 63-2 led to a significant increase in the length of mitosis, in particular, prometaphase and metaphase, and therefore caused an increase in mitotic index. This increase was reversed when the SAC was inactivated by depletion of Mad2 by RNAi, which indicated that the delay in mitosis was due to the inability of Cep63 RNAi treated cells to satisfy the SAC.

Cep63 RNAi using siRNA 63-2 caused a large increase in mitotic index, whereas siRNA 63-1 only caused a slight increase (figure 53a). RNAi with 63-1 was not as efficient at depleting Cep63 from the centrosome, as observed by immunofluorescence (not shown), which offered an explanation for the difference in phenotype. However, experiments to verify whether the mitotic index phenotype was indeed due to the lack of Cep63, rather than an off-target effect of siRNA 63-2 suggested that off target effects may indeed be responsible for this phenotype (figure 56). Control RNAi or Cep63 RNAi in U2OS cell lines stably expressing GFP alone or GFP-Cep63 W, which is the wobble mutant of Cep63 that is resistant to siRNA 63-2 were performed. RNAi with 63-2 caused an increase in mitotic index in both GFP-Empty and GFP-Cep63 W cell lines, which indicated that it was causing a mitotic delay independent of Cep63 status. GFP-Cep63 W was resistant to siRNA 63-2 (figure 56b).

Therefore the increase in mitotic index could have been due to either an off-target effect of the siRNA or due to the depletion of the other Cep63 isoforms. All four predicted isoforms of Cep63 are expressed in U2OS cells (figure 32)(Loffler et al., 2011) and all four transcript variants are targeted by siRNA 63-2 (figure 33). GFP-Cep63 W encodes isoform b and therefore only isoform b would have been present in the 63-2 treated GFP-Cep63 W cells, compared to all four isoforms (plus GFP-Cep63 W) in the control cells. This GFP-Cep63 W construct was able to rescue the centrosome reduplication phenotype, but it was not able to rescue the mitotic index phenotype. RNAi experiments in cells expressing siRNA resistant forms of all four different isoforms must be performed in order to reach a final conclusion.

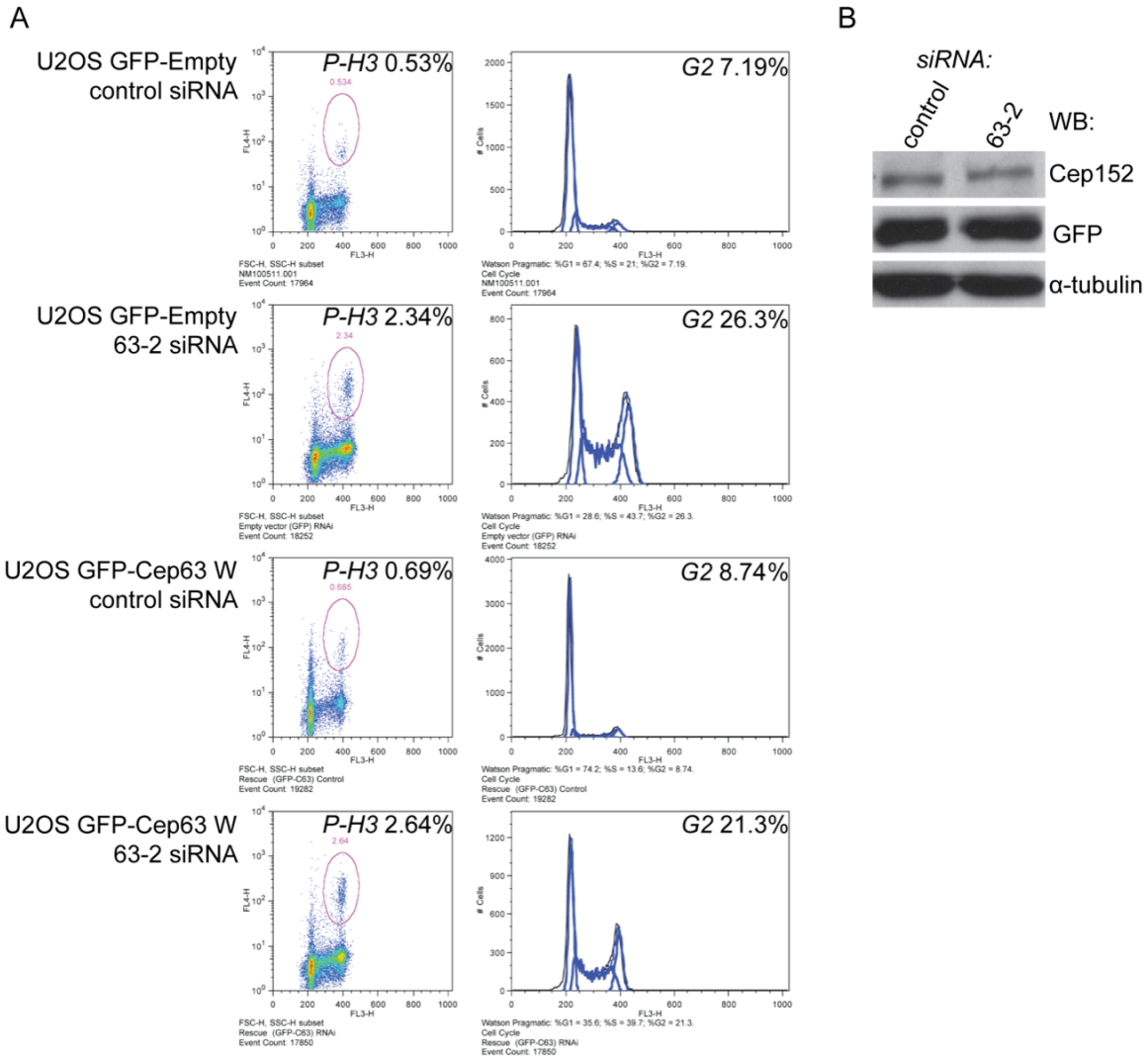

Figure 56 Cep63 RNAi induced mitotic delay is not rescued by siRNA resistant Cep63

(A) FACS analysis of DNA content (PI, x-axis) and phospho-histone H3 staining (P-H3, y-axis). U2OS cell lines stably expressing GFP only (GFP-Empty) or GFP-Cep63 resistant to siRNA 63-2 (GFP-Cep63 W) were transfected with control or 63-2 siRNAs and collected after 4 days. The percentages of phospho-histone H3 positive mitotic cells are indicated in the left hand panels and the percentages of cells with G2 DNA content are indicated in the right panels. (B) Western blot of U2OS GFP-Cep63 W cells after control or 63-2 RNAi with anti-Cep152, GFP antibodies with α-tubulin as a loading control. Cep152 is not depleted by Cep63 RNAi and GFP-Cep63 W is resistant to Cep63 siRNA 63-2.

4.6 Phosphorylation of Cep63 – preliminary data

Xenopus laevis Cep63, XCep63, is a target of ATM/ATR kinase signalling in response to DNA damage in egg extract (Smith et al., 2009). XCep63 is phosphorylated on serine 560, which is part of a novel ATM consensus site consisting of the consecutive amino acids; SLE. The canonical ATM consensus site is either SQ or TQ, with the serine or threonine being phosphorylated (Sancar et al., 2004). Cep63 is conserved amongst vertebrates, but serine 560 is not. However, there are many other SQ, TQ and SLE sequences that could be potential ATM/ATR targets for phosphorylation (figure 57).

Since XCep63 is phosphorylated in response to DNA damage, experiments were carried out to see if the same was true for the human protein. First of all, a Flag IP from Flag-Cep63 293 cells untreated or incubated with Phleomycin for two hours to induce DNA damage was undertaken (figure 27, section 3.2.1). The eluate was separated by SDS-PAGE and the gel was cut into slices for mass spectrometry analysis by LC-MS. There was only 16% peptide coverage for Cep63, which was not sufficient for this experiment. Although 5 of the 11 putative ATM/ATR phospho sites were covered within the peptides identified (black lines, figure 57), no phosphorylation was detected. In order to improve the protein coverage with this technique it will be necessary to increase the amount of protein used for mass spectrometry analysis. Identification of the phosphorylated residues by mass spectrometry could indicate the kinase responsible if the phosphorylated residue is part of a known consensus sequence, and it would allow verification that it is Cep63 that is phosphorylated and not the Flag tag.

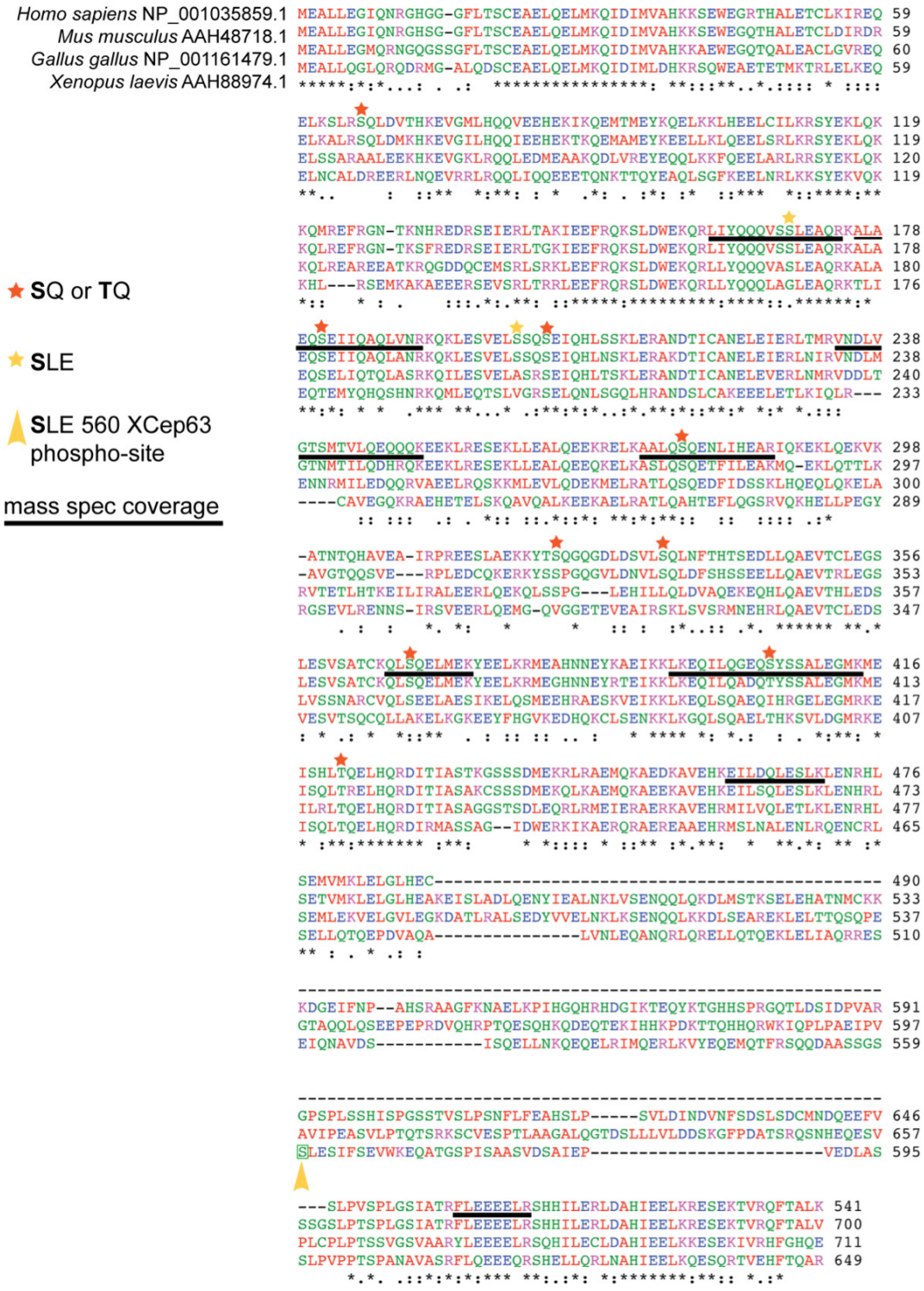

Figure 57 Multiple alignment of Cep63 protein sequences
Human Cep63 (isoform b) was aligned with mouse, chicken and *Xenopus* (top to bottom) Cep63 protein sequences using ClustalW alignment tool. Serine 560, which is phosphorylated by ATM in *X. laevis.* is indicated by a yellow arrowhead. Putative ATM target sequences (SQE or TQE) are indicated by orange stars and putative SLE target sites by yellow stars. Black lines indicate peptides of the human protein that were identified by mass spectrometry analysis of Flag-Cep63.

Since XCep63 undergoes an electrophoretic mobility shift upon phosphorylation by ATM/ATR in egg extract (figure 27)(Smith et al., 2009), experiments were performed to examine whether human Cep63 might also be phosphorylated in egg extract. MBP-XCep63 and MBP-Cep63 (human) were incubated in egg extract with or without short linear double strand DNA fragments to activate ATM (pA/pT, figure 58). Although XCep63 showed decreased mobility (upward shift) after incubation in extracts with pA/pT on a 10% SDS-PAGE gel and a 10% SDS-PAGE gel containing Phos-tag™ reagent, the human MBP-Cep63 did not (figure 58a). Phos-tag™ acrylamide specifically binds phosphate groups and therefore specifically slows the migration of phospho-proteins through SDS-PAGE gels. Using these conditions for the Phos-tag gel (40 μM Phos-tag, 40 μM $MnCl_2$), phospho-MBP-XCep63 did not show any slower migration than on the 10% SDS-PAGE gel. MBP-hCep63 had the same mobility with or without DNA damage checkpoint activation in the absence or presence of Phos-tag, which indicated that human Cep63 was not phosphorylated by DNA damage kinases in *Xenopus* egg extracts. However, this did not rule out the possibility of Cep63 being phosphorylated, as the reaction may be species specific, such that *Xenopus* ATM might not be able to bind and phosphorylate Cep63, as it does to XCep63.

In order to determine whether Cep63 was phosphorylated in human cells, cell lysates from YFP-Cep63 293 stable cell line were analysed by Western blotting after treatment of the cells with 10 Gy γ-irradiation (IR, figure 58b). Cells were irradiated then collected at time points up to 2 hours in the presence or absence of phosphatase inhibitors. No mobility shift was observed for YFP-Cep63 after DNA damage treatment when samples were analysed on a 10% SDS-PAGE gel. However, not all phospho-proteins show reduced mobility in SDS-PAGE electrophoresis.

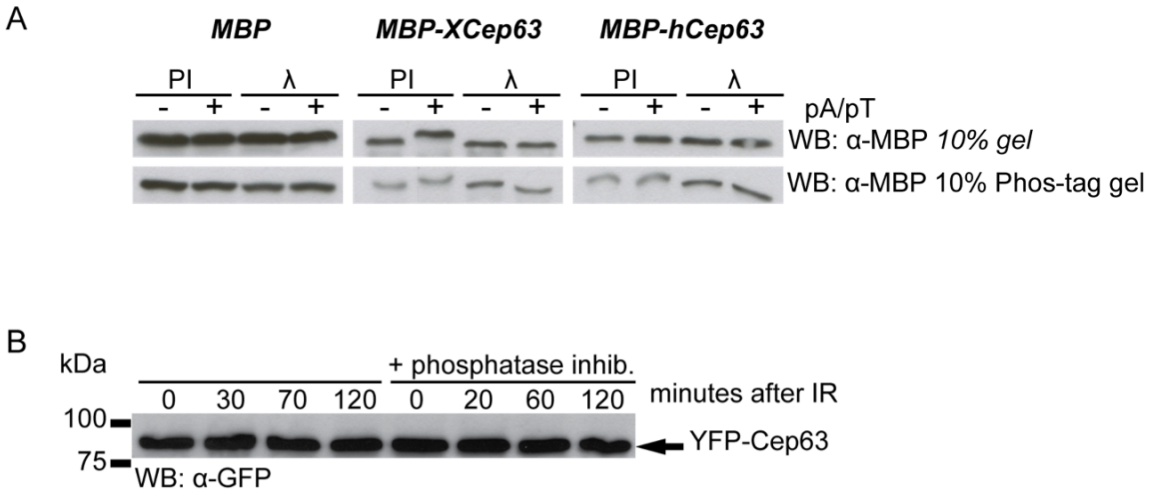

Figure 58 MBP-hCep63 and MBP-XCep63 incubation with Xenopus egg extracts +/- DNA damage
(A) MBP, MBP-XCep63 or MBP-hCep63 (human Cep63) were incubated in *Xenopus laevis* CSF extract in the absence or presence of short double stranded DNA oligonucleotides (pA/pT). Extracts were treated with phosphatase inhibitors (PI) or lambda phosphatase (λ) and separated on a 10% SDS-PAGE gel (upper panels) or a 10% gel containing Phos-tag reagent (lower panels). Western blotting was carried out with anti-MBP antibody. (B) 293 YFP-Cep63 cells were treated with gamma-irradiation (IR) and collected at the indicated times in the absence or presence of phosphatase inhibitors (+ phosphatase inhib.). Cell lysates were analysed on a 10% SDS-PAGE gel and Western blotting with anti-GFP antibody (rabbit).

Since there was no evident mobility shift of exogenous Cep63 on standard SDS-PAGE gels after cells were treated with γ-IR, samples were then analysed using SDS-PAGE gels containing Phos-tag acrylamide. Flag-Cep63 293 cells were treated with UV (10 Jm-2) or γ-IR (10 Gy) followed by incubation for one hour before collection (figure 59). Additionally, cells arrested in mitosis by 16-hour incubation with nocodazole (100 ng/ml) or arrested in mitosis then irradiated with 10 Gy γ-IR were also analysed. Cell lysates were separated by SDS-PAGE on a 10% gel plus Phos-tag and Western blotting was carried out with anti-Flag antibody. Interestingly, Flag-Cep63 migrated as a doublet in cells treated with nocodazole (figure 59a), which indicated that a proportion of Flag-Cep63 was phosphorylated in this condition. The bands on this gel did not migrate in a straight line, which was due to EDTA in the lysis buffer, which chelates the manganese ions required for Phos-tag reagent to bind to phosphate groups. Therefore, future Phos-tag analysis was carried out using eluates from Flag IPs from Flag-Cep63 containing cell lysates. Anti-Flag beads were washed with PBS, then protein was eluted with Laemmli loading buffer to avoid the presence of salt and EDTA in samples. Also, the concentration of Phos-tag and $MnCl_2$ was lowered from 40 to 20 μM. This combination resulted in the Flag-Cep63 band shift after nocodazole to become more evident (figure 59b).

Analysis of the same Flag-Cep63 eluate on a Phos-tag gel and a standard gel without Phos-tag showed that Flag-Cep63 appeared as two bands in a Phos-tag dependent manner (figure 59b). In the absence of Phos-tag, Flag-Cep63 migrated as a single band, which indicated that the upper band observed upon Phos-tag SDS-PAGE was a phosphorylated version of Flag-Cep63. Interestingly, the upper Flag-Cep63 band was only a small proportion of total Flag-Cep63, indicating that only a subset of Flag-Cep63 was phosphorylated. The upper Flag-Cep63 band was proportionally greater in nocodazole treated cells, but it was also apparent in untreated asynchronous cells.

In order to conclude whether the upper Flag-Cep63 band was due to phosphorylation, Flag-IP of Flag-Cep63 was carried out from lysates of 293 cells arrested in mitosis by different methods (figure 59c) and each sample was compared before and after

treatment with λ-phosphatase. λ-phosphatase removed the upper band of Flag-Cep63 from all samples, which confirmed that this band was a phosphorylated form of Flag-Cep63. Cells were arrested in mitosis by incubation with nocodazole; nocodazole release into medium containing MG132 proteasome inhibitor to prevent anaphase onset; or S-Trityl-L-Cysteine, which inhibits Eg5, a kinesin motor protein required for proper mitotic spindle assembly and therefore arrests cells in mitosis because they cannot form a spindle and satisfy the spindle assembly checkpoint (Skoufias et al., 2006). In this experiment phospho-Flag-Cep63 was also present in the untreated, asynchronous cells, although the proportion of the phosphorylated protein increased in cells that were arrested in mitosis. However, it is unlikely that this is a phosphorylation event that occurs during all mitoses, because only a small proportion of Flag-Cep63 was phosphorylated when all cells were arrested in mitosis. Perhaps this phosphorylation occurs in only a subset of mitotic cells where ATM and/or ATR is active. Alternatively, perhaps the phosphorylated proportion of Flag-Cep63 represents the portion of the protein that is present at a particular location, for example the centrosome, or cytoplasm.

In order to try and determine the kinase responsible for phosphorylation of Flag-Cep63, analysis of Flag-Cep63 293 cell lysates from cells treated with UV (UV was seen to cause an increase in phospho-Flag-Cep63 in a previous experiment) in the absence or presence of different specific inhibitors of DNA damage signalling proteins was carried out (figure 59d). UCN01, a Chk1 inhibitor (Graves et al., 2000); am ATM specific inhibitor (Jazayeri et al., 2006); an ATR specific inhibitor; and an ATM/ATR dual inhibitor, both from Oscar Fernandez-Capetillo (Toledo et al., 2011) were used. Although the phospho-Flag-Cep63 band was present after UV, the proportion was not visibly different from untreated cells, which indicated that the modification might not have been DNA damage dependent. Furthermore, the proportion of phospho-Flag-Cep63 remained unchanged in cells treated with UV in the presence of each of the DNA damage kinase inhibitors.

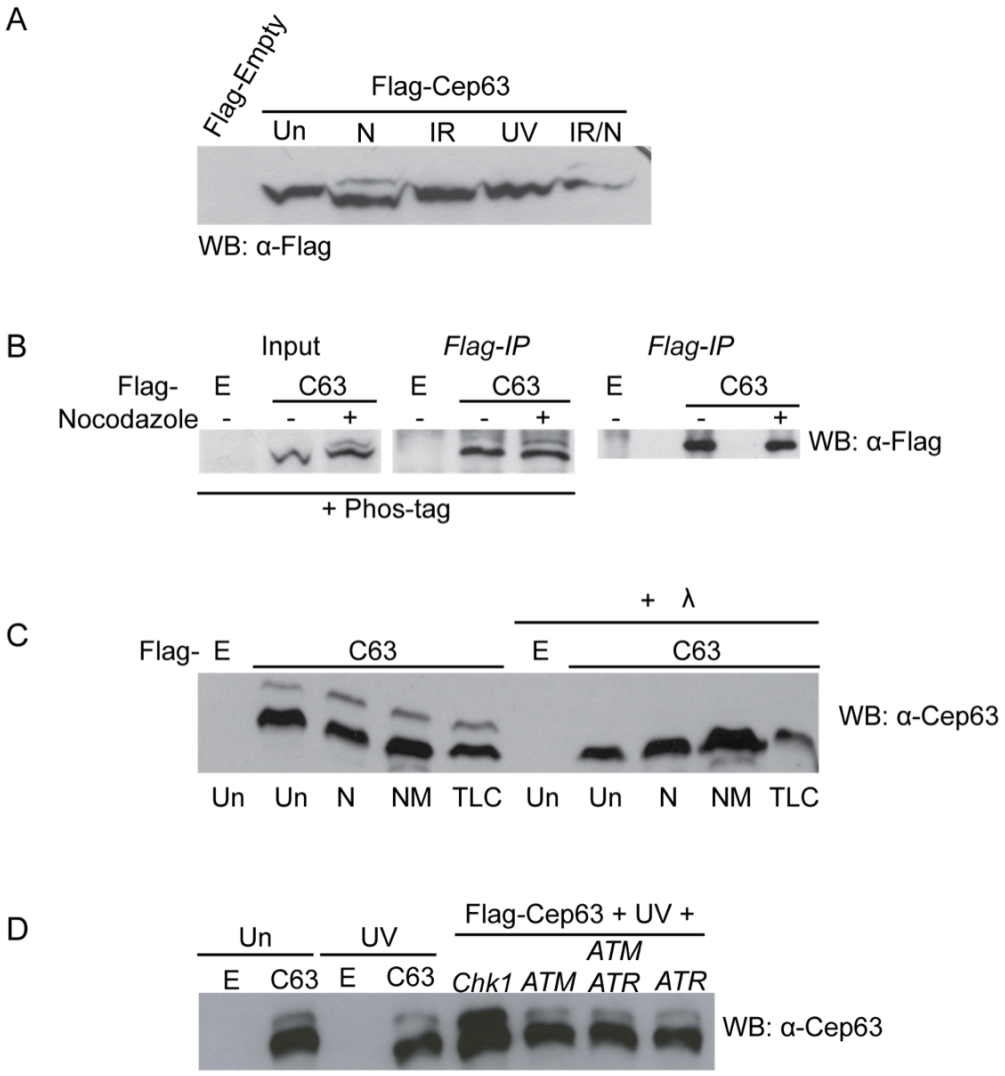

Figure 59 Flag-Cep63 DNA damage independent phosphorylation
(A) Flag-Cep63 293 cells were untreated (Un), incubated for 16 hours in 100 ng/ml nocodazole (N), treated with 10 Jm^{-2} UV (UV), treated with 10 Gy γ-irradiation (IR) or treated with γ-irradiation after 16 hour incubation with nocodazole. Cell lysates were analysed by SDS-PAGE on a 10% gel containing 40 μM Phos-tag reagent followed by Western blotting with anti-Flag M2 antibody. (B) Flag-Cep63 293 cells were untreated (-) or incubated for 16 hours in nocodazole (+). Cell lysates were analysed by SDS-PAGE on a 7.5% Phos-tag gel (left panel). Flag IPs were carried out using the same cell lysates and eluates were analysed on a 7.5% Phos-tag gel (middle) or on a 10% standard SDS-PAGE gel (right). Western blotting was carried out with anti-Flag M2 antibody. (C) Flag-Cep63 293 cells were untreated (Un); incubated with nocodazole for 16 hours (N); incubated with nocodazole for 16 hours then release in the presence of MG132 for 2 hours (NM); or incubated with S-trityl-L-Cysteine for 16 hours. Flag-Cep63 was isolated by Flag-IP from cell lysates and was analysed before and after treatment with λ phosphatase (+λ) on a 7.5% Phos-tag gel followed by Western blotting with anti-Cep63 49AP. (D) Flag-Cep63 293 cells were treated with 10 Jm-2 UV (UV) in the absence or presence of specific inhibitors of DNA damage signalling proteins (Chk1, ATM, ATM/ATR dual inhibitor and ATR). Flag-Cep63 was isolated by Flag-IP from cell lysates and analysed on a 7.5% Phos-tag gel followed by Western blotting with anti-Cep63 49AP. Flag-Empty cell lysate was used as a negative control for the identification of Flag-Cep63 specific bands (B-D). 7.5% Phos-tag gels contained 20 μM Phos-tag (B-D).

In conclusion to these preliminary experiments: a small proportion of Flag-Cep63 was phosphorylated in asynchronous 293 Flag-Cep63 cells, which increased slightly upon synchronisation of the cells in mitosis, but was still less than 50% of the total protein. The phospho-Flag-Cep63 band was still present after incubation of cells with different specific inhibitors of DNA damage signalling proteins and there was little increase in the proportion of phospho-Flag-Cep63 relative to the total amount in cells treated with UV. Many more experiments need to be carried out in order to determine the kinase responsible for this phosphorylation; the cause of the phosphorylation and ultimately, its function. However, this preliminary data is interesting as it leads to the hypothesis that Cep63 might be regulated by phosphorylation, perhaps by cell cycle dependent kinases, kinases involved in centriole duplication or perhaps DNA damage signalling kinases.

4.7 Chapter 4 conclusions

Cep63, and its binding partner Cep152, play a role in the positive regulation of centriole duplication. Cep63 depletion by RNAi led to inhibition of centrosome reduplication, which occurs in U2OS cells arrested with DNA replication stalling agents. Cep63 depletion leads to inefficient centriole duplication such that around 50% of cells enter mitosis with fewer than four centrioles, but Cep63 appears not to be absolutely required for centriole duplication.

Cep63 likely regulates centriole duplication via modulation of its interacting partner Cep152. Cep63 interacts with and recruits Cep152 to the centrosome. Conversely, Cep63 also depends on Cep152 for centrosomal localisation, although Cep63 N-terminal fragments that cannot interact with Cep152 are able to localise to the centrosome with reduced efficiency. Studies detailed in this chapter led to the conclusion that Cep63 is required for efficient and timely centriole duplication, but that it is not required for efficient bipolar spindle assembly and mitotic progression. Furthermore, a proportion of exogenous Cep63 is phosphorylated when expressed in human cells. The kinase(s) responsible for this modification(s) has not yet been identified.

Chapter 5. Cep63 gene-trap mouse embryonic fibroblasts

Centrosomes have multiple functions some of which are more important in some cell types than others. For example, centrosomes act as the principle microtubule organising centre (MTOC) in dividing cells, but differentiated cells, neuronal, epithelial and muscle cells for example, also use other cellular structures for the nucleation of microtubules (Keating and Borisy, 1999). Furthermore, centrosomes are not required to organise spindle assembly in certain cell types: oocytes are one example (Doubilet and McKim, 2007). However, in some cell types, particularly in neural stem and progenitor cells during mammalian embryonic brain development, centrosomes have important functions in positioning of the mitotic spindle (Farkas and Huttner, 2008). Cell division plane positioning regulates the switch of cell fate between proliferation and differentiation, as described in 1.2.4. The switch from proliferation to differentiation of neuroepithelial cells (NE) during embryonic development is a key determinant of brain size. Before the onset of neurogenesis, NE cells divide symmetrically, which generates two NE progenitors. At the onset of neurogenesis, NE cell division becomes asymmetric and one daughter becomes a differentiated neuron, while the other retains proliferative potential. This topic is complex and many more factors than the centrosome are involved: the subject is reviewed in (Farkas and Huttner, 2008). The important point to emphasise here is that while some centrosome proteins may play a minor role in one particular cell type, they may play a more crucial role in another cell type or at a particular stage of development. As such, an animal model for Cep63 may shed more light on the function of the protein by illuminating a particular cell type, organ or developmental stage in which the protein is required.

Additionally, there is growing evidence that centrosome proteins are important during embryonic brain development as several centrosome components have been linked to primary microcephaly, as described in 1.2.4. Interestingly, mutations in Cep152 have recently been identified as the cause of microcephaly in several patients (Guernsey et al., 2010, Kalay et al., 2011).

The generation of Cep63 null embryos would also allow analysis of cells in culture that are devoid of Cep63 without relying on RNAi mediated depletion of the protein, which may not be complete and can sometimes result in off-target effects. We collaborated with Dr Travis Stracker from the Institute for Research in Biomedicine (IRB) in Barcelona for the generation of Cep63 deficient mice and mouse embryonic fibroblast cell lines. At the time of writing these efforts have yielded one Cep63 homozygous mutant cell line and a wild type littermate control cell line. Thus all experiments detailed in this chapter are carried out with cells derived from one embryo (plus the wild type control) only. All data will need to be validated by repeating experiments in other Cep63 mutant cell lines.

5.1 Checking the Cep63 gene-trap mouse ES cells

Mouse embryonic stem (ES) cells with a gene-trap cassette inserted in the Cep63 gene (one allele) were purchased from the EUCOMM consortium (European Conditional Mouse Mutagenesis Programme). Although the targeting construct used was intended to enable a Flp and Cre recombinase mediated conditional mutation in the gene, the 3' Lox P site was lost during the targeting process and thus the cassette in Cep63 could not be excised (see diagram, figure 60). Thus, the ES cells could not be used to generate a conditional knockout mouse. The ES cells were cultured and, after freezing down an early passage for blastocyst injection, genomic DNA was extracted to check for the insertion of the cassette by PCR (figure 60). Four of the 6 PCR reactions were positive, which confirmed that the construct was in the expected position: between the first and second exon of the Cep63 gene. A Southern blot of restriction enzyme digested genomic DNA from the ES cells was carried out to check for potential mistargeting events. A radioactive probe was generated using the β-galactosidase and neomycin resistance gene sequence as a template, which are present in the cassette. The Southern blot contained one band of expected size for each of the three digest experiments carried out (figure 61) and no other bands were seen, which indicated that the cassette was inserted only in one position in the genome: the Cep63 gene. As a control for probe specificity, genomic DNA from mouse ES cells that did not contain the cassette was subjected to the same analysis; no non-specific bands were seen.

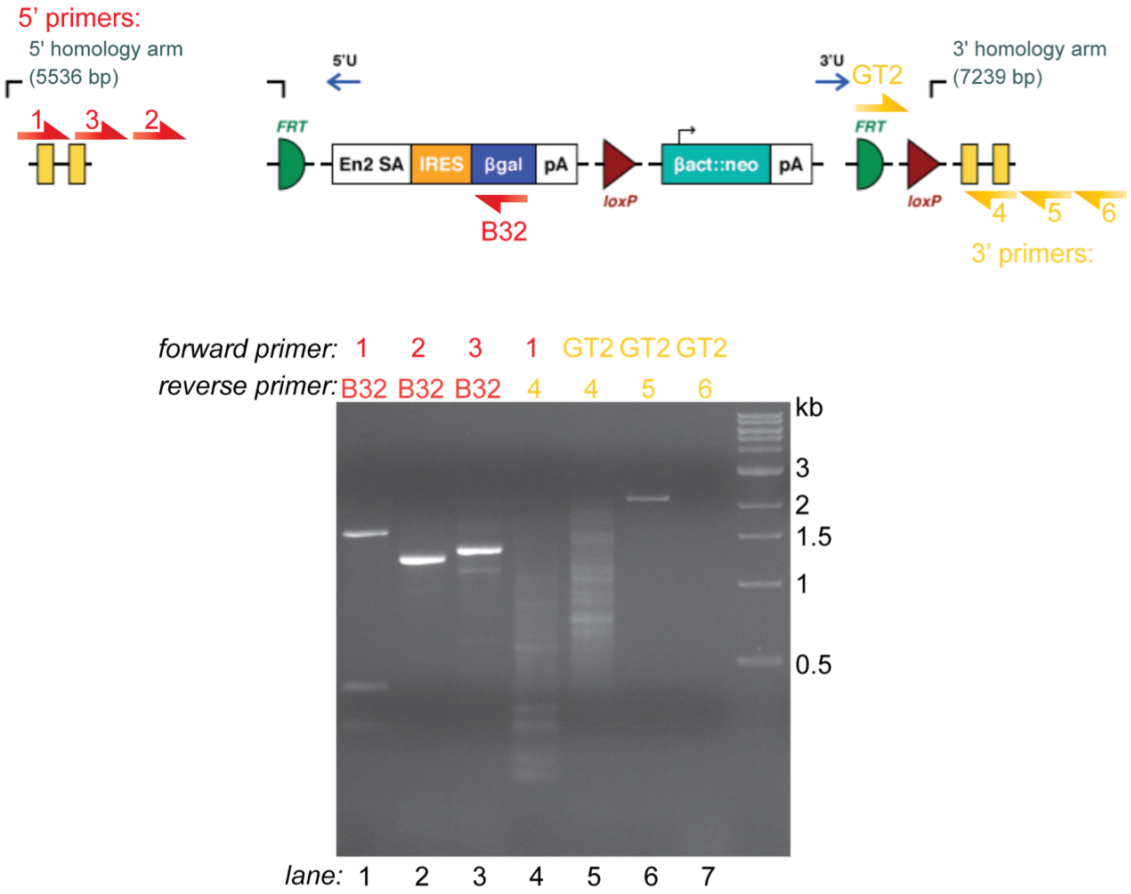

Figure 60 Cep63 gene-trap mouse embryonic stem cells
Genomic DNA from mouse embryonic stem (ES) cells containing a Cep63 gene-trap (from EUCOMM) was analysed by PCR. Primer sequences present in the Cep63 gene surrounding the expected cassette position (1 – 6) were used with primers specific for sequences present in the gene-trap cassette (B32 and GT2). The diagram illustrates the composition of the gene-trap cassette and the position of the primers used (not to scale). Lower panel: PCR products were analysed on a 1% agarose gel containing ethidium bromide and DNA was visualised by UV trans-illumination. PCR reactions in lanes 4, 5 and 7 generated no specific products. Reactions in lanes 1, 2, 3 and 5 generated products of the predicted size. A 1 kb DNA ladder was used for comparison of DNA fragment size (right hand lane).

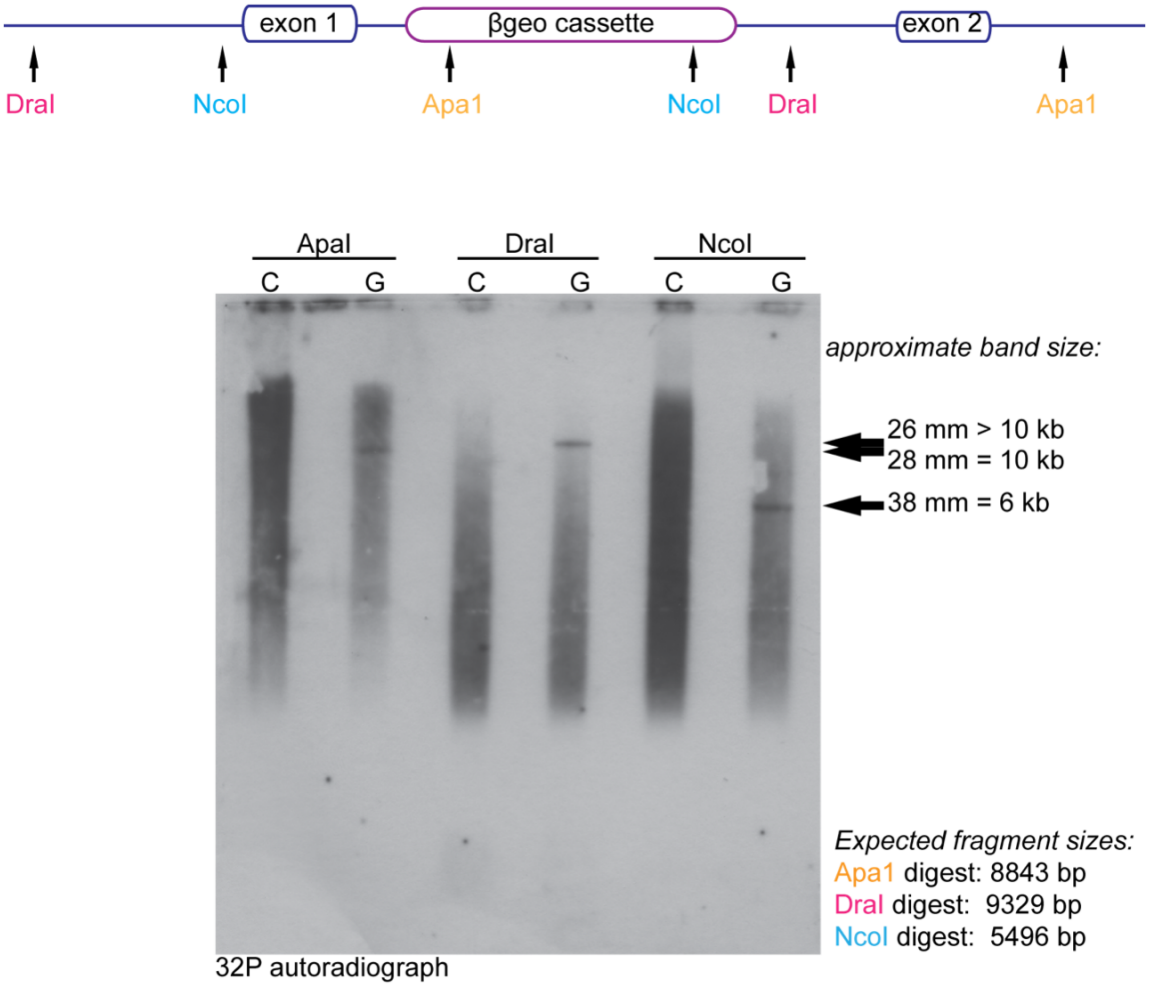

Figure 61 Southern blot of Cep63 gene-trap mouse ES cell genomic DNA
The diagram illustrates the position of the gene-trap cassette relative to exons 1 and 2 of the cep63 gene and the position of restriction sites of three selected restriction enzymes (DraI, NcoI and ApaI) within the cassette and the surrounding gene. Lower panel: the indicated restriction digests were carried out on genomic DNA from wild type ES cells as a negative control (C) or ES cells with the Cep63 gene-trap (G). The resulting DNA fragments were separated on a 0.7% agarose gel without ethidium bromide and transferred onto a nitrocellulose membrane for subsequent Southern blotting with a ^{32}P-αdATP labelled probe generated using the β-geo cassette DNA as a template. Radioactive signals were detected using autoradiography film. Distance of the bands from the well in the gel and the corresponding approximate molecular sizes are indicated on the right.

Since both the PCR and Southern blot indicated that the gene-trap cassette was present in the expected position and not in any off-target location, the ES cells were injected into blastocysts in order to generate chimeric mice for breeding. All mouse work was carried out in Dr Stacker's lab at the IRB. This includes injection, breeding, genotyping and generation of mouse embryonic fibroblasts (MEFs).

5.2 Mouse embryonic fibroblast (MEF) cell lines

Genotyping of 6 embryos from one litter indicated that one was homozygous for the Cep63 gene-trap (number 2, figure 62) and one was heterozygous (number 6), the rest were wild type homozygotes. Genotyping was carried out using primers for the intron between Cep63 exons 1 and 2 and also the B32 reverse primer, which anneals to a site in the gene-trap. Reactions carried out with primer pairs that anneal to the Cep63 gene showed that the expected product (for the wild type gene) was present in all embryos except number 2 (figure 62). This was true for both reactions carried out using primer pairs to detect the wild type allele. Absence of a product at this size indicated that the gene-trap must have been inserted in both alleles in this embryo (2). The presence of the gene-trap results in the primer pairs being separated such that the PCR reaction cannot be completed in the extension time used for the reactions. Embryo number 6 was positive for the presence of the cassette (B32 primer) and the wild type allele and was therefore heterozygous for the gene-trap Cep63 allele (figure 62).

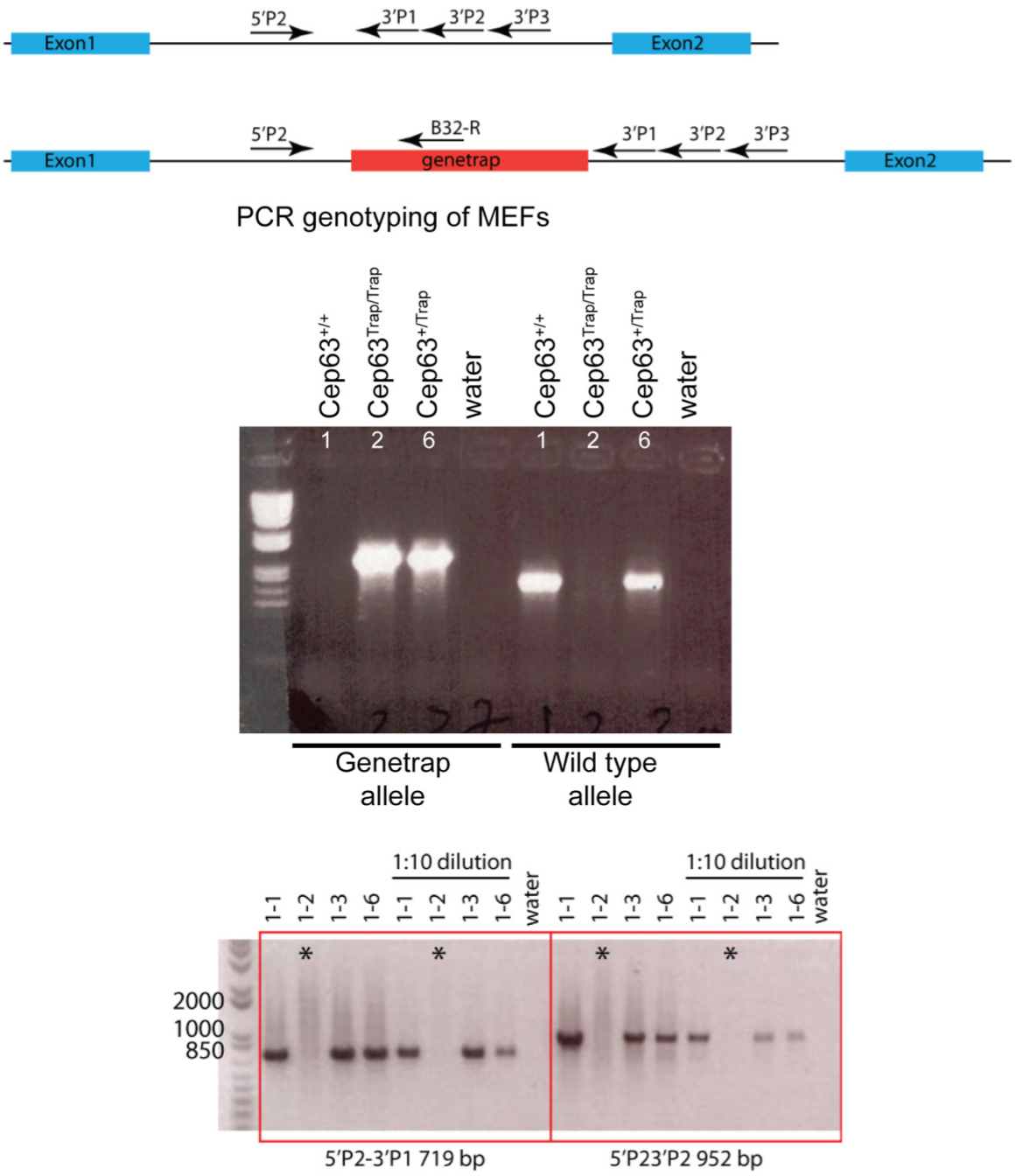

Figure 62 Genotyping embryos from Cep63 gene-trap heterozygote breeding
Figure provided by Dr Travis Stracker. PCR was carried out with genomic DNA from embryos 1, 2, 3 and 6. Reactions with a gene-trap specific primer (middle panel) indicated that embryos 2 and 6 contained the gene-trap cassette. PCR reactions using primers specific for the region of Cep63 flanking the cassette (middle panel, right hand lanes and bottom panel) indicated that embryo 6 also contained a wild type allele (heterozygous), whereas embryo 2 did not. Diagram indicates the position of the primers used in the bottom panel, with respect to Cep63 exons and the gene-trap cassette.

Embryos 1 (wt/wt), 2 (gt/gt) and 6 (wt/gt) were used to generate MEF cell lines. Initial culturing of the MEFs was also carried out by Dr Stracker. A 3T3 assay was carried out, which involved the passage of 300,000 cells into a 60 mm tissue culture plate, every 3 days. During this time, cells numbers were recorded (figure 63a). Growth rates between the cell lines were comparable during early passages and FACS analyses of the cells showed that cell cycle distribution was comparable between cell lines (figure 63b).

Intriguingly, cell line 2 (gt/gt) immortalised at a much earlier passage than wild type cell line 1 (figure 63a) and also in a much shorter time than previously observed in the lab for any other cell line. The cell lines entered a crisis period at around the same time, where the cells start to become senescent; around passage 7, 18 days (figure 63a). However, cell line 2 (gt/gt) bypassed senescence and spontaneously immortalised around passage 10, day 25. Cells started to form tightly packed colonies at this time, showing that they were overcoming contact inhibition. In comparison, the cell line 1 (wt/wt) did not begin cell doubling again until after passage 20. The Cep63 gene-trap cell line (2) also spontaneously immortalised when cells were left at confluence at passage 6, for 2.5 weeks with regular media changes, whereas the wild type cell line took around 3 weeks to undergo spontaneous immortalisation under the same conditions.

This phenotype was extremely interesting as it could be an indication that Cep63 is involved in the maintenance of genome stability. Inactivation of Cep63 could lead to cell division aberrations, possibly through its role in centriole duplication, and provide a background with high genome instability, thus creating an environment suitable for mutations to occur at a high rate and allow loss of growth inhibition. However, this phenotype could be due to differential loss of tumour suppressor functions, for example. Further investigation is required in order to conclude on this topic. Analysis of additional MEF cell lines will be required and expression of exogenous Cep63 in the gene-trap homozygous MEFs will provide a way to validate this data and conclude whether the difference observed here is specifically due to lack of Cep63.

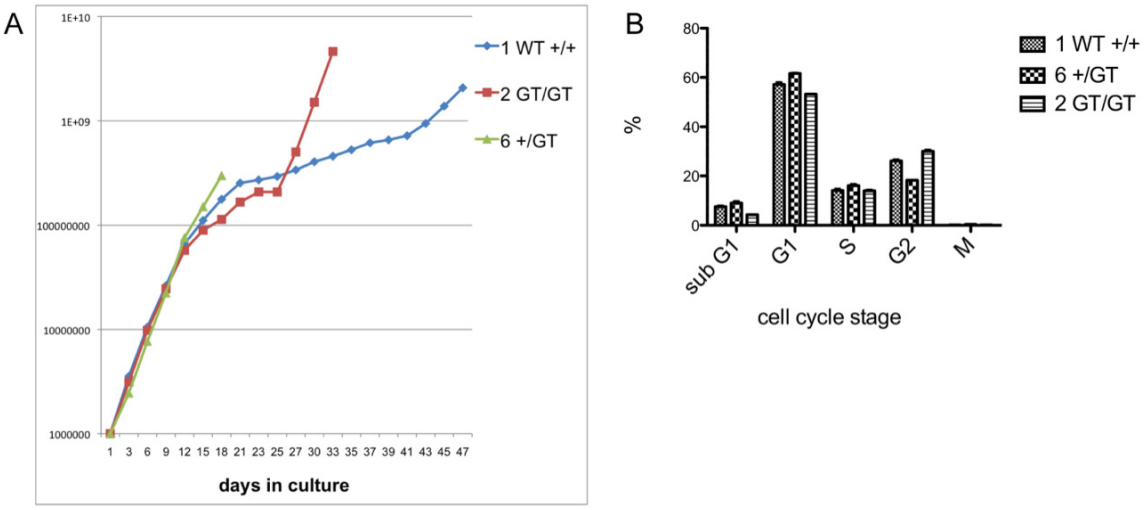

Figure 63 Cep63 MEF growth curve and cell cycle analysis
(A) Provided by Dr Stracker: Growth curve of Cep63 wild type 1 (WT +/+), gene-trap 2 (GT/GT) and heterozygous 6 (+/GT) cell lines. Cells were counted in triplicate every 3 days. Cell number (y axis) is plotted on a logarithmic scale. (B) Cell cycle stage analysis carried out by FACS of propidium iodide stained fixed cells in order to measure DNA content. FACS analyses carried out in duplicate. Graph shows the mean and standard deviation.

Immunofluorescence analysis of wild type (1) and gene-trap (2) cell lines from the fourth passage was carried out to determine the Cep63 protein status (figure 64). Anti-Cep63 49AP antibody stained the centrosome specifically in wild type cells, but not gene-trap homozygous cells. Co-staining was carried out with γ-tubulin to determine the position of centrosomes. Cells in all stages of the cell cycle were analysed and no Cep63 was detected at the centrosome in any of the Cep63 gene-trap 2 cells (figure 64). Anti-Cep63 49AP antibody recognised the N-terminal, middle (SMC-like domain) and C-terminal thirds of the human Cep63 protein. Although the specificity for the entire length of the mouse Cep63 protein has not been tested, the absence of any Cep63 staining in gene-trap cells led us to a tentative conclusion that there were no Cep63 proteins produced in these cells. Certainly, there was no detectable Cep63 at the centrosome, and no staining was observed elsewhere in the cell.

Absence of Cep63, full length or truncated or alternatively spliced transcripts, was further verified by reverse transcriptase-PCR (RT-PCR) analysis of mRNA from the cell lines using primer pairs covering the length of the Cep63 coding region. No PCR products were observed in the Cep63 gene-trap cell line 2 (figure 65), which indicated that there were no Cep63 transcripts present.

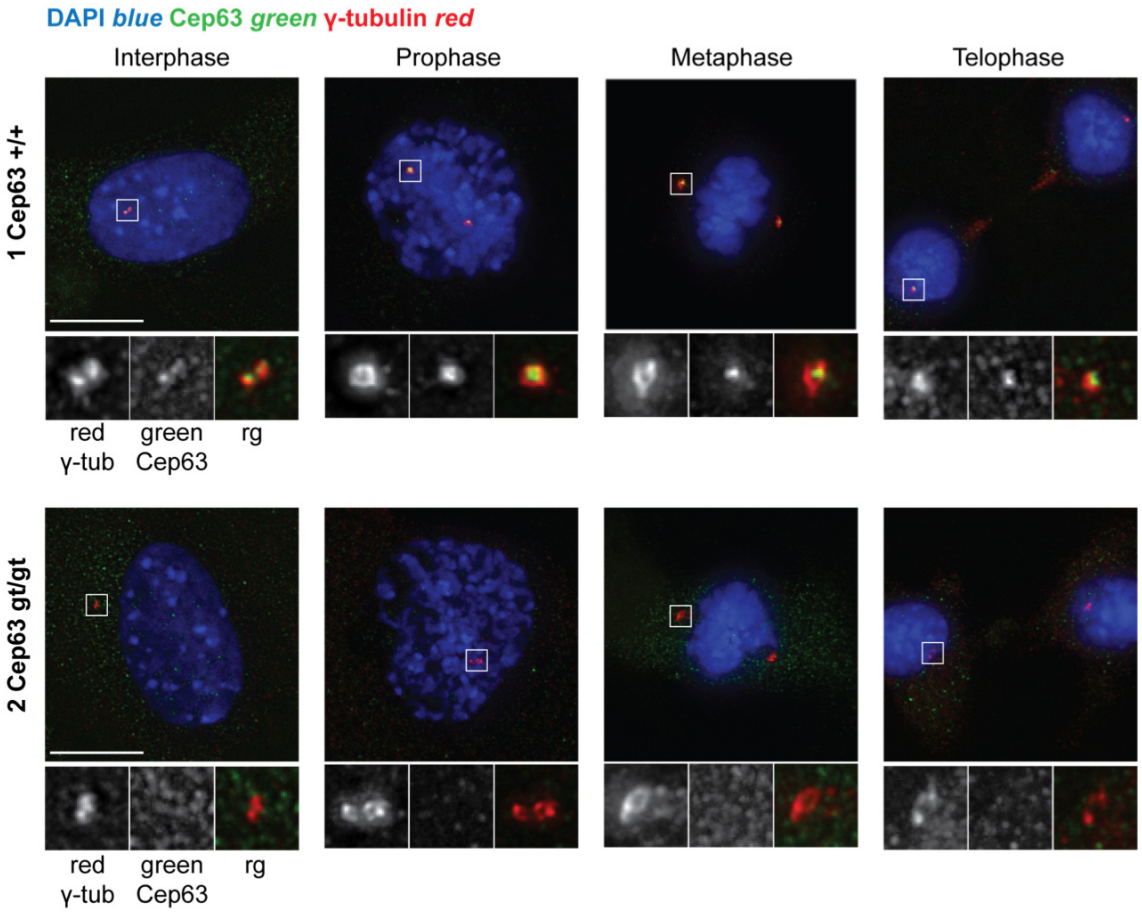

Figure 64 Cep63 gene-trap MEFs lack Cep63 immunofluorescence at the centrosome
Cells from the fourth passage of the Cep63 gt/gt (2) or +/+ (1) cell lines were fixed and stained with anti-Cep63 (green) and γ-tubulin (red) antibodies and DAPI (blue). Cells in interphase, prophase, metaphase and telophase/G1 are shown. Small panels show 3 times enlargements of the boxed areas. Scale bar 10 μm. Images are maximum projections of deconvolved z-sections.

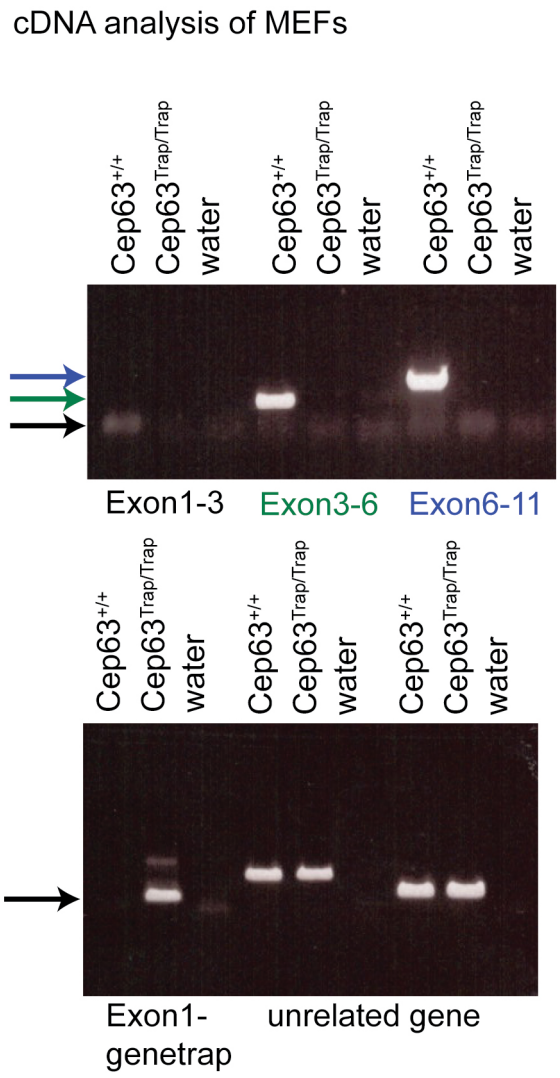

Figure 65 RT-PCR analysis of mRNA from Cep63 gene-trap cell lines
Figure provided by Dr Stracker. RT-PCR analysis of mRNA from MEF cell lines: wild type (+/+) and gene-trap (trap/trap) with primers spanning different regions of the Cep63 coding sequence, as indicated at the bottom of each panel. Cep63 specific primers only produced a product in wild type MEFs. No products were detected in Cep63 gene-trap MEFs. Control reactions (unrelated gene) showed that input mRNA levels were the same for each cell line and that the preparation was proficient for RT-PCR.

5.3 Centriole and centrosome analyses in primary MEFs

Cep63 gene-trap cell lines were analysed further by immunofluorescence in order to determine their centrosome and centriole status. Cep63 RNAi in the human cell line U2OS caused a loss of centrioles, such that over half of mitotic cells contained fewer than the usual 4 centrioles (56% versus 5% in control treated cells, figure 46). This phenotype was stochastic, such that some cells lacking Cep63 were able to duplicate their centrioles in time for the entry into mitosis, while others were not. However, since RNAi did not completely remove Cep63 from these cells, the stochastic nature of the phenotype may have been due to the RNAi technique rather than the function of Cep63 in centriole duplication. Analysis of Cep63 gene-trap MEFs with no detectable Cep63 removed this layer of ambiguity.

Firstly, centrosomes were counted by scoring γ-tubulin foci in all cells in wild type (1, wt/wt) and gene-trap (2, gt/gt) cells from the fourth passage (figure 66). Since FACS analysis showed that these cell lines have very similar cell cycle profiles, it was possible to compare centrosome counts from all cells and deduce that any difference seen would be due to centrosome duplication differences, rather than cell cycle differences. There was clearly a greater number of cells with only one centrosome in cell line 2 (gt/gt), which indicated that there might be a problem with centrosome duplication in these cells (figure 66a). Whereas the number of cells in G1 was roughly equal in wild type and gene-trap cell lines (57% and 53% respectively), the number of cells with only one centrosome was quite different (7% and 21% respectively).

Interestingly, the number of cells with more than 2 γ-tubulin foci was similar between wild type and gene-trap cell lines. The maximum number of γ-tubulin foci throughout the cell cycle should be 2, in theory, since γ-tubulin is a centrosome marker. Thus, Cep63 gene-trap cells can accumulate extra centrosomes, just as wild type cells can. This observation, and the fact that 56% (compared to 67% in wild type) of cells contain 2 centrosomes, indicated that centrosomes without Cep63 were able to duplicate, although duplication efficiency was perturbed.

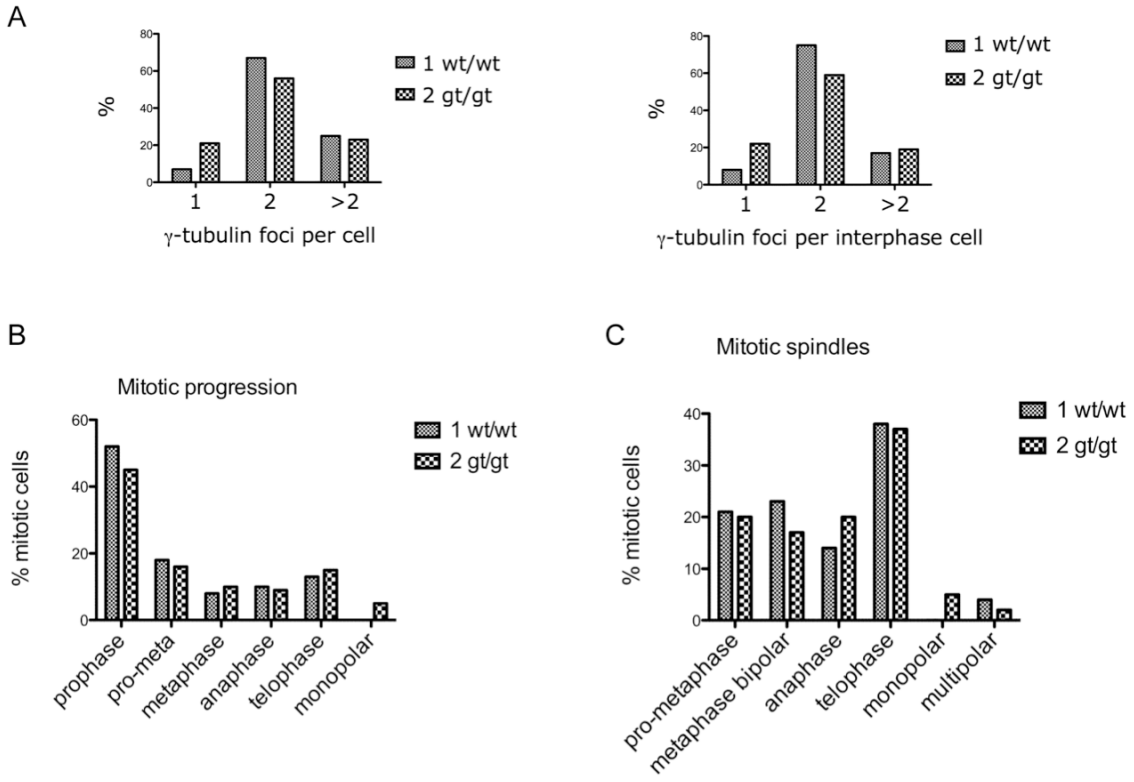

Figure 66 Inefficient centrosome duplication in Cep63 gene-trap MEFs, but normal mitotic progression

(A) Wild type cell line 1 (1 wt/wt) and gene-trap cell line 2 (2 gt/gt) cells from passage 4 were fixed and stained with γ-tubulin antibody. The number of γ-tubulin foci was recorded, n = 250. Graphs show γ-tubulin number in cells from all cell cycle stages (left) or interphase cells only (right). (B) Cell lines 1 and 2 were fixed and stained with γ-tubulin and phospho-histone H3 antibodies to mark centrosomes and mitotic cells, respectively, and DAPI to stain DNA. All phospho-H3 positive cells were counted and categorised into mitotic stages depending on the shape of mitotic chromosomes; n > 160 phospho-H3 positive cells. (C) Cell lines 1 and 2 were fixed and stained with α-tubulin and pericentrin antibodies to mark microtubules and centrosomes, respectively and DAPI to visualise DNA. Cells with mitotic spindles were counted and categorised depending on the shape of the spindle and the mitotic chromosomes; n > 65 cells with mitotic spindles.

Analysis of mitotic progression demonstrated that Cep63 gene-trap cells were able to progress through all stages of mitosis with similar kinetics to wild type cells (figure 66). If there was a block or delay in any stage of the cell cycle, FACS analysis of DNA content would have shown an increase in that cell cycle stage. Since cell cycle analysis by flow cytometry showed that wild type and gene-trap cell lines have a similar profile, this indicated that Cep63 deficiency did not cause a delay or block in any cell cycle phase, including mitosis. However, to analyse this in more detail, the different stages of mitosis were examined in order to identify any potential mitotic processes, e.g. spindle assembly that may be slowed down in Cep63 deficient gene-trap cells. This was not the case as analysis of all mitotic cells, identified by positive phospho-histone H3 Serine 10 staining, showed that the proportion of cells in each mitotic stage was similar between cell lines (figure 66b).

Analysis with α-tubulin immunofluorescence showed that Cep63 deficient cells were able to progress through mitosis and form a proper mitotic spindle (figure 66c). However, the Cep63 gene-trap cell line did show a small percentage of cells with monopolar spindles, with just one centrosome at the pole: 5% of mitotic cells compared with zero in the wild type cell line (figure 66c). Since there was an increase in cells with one centrosome as indicated by γ-tubulin staining and no increase in the proportion of G1 cells (figure 66a and 63b), it follows that some cells contain only one centrosome despite having progressed through S phase.

Further to the γ-tubulin counts in asynchronous cells, γ-tubulin foci in mitotic cells (identified by phospho-histone H3 staining) were examined (figure 67). All stages of mitosis were included in the analysis: γ-tubulin counts were carried out using the cells represented in figure 67b. As expected from the γ-tubulin counts in asynchronous cells (figure 66a), the Cep63 gene-trap cell line contained cells with only one γ-tubulin focus (15% compared to 2% in wild type). Despite this, cells were able to progress through all stages of mitosis (figure 67b), perhaps by forming a second, acentrosomal spindle pole. Both wild type and gene-trap cell lines contained cells with diffuse γ-tubulin foci or extra, smaller γ-tubulin foci in addition to the larger foci at spindle poles. However,

examples of these were more common in Cep63 gene-trap cell line 2 (figure 67b). Since γ-tubulin stains the centrosome and the spindle pole, it was not possible to tell whether the cells with diffuse γ-tubulin foci contained centrosomes or not. In order to determine the centrosome status of these cells, centrin immunofluorescence was carried out to mark the distal end of centrioles and therefore indicate the position of the centrosomes.

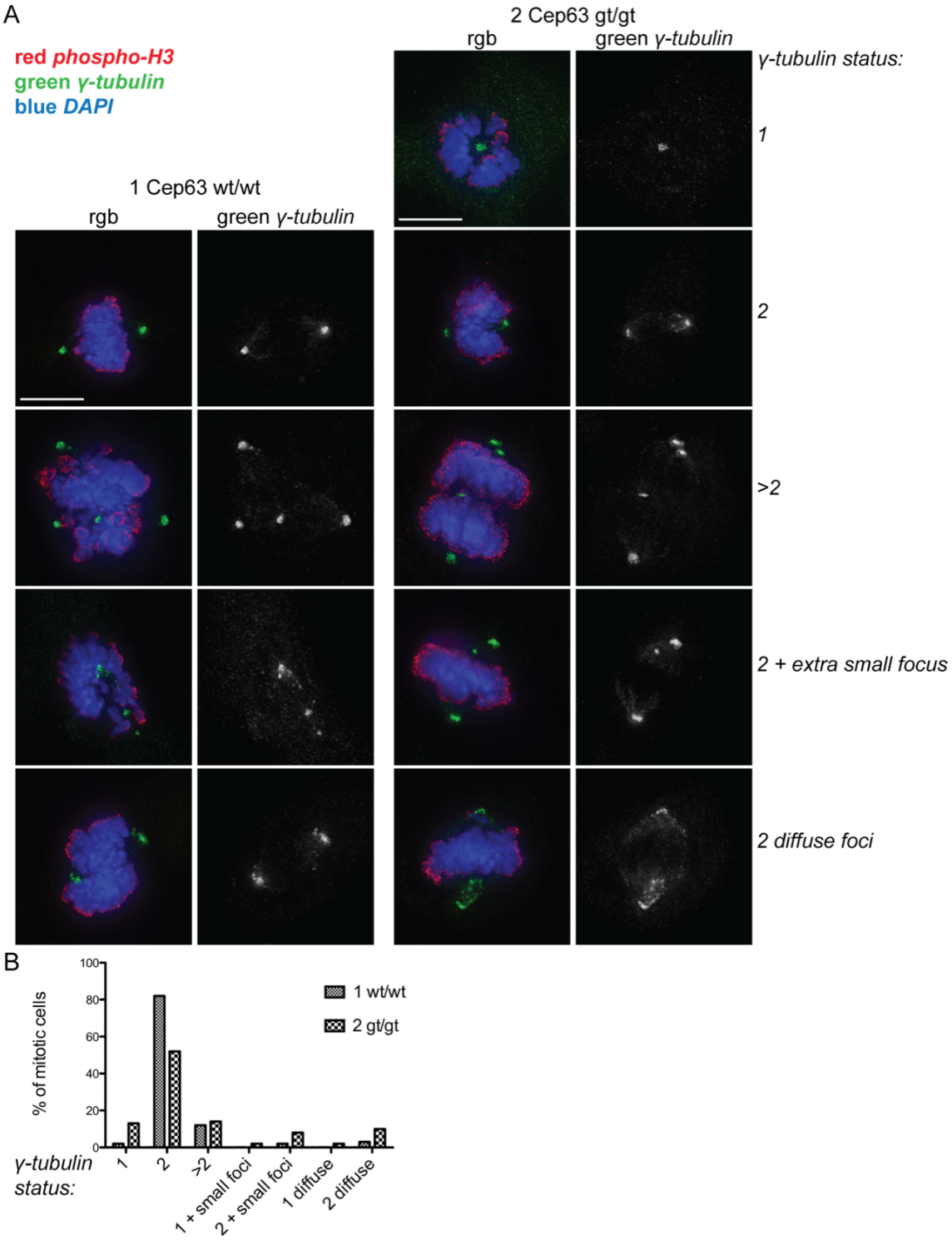

Figure 67 Extra mitotic γ-tubulin foci in Cep63 gene-trap MEFs
(A) Wild type (1 wt/wt) and Cep63 gene-trap (2 gt/gt) cell lines were fixed and stained with γ-tubulin and phospho-histone H3 antibodies to mark centrosomes and mitotic cells, respectively, and DAPI to stain DNA. All phospho-H3 positive cells were analysed. Images show examples of γ-tubulin foci appearance in wild type and gene-trap cells. Images are maximum projections of deconvolved z-sections. Scale bar 10 µm. (B) Quantification of the categories of γ-tubulin focus illustrated in A; n >160.

Immunofluorescence with γ-tubulin and Centrin 2 antibodies was performed to identify centrosomes and centrioles respectively (figure 68). Centrin 2 staining was variable in wild type cells, such that some mitotic cells contained 4 very clear centrin foci with little background, while others contained high levels of Centrin 2 staining in multiple foci all over the cell. Centrin 2 immunofluorescence was also variable between different samples from the same cell line. So, for each sample, cells were counted from a single coverslip all of which were stained at the same time. Centrin 2 analysis of mitotic cells indicated that Cep63 gene-trap cells contained fewer than the expected 4 centrioles: 45% of gene-trap cells contained less than 4 centrioles compared to 17% of wild type cells. There was a high number of wild type cells with 3 centrioles (17%), which might have been due to there only being 3 centrioles, or due to staining limitations of Centrin 2 immunofluorescence. However, while numbers of cells with only 3 centrioles was similar in wild type and gene-trap cell lines, cells with less than 3 centrioles were only detected in the gene-trap cell line (30% compared to zero in wild type, figure 68b). Therefore, lack of Cep63 led to inefficiency of centriole duplication in these cultured primary MEFs. While Cep63 must have a role in centriole duplication, it is not required because 47% of Cep63 gene-trap cells are able to duplicate their centrioles and centrosomes in time for entry into mitosis (compared with 83% in wild type).

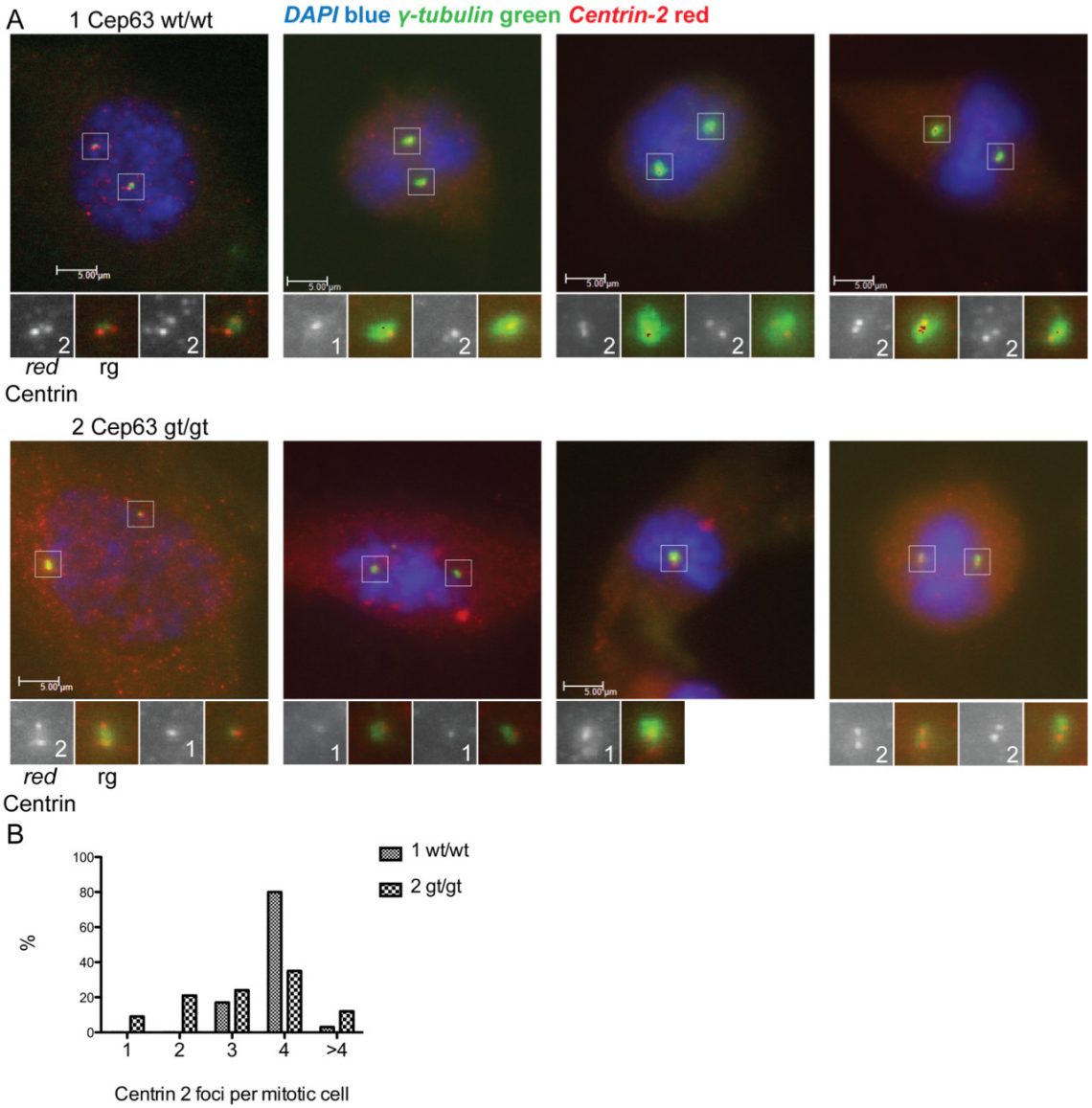

Figure 68 Centriole duplication defect in Cep63 gene-trap MEFs
Wild type (1 wt/wt) and Cep63 gene-trap (2 gt/gt) cell lines were fixed and stained with γ-tubulin (green) and Centrin 2 (red) antibodies to mark centrosomes and centrioles, respectively, and DAPI to stain DNA. Mitotic cells were scored for centrin foci number. (A) Images show examples of cells with different numbers of centrin foci in wild type and gene-trap cells. The number of centrin foci is indicated in the small panels, which are 3 times enlargements of the boxed regions. Scale bars are 5 μm. Images are maximum projections of z-sections without deconvolution. (B) Quantification of cells illustrated in A; n >30 mitotic cells.

Dr Jens Luders (IRB, Barcelona) carried out additional counts using γ-tubulin and a different centrin antibody that was a gift to his lab (figure 69). All cells were counted, regardless of cell cycle stage and, in concurrence with my analysis; Cep63 gene-trap cells had fewer centrioles. As daughter cells are born, they should contain two centrioles (two centrin foci), then during centriole duplication in G1 and through S phase, 2 new centrioles are formed. Therefore cells should contain either 2 or 4 centrioles. There are fewer Cep63 gene-trap cells with 4 centrioles (12%) compared to wild type (32%) and a concomitant increase in cells containing less than 2 centrioles (19% compared to 2% in wild type cells). The number of cells containing 3 centrioles was very similar between the two cell lines, but the arrangement of these centrioles differed, i.e. whether there was a pair of centrin foci plus a single one (2+1) or whether there were three single foci (1+1+1) (figure 69b).

Data presented in categories of γ-tubulin and centrin foci arrangement showed that there was a decrease in 'normal' arrangements (blue arrows, figure 69b). Normal γ-tubulin and centrin arrangements include 1 γ-tubulin to 2 centrin foci in early G1; 2:2 just before new centrioles are formed; then 2:4 through G2 and mitosis when cells have fully duplicated centrioles and centrosomes, as illustrated in figure 69c. The γ-tubulin and centrin arrangements were heterogeneous in both cell lines, possibly due to some centrioles not being detected by centrin immunofluorescence and the presence of non-specific background staining. However, the Cep63 gene-trap cell line clearly showed more examples of abnormal arrangements including increased incidence of cells with one centrin foci per γ-tubulin focus (76% compared to 56% in wild type).

Interestingly, this analysis also showed that Cep63 gene-trap cells show a higher incidence of abnormal γ-tubulin foci number, as seen previously (figure 66-68). Cells should contain one or two γ-tubulin foci depending on cell cycle stage, yet Cep63 gene-trap cells contained cells with no γ-tubulin focus (4% compared to zero in wild type cells) and cells with greater than 2 γ-tubulin foci (20% compared to 12% in wt). Also, there were more Cep63 gt cells with only one γ-tubulin focus (17% compared to 4% in wt).

These data support the conclusion that primary MEFs lacking Cep63 were unable to duplicate centrioles in an efficient and timely manner such that some cells enter mitosis with fewer than 4 centrioles and a proportion of these, with only one centrosome. Despite the lack of centrioles and, in some cases, centrosomes, Cep63 deficient cells were able to progress through all stages of mitosis with no detectable delay. Perhaps the diffuse γ-tubulin foci observed in some mitotic cells were due to the lack of a centrosome at the spindle pole, which would lead to less efficient microtubule focussing. Further to this, Cep63 gene-trap cells displayed heterogeneity in γ-tubulin foci number. Importantly, as illustrated in figure 69b, the extra γ-tubulin foci observed in Cep63 gene-trap cells were not entire centrosomes as the majority only contained one centrin focus. Electron microscopy analysis of Cep63 deficient MEFs would clarify the centriole status of these extra γ-tubulin foci.

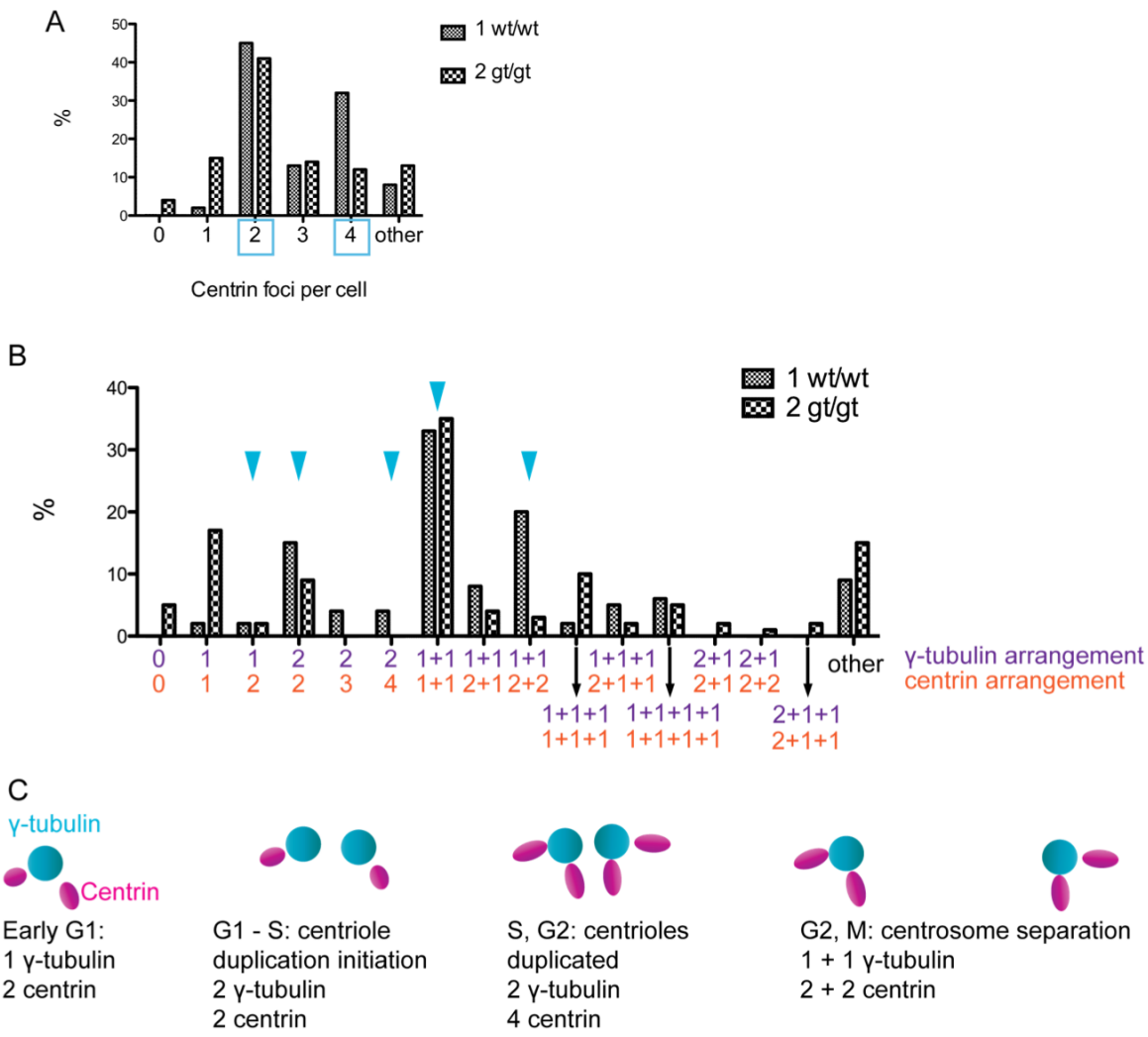

Figure 69 Cep63 gene-trap MEFs show heterogeneity in centriole and centrosome number

Centrin and γ-tubulin arrangement was analysed in wild type (1 wt/wt) and Cep63 gene-trap (2 gt/gt) by Dr Jens Luders (IRB, Barcelona). All cells were counted in an asynchronous population, n >110. (A) Graph shows the total number of centrin foci per cell. (B) Graph shows γ-tubulin and centrin ratio arrangement in the cell 2 indicated 2 foci together, whereas 1+1 indicates two separated foci. Bars marked with blue arrows show 'normal' centrosome arrangements that would be expected throughout the cell cycle. (C) Diagram shows centrin and γ-tubulin arrangement throughout the centrosome duplication cycle. Each of these configurations is marked with a blue arrow in B.

5.4 Functional DNA damage checkpoint in Cep63 gene-trap cells

As described previously, *Xenopus laevis* Cep63 is an ATM/ATR kinase target, which is phosphorylated upon DNA damage induction in *Xenopus* egg extract. Due to the possible implication of the mouse Cep63 orthologue also being involved in DNA damage checkpoint signalling, the competence of Cep63 gene-trap cells to initiate a DNA damage checkpoint induced cell cycle arrest was tested. When asynchronous cell cultures are subjected to DNA damage treatments they initiate a DNA damage signalling cascade via ATM or ATR DNA damage signalling kinases and the cell cycle is halted at the G1/S phase transition, during S phase or in G2. Entry into mitosis is prevented in the presence of DNA damage signalling and therefore, the mitotic index of asynchronous cell cultures subjected to DNA damage treatments is lower than untreated cultures. If cells are deficient in a checkpoint signalling protein, the cell cycle will not be halted and the mitotic index will remain unchanged after DNA damage treatment. This is true for ATM and ATR deficient cells and for deficiencies in other proteins downstream of these kinases (Griffith et al., 2008).

UV irradiation primarily induces an ATR kinase signalling response. γ-irradiation predominantly causes double strand DNA breaks and activates ATM dependent signalling. Therefore, cells defective in ATR signalling show a G2/M checkpoint response after γ-irradiation, but not after UV and *vice versa* for cells defective in ATM signalling (Griffith et al., 2008). The G2/M checkpoint was assayed by counting phospho-histone H3 positive (mitotic) cells by FACS before and after UV or γ-irradiation treatment. Dr Stacker carried out these experiments. Cep63 gene-trap cells showed efficient ATM and ATR-dependent checkpoint signalling (figure 70). The G2/M checkpoint was activated in Cep63 gene-trap cells, as in wild type cells, after both UV and γ-irradiation, as determined by a decrease in mitotic index (figure 70a). Importantly, mitotic index in untreated cells was very similar between wild type and gene-trap cells, which further confirmed that these cells had no problems with the timing of mitosis.

DNA damage signalling proficiency was assayed by immunofluorescence with antibodies that detect activated DNA damage signalling proteins (figure 70b). Histone variant H2AX is a target of the DNA damage signalling pathways and its phosphorylated form (γH2AX) can be detected by immunofluorescence with an antibody that specifically recognises the phosphorylated form of the protein. H2AX is phosphorylated by ATM and ATR checkpoint kinases on regions of chromatin surrounding the DNA lesion (Rogakou et al., 1998, Stiff et al., 2004). First of all, γ-H2AX immunofluorescence showed that there was no activation of DNA damage signalling cascades in untreated cells, but as in wild type, Cep63 gene-trap cells were able to respond to DNA damage in the form of hydroxyurea (HU) treatment, as determined by detection of γ-H2AX foci in the nucleus. 53BP1 is another marker of DNA damage, which is also recruited to the site of the DNA lesion (Huyen et al., 2004). Using an anti-53BP1 antibody, HU induced 53BP1 foci were observed in Cep63 gene-trap and wild type cells (not shown). In conclusion, Cep63 gene-trap cells showed no deficiency in DNA damage checkpoint signalling and subsequent cell cycle arrest.

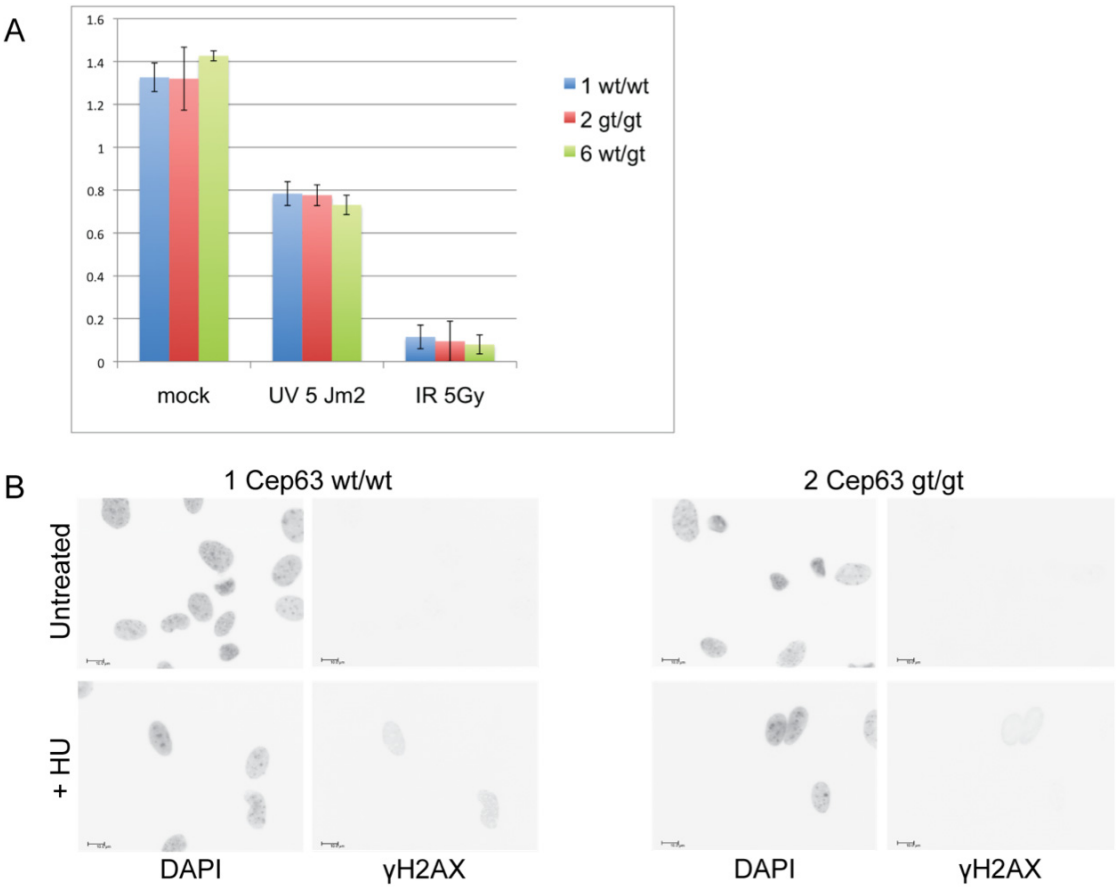

Figure 70 DNA damage checkpoint signalling in Cep63 gene-trap MEFs
(A) Experiment carried out by Dr Stacker. Cells were untreated (mock) or irradiated with 5 Jm^{-2} UV or 5 Gy γ-irradiation then incubated for 1 hour before collection and analysis of mitotic index by FACS of phospho-histone H3 positive cells. The y-axis shows % of mitotic cells. Wild type (1 wt/wt), Cep63 gene-trap homozygous (2 gt/gt) and heterozygous (6 wt/gt) MEFs were used. Experiments were carried out in triplicate; error bars show the standard deviation. (B) MEFs were treated with 4 mM HU for 1 hour then fixed for immunofluorescence with anti-γ-H2AX. Blue (DAPI) and green (γ-H2AX) channels are shown in black and white and inverted. Cells were co-stained with DAPI to visualise DNA. Images show one section without deconvolution. Scale bar 10 μm.

5.5 Centriole analysis of Cep63 gene-trap 3T3 transformed MEFs

Centriole analysis in primary MEFs was limited by the number of primary cells available and their limited growth capacity. These experiments were continued by analysing the resulting MEFs after spontaneous immortalisation by the 3T3 protocol.

Cep63 protein levels were examined by immunofluorescence in case there was any kind of mutation in the Cep63 gene-trap cells that allowed Cep63 to be expressed either in part or in full. Cep63 localised to the centrosome throughout the cell cycle in wild type cells, but there was no detectable Cep63 in the Cep63 gene-trap (gt) 3T3 cells (3T3-2, figure 71).

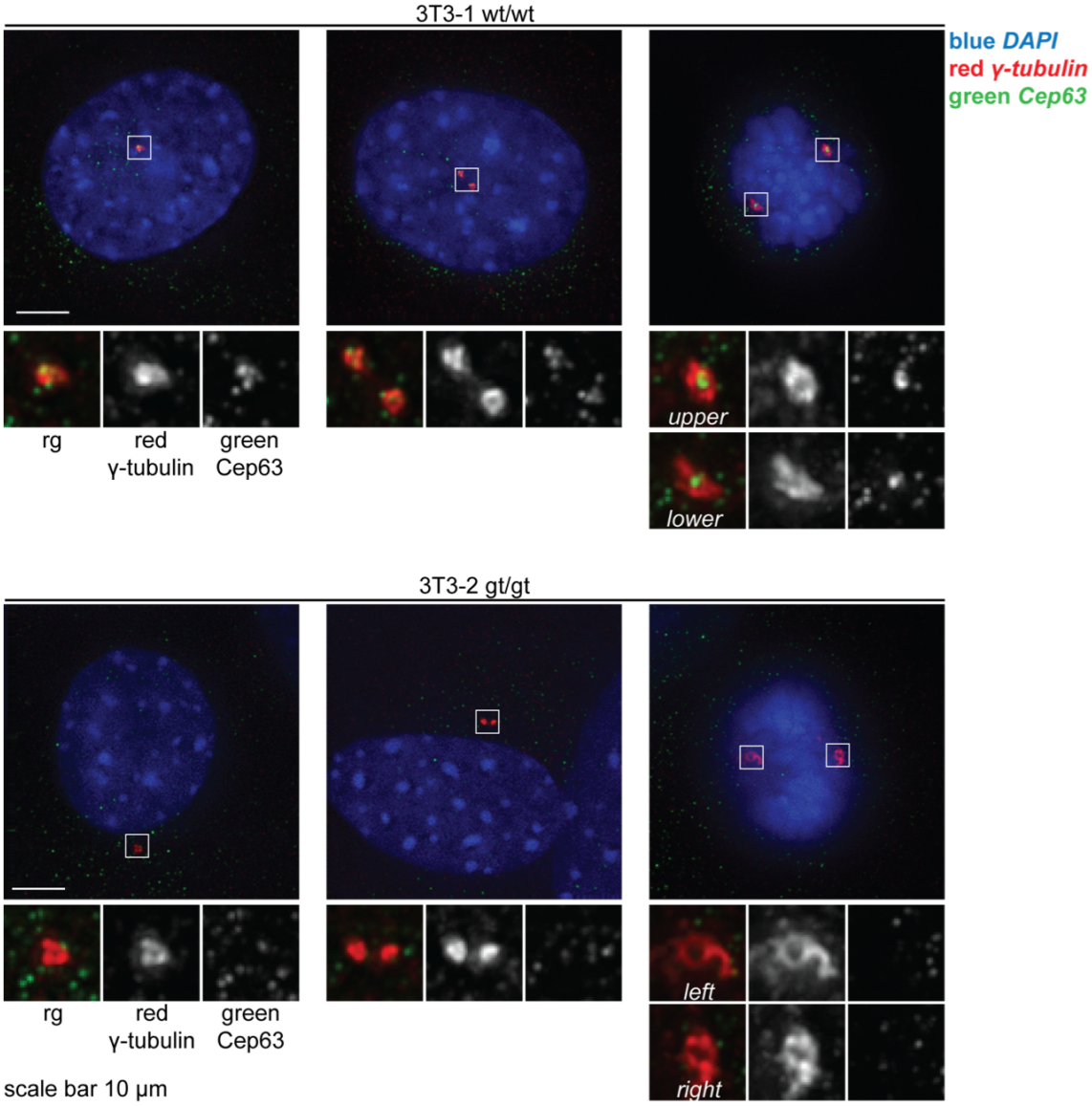

Figure 71 Cep63 immunofluorescence in transformed MEF cell lines
Wild type (3T3-1 wt/wt) and Cep63 gene-trap (3T3-2 gt/gt) immortalised MEFs were fixed and stained with anti-Cep63 49AP (green) and γ-tubulin (red) antibodies and DAPI to visualise DNA. Cells in G1, G2 and mitosis are shown (left to right). Small panels show enlargements of the boxed regions (centrosomes). Images are maximum projections of deconvolved z-sections. Scale bar 10 µm. 3T3-2 Cep63 gt/gt cells show no Cep63 staining at the centrosome.

Next, centriole number in the transformed MEFs cells was analysed using a Centrin 3 antibody to mark centrioles and a pericentrin antibody to mark centrosomes and spindle poles. Only mitotic cells were scored in order to make a direct comparison of centriole number from all cells and to reduce centrin staining ambiguity seen in interphase cells. Centrin staining was much clearer in mitotic cells compared to interphase because interphase nuclei stained very strongly with centrin antibodies, but upon nuclear envelope breakdown the staining was less intense.

As observed in the analysis of mitotic primary MEFs (figure 68), Cep63 gene-trap transformed MEFs (3T3-2) entered mitosis with fewer than the expected 4 centrioles (figure 72). There were fewer gene-trap cells with 4 centrioles (3T3-2) than wild type (3T3-1): only 45% of 3T3-2 cells in mitosis contained 4 centrioles, compared with 75% of 3T3-1 (figure 72b). There was a concomitant increase in cells with less than 4 centrioles, which contained a range of centriole numbers and arrangements (figure 72c). Overall, there was an increase in cells with one unpaired centrin focus per spindle pole (24% of gt 3T3-2 compared to 10% of wt 3T3-1) and cells with no centrin foci at the spindle pole (26% of gt 3T3-2, 12% of wt 3T3-1, figure 72d). Although wild type 3T3-1 cells did contain some spindle poles with only one detectable centrin focus, the opposite spindle pole in these cells contained a pair of centrin foci (figure 72c). Mitotic cells with fewer than 3 centrioles were much more common in 3T3-2 cell samples with 30% of cells with less than 3 centrioles compared to 5% of wild type 3T3-1 cells.

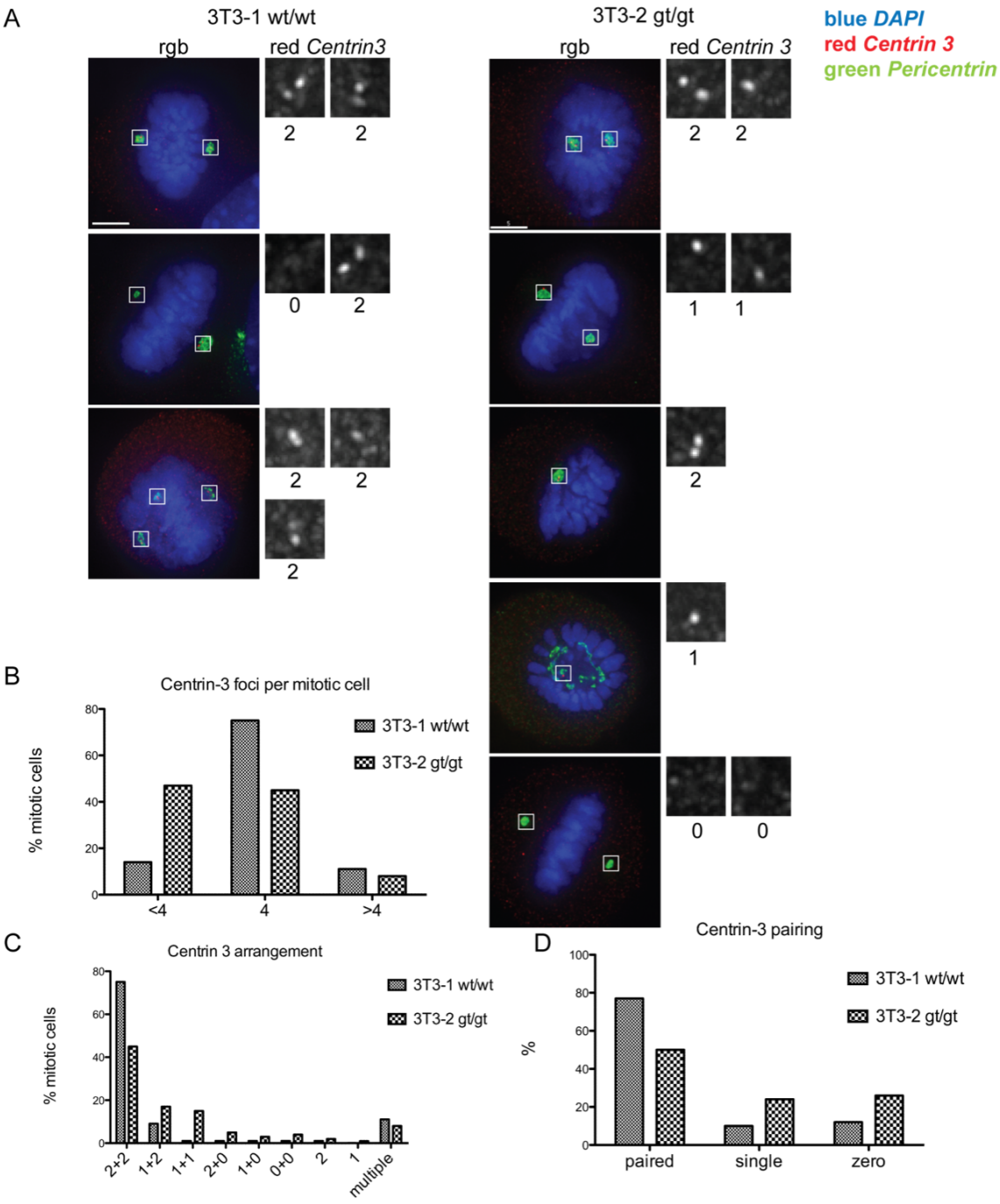

Figure 72 Reduced centriole numbers in Cep63 gene-trap 3T3 MEFs
(A) Wild type (3T3-1) and Cep63 gene-trap (3T3-2) transformed cells were incubated for 7 hours with 100 ng/µl nocodazole to arrest cells in mitosis, then released into medium containing 10 µg/ml MG132 to prevent mitotic exit for 1 hour. Cells were fixed and stained with anti-Centrin 3 (red) and pericentrin (green) antibodies and DAPI (blue). Images are maximum projections of deconvolved z-sections. Right hand panels show 3 times enlargements of the boxed regions and the number of Centrin 3 foci is indicated below. Scale bar 5 µm. (B) Total number of Centrin 3 foci per cell. (C) Mitotic cells were categorised depending on Centrin 3 arrangement. (D) Number of paired, single or no Centrin 3 foci per spindle pole. N = 100 mitotic cells.

Following the RNAi studies and YFP-Cep63 truncation protein overexpression in human cell lines (chapter 4), which showed that the localisation of one of the Cep63-Cep152 binding partners to the centrosome was reduced in the absence of the other, an analysis of Cep152 localisation to the centrosome in transformed MEF cell lines was conducted.

It was not possible to visualise endogenous mouse Cep152 by immunofluorescence or Western blot, as the antibody used to detect the human protein gave no signal by either method. This antibody was raised against a peptide from the human protein and was probably unable to recognise the mouse orthologue. Consequently, transformed MEF cell lines were transfected with the human GFP-Cep152 expression vector used for previous experiments in human cell lines (figure 73a). Experiments with GFP-Cep63 transfection were carried out simultaneously, for comparison (73b). After 48 hours, cells were collected and stained with γ-tubulin antibody for identification of the centrosome by immunofluorescence; and centrosomes were scored for the presence of GFP fluorescence. Importantly, all three cell lines used were able to express GFP-Cep152 and GFP-Cep63. Cell line SP-2 was an additional transformed cell line generated from embryo 2 (gt/gt) primary MEFs by spontaneous transformation of cells left at confluence for 2.5 weeks. At the time of this experiment the wild type (1) MEFs had not yet transformed by this method. GFP-Cep152 localised to the centrosome in wild type cells, but none was detected at centrosomes in Cep63 gene-trap cells (3T3-2, SP-2, figure 73a). Interestingly, all three cell lines were able to incorporate GFP-Cep63 into their centrosomes, although Cep63 gene-trap cell lines (3T3-2 and SP-2) showed reduced efficiency. Perhaps this was due to wild type centrosomes already containing some Cep63, and consequently some Cep152, which would make localisation of new GFP-Cep63 more efficient, according to previous data from human cell RNAi experiments Cep152 also mediates the centrosomal localisation of Cep63 (figure 49). This data provides additional support to RNAi experiments, which showed the inter-dependency of Cep63 and Cep152 for their centrosome localisation.

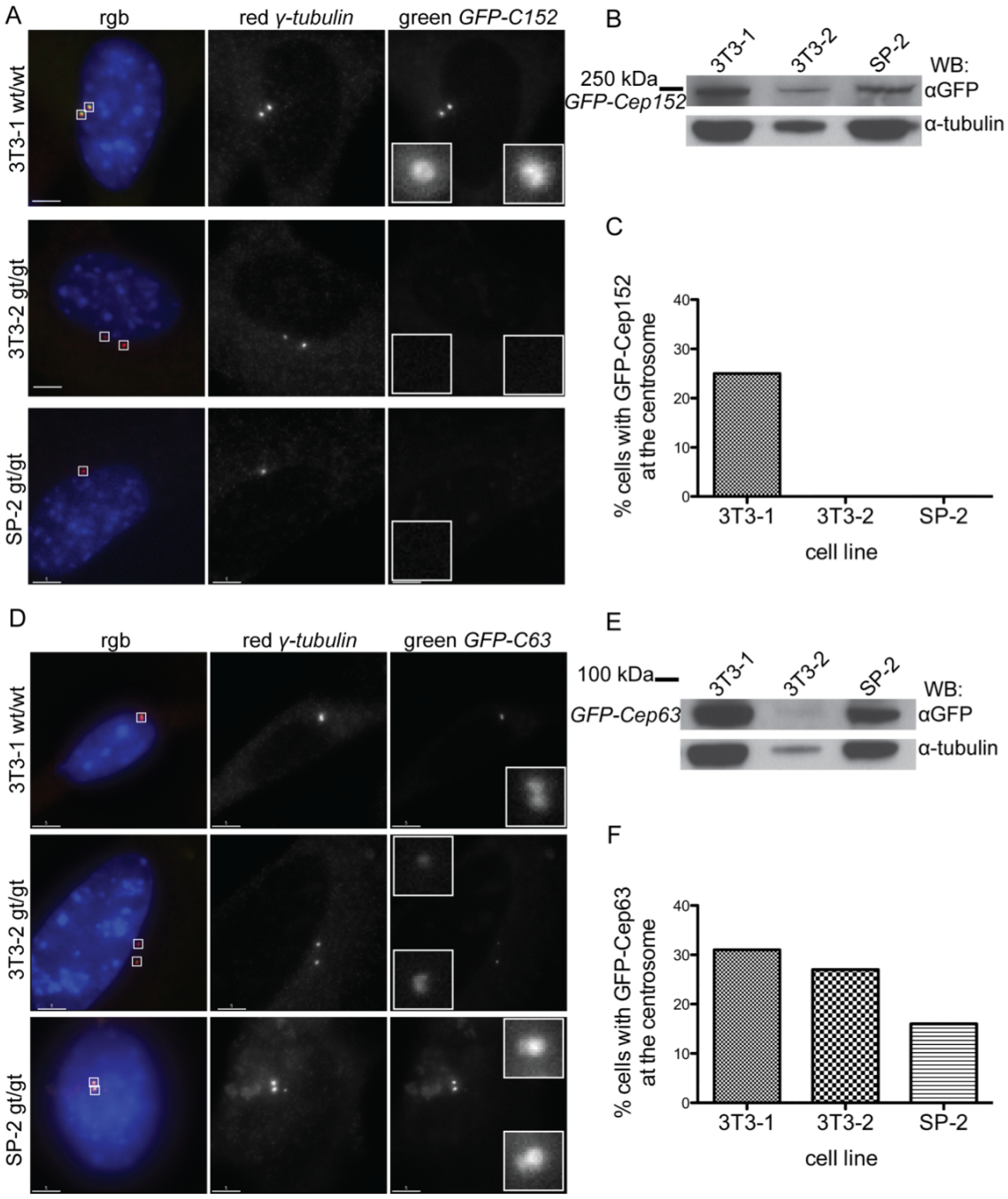

Figure 73 Cep63 is required for GFP-Cep152 incorporation into centrosomes
(A) Transformed MEF cell lines (3T3-1 (wt/wt), 3T3-2 (gt/gt) and SP-2 (gt/gt)) were transfected with human GFP-Cep152 and immunofluorescence was carried out with γ-tubulin antibody (red) to mark centrosomes and DAPI (blue). GFP-Cep152 was detected by direct fluorescence (green). Western blot of whole cell lysates with anti-GFP antibody showed that GFP-Cep152 was expressed in all cell lines, the α-tubulin Western blot indicates the amount of cell lysate loaded. Graph shows the percentage of cells with GFP fluorescence at the centrosome. (B) The same experiment was carried out using GFP-Cep63. Small panels show 3 times enlargement of the GFP signal at centrosomes indicated by boxes in the rgb image. Images are maximum projections of deconvolved z-sections. N = 100 cells per sample. Scale bars 5 μm.

5.6 Chapter 5 conclusions

In conclusion to the work carried out using Cep63 gene-trap MEFs: Cep63 is involved in the regulation of centriole duplication, but is not absolutely required for duplication to occur. Cep63 gene-trap cells did not show any Cep63 protein expression, as determined by immunofluorescence of cells and RT-PCR analysis of mRNA. These Cep63-deficient cells were able to grow at the same rate as a wild type littermate control cell line. The Cep63 gt/gt studied here showed premature spontaneous immortalisation under two different growth conditions, which is indicative of genome instability. However, this phenotype could be due to differential loss of tumour suppressor functions rather than directly due to loss of Cep63. This remains to be fully investigated. Cep63 deficient and wild type MEFs cells showed very similar cell cycle progression. Furthermore, Cep63 deficient cells were able to elicit a DNA damage signalling response and cell cycle arrest to the same extent as wild type cells in response to DNA damage.

Analysis of centriole and centrosome number showed that Cep63 deficiency resulted in reduced centriole number and aberrant centrosome number, as determined by centrin and γ-tubulin staining, respectively. Approximately half of the Cep63 deficient MEFs entered mitosis with fewer than 4 centrioles and half were able to duplicate their centrioles in time for mitotic entry. A smaller proportion of these cells entered mitosis with only one or two detectable centrioles. The stochastic nature of this phenotype led to the conclusion that Cep63 is not absolutely required for centriole duplication, but it is required for fully efficient duplication that is tightly coordinated with the cell cycle to ensure faithful inheritance of 2 centrioles per daughter cell. Data presented in this chapter are in accordance with data presented in chapter 4. Both studies in Cep63 deficient MEFs and Cep63 depleted human cell lines showed that Cep63 has a role in centriole duplication, perhaps via Cep152 binding and recruitment to the centrosome.

Further to the analysis of cellular behaviour, the Cep63 gt/gt embryo number 2 showed defects in the head upon collection for MEF generation at embryonic day 14.5. Another

litter of Cep63 gene-trap embryos has recently been collected and one of two homozygous gene-trap homozygotes also had a structural defect in the head area, which is reminiscent of exencephaly, a defect in neural tube closure leading to growth of neural tissue outside of the skull (figure 74). This intriguing phenotype is discussed further in chapter 6.

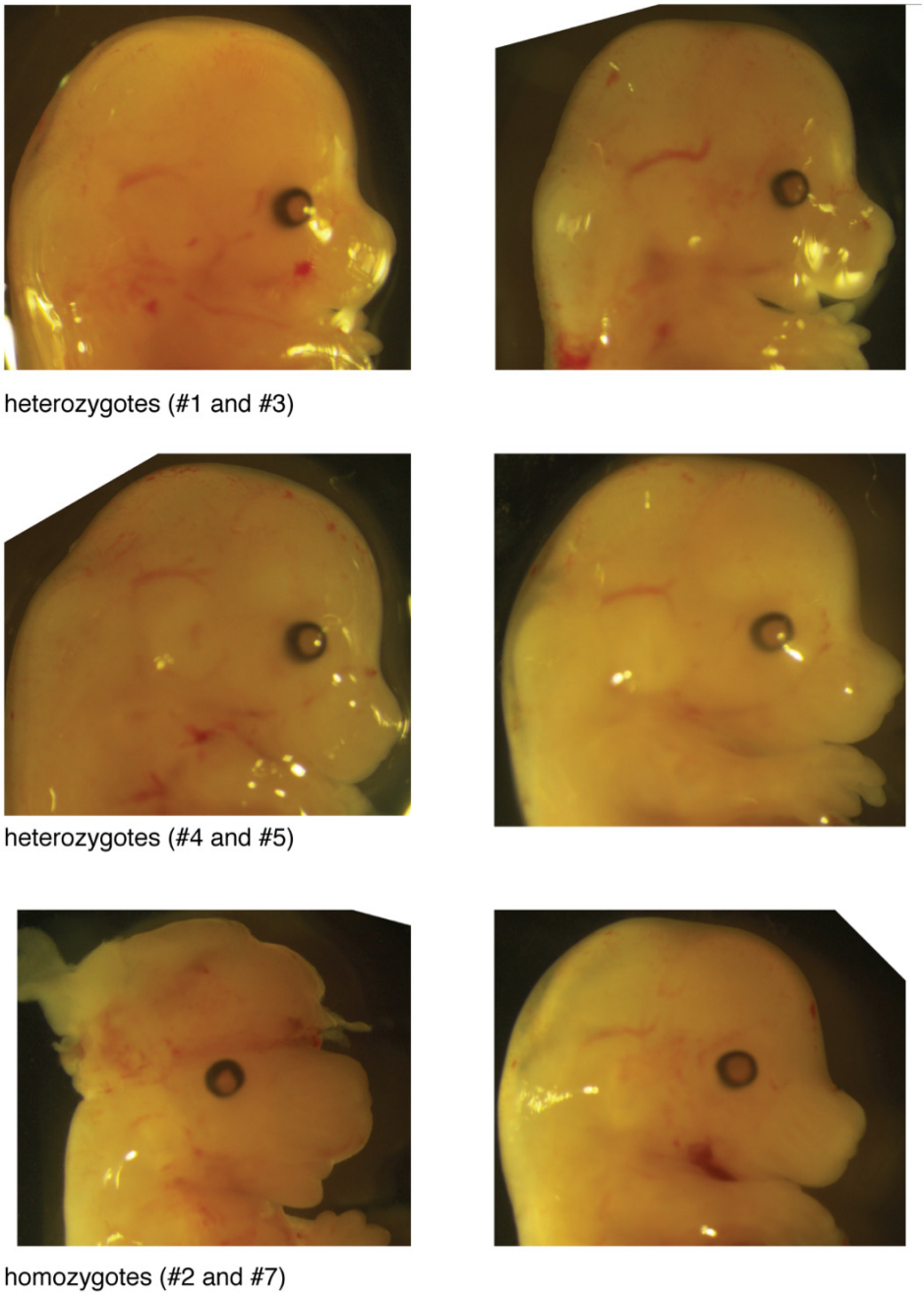

Figure 74 Cep63 gene-trap embryos, litter 2.
This litter of embryos was collected at embryonic day 14.5, pictures were provided by Dr Stracker. One of the gene-trap homozygotes shows a structural defect of the head (bottom left). Heterozygote controls are shown, there were no wild type embryos in this litter. Pictures from litter 1 were not available.

Chapter 6. Discussion

The aim of this study was to determine the function of human Cep63. This thesis provides evidence for the following:

- Cep63 localises to the PCM throughout the cell cycle.
- Characterisation of Cep63 directed antibody, which specifically stains Cep63 by immunofluorescence.
- The interaction between Cep63 and Cep152.
- Cep63 is required for efficient centriole duplication.
- Cep63 and Cep152 centrosomal localisation is inter-dependent.
- The role of Cep63 in centriole duplication is conserved in mice.

6.1 Cep63 in centriole duplication

Cep63 interacts with Cep152, a PCM component required for centriole duplication due to its role in recruiting CPAP and facilitating the recruitment of Plk4 to the centrosome. Cep63 colocalises precisely with both Cep152 and Plk4, to the PCM surrounding the proximal end of the centriole wall, which is the area where daughter centriole formation is initiated. Without Cep63, Cep152 fails to localise to the centrosome and centriole duplication does not occur efficiently. Although Cep63 deficient cells were able to duplicate their centrioles, around half of the population entered mitosis with less than 4 centrioles, and a smaller proportion with only one centrosome. As Cep63 is required for localisation of Cep152 to the centrosome, Cep152 is also required for efficient localisation of Cep63 to the centrosome. Thus, it is likely that the two proteins, Cep63 and Cep152, interact with each other upon translation in the cytoplasm and move to the centrosome together where the interface of the combined protein complex is important for stable maintenance of both proteins in the PCM. The role of Cep63 in centriole duplication is therefore likely to be mediated through its interaction with Cep152 and, in turn, Cep152-mediated recruitment of Plk4 and CPAP (figure 75).

However, Cep152 is absolutely required for centriole duplication whereas Cep63 deficient cells show a stochastic phenotype. The root of this difference in phenotypes is likely due to alternative recruitment of Plk4 and CPAP to the centrosome, via Cep63 independent recruitment of Cep152 to the PCM. The Cep63-Cep152 interaction is clearly required for efficient recruitment of Cep152 to the centrosome, but perhaps Cep152 localisation to the centrosome can occur via both Cep63-dependent and Cep63-independent pathways. Precise centrosomal levels of Plk4 and CPAP are required for centriole duplication: too much of either lead to centriole reduplication or increase in centriole length, respectively (Kleylein-Sohn et al., 2007, Kohlmaier et al., 2009, Schmidt et al., 2009). Conversely, depletion of either Plk4 or CPAP, or their recruitment factor, Cep152, leads to inhibition of centriole duplication (Habedanck et al., 2005, Tang et al., 2009, Hatch et al., 2010a, Cizmecioglu et al., 2010). Cep63 depletion impairs Cep152 localisation to the centrosome and thus the critical threshold level of these essential duplication components may not always be reached. Perhaps centrosome recruitment of these proteins is slower in the absence of Cep63 and consequently cells that spend longer in G1 and S phase may be able to reach the critical level in time for duplication of both centrioles before entry into mitosis, whereas cells that progress more quickly will contain one or both centrioles that do not accumulate enough Plk4 and CPAP in order to duplicate. One could imagine that in cells where one centriole is able to duplicate, but not the other, it would be the grandmother centriole (the mother in the previous cell cycle) that would be able to duplicate due to it having more PCM at an earlier stage in the cell cycle.

Although evidence points to a regulatory role for Cep63 in centriole duplication as described above, an additional role for Cep63 in centriole duplication is not ruled out. Interestingly, Loffler and colleagues have recently shown that the N-terminal 209 amino acids were sufficient to drive centrosome reduplication (Loffler et al., 2011), which confirms that Cep63 is a positive regulator of centrosome duplication and shows that it may have an additional role in centriole duplication other than recruitment of Cep152 to the centrosome, as this region is not able to bind Cep152. Perhaps Cep63 acts as a scaffold component of the PCM and regulates the binding of several centriole duplication factors, including Cep152. It is a possibility that Cep152 functions alone in

the recruitment and maintenance of CPAP and Plk4 at the centrosome, but the Cep152-Cep63 complex is important for other regulatory processes. If this was the situation, centriole duplication would not be possible in Cep152 depleted cells due to loss of centrosomal Plk4 and CPAP, and loss of Cep63 would impinge on the regulation of centriole duplication via an unknown pathway, but CPAP and Plk4 recruitment would not be affected and centriole duplication would still be able to occur, albeit at reduced efficiency.

In order to test these hypotheses it will be important to assess the ability of Plk4 and CPAP to localise to the centrosome in the absence of Cep63. Furthermore, generation of a non-rabbit Cep63 or Cep152 specific antibody could be used to simultaneously monitor Cep63 and Cep152 levels at the same centrosome. Additionally, an antibody that recognises the mouse Cep152 orthologue will be important for studying endogenous Cep152 in Cep63 gene-trap MEFs. Detailed analysis with a series of different centriole antibodies will shed light on the duplication defect in Cep63 depleted cells. Is Sas-6 recruited to form the cartwheel structure; are proteins of the central tube recruited; is CPAP recruited? This type of analysis would help determine the point at which Cep63 plays a regulatory role in centriole duplication. From evidence described so far, the prediction for Cep63 would be that it works with Cep152 to recruit Plk4 and CPAP and is therefore required for initiation of procentriole formation, beginning with recruitment of Sas-6, and at a later stage in centriole elongation (recruitment of CPAP). Thus the expected observed phenotype would be that centrosomes in G2/M Cep63 deficient cells that have only one centrin focus have only one centriole and no visible procentriole (Sas-6 negative). Correlative EM to visualise centriole structure in cells depleted of Cep63 would also be useful for determining the stage at which duplication is prevented.

The work presented in this thesis adds another player to the field of centriole duplication. Cep63 has not previously been described as a regulator of centriole duplication and the evidence that it provides an additional layer of regulation in vertebrates, where Cep63 orthologues are present, may lead to further understanding of

the evolutionary changes in the regulation of this process. Despite the conservation of centriole structure, there is quite some variety in centriole protein sequence (Carvalho-Santos et al., 2010). Sas-6, Cep135 and CPAP comprise a universally conserved module that defines centriole architecture. However, other proteins essential for regulation of centriole duplication are not well conserved including Plk4, for which there is an orthologue in flies, but not in worms, as determined by sequence or structural similarity (Carvalho-Santos et al., 2010). Furthermore, although Plk4 is conserved between humans and flies there is a functional difference between the orthologues reflected by the inability of one to cause centriole reduplication in cells from the other species (Carvalho-Santos et al., 2010). This example of divergence in centriole duplication between flies and humans may be linked to the presence of Cep63 in humans, but not flies. In the least, it provides evidence that although the structure of centrioles and regulation of centriole biogenesis are highly conserved, there are emerging differences in the molecular mechanisms of centriole duplication regulation. The main players may still have their role, but additional layers of regulation have been added. An interesting line of investigation will be to determine the capabilities that have been acquired by the addition of these regulatory controls. Study of Cep63 will further our understanding of the regulation of centriole duplication when compared across different vertebrate species and in comparison to those species lacking Cep63. Fundamental to these future studies will be the study of Cep63 at the level of the whole organism. Cep63 may offer an additional layer of regulation for centriole duplication that is important for a particular tissue or developmental process specific to vertebrates.

A Cep63 deficient mouse would be an extremely useful model for the study of centriole duplication deficiencies since mice null for other essential centriole regulatory proteins are embryonic lethal, for example, Plk4 mutant homozygotes (Harris et al., 2011).

6.2 Cep63 and cell cycle control

Loffler and colleagues propose a role for Cep63 in mitotic entry via recruitment of Cdk1 to the centrosome (Loffler et al., 2011). In this study, Loffler and colleagues show that depletion of Cep63 in U2OS cells by RNAi lead to an increase in polyploid cells (11% compared to 3.5% control siRNA) (Loffler et al., 2011). This phenotype was observed with two other siRNAs to a lesser extent (6.6% and 4.38% compared to 2.48% with control siRNA). The phenotype was inferred to be specific to Cep63 due to the repeated observations with different siRNAs targeting Cep63, but no complementation experiment was carried out. The authors conclude that polyploidisation occurs due to mitotic skipping, which is the inability of cells to enter mitosis followed by another round of DNA replication. Indeed, upon Cep63 RNAi centrosomal levels of Cdk1 are reduced (Loffler et al., 2011). Additionally, a small proportion of Cdk1 interacts with GFP-Cep63. Thus, Cep63 plays a role in regulation of mitotic entry at the centrosome by ensuring the centrosomal localisation of Cdk1. However, this phenotype was not observed with the three siRNAs used in this thesis, two of which successfully depleted Cep63 from the centrosome. One of these siRNAs caused an increase in the percentage of cells with 4N DNA content, but this was likely off target (described in 4.5). However, polyploid cells were not observed by FACS analysis. Furthermore, Cep63 gene-trap primary MEFs did not show signs mitotic skipping or polyploidisation. It will be important to look carefully at the efficiency of the G2 to M transition and the efficiency of the G2/M checkpoint in additional Cep63 deficient MEF cell lines.

Furthermore, there is a potential role for Cep63 in the DNA damage signalling pathway as determined by the work carried out in the Costanzo lab using *Xenopus laevis* Cep63 (Smith et al., 2009). Although functions may not be fully conserved between the *Xenopus* and human Cep63 orthologues, the possibility of human Cep63 being involved in a DNA damage signalling pathway has not been ruled out. Certainly, Cep63 deficient primary MEFs are proficient in DNA damage checkpoints, but Cep63 may be important for the less well characterised response to DNA damage in mitosis, or perhaps a constitutive mitotic signalling pathway present during unperturbed mitoses, involving DNA damage signalling kinases such as ATM and ATR. Identification for role of human Cep63 in DNA damage signalling processes is yet to be demonstrated:

phosphorylation site identification will provide an important starting point in this investigation.

6.3 Cep63 in genome stability

Unusually early spontaneous immortalisation of a Cep63-deficient MEF line points to an important role for Cep63 in genome stability. Transformation requires several genetic changes to occur and is therefore promoted in genetically unstable backgrounds (Hanahan and Weinberg, 2000). This preliminary, but exciting, finding is an indication for the implication of Cep63 in cancer. Genome stability could arise in Cep63 deficient cells through centriole duplication defects leading to aberrant mitoses and consequent aneuploidy. Centrosome aberrations are observed in tumours and although there is little direct evidence for centrosomes in causing cancer, centrosome aberrations are found in early pre-malignant lesions; coincident with chromosome aberrations; and they correlate with poor clinical outcome (Nigg, 2002). Interestingly, the presence of multiple centrosomes can initiate tumourigenesis in flies: when Plk4 over-expressing *Drosophila* larval brain cells are transplanted into the abdomen of adult flies, the cells over-proliferate and form tumours (Basto et al., 2008). In addition to the effects of centrosome abnormalities on cell division, centrosomes may also play a role in cancer progression via microtubule organisation effects on cell shape, polarity, and motility, and consequently the ability of cells to metastasise (Nigg and Raff, 2009).

As a protein that is involved in the regulation of centrosome duplication and cell cycle control, Cep63 is an interesting candidate for maintenance of genome stability. Although there is not yet sufficient evidence for ascribing a role for Cep63 in genome stability maintenance, it will be interesting to investigate this further. Firstly and most importantly, the effect of Cep63 deficiency on immortalisation timing needs to be examined in duplicate experiments with the generation of more Cep63 gene-trap MEF cell lines and complementation experiments with exogenous Cep63 must be carried out to validate any findings. Further to this, generation of Cep63 gene-trap homozygous mice will, amongst other things, allow the study of the effect of Cep63 deficiency on

cancer predisposition and cancer progression. Interestingly there is correlative evidence for a role for Cep63 as a tumour suppressor in humans (Buim et al., 2005).

6.4 Cep63 and brain development

The striking head defect seen in two (of three) Cep63 gene-trap homozygous mouse embryos is reminiscent of exencephaly. Exencephaly is a condition of neural overgrowth outside of the skull due to a defect in neural tube closure, which therefore indicates a role for Cep63 in brain development. Intriguingly, Cep63 mutation have recently been found in primary microcephaly in humans, although details are currently unpublished (Fanni Gergely, CRUK Cambridge Research Institute, personal communication). As described in chapter 1.2.4, the cause of microcephaly at the molecular and cellular level is under investigation, but no unifying theme has arisen from studies so far. Of the seven identified primary microcephaly genes, four are constitutive centrosome proteins and the other three are associated with mitotic spindle poles, which indicates the importance of mitotic spindle organisation in neuroepithelial (NE) cell divisions. Molecular and cellular roles have been described for MCPH1, Cdk5Rap2, Cep152, ASPM, CPAP and STIL. These proteins are all involved in centrosome function, whether it may be centriole duplication (Cep152, CPAP); spindle pole focussing (ASPM); centrosome to spindle pole attachment (Cdk5Rap2); or regulation of the G2/M checkpoint at the centrosome (MCPH1) (introduction 1.2.4).

DNA damage signalling is also a common theme in patients with a range of microcephaly causing syndromes: ATR, pericentrin, MCPH1, and Cdk5Rap2 are all required for efficient G2/M checkpoint although phenotypes of these patients and patient-derived cell lines are not all overlapping. ATR and pericentrin mutations cause Seckel syndrome (O'Driscoll et al., 2003, Griffith et al., 2008), although most patients with pericentrin mutations are clinically described as MOPD II, which has many overlapping clinical features with Seckel syndrome (Piane et al., 2009). At a cellular level, ATR-Seckel and pericentrin-Seckel cell lines share the features of defective G2/M arrest after UV treatment; nuclear fragmentation upon prolonged hydroxyurea

treatment; and supernumerary centrosomes (Griffith et al., 2008). MCPH1 mutations also result in these cellular phenotypes (Alderton et al., 2006), yet MCPH1 patients have primary microcephaly without the short stature seen in Seckel syndrome. Furthermore, Cdk5Rap2 mutation causes primary microcephaly, and at a cellular level, G2/M checkpoint signalling is defective (Barr et al., 2010). Interestingly, one particular CPAP (CENPJ) mutation has also been observed in Seckel syndrome patients, which differs from other CPAP mutations that cause MCPH, although the cellular phenotypes have not been described (Al-Dosari et al., 2010). In addition to Seckel syndrome and MOPD II, microcephalic primordial dwarfism, which comprises microcephaly as well as severe short stature, is observed Meier-Gorlin syndrome (MGS), which is caused by mutations in pre-replicative complex proteins required for DNA replication licensing (Bicknell et al., 2011a). Interestingly, not all Meier-Gorlin syndrome mutations cause microcephaly, but microcephaly is associated with MGS patients with Orc1 mutations, which may be due to its reduced function in replication origin licensing, or in centriole duplication (Bicknell et al., 2011b).

In summary, the clinical feature of microcephaly is caused by a wide variety of mutations. However, other associated clinical features and cellular phenotypes are not always conserved from mutation in one microcephaly gene to the next. Studies carried out so far highlight several cellular processes that are defective in microcephaly patients, mouse models, and cell culture: centrosome function in spindle assembly, mitotic spindle pole maintenance, centrosome duplication, and DNA damage signalling. Microcephaly genes and their associated clinical classifications are outlined in figure 75. Cep63 is important for the proper regulation of centriole duplication and centriole number, and may also be involved in DNA damage signalling, and cell cycle regulation, which therefore places it as a potential microcephaly gene and indeed this is the case.

Perhaps the centriole duplication defects caused by Cep63 depletion would cause microcephaly via knock-on effects in centrosome dependent spindle organisation. Although spindle organisation appears not to be affected in tissue culture cells depleted of Cep63, the precise regulation and positioning of the mitotic spindle in NE cells is

important in regulating division plane positioning and can affect the fate of the division; symmetric proliferative versus asymmetric neurogenic. Cep63 deficient NE cells unable to duplicate their centrioles would end up with asymmetric spindle poles, such that there may be a pair of centrioles at one pole and only one centriole at the other; or one centriole at one spindle pole with an acentrosomal spindle pole opposite. Thus, control of mitotic spindle positioning and the consequent division plane position may be deregulated. Spindle positioning relies on interaction of astral microtubules emanating from the centrosome with the cell cortex. Cep63 may have an indirect role in spindle positioning via regulation of centriole duplication; or alternatively it could play more direct role via the organisation of astral microtubules.

Aside from positioning of the mitotic spindle in NE cells, Cep63 may play a role at the centrosome in determining symmetry of cell fate determinants orchestrated by centrosomes and the carriage of components by motor proteins on spindle microtubules. Like ASPM, it could maintain symmetry of cell division such that its absence would cause an increase in asymmetric cell divisions at earlier stages of developments where symmetric divisions are important to build the population of neural progenitors (Fish et al., 2006). Animals with this kind of defect would have depleted neural progenitor pools and the number of neurons produced would consequently be much lower. Alternatively, if Cep63 regulated symmetry of cell fate determinants required for cell cycle progression, the asymmetric divisions induced upon loss of Cep63 could generate a daughter cell that exits the cell cycle prematurely, while the other daughter continues to cycle. Indeed, this type of asymmetric cell division is a phenotype observed in several cancer cell lines and tumours after irradiation treatment, although the causative mechanisms have not yet been described (Dey-Guha et al., 2011). In this case, Cep63 deficiency would result in a reduced number of cell divisions, which may not be evident in most organs where the phenotype would be masked by ongoing cell division that occurs through development and postnatal life. In the development of the cerebral cortex, on the other hand, NE cell divisions and neurogenesis is limited to a particular developmental window of time. In this case, a decrease in cell divisions due to premature cell cycle exit of a subpopulation of NE cells would lead to a decreased neural progenitor pool and consequently reduced neuron number. Premature cell cycle

exit and increased levels of apoptosis are a likely cause of microcephaly observed in mice with Cdk5Rap2 mutations (Buchman et al., 2010).

The primary cilium may also be important in embryonic neurogenesis. As opposed to the motile cilia that are found in specialised epithelial cells of the respiratory tract, for example, most vertebrate cells can form a primary cilium, which is a non-motile array of 9 microtubules organised by the mother centriole. Primary cilia play important roles during vertebrate development via their role in sonic hedgehog (shh) signalling. Ssh signalling is used in many different tissues throughout development and most shh signalling in mice requires primary cilia, whereas shh signalling can occur in the absence of a primary cilium in *Drosophila melanogaster* (Nigg and Raff, 2009). The primary cilium is important for both shh and wnt signalling in the detection of extracellular signals in the later stages of brain development (Farkas and Huttner, 2008). Perhaps there is also a role for the primary cilium in embryonic development of the cerebral cortex and the potential for microcephaly resulting from defective centriole structure or function. In fact, multiple cilia, as well as multiple centrosomes, were observed in one mouse model of MCPH3 with truncation of Cdk5Rap2, although this particular model did not show microcephaly (Barrera et al., 2010). The role of Cep63 in primary cilium formation has not yet been studied and it will be important to investigate this further in human tissue culture cells and in the mouse model.

Evolutionary studies of the Cep152 gene show that it is under positive selection in the human lineage, compared to primates and other vertebrates (Guernsey et al., 2010). The same is found for other MCPH genes, MCPH1 and ASPM (Kouprina et al., 2004, Evans et al., 2004, Ponting and Jackson, 2005). These findings, in addition to mutations in these genes causing microcephaly, support the conclusion that there is a causative link between changes in MCPH genes and the increase in brain size evident in humans compared to hominoid ancestors (Bond et al., 2002, Woods et al., 2005). Furthermore, these studies may provide an explanation for the differences seen between human MCPH patient phenotypes and mouse model phenotypes. For example, mouse models of MCPH5 (Aspm) show very slight or insignificant reductions in the size of the

neocortex compared to human patients with similar mutations (Pulvers et al., 2010). An equivalent evolutionary study of Cep63 would be extremely interesting, as it has arisen at a later evolutionary time point than Cep152: Cep63 is present only in vertebrates whereas flies have a Cep152 orthologue. Cep63 may also be under positive selection for a role in neuroepithelial cell divisions and neocortex expansion.

It will be exciting to study Cep63 gene-trap homozygous embryos and, if possible, adult mice in order to determine if Cep63 deficiency does indeed cause microcephaly and to understand the cause of this microcephaly. Further investigation should begin with measuring the cerebral cortex in Cep63 gene-trap homozygous embryos and adults, including brain sectioning to observe cell numbers and carry out immunohistochemistry (ICH) of centrosome and spindle components; cell cycle stage markers; and markers of apoptosis. Analysis of wild type mouse neuroepithelium between embryonic day 9 to 14 by FISH (fluorescent in situ hybridisation) or ICH will be important to determine whether Cep63 is expressed in neuroepithelium at the time of neurogenesis like other microcephaly genes. Analysis of cleavage plane orientation and symmetric versus asymmetric inheritance of the apical membrane in NE cell of Cep63 deficient embryos will also be interesting. Establishing neural cell cultures *in vitro* from Cep63 gene-trap and wild type mice would provide a useful model for determining the role of Cep63 in neural cell divisions. Further to the potential microcephaly phenotype, analysis of Cep63 deficient embryos and adults will be extremely important in identifying alternative developmental processes in which Cep63 is involved, as well as non developmental processes. A Cep63 mouse model will provide a possibility of studying the effects of Cep63 deficiency on genome stability.

One additional hypothesis for Cep63 deficiency is that it may cause problems in spermatogenesis. The *Drosophila melanogaster* orthologue of Cep152, *asterless*, is essential for proper spindle assembly and meiotic cell division during spermatogenesis (Bonaccorsi et al., 1998). Furthermore, mice with a heterozygous mutation in Plk4 have defects in spermatogenesis (Harris et al., 2011), and mouse models of MCPH1 and

MCPH3 (Cdk5Rap2) also cause male infertility (Liang et al., 2010, Lizarraga et al., 2010).

6.5 Conclusions

Cep63 is a constitutive PCM component that is involved in the regulation of centriole duplication. In the absence of Cep63 centrioles can duplicate, but do so with reduced efficiency. The role of Cep63 in centriole duplication is predicted to be mediated through its binding partner, Cep152, which is required for centriole duplication due to its role in recruiting Plk4 and CPAP to the centrosome. This study is the first to implicate Cep63 in centriole duplication; identify and characterise the interaction between Cep63 and Cep152; and show the requirement for Cep63 in localisation of Cep152 to the centrosome. Other than the primary phenotype of a defect in centriole duplication, preliminary evidence from Cep63 null mouse embryos and derived cell lines show evidence for a potential role for Cep63 in embryonic brain development.

Figure 75 depicts the hypothesis drawn from Cep63 studies described in this thesis. Although the situation is likely to be much more complicated than depicted, this model serves as a good basis for designing future experiments to understand Cep63 function at the molecular level more thoroughly. Further to the characterisation of the molecular details of the involvement of Cep63 in centriole duplication, study of Cep63 deficient mice will provide information on the importance and the role of Cep63 in different cell types and during development. The Cep63 deficient mouse model may prove a useful system for understanding the molecular and cellular phenotypes underlying primary microcephaly.

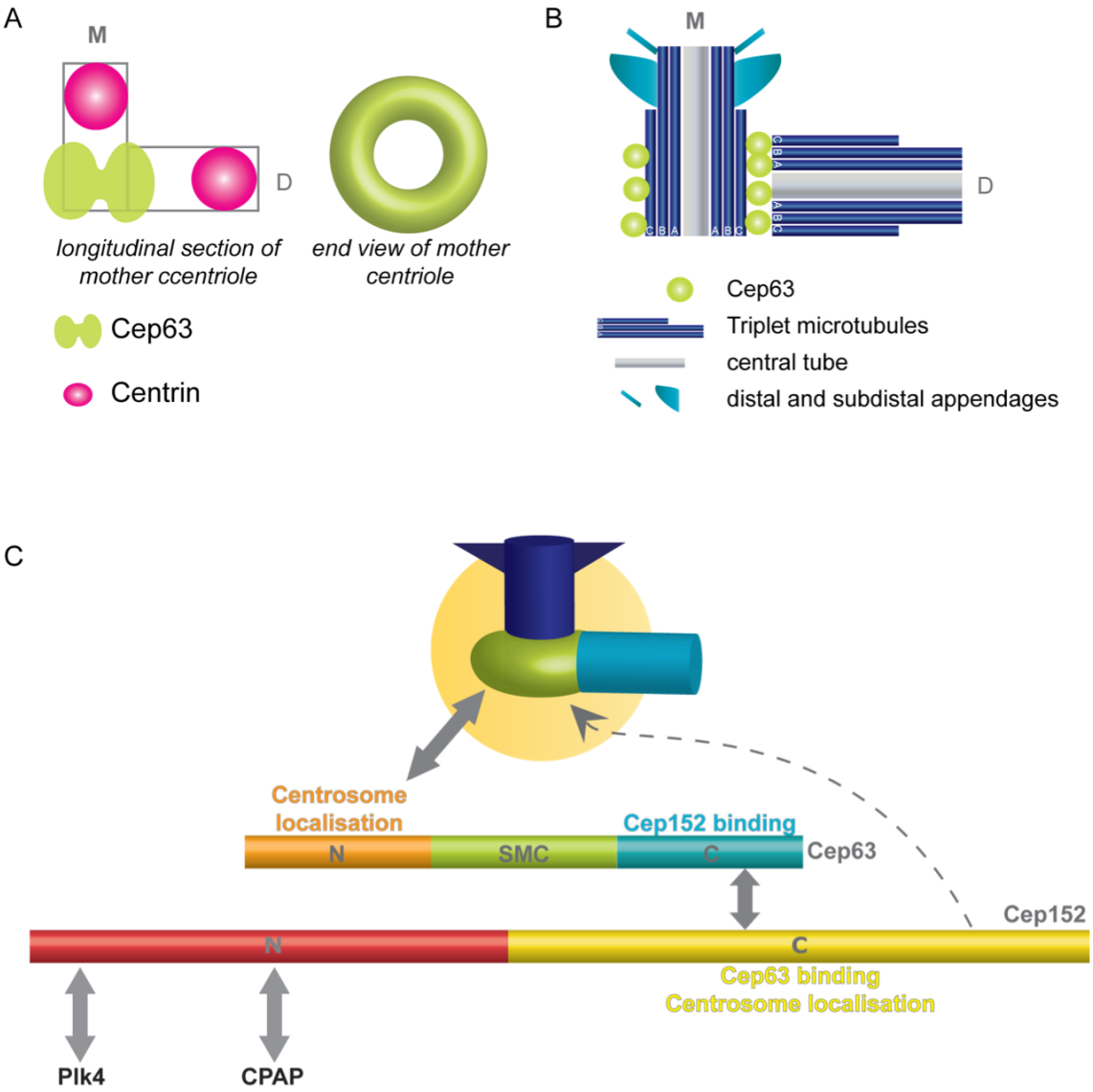

Figure 75 Hypothesis
(A) Cep63 is a constitutive PCM protein that localises around the outside of the proximal centriole wall, which is visualised as a bi-lobed (left) or doughnut-shaped (right) appearance by immunofluorescence. (B) Predicted localisation of Cep63 with respect to mother and daughter centrioles; to be tested by immuno-electron microscopy. (C) Cep63 functions in promoting centriole duplication by recruiting Cep152 to the centrosome. Cep152, in turn, recruits CPAP and aids recruitment of Plk4 to promote pro-centriole formation. The dashed arrow represents a possible alternative mode of recruitment of Cep152 to the centrosome that could occur in the absence of Cep63.

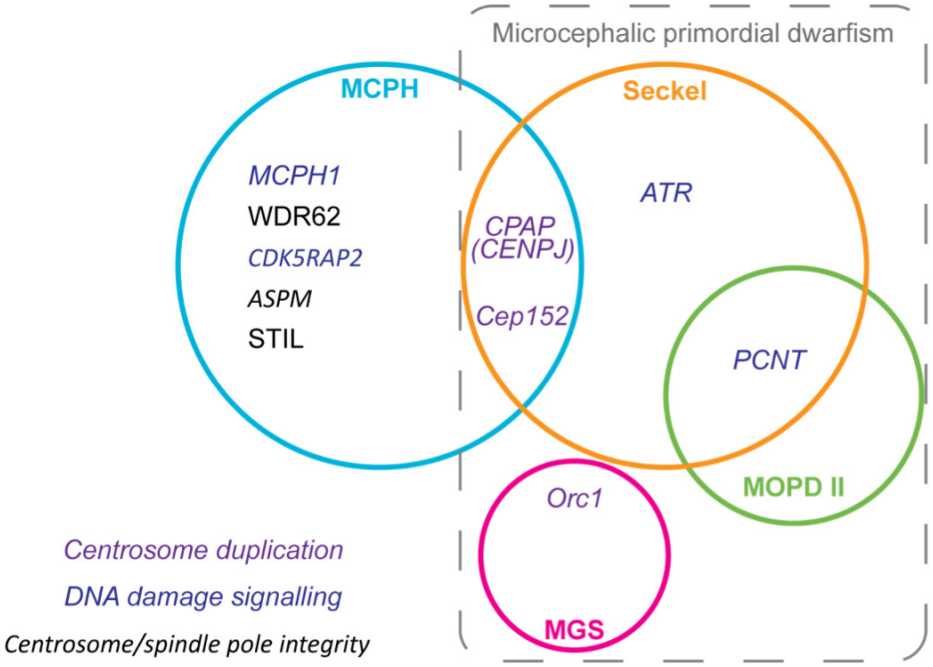

Figure 76 Microcephaly genes
MCPH1, WDR62, Cdk5Rap2, ASPM, STIL, CPAP and Cep152 mutations cause primary microcephaly. CPAP and Cep152 mutations have also been found in patients with Seckel syndrome. ATR and pericentrin (PCNT) mutations cause Seckel syndrome, although most patients with PCNT mutations are diagnosed with MOPD II. A subset of Meier-Gorlin syndrome (MGS) patients have microcephaly, these patients have Orc1 mutations. Of the microcephaly genes whose proteins have been characterised at a cellular level (*italics*), MCPH1, Cdk5Rap2, ATR, and PCNT are required for efficient DNA damage signalling; CPAP, Cep152, and Orc1 are required for proper centrosome duplication; and Cdk5Rap2 and ASPM are required for mitotic spindle pole integrity. Perhaps Cep63 will also be placed in the MCPH category.

Reference List

ABAL, M., PIEL, M., BOUCKSON-CASTAING, V., MOGENSEN, M., SIBARITA, J. B. & BORNENS, M. 2002. Microtubule release from the centrosome in migrating cells. *J Cell Biol,* 159**,** 731-7.

ACILAN, C. & SAUNDERS, W. S. 2008. A tale of too many centrosomes. *Cell,* 134**,** 572-5.

AL-DOSARI, M. S., SHAHEEN, R., COLAK, D. & ALKURAYA, F. S. 2010. Novel CENPJ mutation causes Seckel syndrome. *J Med Genet,* 47**,** 411-4.

ALDERTON, G. K., GALBIATI, L., GRIFFITH, E., SURINYA, K. H., NEITZEL, H., JACKSON, A. P., JEGGO, P. A. & O'DRISCOLL, M. 2006. Regulation of mitotic entry by microcephalin and its overlap with ATR signalling. *Nat Cell Biol,* 8**,** 725-33.

ANDERSEN, J. S., WILKINSON, C. J., MAYOR, T., MORTENSEN, P., NIGG, E. A. & MANN, M. 2003. Proteomic characterization of the human centrosome by protein correlation profiling. *Nature.*

ARCHINTI, M., LACASA, C., TEIXIDÓ-TRAVESA, N. & LÜDERS, J. 2010. SPICE--a previously uncharacterized protein required for centriole duplication and mitotic chromosome congression. *Journal of Cell Science.*

AZIMZADEH, J., HERGERT, P., DELOUVEE, A., EUTENEUER, U., FORMSTECHER, E., KHODJAKOV, A. & BORNENS, M. 2009. hPOC5 is a centrin-binding protein required for assembly of full-length centrioles. *J Cell Biol,* 185**,** 101-14.

AZIMZADEH, J. & MARSHALL, W. F. 2010. Building the centriole. *Curr Biol,* 20**,** R816-25.

BAHE, S., STIERHOF, Y. D., WILKINSON, C. J., LEISS, F. & NIGG, E. A. 2005. Rootletin forms centriole-associated filaments and functions in centrosome cohesion. *J Cell Biol,* 171**,** 27-33.

BAHMANYAR, S., KAPLAN, D. D., DELUCA, J. G., GIDDINGS, T. H., JR., O'TOOLE, E. T., WINEY, M., SALMON, E. D., CASEY, P. J., NELSON, W. J. & BARTH, A. I. 2008. beta-Catenin is a Nek2 substrate involved in centrosome separation. *Genes Dev,* 22**,** 91-105.

BALCZON, R., BAO, L., ZIMMER, W. E., BROWN, K., ZINKOWSKI, R. P. & BRINKLEY, B. R. 1995. Dissociation of centrosome replication events from cycles of DNA synthesis and mitotic division in hydroxyurea-arrested Chinese hamster ovary cells. *J Cell Biol,* 130**,** 105-15.

BARR, A. R., KILMARTIN, J. V. & GERGELY, F. 2010. CDK5RAP2 functions in centrosome to spindle pole attachment and DNA damage response. *The Journal of Cell Biology.*

BARRERA, J. A., KAO, L. R., HAMMER, R. E., SEEMANN, J., FUCHS, J. L. & MEGRAW, T. L. 2010. CDK5RAP2 regulates centriole engagement and cohesion in mice. *Dev Cell,* 18**,** 913-26.

BASTO, R., BRUNK, K., VINADOGROVA, T., PEEL, N., FRANZ, A., KHODJAKOV, A. & RAFF, J. W. 2008. Centrosome amplification can initiate tumorigenesis in flies. *Cell,* 133**,** 1032-42.

BASTO, R., LAU, J., VINOGRADOVA, T., GARDIOL, A., WOODS, C. G., KHODJAKOV, A. & RAFF, J. W. 2006. Flies without centrioles. *Cell.*

BETTENCOURT-DIAS, M. & GLOVER, D. M. 2007. Centrosome biogenesis and function: centrosomics brings new understanding. *Nat Rev Mol Cell Biol.*

BHAT, V., GIRIMAJI, S., MOHAN, G., ARVINDA, H., SINGHMAR, P., DUVVARI, M. & KUMAR, A. 2011. Mutations in WDR62, encoding a centrosomal and nuclear protein, in Indian primary microcephaly families with cortical malformations. *Clin Genet*.

BICKNELL, L. S., BONGERS, E. M., LEITCH, A., BROWN, S., SCHOOTS, J., HARLEY, M. E., AFTIMOS, S., AL-AAMA, J. Y., BOBER, M., BROWN, P. A., VAN BOKHOVEN, H., DEAN, J., EDREES, A. Y., FEINGOLD, M., FRYER, A., HOEFSLOOT, L. H., KAU, N., KNOERS, N. V., MACKENZIE, J., OPITZ, J. M., SARDA, P., ROSS, A., TEMPLE, I. K., TOUTAIN, A., WISE, C. A., WRIGHT, M. & JACKSON, A. P. 2011a. Mutations in the pre-replication complex cause Meier-Gorlin syndrome. *Nat Genet,* 43**,** 356-9.

BICKNELL, L. S., WALKER, S., KLINGSEISEN, A., STIFF, T., LEITCH, A., KERZENDORFER, C., MARTIN, C. A., YEYATI, P., AL SANNA, N., BOBER, M., JOHNSON, D., WISE, C., JACKSON, A. P., O'DRISCOLL, M. & JEGGO, P. A. 2011b. Mutations in ORC1, encoding the largest subunit of the origin recognition complex, cause microcephalic primordial dwarfism resembling Meier-Gorlin syndrome. *Nat Genet,* 43**,** 350-5.

BIGNOLD, L. P., COGHLAN, B. L. & JERSMANN, H. P. 2006. Hansemann, Boveri, chromosomes and the gametogenesis-related theories of tumours. *Cell Biol Int,* 30**,** 640-4.

BILGUVAR, K., OZTURK, A. K., LOUVI, A., KWAN, K. Y., CHOI, M., TATLI, B., YALNIZOGLU, D., TUYSUZ, B., CAGLAYAN, A. O., GOKBEN, S., KAYMAKCALAN, H., BARAK, T., BAKIRCIOGLU, M., YASUNO, K., HO, W., SANDERS, S., ZHU, Y., YILMAZ, S., DINCER, A., JOHNSON, M. H., BRONEN, R. A., KOCER, N., PER, H., MANE, S., PAMIR, M. N., YALCINKAYA, C., KUMANDAS, S., TOPCU, M., OZMEN, M., SESTAN, N., LIFTON, R. P., STATE, M. W. & GUNEL, M. 2010. Whole-exome sequencing identifies recessive WDR62 mutations in severe brain malformations. *Nature,* 467**,** 207-10.

BLACHON, S., GOPALAKRISHNAN, J., OMORI, Y., POLYANOVSKY, A., CHURCH, A., NICASTRO, D., MALICKI, J. & AVIDOR-REISS, T. 2008. Drosophila asterless and vertebrate Cep152 Are orthologs essential for centriole duplication. *Genetics.*

BOBINNEC, Y., KHODJAKOV, A., MIR, L. M., RIEDER, C. L., EDDE, B. & BORNENS, M. 1998. Centriole disassembly in vivo and its effect on centrosome structure and function in vertebrate cells. *J Cell Biol,* 143**,** 1575-89.

BONACCORSI, S., GIANSANTI, M. G. & GATTI, M. 1998. Spindle Self-organization and Cytokinesis During Male Meiosis in

asterless Mutants of Drosophila melanogaster. *The Journal of Cell Biology.*

BOND, J., ROBERTS, E., MOCHIDA, G. H., HAMPSHIRE, D. J., SCOTT, S., ASKHAM, J. M., SPRINGELL, K., MAHADEVAN, M., CROW, Y. J., MARKHAM, A. F., WALSH, C. A. & WOODS, C. G. 2002. ASPM is a major determinant of cerebral cortical size. *Nat Genet,* 32**,** 316-20.

BOND, J., ROBERTS, E., SPRINGELL, K., LIZARRAGA, S. B., SCOTT, S., HIGGINS, J., HAMPSHIRE, D. J., MORRISON, E. E., LEAL, G. F., SILVA, E. O., COSTA, S. M., BARALLE, D., RAPONI, M., KARBANI, G., RASHID,

Y., JAFRI, H., BENNETT, C., CORRY, P., WALSH, C. A. & WOODS, C. G. 2005. A centrosomal mechanism involving CDK5RAP2 and CENPJ controls brain size. *Nat Genet,* 37**,** 353-5.

BOND, J., SCOTT, S., HAMPSHIRE, D. J., SPRINGELL, K., CORRY, P., ABRAMOWICZ, M. J., MOCHIDA, G. H., HENNEKAM, R. C., MAHER, E. R., FRYNS, J. P., ALSWAID, A., JAFRI, H., RASHID, Y., MUBAIDIN, A., WALSH, C. A., ROBERTS, E. & WOODS, C. G. 2003. Protein-truncating mutations in ASPM cause variable reduction in brain size. *Am J Hum Genet,* 73**,** 1170-7.

BONNET, J., COOPMAN, P. & MORRIS, M. C. 2008. Characterization of centrosomal localization and dynamics of Cdc25C phosphatase in mitosis. *Cell Cycle.*

BORNENS, M. 2002. Centrosome composition and microtubule anchoring mechanisms. *Curr Opin Cell Biol,* 14**,** 25-34.

BORNENS, M., PAINTRAND, M., BERGES, J., MARTY, M.-C. & KARSENTI, E. 1987. structural and chemical characterization of isolated centrosomes. *Cell Motil Cytoskeleton.*

BOULTON, S. J. 2006. Cellular functions of the BRCA tumour-suppressor proteins. *Biochem Soc Trans,* 34**,** 633-45.

BRITTLE, A. L. & OHKURA, H. 2005. Centrosome maturation: Aurora lights the way to the poles. *Curr Biol,* 15**,** R880-2.

BROWN, N. & COSTANZO, V. 2009. An ATM and ATR dependent pathway targeting centrosome dependent spindle assembly. *Cell Cycle.*

BUCHMAN, J. J., TSENG, H. C., ZHOU, Y., FRANK, C. L., XIE, Z. & TSAI, L. H. 2010. Cdk5rap2 interacts with pericentrin to maintain the neural progenitor pool in the developing neocortex. *Neuron,* 66**,** 386-402.

BUIM, M. E., SOARES, F. A., SARKIS, A. S. & NAGAI, M. A. 2005. The transcripts of SFRP1,CEP63 and EIF4G2 genes are frequently downregulated in transitional cell carcinomas of the bladder. *Oncology,* 69**,** 445-54.

CARAZO-SALAS, R. E., GUARGUAGLINI, G., GRUSS, O. J., SEGREF, A., KARSENTI, E. & MATTAJ, I. W. 1999. Generation of GTP-bound Ran by RCC1 is required for chromatin-induced mitotic spindle formation. *Nature,* 400**,** 178-81.

CARVALHO-SANTOS, Z., MACHADO, P., BRANCO, P., TAVARES-CADETE, F., RODRIGUES-MARTINS, A., PEREIRA-LEAL, J. B. & BETTENCOURT-DIAS, M. 2010. Stepwise evolution of the centriole-assembly pathway. *Journal of Cell Science.*

CASTIEL, A., DANIELI, M. M., DAVID, A., MOSHKOVITZ, S., APLAN, P. D., KIRSCH, I. R., BRANDEIS, M., KRAMER, A. & IZRAELI, S. 2011. The Stil protein regulates centrosome integrity and mitosis through suppression of Chfr. *J Cell Sci,* 124**,** 532-9.

CAZALES, M., SCHMITT, E., MONTEMBAULT, E., DOZIER, C., PRIGENT, C. & DUCOMMUN, B. 2005. CDC25B phosphorylation by Aurora-A occurs at the G2/M transition and is inhibited by DNA damage. *Cell Cycle,* 4**,** 1233-8.

CHANG, J., CIZMECIOGLU, O., HOFFMANN, I. & RHEE, K. 2010. PLK2 phosphorylation is critical for CPAP function in procentriole formation during the centrosome cycle. *EMBO J.*

CHANG, P., COUGHLIN, M. & MITCHISON, T. J. 2009. Interaction between Poly(ADP-ribose) and NuMA contributes to mitotic spindle pole assembly. *Molecular Biology of the Cell.*

CHEESEMAN, I. M. & DESAI, A. 2008. Molecular architecture of the kinetochore-microtubule interface. *Nat Rev Mol Cell Biol.*

CHO, J. H., CHANG, C. J., CHEN, C. Y. & TANG, T. K. 2006. Depletion of CPAP by RNAi disrupts centrosome integrity and induces multipolar spindles. *Biochem Biophys Res Commun,* 339**,** 742-7.

CHOW, J. P., SIU, W. Y., FUNG, T. K., CHAN, W. M., LAU, A., AROOZ, T., NG, C. P., YAMASHITA, K. & POON, R. Y. 2003. DNA damage during the spindle-assembly checkpoint degrades CDC25A, inhibits cyclin-CDC2 complexes, and reverses cells to interphase. *Mol Biol Cell,* 14**,** 3989-4002.

CIZMECIOGLU, O., ARNOLD, M., BAHTZ, R., SETTELE, F., EHRET, L., HASELMANN-WEIS, U., ANTONY, C. & HOFFMANN, I. 2010. Cep152 acts as a scaffold for recruitment of Plk4 and CPAP to the centrosome. *The Journal of Cell Biology.*

CIZMECIOGLU, O., WARNKE, S., ARNOLD, M., DUENSING, S. & HOFFMANN, I. 2008. Plk2 regulated centriole duplication is dependent on its localization to the centrioles and a functional polo-box domain. *Cell Cycle.*

D'ANGIOLELLA, V., DONATO, V., VIJAYAKUMAR, S., SARAF, A., FLORENS, L., WASHBURN, M. P., DYNLACHT, B. & PAGANO, M. 2010. SCF(Cyclin F) controls centrosome homeostasis and mitotic fidelity through CP110 degradation. *Nature.*

DAMMERMANN, A. & MERDES, A. 2002. Assembly of centrosomal proteins and microtubule organization depends on PCM-1. *J Cell Biol,* 159**,** 255-66.

DANTAS, T. J., WANG, Y., LALOR, P., DOCKERY, P. & MORRISON, C. G. 2011. Defective nucleotide excision repair with normal centrosome structures and functions in the absence of all vertebrate centrins. *J Cell Biol,* 193**,** 307-18.

DEY-GUHA, I., WOLFER, A., YEH, A. C., J, G. A., DARP, R., LEON, E., WULFKUHLE, J., PETRICOIN, E. F., 3RD, WITTNER, B. S. & RAMASWAMY, S. 2011. Asymmetric cancer cell division regulated by AKT. *Proc Natl Acad Sci U S A,* 108**,** 12845-50.

DIVIANI, D., LANGEBERG, L. K., DOXSEY, S. J. & SCOTT, J. D. 2000. Pericentrin anchors protein kinase A at the centrosome through a newly identified RII-binding domain. *Curr Biol,* 10**,** 417-20.

DO CARMO AVIDES, M. & GLOVER, D. M. 1999. Abnormal spindle protein, Asp, and the integrity of mitotic centrosomal microtubule organizing centers. *Science,* 283**,** 1733-5.

DODSON, H., BOURKE, E., JEFFERS, L. J., VAGNARELLI, P., SONODA, E., TAKEDA, S., EARNSHAW, W. C., MERDES, A. & MORRISON, C. 2004. Centrosome amplification induced by DNA damage occurs during a prolonged G2 phase and involves ATM. *EMBO J,* 23**,** 3864-73.

DOUBILET, S. & MCKIM, K. S. 2007. Spindle assembly in the oocytes of mouse and Drosophila--similar solutions to a problem. *Chromosome Res,* 15**,** 681-96.

DOXSEY, S., ZIMMERMAN, W. & MIKULE, K. 2005. Centrosome control of the cell cycle. *Trends Cell Biol,* 15**,** 303-11.

DUCAT, D. & ZHENG, Y. 2004. Aurora kinases in spindle assembly and chromosome segregation. *Exp Cell Res,* 301**,** 60-7.

DUENSING, A., GHANEM, L., STEINMAN, R. A., LIU, Y. & DUENSING, S. 2006. p21(Waf1/Cip1) deficiency stimulates centriole overduplication. *Cell Cycle,* 5**,** 2899-902.

DUENSING, A., LIU, Y., PERDREAU, S. A., KLEYLEIN-SOHN, J., NIGG, E. A. & DUENSING, S. 2007. Centriole overduplication through the concurrent formation of multiple daughter centrioles at single maternal templates. *Oncogene,* 26**,** 6280-8.

DUTERTRE, S., CAZALES, M., QUARANTA, M., FROMENT, C., TRABUT, V., DOZIER, C., MIREY, G., BOUCHE, J. P., THEIS-FEBVRE, N., SCHMITT, E., MONSARRAT, B., PRIGENT, C. & DUCOMMUN, B. 2004. Phosphorylation of CDC25B by Aurora-A at the centrosome contributes to the G2-M transition. *J Cell Sci,* 117**,** 2523-31.

DZHINDZHEV, N. S., YU, Q. D., WEISKOPF, K., TZOLOVSKY, G., CUNHA-FERREIRA, I., RIPARBELLI, M., RODRIGUES-MARTINS, A., BETTENCOURT-DIAS, M., CALLAINI, G. & GLOVER, D. M. 2010a. Asterless is a scaffold for the onset of centriole assembly. *Nature.*

DZHINDZHEV, N. S., YU, Q. D., WEISKOPF, K., TZOLOVSKY, G., CUNHA-FERREIRA, I., RIPARBELLI, M., RODRIGUES-MARTINS, A., BETTENCOURT-DIAS, M., CALLAINI, G. & GLOVER, D. M. 2010b. Asterless is a scaffold for the onset of centriole assembly. *Nature,* 467**,** 714-8.

ERICKSON, H. P., TAYLOR, D. W., TAYLOR, K. A. & BRAMHILL, D. 1996. Bacterial cell division protein FtsZ assembles into protofilament sheets and minirings, structural homologs of tubulin polymers. *Proc Natl Acad Sci U S A,* 93**,** 519-23.

EVANS, P. D., ANDERSON, J. R., VALLENDER, E. J., GILBERT, S. L., MALCOM, C. M., DORUS, S. & LAHN, B. T. 2004. Adaptive evolution of ASPM, a major determinant of cerebral cortical size in humans. *Hum Mol Genet,* 13**,** 489-94.

EVANS, T., ROSENTHAL, E. T., YOUNGBLOM, J., DISTEL, D. & HUNT, T. 1983. Cyclin: a protein specified by maternal mRNA in sea urchin eggs that is destroyed at each cleavage division. *Cell,* 33**,** 389-96.

FALINI, B., LENZE, D., HASSERJIAN, R., COUPLAND, S., JAEHNE, D., SOUPIR, C., LISO, A., MARTELLI, M. P., BOLLI, N., BACCI, F., PETTIROSSI, V., SANTUCCI, A., MARTELLI, M. F., PILERI, S. & STEIN, H. 2007. Cytoplasmic mutated nucleophosmin (NPM) defines the molecular status of a significant fraction of myeloid sarcomas. *Leukemia,* 21**,** 1566-70.

FARKAS, L. M. & HUTTNER, W. B. 2008. The cell biology of neural stem and progenitor cells and its significance for their proliferation versus differentiation during mammalian brain development. *Curr Opin Cell Biol.*

FISH, J. L., KOSODO, Y., ENARD, W., PAABO, S. & HUTTNER, W. B. 2006. Aspm specifically maintains symmetric proliferative divisions of neuroepithelial cells. *Proc Natl Acad Sci U S A,* 103**,** 10438-43.

FISK, H. A., MATTISON, C. P. & WINEY, M. 2003. Human Mps1 protein kinase is required for centrosome duplication and normal mitotic progression. *Proc Natl Acad Sci U S A,* 100**,** 14875-80.

FISK, H. A. & WINEY, M. 2001. The mouse Mps1p-like kinase regulates centrosome duplication. *Cell,* 106**,** 95-104.

FURUNO, N., DEN ELZEN, N. & PINES, J. 1999. Human cyclin A is required for mitosis until mid prophase. *J Cell Biol,* 147**,** 295-306.

GATLIN, J. C. & BLOOM, K. 2010. Microtubule motors in eukaryotic spindle assembly and maintenance. *Semin Cell Dev Biol,* 21**,** 248-54.

GILLINGHAM, A. K. & MUNRO, S. 2000. The PACT domain, a conserved centrosomal targeting motif in the coiled-coil proteins AKAP450 and pericentrin. *EMBO Rep.*

GOLAN, A., PICK, E., TSVETKOV, L., NADLER, Y., KLUGER, H. & STERN, D. F. 2010. Centrosomal Chk2 in DNA damage responses and cell cycle progression. *Cell Cycle,* 9**,** 2647-56.

GOMEZ-FERRERIA, M. & PELLETIER, L. 2010. Centrosome biogenesis: centrosomin sizes things up! *Curr Biol,* 20**,** R1069-71.

GRAVES, P. R., YU, L., SCHWARZ, J. K., GALES, J., SAUSVILLE, E. A., O'CONNOR, P. M. & PIWNICA-WORMS, H. 2000. The Chk1 protein kinase and the Cdc25C regulatory pathways are targets of the anticancer agent UCN-01. *J Biol Chem,* 275**,** 5600-5.

GRIFFITH, E., WALKER, S., MARTIN, C.-A., VAGNARELLI, P., STIFF, T., VERNAY, B., SANNA, N. A., SAGGAR, A., HAMEL, B., EARNSHAW, W. C., JEGGO, P. A., JACKSON, A. P. & O'DRISCOLL, M. 2008. Mutations in pericentrin cause Seckel syndrome with defective ATR-dependent DNA damage signaling. *Nat Genet.*

GUDERIAN, G., WESTENDORF, J., ULDSCHMID, A. & NIGG, E. A. 2010. Plk4 trans-autophosphorylation regulates centriole number by controlling betaTrCP-mediated degradation. *Journal of Cell Science.*

GUDI, R., ZOU, C., LI, J. & GAO, Q. 2011. Centrobin-tubulin interaction is required for centriole elongation and stability. *The Journal of Cell Biology.*

GUERNSEY, D. L., JIANG, H., HUSSIN, J., ARNOLD, M., BOUYAKDAN, K., PERRY, S., BABINEAU-STURK, T., BEIS, J., DUMAS, N., EVANS, S. C., FERGUSON, M., MATSUOKA, M., MACGILLIVRAY, C., NIGHTINGALE, M., PATRY, L., RIDEOUT, A. L., THOMAS, A., ORR, A., HOFFMANN, I., MICHAUD, J. L., AWADALLA, P., MEEK, D. C., LUDMAN, M. & SAMUELS, M. E. 2010. Mutations in centrosomal protein CEP152 in primary microcephaly families linked to MCPH4. *Am J Hum Genet.*

GUO, J., YANG, Z., SONG, W., CHEN, Q., WANG, F., ZHANG, Q. & ZHU, X. 2006. Nudel contributes to microtubule anchoring at the mother centriole and is involved in both dynein-dependent and -independent centrosomal protein assembly. *Mol Biol Cell,* 17**,** 680-9.

HABEDANCK, R., STIERHOF, Y.-D., WILKINSON, C. J. & NIGG, E. A. 2005. The Polo kinase Plk4 functions in centriole duplication. *Nat Cell Biol.*

HANAHAN, D. & WEINBERG, R. A. 2000. The hallmarks of cancer. *Cell,* 100**,** 57-70.

HANAHAN, D. & WEINBERG, R. A. 2011. Hallmarks of cancer: the next generation. *Cell,* 144**,** 646-74.

HAREN, L., GNADT, N., WRIGHT, M. & MERDES, A. 2009a. NuMA is required for proper spindle assembly and chromosome alignment in prometaphase. *BMC Res Notes.*

HAREN, L., REMY, M. H., BAZIN, I., CALLEBAUT, I., WRIGHT, M. & MERDES, A. 2006. NEDD1-dependent recruitment of the gamma-tubulin ring complex to the centrosome is necessary for centriole duplication and spindle assembly. *J Cell Biol,* 172**,** 505-15.

HAREN, L., STEARNS, T. & LÜDERS, J. 2009b. Plk1-dependent recruitment of gamma-tubulin complexes to mitotic centrosomes involves multiple PCM components. *PLoS ONE.*

HARRIS, R. M., WEISS, J. & JAMESON, J. L. 2011. Male Hypogonadism and Germ Cell Loss Caused by a Mutation in Polo-Like Kinase 4. *Endocrinology*.

HATCH, E. M., KULUKIAN, A., HOLLAND, A. J., CLEVELAND, D. W. & STEARNS, T. 2010a. Cep152 interacts with Plk4 and is required for centriole duplication. *J Cell Biol,* 191**,** 721-9.

HATCH, E. M., KULUKIAN, A., HOLLAND, A. J., CLEVELAND, D. W. & STEARNS, T. 2010b. Cep152 interacts with Plk4 and is required for centriole duplication. *The Journal of Cell Biology.*

HEALD, R., TOURNEBIZE, R., BLANK, T., SANDALTZOPOULOS, R., BECKER, P., HYMAN, A. & KARSENTI, E. 1996. Self-organization of microtubules into bipolar spindles around artificial chromosomes in Xenopus egg extracts. *Nature,* 382**,** 420-5.

HEALD, R., TOURNEBIZE, R., HABERMANN, A., KARSENTI, E. & HYMAN, A. 1997. Spindle assembly in Xenopus egg extracts: respective roles of centrosomes and microtubule self-organization. *J Cell Biol,* 138**,** 615-28.

HEMERLY, A. S., PRASANTH, S. G., SIDDIQUI, K. & STILLMAN, B. 2009. Orc1 controls centriole and centrosome copy number in human cells. *Science.*

HIROTA, T., KUNITOKU, N., SASAYAMA, T., MARUMOTO, T., ZHANG, D., NITTA, M., HATAKEYAMA, K. & SAYA, H. 2003. Aurora-A and an interacting activator, the LIM protein Ajuba, are required for mitotic commitment in human cells. *Cell,* 114**,** 585-98.

HOLLAND, A. J., LAN, W., NIESSEN, S., HOOVER, H. & CLEVELAND, D. W. 2010. Polo-like kinase 4 kinase activity limits centrosome overduplication by autoregulating its own stability. *J Cell Biol,* 188**,** 191-8.

HUNG, L. Y., TANG, C. J. & TANG, T. K. 2000. Protein 4.1 R-135 interacts with a novel centrosomal protein (CPAP) which is associated with the gamma-tubulin complex. *Mol Cell Biol,* 20**,** 7813-25.

HUYEN, Y., ZGHEIB, O., DITULLIO, R. A., JR., GORGOULIS, V. G., ZACHARATOS, P., PETTY, T. J., SHESTON, E. A., MELLERT, H. S., STAVRIDI, E. S. & HALAZONETIS, T. D. 2004. Methylated lysine 79 of histone H3 targets 53BP1 to DNA double-strand breaks. *Nature,* 432**,** 406-11.

INANÇ, B., DODSON, H. & MORRISON, C. G. 2010. A Centrosome-autonomous Signal that Involves Centriole Disengagement Permits Centrosome Duplication in G2 Phase After DNA Damage. *Molecular Biology of the Cell.*

IZRAELI, S., LOWE, L. A., BERTNESS, V. L., GOOD, D. J., DORWARD, D. W., KIRSCH, I. R. & KUEHN, M. R. 1999. The SIL gene is required for mouse embryonic axial development and left-right specification. *Nature,* 399**,** 691-4.

JACKMAN, M., LINDON, C., NIGG, E. A. & PINES, J. 2003. Active cyclin B1–Cdk1 first appears on centrosomes in prophase. *Nat Cell Biol.*

JACKSON, A. P., EASTWOOD, H., BELL, S. M., ADU, J., TOOMES, C., CARR, I. M., ROBERTS, E., HAMPSHIRE, D. J., CROW, Y. J., MIGHELL, A. J., KARBANI, G., JAFRI, H., RASHID, Y., MUELLER, R. F., MARKHAM, A. F. & WOODS, C. G. 2002. Identification of microcephalin, a protein implicated in determining the size of the human brain. *Am J Hum Genet,* 71**,** 136-42.

JACKSON, S. P. & BARTEK, J. 2009. The DNA-damage response in human biology and disease. *Nature,* 461**,** 1071-8.

JAKOBSEN, L., VANSELOW, K., SKOGS, M., TOYODA, Y., LUNDBERG, E., POSER, I., FALKENBY, L. G., BENNETZEN, M., WESTENDORF, J., NIGG, E. A., UHLEN, M., HYMAN, A. A. & ANDERSEN, J. S. 2011. Novel asymmetrically localizing components of human centrosomes identified by complementary proteomics methods. *The EMBO Journal.*

JAZAYERI, A., FALCK, J., LUKAS, C., BARTEK, J., SMITH, G. C. M., LUKAS, J. & JACKSON, S. P. 2006. ATM- and cell cycle-dependent regulation of ATR in response to DNA double-strand breaks. *Nat Cell Biol.*

JOUKOV, V., DE NICOLO, A., RODRIGUEZ, A., WALTER, J. C. & LIVINGSTON, D. M. 2010. Centrosomal protein of 192 kDa (Cep192) promotes centrosome-driven spindle assembly by engaging in organelle-specific Aurora A activation. *Proc Natl Acad Sci U S A,* 107**,** 21022-7.

KALAY, E., YIGIT, G., ASLAN, Y., BROWN, K. E., POHL, E., BICKNELL, L. S., KAYSERILI, H., LI, Y., TÜYSÜZ, B., NÜRNBERG, G., KIESS, W., KOEGL, M., BAESSMANN, I., BURUK, K., TORAMAN, B., KAYIPMAZ, S., KUL, S., IKBAL, M., TURNER, D. J., TAYLOR, M. S., AERTS, J., SCOTT, C., MILSTEIN, K., DOLLFUS, H., WIECZOREK, D., BRUNNER, H. G., HURLES, M., JACKSON, A. P., RAUCH, A., NÜRNBERG, P., KARAGÜZEL, A. & WOLLNIK, B. 2011. CEP152 is a genome maintenance protein disrupted in Seckel syndrome. *Nat Genet.*

KEATING, T. J. & BORISY, G. G. 1999. Centrosomal and non-centrosomal microtubules. *Biol Cell,* 91**,** 321-9.

KEATING, T. J. & BORISY, G. G. 2000. Immunostructural evidence for the template mechanism of microtubule nucleation. *Nat Cell Biol,* 2**,** 352-7.

KELLER, A., NESVIZHSKII, A. I., KOLKER, E. & AEBERSOLD, R. 2002. Empirical statistical model to estimate the accuracy of peptide identifications made by MS/MS and database search. *Anal Chem,* 74**,** 5383-92.

KERYER, G., DI FIORE, B., CELATI, C., LECHTRECK, K. F., MOGENSEN, M., DELOUVEE, A., LAVIA, P., BORNENS, M. & TASSIN, A.-M. 2003. Part of Ran is associated with AKAP450 at the centrosome: involvement in microtubule-organizing activity. *Molecular Biology of the Cell.*

KHODJAKOV, A., COPENAGLE, L., GORDON, M. B., COMPTON, D. A. & KAPOOR, T. M. 2003. Minus-end capture of preformed kinetochore fibers contributes to spindle morphogenesis. *J Cell Biol,* 160**,** 671-83.

KHODJAKOV, A. & RIEDER, C. L. 1999. The sudden recruitment of gamma-tubulin to the centrosome at the onset of mitosis and its dynamic exchange throughout the cell cycle, do not require microtubules. *J Cell Biol,* 146**,** 585-96.

KHODJAKOV, A., RIEDER, C. L., SLUDER, G., CASSELS, G., SIBON, O. & WANG, C. L. 2002. De novo formation of centrosomes in vertebrate cells arrested during S phase. *J Cell Biol,* 158**,** 1171-81.

KITAGAWA, D., VAKONAKIS, I., OLIERIC, N., HILBERT, M., KELLER, D., OLIERIC, V., BORTFELD, M., ERAT, M. C., FLÜCKIGER, I., GÖNCZY, P. & STEINMETZ, M. O. 2011. Structural Basis of the 9-Fold Symmetry of Centrioles. *Cell.*

KLEYLEIN-SOHN, J., WESTENDORF, J., LE CLECH, M., HABEDANCK, R., STIERHOF, Y.-D. & NIGG, E. A. 2007. Plk4-induced centriole biogenesis in human cells. *Dev Cell.*

KLINE-SMITH, S. L. & WALCZAK, C. E. 2004. Mitotic spindle assembly and chromosome segregation: refocusing on microtubule dynamics. *Mol Cell,* 15**,** 317-27.

KLOTZ, C., DABAUVALLE, M. C., PAINTRAND, M., WEBER, T., BORNENS, M. & KARSENTI, E. 1990. Parthenogenesis in Xenopus eggs requires centrosomal integrity. *J Cell Biol,* 110**,** 405-15.

KOHLMAIER, G., LONCAREK, J., MENG, X., MCEWEN, B. F., MOGENSEN, M. M., SPEKTOR, A., DYNLACHT, B. D., KHODJAKOV, A. & GÖNCZY, P. 2009. Overly long centrioles and defective cell division upon excess of the SAS-4-related protein CPAP. *Curr Biol.*

KONG, X., BALL, A. R., JR, SONODA, E., FENG, J., TAKEDA, S., FUKAGAWA, T., YEN, T. J. & YOKOMORI, K. 2009. Cohesin Associates with Spindle Poles in a Mitosis-specific Manner and Functions in Spindle Assembly in Vertebrate Cells

. *Molecular Biology of the Cell.*

KOUPRINA, N., PAVLICEK, A., MOCHIDA, G. H., SOLOMON, G., GERSCH, W., YOON, Y. H., COLLURA, R., RUVOLO, M., BARRETT, J. C., WOODS, C. G., WALSH, C. A., JURKA, J. & LARIONOV, V. 2004. Accelerated evolution of the ASPM gene controlling brain size begins prior to human brain expansion. *PLoS Biol,* 2**,** E126.

KRAUSE, A. & HOFFMANN, I. 2010. Polo-like kinase 2-dependent phosphorylation of NPM/B23 on serine 4 triggers centriole duplication. *PLoS ONE.*

KUMAR, A., GIRIMAJI, S. C., DUVVARI, M. R. & BLANTON, S. H. 2009. Mutations in STIL, encoding a pericentriolar and centrosomal protein, cause primary microcephaly. *Am J Hum Genet,* 84**,** 286-90.

KURIYAMA, R., TERADA, Y., LEE, K. S. & WANG, C. L. 2007. Centrosome replication in hydroxyurea-arrested CHO cells expressing GFP-tagged centrin2. *J Cell Sci,* 120**,** 2444-53.

LA TERRA, S., ENGLISH, C. N., HERGERT, P., MCEWEN, B. F., SLUDER, G. & KHODJAKOV, A. 2005. The de novo centriole assembly pathway in HeLa cells: cell cycle progression and centriole assembly/maturation. *J Cell Biol,* 168**,** 713-22.

LANE, H. A. & NIGG, E. A. 1996. Antibody microinjection reveals an essential role for human polo-like kinase 1 (Plk1) in the functional maturation of mitotic centrosomes. *J Cell Biol,* 135**,** 1701-13.

LEIDEL, S., DELATTRE, M., CERUTTI, L., BAUMER, K. & GÖNCZY, P. 2005. SAS-6 defines a protein family required for centrosome duplication in C. elegans and in human cells. *Nat Cell Biol.*

LI, X. & NICKLAS, R. B. 1995. Mitotic forces control a cell-cycle checkpoint. *Nature,* 373**,** 630-2.

LIANG, Y., GAO, H., LIN, S. Y., PENG, G., HUANG, X., ZHANG, P., GOSS, J. A., BRUNICARDI, F. C., MULTANI, A. S., CHANG, S. & LI, K. 2010. BRIT1/MCPH1 is essential for mitotic and meiotic recombination DNA repair and maintaining genomic stability in mice. *PLoS Genet,* 6**,** e1000826.

LINDQVIST, A., KALLSTROM, H., LUNDGREN, A., BARSOUM, E. & ROSENTHAL, C. K. 2005. Cdc25B cooperates with Cdc25A to induce mitosis but has a unique role in activating cyclin B1-Cdk1 at the centrosome. *J Cell Biol,* 171**,** 35-45.

LIZARRAGA, S. B., MARGOSSIAN, S. P., HARRIS, M. H., CAMPAGNA, D. R., HAN, A. P., BLEVINS, S., MUDBHARY, R., BARKER, J. E., WALSH, C. A. & FLEMING, M. D. 2010. Cdk5rap2 regulates centrosome function and chromosome segregation in neuronal progenitors. *Development,* 137**,** 1907-17.

LÖFFLER, H., BOCHTLER, T., FRITZ, B., TEWS, B., HO, A. D., LUKAS, J., BARTEK, J. & KRÄMER, A. 2007. DNA damage-induced accumulation of centrosomal Chk1 contributes to its checkpoint function. *Cell Cycle.*

LOFFLER, H., FECHTER, A., MATUSZEWSKA, M., SAFFRICH, R., MISTRIK, M., MARHOLD, J., HORNUNG, C., WESTERMANN, F., BARTEK, J. & KRAMER, A. 2011. Cep63 Recruits Cdk1 to the Centrosome: Implications for Regulation of Mitotic Entry, Centrosome Amplification, and Genome Maintenance. *Cancer Research.*

LONCAREK, J., HERGERT, P. & KHODJAKOV, A. 2010. Centriole reduplication during prolonged interphase requires procentriole maturation governed by Plk1. *Curr Biol,* 20**,** 1277-82.

LONCAREK, J., HERGERT, P., MAGIDSON, V. & KHODJAKOV, A. 2008. Control of daughter centriole formation by the pericentriolar material. *Nat Cell Biol,* 10**,** 322-8.

LUDERS, J., PATEL, U. K. & STEARNS, T. 2006. GCP-WD is a gamma-tubulin targeting factor required for centrosomal and chromatin-mediated microtubule nucleation. *Nat Cell Biol,* 8**,** 137-47.

LUKAS, C., SORENSEN, C. S., KRAMER, E., SANTONI-RUGIU, E., LINDENEG, C., PETERS, J. M., BARTEK, J. & LUKAS, J. 1999. Accumulation of cyclin B1 requires E2F and cyclin-A-dependent rearrangement of the anaphase-promoting complex. *Nature,* 401**,** 815-8.

MAHJOUB, M. R., XIE, Z. & STEARNS, T. 2010. Cep120 is asymmetrically localized to the daughter centriole and is essential for centriole assembly. *J Cell Biol,* 191**,** 331-46.

MARCHLER-BAUER, A., LU, S., ANDERSON, J. B., CHITSAZ, F., DERBYSHIRE, M. K., DEWEESE-SCOTT, C., FONG, J. H., GEER, L. Y., GEER, R. C., GONZALES, N. R., GWADZ, M., HURWITZ, D. I., JACKSON, J. D., KE, Z., LANCZYCKI, C. J., LU, F., MARCHLER, G. H., MULLOKANDOV, M., OMELCHENKO, M. V., ROBERTSON, C. L., SONG, J. S., THANKI, N., YAMASHITA, R. A., ZHANG, D., ZHANG, N., ZHENG, C. & BRYANT, S. H. 2011. CDD: a Conserved Domain Database for the functional annotation of proteins. *Nucleic Acids Res,* 39**,** D225-9.

MARESCA, T. J. & SALMON, E. D. 2009. Intrakinetochore stretch is associated with changes in kinetochore phosphorylation and spindle assembly checkpoint activity. *J Cell Biol,* 184**,** 373-81.

MARESCA, T. J. & SALMON, E. D. 2010. Welcome to a new kind of tension: translating kinetochore mechanics into a wait-anaphase signal. *J Cell Sci,* 123**,** 825-35.

MAYOR, T., STIERHOF, Y. D., TANAKA, K., FRY, A. M. & NIGG, E. A. 2000. The centrosomal protein C-Nap1 is required for cell cycle-regulated centrosome cohesion. *J Cell Biol,* 151**,** 837-46.

MEANI, N. & ALCALAY, M. 2009. Role of nucleophosmin in acute myeloid leukemia. *Expert Rev Anticancer Ther,* 9**,** 1283-94.

MEGRAW, T. L., SHARKEY, J. T. & NOWAKOWSKI, R. S. 2011. Cdk5rap2 exposes the centrosomal root of microcephaly syndromes. *Trends Cell Biol,* 21**,** 470-80.

MERALDI, P., LUKAS, J., FRY, A. M., BARTEK, J. & NIGG, E. A. 1999. Centrosome duplication in mammalian somatic cells requires E2F and Cdk2-cyclin A. *Nat Cell Biol,* 1**,** 88-93.

MERDES, A., HEALD, R., SAMEJIMA, K., EARNSHAW, W. C. & CLEVELAND, D. W. 2000. Formation of spindle poles by dynein/dynactin-dependent transport of NuMA. *J Cell Biol,* 149**,** 851-62.

MIDDENDORP, S., KUNTZIGER, T., ABRAHAM, Y., HOLMES, S., BORDES, N., PAINTRAND, M., PAOLETTI, A. & BORNENS, M. 2000. A role for centrin 3 in centrosome reproduction. *J Cell Biol,* 148**,** 405-16.

MIKHAILOV, A., COLE, R. W. & RIEDER, C. L. 2002. DNA Damage during Mitosis in Human Cells Delays the Metaphase/Anaphase Transition via the Spindle-Assembly Checkpoint

. *Current Biology.*

MIMITOU, E. P. & SYMINGTON, L. S. 2009. Nucleases and helicases take center stage in homologous recombination. *Trends Biochem Sci,* 34**,** 264-72.

MITCHISON, T. & KIRSCHNER, M. 1984. Microtubule assembly nucleated by isolated centrosomes. *Nature,* 312**,** 232-7.

MITRA, J. & ENDERS, G. H. 2004. Cyclin A/Cdk2 complexes regulate activation of Cdk1 and Cdc25 phosphatases in human cells. *Oncogene,* 23**,** 3361-7.

MOGENSEN, M. M., MALIK, A., PIEL, M., BOUCKSON-CASTAING, V. & BORNENS, M. 2000. Microtubule minus-end anchorage at centrosomal and non-centrosomal sites: the role of ninein. *Journal of Cell Science.*

MOSS, D. K., BELLETT, G., CARTER, J. M., LIOVIC, M., KEYNTON, J., PRESCOTT, A. R., LANE, E. B. & MOGENSEN, M. M. 2007. Ninein is released from the centrosome and moves bi-directionally along microtubules. *J Cell Sci,* 120**,** 3064-74.

MURRAY, A. W. & KIRSCHNER, M. W. 1989. Cyclin synthesis drives the early embryonic cell cycle. *Nature,* 339**,** 275-80.

MURRAY, A. W., SOLOMON, M. J. & KIRSCHNER, M. W. 1989. The role of cyclin synthesis and degradation in the control of maturation promoting factor activity. *Nature,* 339**,** 280-6.

MUSACCHIO, A. & SALMON, E. D. 2007. The spindle-assembly checkpoint in space and time. *Nat Rev Mol Cell Biol.*

NEGRINI, S., GORGOULIS, V. G. & HALAZONETIS, T. D. 2010. Genomic instability--an evolving hallmark of cancer. *Nat Rev Mol Cell Biol,* 11**,** 220-8.

NICHOLAS, A. K., KHURSHID, M., DESIR, J., CARVALHO, O. P., COX, J. J., THORNTON, G., KAUSAR, R., ANSAR, M., AHMAD, W., VERLOES, A., PASSEMARD, S., MISSON, J. P., LINDSAY, S., GERGELY, F., DOBYNS, W. B., ROBERTS, E., ABRAMOWICZ, M. & WOODS, C. G. 2010. WDR62 is

associated with the spindle pole and is mutated in human microcephaly. *Nat Genet,* 42**,** 1010-4.

NICHOLAS, A. K., SWANSON, E. A., COX, J. J., KARBANI, G., MALIK, S., SPRINGELL, K., HAMPSHIRE, D., AHMED, M., BOND, J., DI BENEDETTO, D., FICHERA, M., ROMANO, C., DOBYNS, W. B. & WOODS, C. G. 2009. The molecular landscape of ASPM mutations in primary microcephaly. *J Med Genet,* 46**,** 249-53.

NIGG, E. 2002. Centrosome aberrations: cause or consequence of cancer progression? *Nat Rev Cancer.*

NIGG, E. A. 2007. Centrosome duplication: of rules and licenses. *Trends Cell Biol.*

NIGG, E. A. & RAFF, J. W. 2009. Centrioles, centrosomes, and cilia in health and disease. *Cell,* 139**,** 663-78.

NITTA, M., KOBAYASHI, O., HONDA, S., HIROTA, T., KUNINAKA, S., MARUMOTO, T., USHIO, Y. & SAYA, H. 2004. Spindle checkpoint function is required for mitotic catastrophe induced by DNA-damaging agents. *Oncogene.*

NORBURY, C., BLOW, J. & NURSE, P. 1991. Regulatory phosphorylation of the p34cdc2 protein kinase in vertebrates. *EMBO J,* 10**,** 3321-9.

O'CONNELL, M. J., RALEIGH, J. M., VERKADE, H. M. & NURSE, P. 1997. Chk1 is a wee1 kinase in the G2 DNA damage checkpoint inhibiting cdc2 by Y15 phosphorylation. *EMBO J,* 16**,** 545-54.

O'DRISCOLL, M., RUIZ-PEREZ, V. L., WOODS, C. G., JEGGO, P. A. & GOODSHIP, J. A. 2003. A splicing mutation affecting expression of ataxia-telangiectasia and Rad3-related protein (ATR) results in Seckel syndrome. *Nat Genet,* 33**,** 497-501.

OHTA, T., ESSNER, R., RYU, J. H., PALAZZO, R. E., UETAKE, Y. & KURIYAMA, R. 2002. Characterization of Cep135, a novel coiled-coil centrosomal protein involved in microtubule organization in mammalian cells. *J Cell Biol,* 156**,** 87-99.

OKUDA, M., HORN, H. F., TARAPORE, P., TOKUYAMA, Y., SMULIAN, A. G., CHAN, P. K., KNUDSEN, E. S., HOFMANN, I. A., SNYDER, J. D., BOVE, K. E. & FUKASAWA, K. 2000. Nucleophosmin/B23 is a target of CDK2/cyclin E in centrosome duplication. *Cell,* 103**,** 127-40.

ON, K. F., CHEN, Y., TANG MA, H., CHOW, J. P. H. & POON, R. Y. C. 2011. Determinants of Mitotic Catastrophe on Abrogation of the G2 DNA Damage Checkpoint by UCN-01. *Mol Cancer Ther.*

OSHIMORI, N., LI, X., OHSUGI, M. & YAMAMOTO, T. 2009. Cep72 regulates the localization of key centrosomal proteins and proper bipolar spindle formation. *EMBO J.*

OSHIMORI, N., OHSUGI, M. & YAMAMOTO, T. 2006. The Plk1 target Kizuna stabilizes mitotic centrosomes to ensure spindle bipolarity. *Nat Cell Biol,* 8**,** 1095-101.

OU, Y. & RATTNER, J. B. 2000. A subset of centrosomal proteins are arranged in a tubular conformation that is reproduced during centrosome duplication. *Cell Motil Cytoskeleton,* 47**,** 13-24.

OU, Y. Y., ZHANG, M., CHI, S., MATYAS, J. R. & RATTNER, J. B. 2003. Higher order structure of the PCM adjacent to the centriole. *Cell Motil Cytoskeleton,* 55**,** 125-33.

PAINTRAND, M., MOUDJOU, M., DELACROIX, H. & BORNENS, M. 1992. Centrosome organization and centriole architecture: their sensitivity to divalent cations. *J Struct Biol,* 108**,** 107-28.

PAOLETTI, A., MOUDJOU, M., PAINTRAND, M., SALISBURY, J. L. & BORNENS, M. 1996. Most of centrin in animal cells is not centrosome-associated and centrosomal centrin is confined to the distal lumen of centrioles. *J Cell Sci,* 109 (Pt 13)**,** 3089-102.

PAWELETZ, N. 2001. Walther Flemming: pioneer of mitosis research. *Nat Rev Mol Cell Biol,* 2**,** 72-5.

PEREZ-MONGIOVI, D., BECKHELLING, C., CHANG, P., FORD, C. C. & HOULISTON, E. 2000. Nuclei and microtubule asters stimulate maturation/M phase promoting factor (MPF) activation in Xenopus eggs and egg cytoplasmic extracts. *J Cell Biol,* 150**,** 963-74.

PERKINS, D. N., PAPPIN, D. J., CREASY, D. M. & COTTRELL, J. S. 1999. Probability-based protein identification by searching sequence databases using mass spectrometry data. *Electrophoresis,* 20**,** 3551-67.

PETRETTI, C., SAVOIAN, M., MONTEMBAULT, E., GLOVER, D. M., PRIGENT, C. & GIET, R. 2006. The PITSLRE/CDK11p58 protein kinase promotes centrosome maturation and bipolar spindle formation. *EMBO Rep,* 7**,** 418-24.

PETRONCZKI, M., LENART, P. & PETERS, J. M. 2008. Polo on the Rise-from Mitotic Entry to Cytokinesis with Plk1. *Dev Cell,* 14**,** 646-59.

PFAFF, K. L., STRAUB, C. T., CHIANG, K., BEAR, D. M., ZHOU, Y. & ZON, L. I. 2007. The zebra fish cassiopeia mutant reveals that SIL is required for mitotic spindle organization. *Mol Cell Biol,* 27**,** 5887-97.

PIANE, M., DELLA MONICA, M., PIATELLI, G., LULLI, P., LONARDO, F., CHESSA, L. & SCARANO, G. 2009. Majewski osteodysplastic primordial dwarfism type II (MOPD II) syndrome previously diagnosed as Seckel syndrome: report of a novel mutation of the PCNT gene. *Am J Med Genet A,* 149A**,** 2452-6.

PIAZZA, F., GURRIERI, C. & PANDOLFI, P. P. 2001. The theory of APL. *Oncogene,* 20**,** 7216-22.

PONTING, C. & JACKSON, A. P. 2005. Evolution of primary microcephaly genes and the enlargement of primate brains. *Curr Opin Genet Dev,* 15**,** 241-8.

POVIRK, L. F. 1996. DNA damage and mutagenesis by radiomimetic DNA-cleaving agents: bleomycin, neocarzinostatin and other enediynes. *Mutation Research/Fundamental and Molecular Mechanisms of Mutagenesis,* 355**,** 71-89.

PUKLOWSKI, A., HOMSI, Y., KELLER, D., MAY, M., CHAUHAN, S., KOSSATZ, U., GRUNWALD, V., KUBICKA, S., PICH, A., MANNS, M. P., HOFFMANN, I., GONCZY, P. & MALEK, N. P. 2011. The SCF-FBXW5 E3-ubiquitin ligase is regulated by PLK4 and targets HsSAS-6 to control centrosome duplication. *Nat Cell Biol,* 13**,** 1004-9.

PULVERS, J. N., BRYK, J., FISH, J. L., WILSCH-BRAUNINGER, M., ARAI, Y., SCHREIER, D., NAUMANN, R., HELPPI, J., HABERMANN, B., VOGT, J., NITSCH, R., TOTH, A., ENARD, W., PAABO, S. & HUTTNER, W. B. 2010. Mutations in mouse Aspm (abnormal spindle-like microcephaly associated) cause not only microcephaly but also major defects in the germline. *Proc Natl Acad Sci U S A,* 107**,** 16595-600.

RAYNAUD-MESSINA, B. & MERDES, A. 2007. Gamma-tubulin complexes and microtubule organization. *Curr Opin Cell Biol,* 19**,** 24-30.

RIEDER, C. L., COLE, R. W., KHODJAKOV, A. & SLUDER, G. 1995. The checkpoint delaying anaphase in response to chromosome monoorientation is mediated by an inhibitory signal produced by unattached kinetochores. *J Cell Biol,* 130**,** 941-8.

ROGAKOU, E. P., PILCH, D. R., ORR, A. H., IVANOVA, V. S. & BONNER, W. M. 1998. DNA double-stranded breaks induce histone H2AX phosphorylation on serine 139. *J Biol Chem,* 273**,** 5858-68.

ROYOU, A., MACIAS, H. & SULLIVAN, W. 2005. The Drosophila Grp/Chk1 DNA Damage Checkpoint

Controls Entry into Anaphase. *Current Biology.*

RUSSELL, P. & NURSE, P. 1987. Negative regulation of mitosis by wee1+, a gene encoding a protein kinase homolog. *Cell,* 49**,** 559-67.

SALISBURY, J. L., SUINO, K. M., BUSBY, R. & SPRINGETT, M. 2002. Centrin-2 is required for centriole duplication in mammalian cells. *Curr Biol,* 12**,** 1287-92.

SANCAR, A., LINDSEY-BOLTZ, L. A., UNSAL-KACMAZ, K. & LINN, S. 2004. Molecular mechanisms of mammalian DNA repair and the DNA damage checkpoints. *Annu Rev Biochem,* 73**,** 39-85.

SCHMIDT, T. I., KLEYLEIN-SOHN, J., WESTENDORF, J., LE CLECH, M., LAVOIE, S. B., STIERHOF, Y. D. & NIGG, E. A. 2009. Control of centriole length by CPAP and CP110. *Curr Biol,* 19**,** 1005-11.

SCHMITT, E., BOUTROS, R., FROMENT, C., MONSARRAT, B., DUCOMMUN, B. & DOZIER, C. 2006. CHK1 phosphorylates CDC25B during the cell cycle in the absence of DNA damage. *J Cell Sci,* 119**,** 4269-75.

SCHOCKEL, L., MOCKEL, M., MAYER, B., BOOS, D. & STEMMANN, O. 2011. Cleavage of cohesin rings coordinates the separation of centrioles and chromatids. *Nat Cell Biol,* 13**,** 966-72.

SILK, A. D., HOLLAND, A. J. & CLEVELAND, D. W. 2009. Requirements for NuMA in maintenance and establishment of mammalian spindle poles. *The Journal of Cell Biology.*

SKOUFIAS, D. A., ANDREASSEN, P. R., LACROIX, F. B., WILSON, L. & MARGOLIS, R. L. 2001. Mammalian mad2 and bub1/bubR1 recognize distinct spindle-attachment and kinetochore-tension checkpoints. *Proc Natl Acad Sci U S A,* 98**,** 4492-7.

SKOUFIAS, D. A., DEBONIS, S., SAOUDI, Y., LEBEAU, L., CREVEL, I., CROSS, R., WADE, R. H., HACKNEY, D. & KOZIELSKI, F. 2006. S-trityl-L-cysteine is a reversible, tight binding inhibitor of the human kinesin Eg5 that specifically blocks mitotic progression. *J Biol Chem,* 281**,** 17559-69.

SLUDER, G. 2005. Two-way traffic: centrosomes and the cell cycle. *Nat Rev Mol Cell Biol,* 6**,** 743-8.

SMITH, E., DEJSUPHONG, D., BALESTRINI, A., HAMPEL, M., LENZ, C., TAKEDA, S., VINDIGNI, A. & COSTANZO, V. 2009. An ATM- and ATR-dependent checkpoint inactivates spindle assembly by targeting CEP63. *Nat Cell Biol.*

STEERE, N., WAGNER, M., BEISHIR, S., SMITH, E., BRESLIN, L., MORRISON, C. G., HOCHEGGER, H. & KURIYAMA, R. 2011. Centrosome amplification

in CHO and DT40 cells by inactivation of cyclin-dependent kinases. *Cytoskeleton (Hoboken)*.

STIFF, T., O'DRISCOLL, M., RIEF, N., IWABUCHI, K., LOBRICH, M. & JEGGO, P. A. 2004. ATM and DNA-PK function redundantly to phosphorylate H2AX after exposure to ionizing radiation. *Cancer Res,* 64**,** 2390-6.

STIFF, T., WALKER, S. A., CEROSALETTI, K., GOODARZI, A. A., PETERMANN, E., CONCANNON, P., O'DRISCOLL, M. & JEGGO, P. A. 2006. ATR-dependent phosphorylation and activation of ATM in response to UV treatment or replication fork stalling. *EMBO J,* 25**,** 5775-82.

STRNAD, P., LEIDEL, S., VINOGRADOVA, T., EUTENEUER, U., KHODJAKOV, A. & GÖNCZY, P. 2007. Regulated HsSAS-6 levels ensure formation of a single procentriole per centriole during the centrosome duplication cycle. *Dev Cell.*

STUCKI, M. & JACKSON, S. P. 2006. gammaH2AX and MDC1: anchoring the DNA-damage-response machinery to broken chromosomes. *DNA Repair (Amst),* 5**,** 534-43.

TANENBAUM, M. E. & MEDEMA, R. H. 2010. Mechanisms of centrosome separation and bipolar spindle assembly. *Dev Cell,* 19**,** 797-806.

TANG, C. J., FU, R. H., WU, K. S., HSU, W. B. & TANG, T. K. 2009. CPAP is a cell-cycle regulated protein that controls centriole length. *Nat Cell Biol,* 11**,** 825-31.

THORNTON, G. K. & WOODS, C. G. 2009. Primary microcephaly: do all roads lead to Rome? *Trends Genet.*

TIBELIUS, A., MARHOLD, J., ZENTGRAF, H., HEILIG, C. E., NEITZEL, H., DUCOMMUN, B., RAUCH, A., HO, A. D., BARTEK, J. & KRAMER, A. 2009. Microcephalin and pericentrin regulate mitotic entry via centrosome-associated Chk1. *J Cell Biol,* 185**,** 1149-57.

TOLEDO, L. I., MURGA, M., ZUR, R., SORIA, R., RODRIGUEZ, A., MARTINEZ, S., OYARZABAL, J., PASTOR, J., BISCHOFF, J. R. & FERNANDEZ-CAPETILLO, O. 2011. A cell-based screen identifies ATR inhibitors with synthetic lethal properties for cancer-associated mutations. *Nat Struct Mol Biol,* 18**,** 721-7.

TSANG, W. Y., SPEKTOR, A., VIJAYAKUMAR, S., BISTA, B. R., LI, J., SANCHEZ, I., DUENSING, S. & DYNLACHT, B. D. 2009. Cep76, a centrosomal protein that specifically restrains centriole reduplication. *Dev Cell.*

TSOU, M.-F. B. & STEARNS, T. 2006. Mechanism limiting centrosome duplication to once per cell cycle. *Nature.*

TSOU, M.-F. B., WANG, W.-J., GEORGE, K. A., URYU, K., STEARNS, T. & JALLEPALLI, P. V. 2009. Polo kinase and separase regulate the mitotic licensing of centriole duplication in human cells. *Dev Cell.*

TSVETKOV, L. 2003. Polo-like Kinase 1 and Chk2 Interact and Co-localize to Centrosomes and the Midbody. *Journal of Biological Chemistry.*

TULU, U. S., FAGERSTROM, C., FERENZ, N. P. & WADSWORTH, P. 2006. Molecular requirements for kinetochore-associated microtubule formation in mammalian cells. *Curr Biol,* 16**,** 536-41.

UCHIDA, K. S., TAKAGAKI, K., KUMADA, K., HIRAYAMA, Y., NODA, T. & HIROTA, T. 2009. Kinetochore stretching inactivates the spindle assembly checkpoint. *J Cell Biol,* 184**,** 383-90.

UETAKE, Y., TERADA, Y., MATULIENE, J. & KURIYAMA, R. 2004. Interaction of Cep135 with a p50 dynactin subunit in mammalian centrosomes. *Cell Motil Cytoskeleton.*

VARMARK, H., LLAMAZARES, S., REBOLLO, E., LANGE, B., REINA, J., SCHWARZ, H. & GONZALEZ, C. 2007. Asterless is a centriolar protein required for centrosome function and embryo development in Drosophila. *Curr Biol.*

VOROBJEV, I. A. & CHENTSOV YU, S. 1982. Centrioles in the cell cycle. I. Epithelial cells. *J Cell Biol,* 93**,** 938-49.

WAKEFIELD, J. G., BONACCORSI, S. & GATTI, M. 2001. The drosophila protein asp is involved in microtubule organization during spindle formation and cytokinesis. *J Cell Biol,* 153**,** 637-48.

WANG, W.-J., SONI, R. K., URYU, K. & BRYAN TSOU, M.-F. 2011. The conversion of centrioles to centrosomes: essential coupling of duplication with segregation. *The Journal of Cell Biology.*

WARNKE, S., KEMMLER, S., HAMES, R. S., TSAI, H.-L., HOFFMANN-ROHRER, U., FRY, A. M. & HOFFMANN, I. 2004. Polo-like kinase-2 is required for centriole duplication in mammalian cells. *Curr Biol.*

WIESE, C. & ZHENG, Y. 2006. Microtubule nucleation: gamma-tubulin and beyond. *J Cell Sci,* 119**,** 4143-53.

WONG, C. & STEARNS, T. 2003. Centrosome number is controlled by a centrosome-intrinsic block to reduplication. *Nat Cell Biol,* 5**,** 539-44.

WOODS, C. G., BOND, J. & ENARD, W. 2005. Autosomal recessive primary microcephaly (MCPH): a review of clinical, molecular, and evolutionary findings. *Am J Hum Genet,* 76**,** 717-28.

WU, J., CHO, H. P., RHEE, D. B., JOHNSON, D. K., DUNLAP, J., LIU, Y. & WANG, Y. 2008. Cdc14B depletion leads to centriole amplification, and its overexpression prevents unscheduled centriole duplication. *J Cell Biol,* 181**,** 475-83.

YAN, X., HABEDANCK, R. & NIGG, E. A. 2006. A complex of two centrosomal proteins, CAP350 and FOP, cooperates with EB1 in microtubule anchoring. *Molecular Biology of the Cell.*

YANG, C. H., KASBEK, C., MAJUMDER, S., YUSOF, A. M. & FISK, H. A. 2010. Mps1 phosphorylation sites regulate the function of centrin 2 in centriole assembly. *Mol Biol Cell,* 21**,** 4361-72.

YANG, J., ADAMIAN, M. & LI, T. 2006. Rootletin interacts with C-Nap1 and may function as a physical linker between the pair of centrioles/basal bodies in cells. *Mol Biol Cell,* 17**,** 1033-40.

YOUNG, A., DICTENBERG, J. B., PUROHIT, A., TUFT, R. & DOXSEY, S. J. 2000. Cytoplasmic dynein-mediated assembly of pericentrin and gamma tubulin onto centrosomes. *Mol Biol Cell,* 11**,** 2047-56.

YU, T. W., MOCHIDA, G. H., TISCHFIELD, D. J., SGAIER, S. K., FLORES-SARNAT, L., SERGI, C. M., TOPCU, M., MCDONALD, M. T., BARRY, B. J., FELIE, J. M., SUNU, C., DOBYNS, W. B., FOLKERTH, R. D., BARKOVICH, A. J. & WALSH, C. A. 2010. Mutations in WDR62, encoding a centrosome-associated protein, cause microcephaly with simplified gyri and abnormal cortical architecture. *Nat Genet,* 42**,** 1015-20.

ZACHOS, G., BLACK, E. J., WALKER, M., SCOTT, M. T., VAGNARELLI, P., EARNSHAW, W. C. & GILLESPIE, D. A. 2009. Chk1 Is Required for Spindle Checkpoint Function. *Dev Cell.*

ZHANG, S., HEMMERICH, P. & GROSSE, F. 2007. Centrosomal localization of DNA damage checkpoint proteins. *J Cell Biochem,* 101**,** 451-65.

ZHONG, X., LIU, L., ZHAO, A., PFEIFER, G. P. & XU, X. 2005. The abnormal spindle-like, microcephaly-associated (ASPM) gene encodes a centrosomal protein. *Cell Cycle,* 4**,** 1227-9.

ZHOU, B. B. & ELLEDGE, S. J. 2000. The DNA damage response: putting checkpoints in perspective. *Nature,* 408**,** 433-9.

ZHU, F., LAWO, S., BIRD, A., PINCHEV, D., RALPH, A., RICHTER, C., MULLER-REICHERT, T., KITTLER, R., HYMAN, A. A. & PELLETIER, L. 2008. The mammalian SPD-2 ortholog Cep192 regulates centrosome biogenesis. *Curr Biol,* 18**,** 136-41.

ZIMMERMAN, W. C., SILLIBOURNE, J., ROSA, J. & DOXSEY, S. J. 2004. Mitosis-specific anchoring of gamma tubulin complexes by pericentrin controls spindle organization and mitotic entry. *Mol Biol Cell,* 15**,** 3642-57.

Books

MORGAN, D. O. 2007. The Cell Cycle: Principles of Control. *New Science Press Ltd*.

SAMBROOK & RUSSELL 2000. Molecular Cloning. *Cold Spring Harbor Laboratory Press, U.S.*

Appendix

Brown, N. & Costanzo, V. 2009. An ATM and ATR dependent pathway targeting centrosome dependent spindle assembly. Cell Cycle, 8, 1997-2001.

This opinion article discusses the topic of DNA damage in mitosis and the effects on mitotic progression. It describes work that was carried out using the *Xenopus laevis* egg extract system to investigate timing of mitotic exit and SAC activation in response to mitotic DNA damage. XMad1 and XMad2 antibodies were generated, purified and verified, and all assays were designed and carried out by N Brown.